Prepared for:

National Institute for Coastal and Marine Management (RIKZ)

Model convergence of SWAN in the Westerschelde estuary

A study on model convergence using the one-dimensional mode of SWAN

March, 1999

H3496

WL | delft hydraulics

Model convergence of SWAN in the Westerschelde estuary

A study on model convergence using the one-dimensional mode of SWAN

R.C. Ris

WL | delft hydraulics

WL | delft hydraulics

CLIENT: National Institute for Coastal and Marine Management (RIKZ)

TITLE: Model convergence of SWAN in the Westerschelde estuary: 'A study on model convergence using the one-dimensional mode of SWAN'

ABSTRACT:

From several studies it has been found that the SWAN model converges rather slowly in computations in the complex field case of the Westerschelde estuary. This study has been performed to get more insight in this observed SWAN model convergence behaviour. To this end a large number of computations have been performed in a one-dimensional situation of the Westerschelde and in a one-dimensional situation of fetch-limited deep water wave growth. The model convergence has been studied by changing the input commands and coefficients in each of the computations. The effect of currents on model convergence has not been investigated in this study.

For the results presented in this study it has been shown that SWAN converges relatively slowly for high wind speeds and that this convergence behaviour is related to the quadruplets and the subsequent limiter that is required to obtain a stable model solution.

On the basis of results of several computations presented in this study, it can be concluded that the model convergence speed can be improved by:

- improving the *first-guess* of SWAN for higher wind speeds;
- changing the strength of the limiter and its distribution over the frequencies.

In addition, further improvement of the SWAN convergence speed is expected from the development of more adequate quadruplet formulations.

REFERENCES: Letters:
1) RIKZ/OS/987223 (dated December 9, 1998) of ir J.J.W. Seyffert
2) order 22990017 (dated January 12, 1999) of ir J.H. Andorka Gal

REV.	ORIGINATOR		DATE	REMARKS	REVIEW		APPROVED BY	
0	R.C. Ris		February 1999		J. Dekker		W.M.K. Tilmans	
1	R.C. Ris		March 1999		J. Dekker		W.M.K. Tilmans	

KEYWORDS: SWAN wave model, Westerschelde estuary, model convergence, first-guess, limiter

CONTENTS:

TEXT PAGES:	13
TABLES:	2
FIGURES:	171
APPENDICES:	1

STATUS: ☐ PRELIMINARY ☐ DRAFT ☒ FINAL

PROJECT IDENTIFICATION: H3496

Contents

Appendices

List of Figures

The results of each test case are presented in four figures (except for the test cases 1, 2 and 3 where only two figures per test case are presented). Here, for reasons of readability, the text of the legend of only the first figure (with index '*a*') is given.

Westerschelde estuary test cases

Deep water test cases

List of Tables

List of Symbols

Roman letters

d	water depth
f	frequency
f_m	mean frequency (defined as $f_m=1/T_{m-2-1}$)
f_{high}, f_{max}	highest discrete frequency in SWAN in Hz
g	acceleration of gravity
H_s	significant wave height (defined as $H_s=4\sqrt{m_0}$)
S_{in}	wind input source term
S_{nl4}	quadruplet source term
S_{wcap}	whitecapping source term
T_{m-2-1}	mean wave period
T_{m01}	mean wave period
U_{10}	wind speed at 10 m height
x	x-co-ordinate

Greek symbols

θ	mean wave direction (Cartesian convention)
θ_w	mean wind direction (Cartesian convention)
θ_o	incident mean wave direction (Cartesian convention) at up-wave boundary
Δx	increment in x-direction
Δf, $\Delta\theta$	increment in frequency- and directional-space, respectively

1 Introduction

1.1 General

The wave model SWAN (see e.g. Booij et al., 1998) has been developed to compute wave conditions in e.g. estuaries and coastal regions. SWAN is widely used and in many complex field cases, the SWAN model performs fairly well. However, it was shown on the basis of several studies that the SWAN model converges rather slowly in complex situations like e.g. the Friesche Zeegat (see e.g. Dunsbergen, 1995). In order to improve the convergence speed, a so-called *first-guess* has been introduced (see Ris, 1997). This first-guess consists of a best possible estimate of the final solution in the first iteration using second-generation formulations.

Although the use of a first-guess has lead to an improvement of the model convergence behaviour in many cases, it has been shown that for cases with (strong) winds, such as the Westerschelde case (see e.g. WL | DELFT HYDRAULICS, 1998 and 1999), SWAN converges very slowly to a final solution. Since it was not been precisely known why the SWAN model converges relatively slowly in the Westerschelde estuary, some investigation regarding this observed model behaviour is called for.

The Dutch Ministry of Public Works and Coastal Management (hereafter to be called RIKZ) therefore invited WL | DELFT HYDRAULICS to submit a proposal in which the observed model convergence is investigated in a one-dimensional situation of the Westerschelde estuary and, in addition, in a one-dimensional situation of fetch-limited wave growth in deep water (reference is made here to the letter of RIKZ with reference number RIKZ/OS/987223 of December 9, 1998). The effect of different model settings and coefficients on model convergence has been investigated in these idealised one-dimensional cases, in order to determine the cause of the slow convergence behaviour of SWAN. It is noted here that the effects of currents on model convergence is not accounted for in this study.

It is noted that the present study has been performed in co-operation with RIKZ and Delft University of Technology (TUD) and that the cases described in this report have mainly been chosen in consultation with RIKZ and TUD while the present study was going on.

1.2 Outline of the report

This report is organised as follows. In Chapter 2, the study after the model convergence behaviour of SWAN is reported. The model schematisation and the model results for different cases are described. The computations have been made with (an experimental version of) **SWAN CYCLE 2, version 45.00**. Conclusions and recommendations are given in Chapter 3.

This project was carried out between February 15 and March 18, 1999 at WL as project H3496. The work was performed by dr R.C. Ris. We thank dr N. Booij, dr L.H. Holthuijsen and IJ. Haagsma of Delft University of Technology (the Netherlands) for their help and advice during the project and for providing us with the results of the DOLPHIN wave model.

2 Study on model convergence behaviour of SWAN

2.1 Introduction

From several studies in the two-dimensional situation of the Westerschelde it has been found that the observed slow model convergence of SWAN is strongly related to relatively high wind speeds and the deep water processes of wind, whitecapping and quadruplets (see WL | DELFT HYDRAULICS, 1998 and 1999). In this section, this observed model behaviour of SWAN is investigated in more detail.

Since the required total computing time for a two-dimensional situation of the Westerschelde is rather large, it has been decided to study the model convergence in a one-dimensional situation using the one-dimensional mode of SWAN. By this the total computing time for a computation is significantly reduced. In addition, two-dimensional wave-propagation effects are also simply avoided by this. This one-dimensional situation represents a section along the main axis of the Westerschelde estuary (see Fig. 0 for the bathymetry of this section). It is noted here that while the present study was going on, RIKZ and TUD have found from additional SWAN computations that the observed model convergence behaviour in the two- and one-dimensional situation of fetch-limited wave growth is similar. This supports that the present approach, i.e. to study the model convergence in a one-dimensional situation, is justified. To avoid any shallow water effects on wave propagation, the model convergence has also been also investigated in the one-dimensional situation of deep water (with a constant depth) with the processes of triads, depth-induced wave breaking and bottom friction de-activated.

The model convergence is investigated in detail by computing the wave evolution along the (one-dimensional) curve using different model settings and parameters. The study concentrates on the computed integral wave parameters, the wave spectra, the source terms at different locations along the fetch for the following iteration levels: 1, 2, 5, 10, 15, 25, and 50.

It is noted here that it may seem that the order of the cases presented in this study have been chosen arbitrarily. However, this is obviously not the case. The order of the cases have been chosen and selected in consultation with RIKZ and TUD while the present study was going and therefore represent conditions which where of interest to investigate at that time.

2.2 Model schematisation

The computations (for both one-dimensional situations of the Westerschelde and the fetch-limited deep water case) have been performed along a curve of 25 km with the one-dimensional mode of SWAN. The resolution in geographical space has been taken equal Δx=100 m. In the computations, a frequency resolution of $\Delta f = 0.1f$ is used between 0.04

Hz and 1 Hz. The computations have been carried out with a directional resolution of $\Delta\theta = 10°$.

By default, the computations are terminated if in more than 97% of the water covered grid points the change in significant wave height H_s between two successive iterations is less than 3% or 0.03 m and the change in intrinsic mean wave period T_{m01} between two successive iterations is less than 3% or 0.3 s. In order to ensure that the computations are terminated on the number of iterations (rather than on the specified absolute and relative accuracy criterion), a rather strict accuracy criterion has been used. The used criterion reads:

1. less than 1.e-5 (relative) or 1.e-5 m change in significant wave height from one iteration to the next, and
2. less than 1.e-5 (relative) or 1.e-5 s change in mean wave period from one iteration to the next, and
3. the conditions a) and b) are fulfilled in 100% of all wet grid points.

In the computations, the wind speed has been varied (i.e. U_{10}=10 m/s, U_{10}=20 m/s and U_{10}=30 m/s).

An example of the SWAN-input file is presented in appendix A.

2.3 Model results

2.3.1 Introduction

For each case, model results are presented in four figures, in order to visualise the iteration process. Information on the integral spectral parameters can be found in the first figure; wave spectra are plotted in the second; the third figure contains source term results and the significant wave height as a function of the number of iterations is presented in the fourth figure. In the following text, these figures are explained in more detail.

The first figure (index a) shows each spectrum parameter as a function of fetch. The parameters are plotted at several moments in the computation (i.e. for the iterations 1, 2, 5, 10, 15, 25, and 50), thus showing their evolution during the iteration process. In the first panel, the significant wave height (H_s, in m) is given. The second panel presents the characteristic wave period (T_{m01}, in s), the third panel contains the mean wave direction (DIR, in °) and in the bottom panel, the directional spreading of the waves (DSPR, in °) is shown.

The second figure (index b) consists of three panels, displaying wave energy spectra for different fetches (i.e. for x = 0 km, x = 12.5 km and x = 25 km) at several iteration levels.

The first panel of the third figure (index c) shows the source terms Swind and Swcap. Swind represents the influence of wind on the energy balance, and Swcap that of the whitecapping process. In the second panel, the source term related to the effect of

quadruplets, S_{nl4}, is plotted. This term can be both positive and negative. The sum of the three source terms is plotted in the third panel.

The fourth figure (index d) shows the significant wave height H_s at x = 12.5 km as a continuous function of the iteration number. This figure gives information about the so-called overshoot and about the speed at which the SWAN model converges.

2.3.2 The Westerschelde estuary (one-dimensional situation)

A listing of the computations, performed in the one-dimensional situation of the Westerschelde, is given in Table 2.1. Note that *Case 1* is the standard reference case.

Case	U_{10} m/s	Computation type and characteristics
1	30	***standard case:* one-dimensional bathymetry; depth along a curve in Westerschelde area**
2	30	depth multiplied by 10^{10}
3	30	deactivated: BREAK, TRIAD, FRIC

Table 2.1 Listing of computations, performed in the one-dimensional situation of the Westerschelde

Case 1 is a standard case for the 1d-situation of the Westerschelde. This bathymetry has been obtained through a two-dimensional computation using the output of depth along a curve (results not shown here; see Fig. 7.1 in WL | DELFT HYDRAULICS, 1999). It has been used for one-dimensional computations with the standard options in SWAN activated. The results (see Figures 1a and 1b) clearly show the convergence problem: no convergence within a few iterations and an overshoot for the H_s.

Case 2 is the same as *Case 1*, apart from the fact that the depth has been multiplied by the factor 10^{10} (i.e. reducing the case to a deep water test). The results are plotted in Figures 2a and 2b. Increasing the depth does not fundamentally change the output of the computation and the observed behaviour is thus related to the deep water processes of wind, whitecapping, and quadruplets.

In Case 3, the formulations of the processes depth-induced breaking, triads and friction have been deactivated (see Figures 3a and 3b). Also here, the results are identical to those presented in Case 2, so the convergence problem must find its cause in the other processes: quadruplets, wind or whitecapping.

Therefore, it has been decided to concentrate on the idealised situation of fetch-limited wave growth in deep water in the remainder of this study.

2.3.3 Fetch-limited deep water wave growth (one-dimensional situation)

The cases for which computations have been made are presented in Table 2.2.

Fetch-limited wave growth in deep water (one-dimensional situation)		
Case	U_{10} m/s	Computation type and characteristics
4	30	***standard case:* third-generation formulations (wind, quadruplets and whitecapping) and the limiter are activated by default.**
5	30	adapted directional sector: dir1 = -90°, dir2 = +90°
6	30	adapted mode of SWAN: second-generation formulations used (GEN2); deactivated: limiter
7	30	adapted number of maximum iterations 500 iterations
8	30	adapted limiter (limiter = 5%)
9	30	adapted S_{nl4} computation (IQUAD = 1)
10	30	adapted S_{nl4} computation; fully explicit method per iteration (IQUAD = 3)
11	30	adapted limiter (limiter = 20%)
12	30	adapted directional resolution: directional increment $\Delta\theta = 2°$
13	30	adapted frequency resolution $f_{i+1} = 1.01*f_i$
14	10	adapted wind speed 10 m/s
15	20	adapted wind speed 20 m/s
16	30	adapted wind speed 30 m/s, *standard computation* (as case 4)
17	10	adapted mode of SWAN: second-generation formulations used (GEN2)
18	20	adapted mode of SWAN: second-generation formulations used (GEN2)
19	30	adapted mode of SWAN: second-generation formulations used (GEN2)
20	30	adapted mode of SWAN: second-generation formulations used (GEN2); quadruplets activated
21	30	deactivated: quadruplets
22	30	no pre-conditioner (no first guess); boundary condition: $H_s = 0.05$ m $T_p = 5$ s
23	30	implicit computation of Swind
24	30	no pre-conditioner; boundary condition: $H_s = 0.05$ m, $T_p = 12$ s
25	30	adapted limiter (limiter = 30%); no pre-conditioner; boundary condition: $H_s = 0.05$ m, $T_p = 12$ s
26	30	effect of incident swell on wave growth: $H_s = 0.05$ m, $T_p = 15$ s, ms = 10
27	30	enhanced first guess by changing coefficients GEN2 mode, adapted coefficients
28	30	adapted coefficient for quadruplets: $\lambda = 0.1$
29	30	adapted coefficients for quadruplets: $c_{nl4} = 1.5*e^7$
30	30	adapted coefficient for quadruplets: $\lambda = 0.2$
31	30	adapted wind speed and direction $U_{10,dir} = 45°$
32	30	adapted frequency range: $f_{low} = 0.04$ Hz, $f_{high} = 0.3$ Hz, MSC = 21
33	30	adapted limiter (limiter = 2%)
34	30	application of self scaling cut-off frequency; coefficient $\delta = 1.5$
35	30	adapted limiter (limiter = 40%)
36	30	adapted limiter; distribution equal (f/f_m)
37	30	adapted limiter; distribution equal $(f/f_m)^2$
38	30	adapted limiter; distribution equal $(f/f_m)^3$
39	30	adapted limiter; distribution equal (f_m/f)
40	30	adapted limiter; distribution equal $(f_m/f)^2$
41	10	adapted limiter; distribution equal $(f_m/f)^2$
42	20	adapted limiter; distribution equal $(f_m/f)^2$
43	10	adapted limiter; distribution equal f/f_m
44	20	adapted limiter; distribution equal f/f_m

Table 2.2 Listing of computations, performed in the idealised case of deep water (one-dimensional situation). Note that *Case 4* is the standard reference case.

For every case, detailed comments on the results have been given below.

Case 4 is the standard case. In this case, the default options have been activated in SWAN. When modelling the physical processes, effects of wind, quadruplets and whitecapping are activated, and the limiter is active at its default value of 10 %. The results of the computations (Figures 4a, 4b, 4c and 4d) have the following characteristics:

- the evolution of the significant wave height (and wave spectra) along the fetch shows an overshoot before converging to the end value;
- the parameter T_{m01} has no significant overshoot, but converges slowly to its end value;
- the direction parameter has an overshoot of ± 2.5° at the first iterations;
- the directional distribution of the energy spectrum has the relatively large value of 40° (it should be about 30° for the wind sea conditions considered). This rather broad directional distribution is ascribed to the modelling of the quadruplets with the DIA (for more information reference is made to Forristall and Ewans, 1998);
- the source terms show sensitivity to small changes in the wave energy;
- the computation traject of H_s at x = 12.5 km shows an overshoot of 0.34 m (with respect to the end value of 3.10 m);
- it takes 35 iterations to converge to the end value for H_s;
- the significant wave height in the first iteration (i.e. the 'first guess': H_s = 2.5 m for x = 12.5 km) is chosen far below the end value.

Case 5 has been carried out in order to investigate the effect of the directional sector being used in the computation. This sector has been changed from 360° into 180° (between -90° and +90°). This setting change does not yield significantly different computation results (Figures 5a to 5d); only the wave spectrum at x = 0 has become zero. This can be explained by the effect of the directional sector on the quadruplets. By changing this sector, the waves that are propagating against the wind direction are not modelled.

Case 6 has been computed using second generation formulations in SWAN. Figure 6a shows that the model converges rather rapidly in this mode. At x = 0, the H_s seems to increase straightforwardly to its end value. The mean wave direction is equal to zero (as it should be) and the width of directional distribution of the energy spectrum equals 30°. Also the model results for the spectra converge rather fast. From the source terms, only the Swind is counted, so that this case represents a limit with respect to this terms. H_s converges to its end value within 3 iterations. This case indicates that the physical processes modelled in the third-generation mode of SWAN (GEN3-mode) and the numerical techniques used in that mode are responsible for the slow convergence process.

Case 7 has been carried out to investigate the iteration behaviour during 500 iteration steps (in other words to check if the model has converged after 50 iterations). The Figures 7a to 7d do not show any differences from the standard case. The final solution is not different from the one found within 50 iterations.

Case 8 has been used for studying the effect of the limiter. The value of the coefficient that controls the strength of this limiter has been changed from its default value into 5%. Although the differences are small (Figures 8a to 8d), the model results clearly show that

the effect of the limiter on the numerical convergence is significant. The overshoot is less pronounced, but H_s has been slightly overestimated, and only after many iteration steps this has been corrected.

In *Case 9*, the S_{nl4} computation method has been changed in a semi-implicit computation per sweep (IQUAD = 1, see SWAN manual). The results (Figures 9a to 9d) reveal that the integration scheme of the quadruplet effect is not responsible for the observed convergence problem.

Like in *Case 9*, in *Case 10*, the S_{nl4} computation has been adapted to a fully explicit computation per iteration (IQUAD = 3, see SWAN manual). The results (Figures 10a to 10d) are exactly the same as those for *Case 4* and *9*.

For *Case 11* computations have been performed with an adapted limiter; the strength parameter value has been increased to 20%. The results (Figures 11a to 11d) show that this affects the overshoot, which gets its maximum within less iterations than in *Case 4*, and the final solution is also found earlier (after 20 iterations).

Increasing the directional resolution (from $\Delta\theta = 10°$ into 2°) as has been done in *Case 12* does not lead towards significant changes in the computation results (Figures 12a to 12d).

Case 13 shows that, apart from a smoother visual presentation, the adapted frequency resolution does not influence the iteration behaviour of the model (Figures 13a to 13d).

Case 14 illustrates that a lower wind speed (10 m/s) yields lower values for H_s, the energy density and the source terms, and although the convergence process is faster, the required number of iterations remains high (Figures 14a to 14d).

Case 15 is more of the same, as here the wind speed is modified (into 20 m/s). Corresponding to this, the results are also more of the same (Figures 15a to 15d).

Case 16 is identical to *Case 4*, and so are the results (Figures 16a to 16d).

In *Case 17* computations have been performed with the second generation mode of SWAN and U_{10}= 10 m/s, and this yields results (Figures 17a to 17d) without the convergence problems that accompany the use of the third generation mode of SWAN. In order to compare the results obtained with the second-generation formulations with those of an other model, the results obtained with the second-generations wave model Dolphin have also been plotted (courtesy to dr Booij for providing us with the data of the Dolphin model)

In *Case 18* the wind speed has been increased (U_{10}= 20 m/s), which lead to different model results (see Figures 18a to 18d). The model results, however, are comparable to those described of *Case 17*. To compare again the results obtained with the second-generation formulations, the results obtained with the second-generations wave model Dolphin have also been plotted.

Increasing the wind speed to 30 m/s also shows the same trend (see Figures 19a to 19d) as in *Case 17* and *18*. Model convergence is obtained within a few iterations. Note that the SWAN model results (in terms of H_s) using second-generation formulations are slightly higher than those of the Dolphin model.

Case 20 has been performed with the second generation mode of SWAN, but with quadruplets activated. This model leads to deviant model results for all parameters and spectra (Figures 20a to 20d). However, the overshoot for H_s is smaller than in the standard case.

Case 21 has been performed with the third generation mode of SWAN but with quadruplets deactivated. The computations for H_s, T_{m01}, DIR and DSPR develop in a different way from *Case 4*, and show that the wave spectrum does not grow. This is obviously because no energy is transferred to the lower frequencies. Computed spectra are smaller. Overshoot problems are even bigger than in the standard *Case 4*. (Figures 21a to 21d).

Case 22 has been carried out without pre-conditioner. (It is noted that to disable the first guess some small modifications to the source code of SWAN have been made. A detailed description of these modifications, however, is beyond the scope of this study.) To start the iteration process, very small waves (H_s =0.05 m, T_p= 5 s) have been used as boundary condition. Omitting the first guess affects the behaviour of the solution during the iteration process, and the positive characteristic of this behaviour is the absence of the overshoot (see Figures 22a to 22d). However, model convergence is still very slowly obtained.

In *Case 23*, implicit formulations have been used to compute Swind. This setting generates some differences in the process but the overshoot and the iteration problem are still present (Figures 23a to 23d).

Case 24 is identical to test *Case 22,* but now the incident wave spectrum has been shifted to the lower frequencies (T_p = 12 s). It is also carried out without the pre-conditioner (i.e. first-guess). This again affects the iteration behaviour, but it takes many iteration steps before the solution is reached (Figures 24a to 24d).

The model settings of *Case 25* (with the limiter = 30%) yield, like in *Case 22* and *24*, different results than the standard case but this has not the wanted effect on the iteration behaviour (Figures 25a to 25d).

In *Case 26* the effect of incident swell on wave growth and the model convergence behaviour is investigated. The results are not fundamentally different from those of *Case 4*, although an extra problem is introduced (in the wave energy spectrum for x = 0) and the H_s converges without overshoot (Figures 26a to 26d). Note that the results of *Case 4* have also been plotted (*Case 4*: no swell, 50 iterations).

In *Case 27*, the computation has been started with an enhanced first-guess (by adapting the coefficients of the second-generation formulations of SWAN). This does not affect the solution itself (Figures 27a to 27d), but it does diminish the number of iterations required for convergence.

The coefficient λ for the quadruplets has been changed into 0.1 in *Case 28*. The model convergence behaviour is affected by this change (Figures 28a to 28d); and it is seen from the figures that no wave growth is obtained. This is presumably due to the modified configuration of the quadruplet interactions. Note that by changing λ, the directional width of the spectrum has decreased and that it is now in better agreement with observations (about 30°).

In *Case 29,* the coefficient of S_{nl4} has been changed as well. This time, the model converges slightly better than in the standard case (the overshoot is less pronounced), but the final solutions for H_s and for DSPR are significantly different (Figures 29a to 29d).

For *Case 30* (Figures 30a to 30d), the same comment can be given as for *Case 28.*

The wind speed and direction have been adapted in *Case 31*; this results into unexpected solutions for all parameters and spectra (Figures 31a to 31d). It is not known why the SWAN model shows this observed behaviour and it should therefore be investigated in more detail. Such an investigation, however, is beyond the scope of this study.

In *Case 32*, the frequency range has been adapted. It is seen from the figures (Figures 32a to 32d) that the overshoot is gone and that model convergence is obtained within a few iterations only. Note, however, that with the selected frequency range, initial wave growth at short fetches is not well resolved.

The adapted limiter in *Case 33* causes a very slow convergence behaviour, but the overshoot is not present in this case (Figures 33a to 33d).

Case 34 has been computed with the use of a self scaling cut-off frequency (see WL | DELFT HYDRAULICS, 1999). The results look promising (see Figures 34a to 34d) since the overshoot is not present. However, the location of the cut-off frequency is located rather close to the peak of the spectrum and the results should be considered with some care.

In *case 35* again the limiter has been set on a different value (limiter = 40%). Although this does affect the model results, the overshoot remains present in the iteration process of the H_s (Figures 35a to 35d).

In *Case 36*, the frequency distribution of the limiter has been adapted. The limiter has been set equal to: limiter = limiter $\times$ (f/f_m). By this adaptation, the limiter is less effective at the lower frequencies and allows a larger change in energy density per iteration step at the higher frequencies. It can be seen that the effect of an adapted limiter speeds up the convergence process (Figures 36a to 36d). The overshoot has almost disappeared.

Therefore, in *Case 37*, again this strategy has been followed; this time, the limiter has been taken as a function of $(f/f_m)^2$. The iteration process has converged after 14 iterations, instead of after 35 iterations, without overshoot (Figures 37a to 37d). Note that the mean wave direction starts to oscillate.

Case 38 has been performed with a limiter that is a function of $(f/f_m)^3$. This introduces different strange solution values for all parameters, and the convergence is slower than in *Case 37* (Figures 38a to 38d).

The limiter has got the form of a function of (f_m/f) in *Case 39.* In this case, the convergence behaviour of the model does not show improvement with respect to *Case 4* (Figures 39a to 39d).

The same holds true for the results in *Case 40* (Figures 40a to 40d). These have been generated using a limiter of the form of a function of $(f_m/f)^2$.

Another case has been carried out using the limiter of the form used in *Case 37*: *Case 41.* In *Case 41*, the effect of the $(f/f_m)^2$ distribution of the limiter has been investigated for $U_{10} = 10$ m/s. The results are promising again, this time computed with a lower wind speed (Figures 41a to 41d). The mean wave direction oscillates; the wave spectrum gets a different form, and although an overshoot is present, convergence is reached after 16 iteration steps.

For a wind speed of 20 m/s, *Case 42* shows very convincing results using the same limiter as in *Case 41* (Figures 42a to 42d). Although the mean wave direction oscillates, the overshoot has diminished and convergence is reached after 16 iterations.

Case 43 has been performed using the same limiter as *Case 36* (f/f_m), with adapted wind speed. The quality of the results is the same as in that case (Figures 43a to 43d).

Case 44 has been based on the same limiter as *Cases 36* and *43* (f/f_m), with another wind speed again. Without question, the improvement of the results is due to the adapted limiter (Figures 44a to 44d).

3 Conclusions and recommendations

3.1 Conclusions

The following conclusions can be drawn from this study:

- the SWAN model converges in all the cases presented in this study (except Case 20, which was unstable), however, the way it converges in all cases is very different;
- if a good estimate of the energy spectrum in the first iteration step is given (i.e. first guess), the model converges faster;
- SWAN with second-generation formulations for the physical processes converges within 3 iterations;
- the standard SWAN computations clearly show an overshoot in the significant wave height (H_s) as a function of the iteration level, which is more pronounced for lower than for higher wind speeds (see Figures 14d, 15d and 16d). The absolute and relative value of the computed overshoot in significant wave height at x = 12.5 km, for a wind speed of 10 m/s, 20 m/s and 30 m/s, are respectively:

U_{10} (m/s)	$H_{s,50\ iters}$ (m)	$H_{s,max}$ (m)	ΔH_s (=$H_{s,max}$ - $H_{s,50\ iters}$) (m)	$\Delta H_s/H_{s,50\ iters}$ (-)
10	0.71	0.90	0.19	27%
20	1.80	2.14	0.34	19%
30	3.11	3.44	0.33	11%

- the limiter and the distribution of the limiter largely affect the model convergence (but not the final solution). Releasing the limiter (with the standard distribution along the frequencies) increases the observed overshoot and vice versa;
- it seems that the formulations of the quadruplets and the subsequent limiter that needs to be applied, are responsible for the observed convergence problems. On the basis of the results presented in Figures 36a to 36d and Figures 37a to 37d, we speculate that the suppression of the change of energy at the higher frequencies per iteration is responsible for these problems;
- the directional distribution of the energy spectra is too large (40°). Changing the value of coefficient λ resulted in a better estimate of the directional energy distribution;
- the results of *Case 31*, in which the wind direction is not taken parallel with that of the computational grid showed some unexpected model behaviour.

3.2 Recommendations

On the basis of the results presented in this study it is recommended:

- to improve the first-guess in SWAN in such a way, that the estimate of the wave spectrum in the first iteration step is in better agreement with the one computed by SWAN in the third-generation mode;
- to investigate the effect of an adapted limiter (using a different distribution over frequencies) on wave growth in idealised fetch-limited conditions and in complex field cases (e.g. Westerschelde);
- to increase the default value (equal 6) of the maximum number of performed iterations;
- to investigate the observed unexpected model behaviour in case of a wind direction that is not parallel with that of the computational grid;
- to study the effect of different coefficient values for λ in the source term of S_{nl4} on wave growth or to investigate to possibility to add one extra quadruplet to SWAN (personal communication with dr G. van Vledder, 1999).

References

Booij, N. R.C. Ris and L.H. Holthuijsen, 1998: A third generation wave model for coastal regions. Part I: Model description and validation, *J. Geoph. Research*, in press

Forristall, G.Z. and K.C. Ewans, 1998: Worldwide measurements of directional wave spectra. *J. of Atmosphere and oceanic technology*, Vol. 15, 440-469

Ris, R.C., 1997: Spectral modelling of wind waves in coastal areas, Ph.D.-dissertation, Delft University of Technology, Department of Civil Engineering, The Netherlands

Ris, R.C., N. Booij, L.H. Holthuijsen and R. Padilla-Hernandez, 1997: User manual for the program SWAN Cycle 2

WL | DELFT HYDRAULICS, 1998: Validation of wave propagation on curvilinear grids in SWAN, N. Doorn and R.C. Ris, Report 3306.20, the Netherlands

WL | DELFT HYDRAULICS, 1999: Effects of a self-scaling cut-off frequency on wave growth in SWAN, R.C. Ris and K.J.Bos, Report 3396, the Netherlands

Figures

12-01-1999

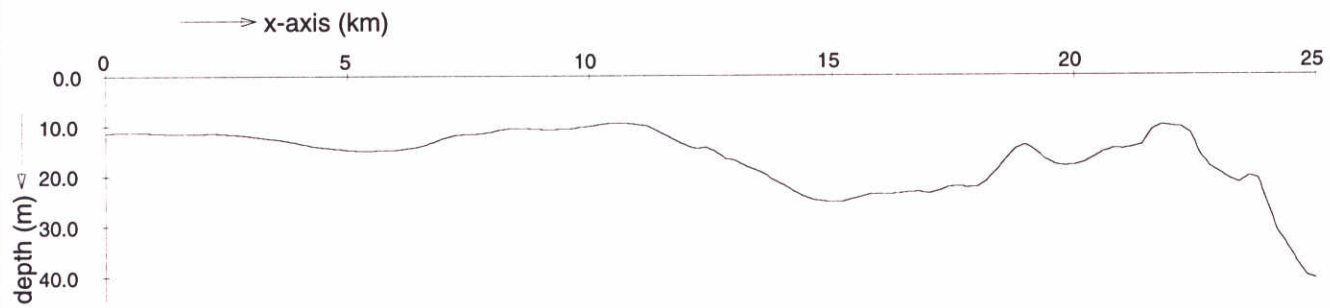

Bathymetry along a curve in the outer region of the Westerschelde estuary for which the one-dimensional SWAN computations are performed (test cases 1, 2 and 3).	SWAN	
WL | delft hydraulics	H3496	Fig. 0

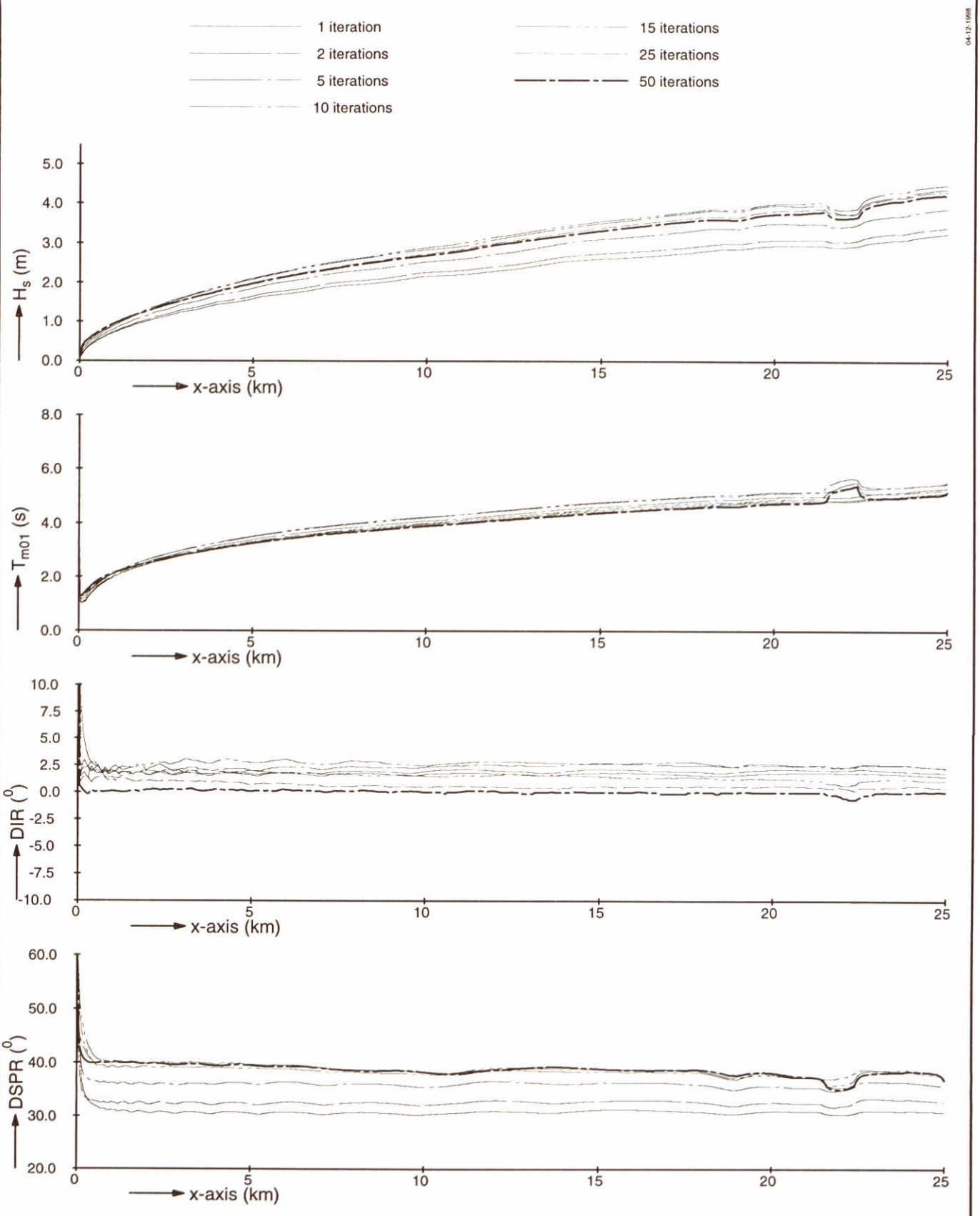

Model convergence behaviour using third-generation formulations Standard computation Bathymetry of Westerschelde	SWAN-1D	U_{10}=30 m/s
WL | delft hydraulics	H3496	Fig. 1a

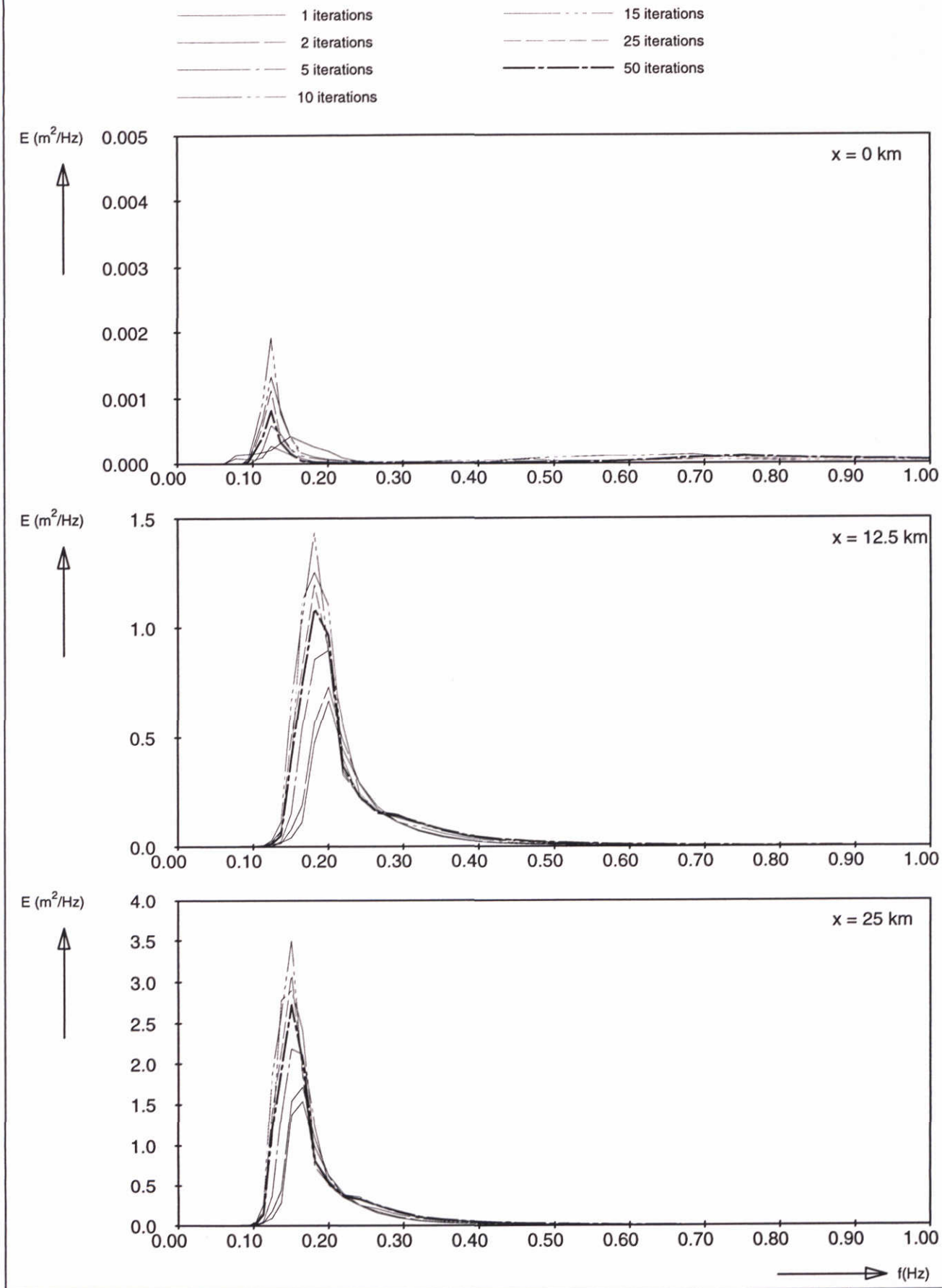

Frequency spectra at 3 locations Standard computation Bathymetry of Westerschelde	SWAN-1D	U_{10}=30 m/s
WL | delft hydraulics	H3496	Fig. 1b

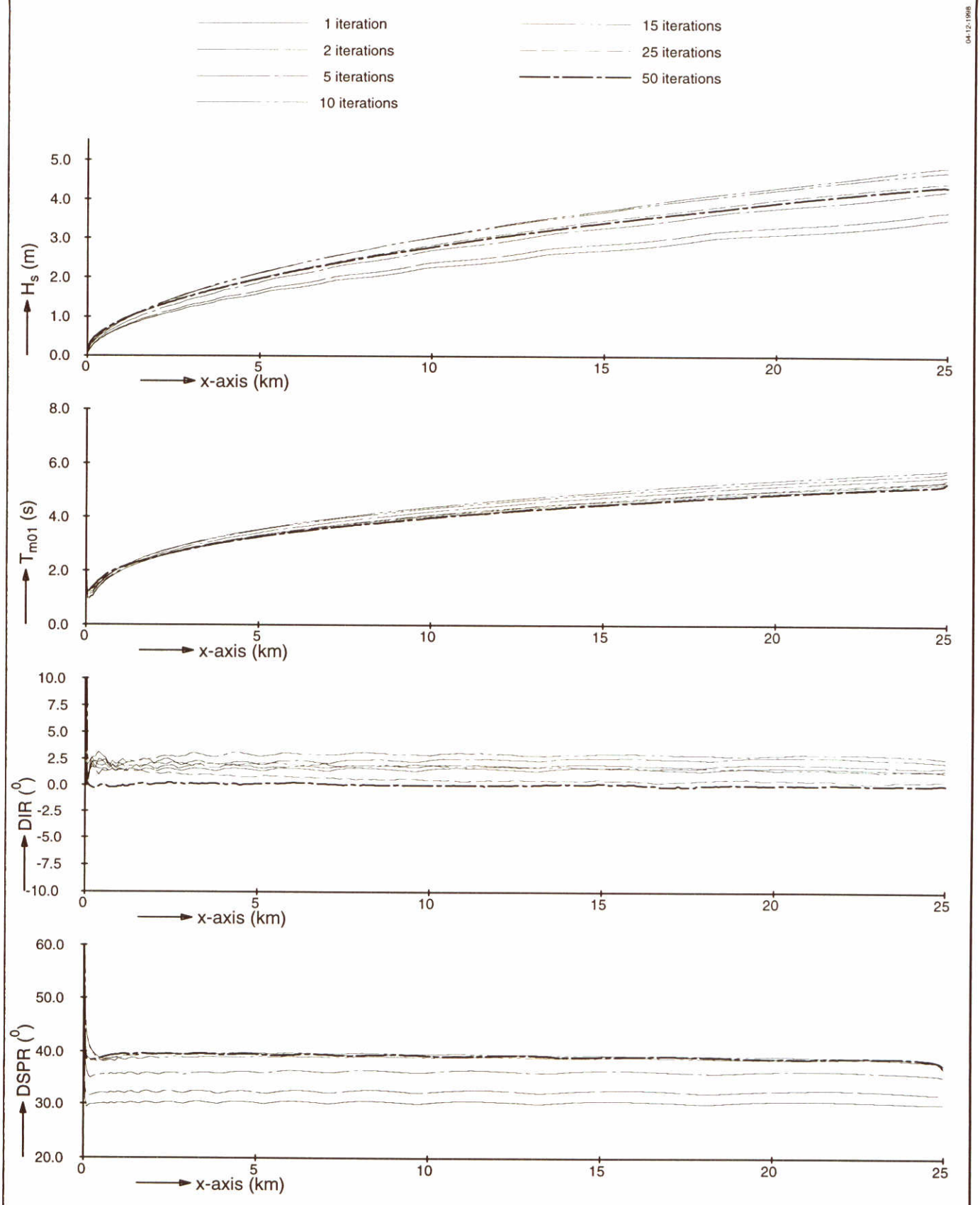

Model convergence behaviour using third-generation formulations Standard computations Bathymetry of Westerschelde: depth * 1.e10	SWAN-1D	U_{10}=30 m/s
WL | delft hydraulics	H3496	Fig. 2a

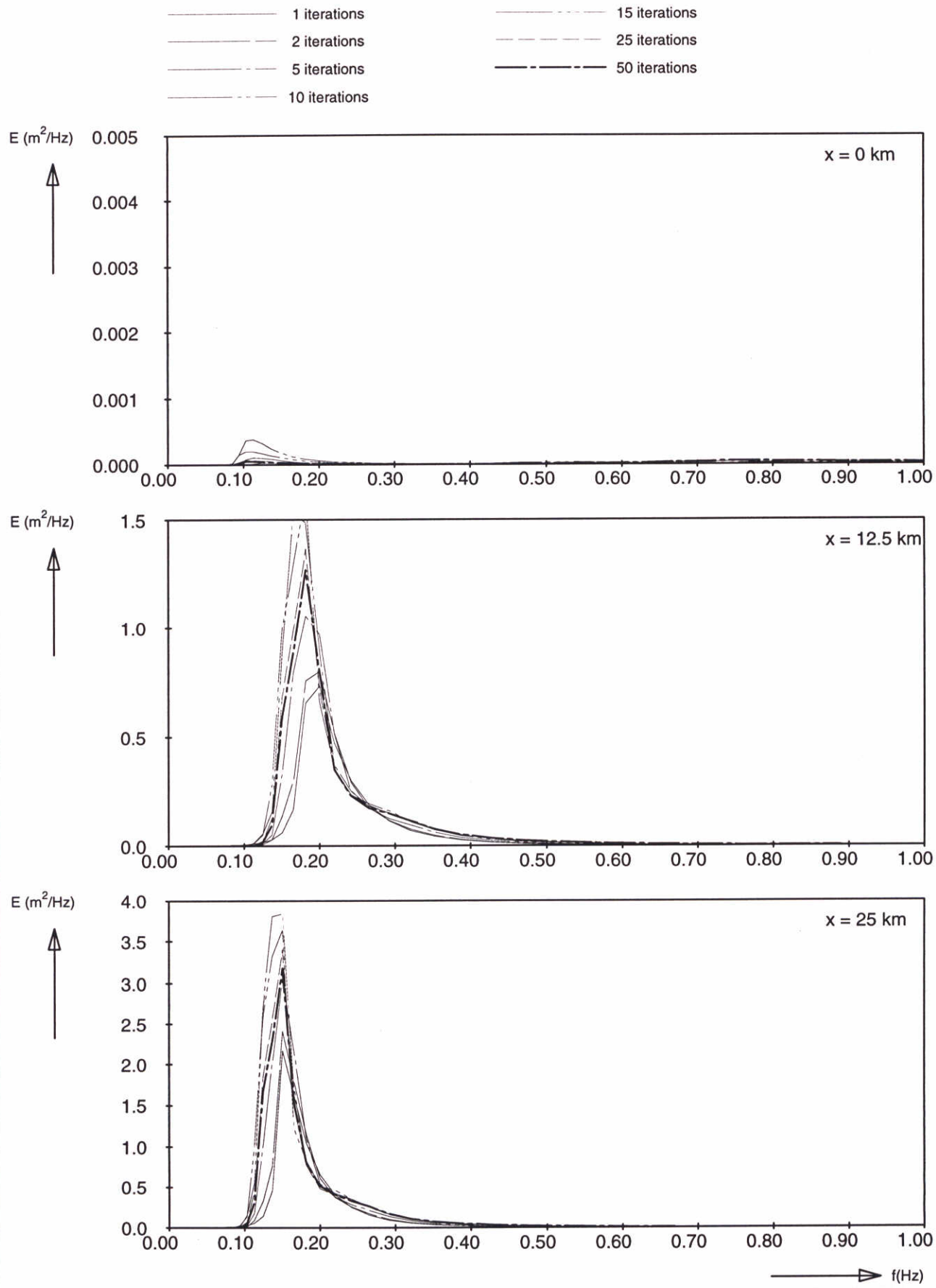

Frequency spectra at 3 locations Standard computation Bathymetry of Westerschelde: depth * 1.e10	SWAN-1D	U_{10}=30 m/s
WL | delft hydraulics	H3496	Fig. 2b

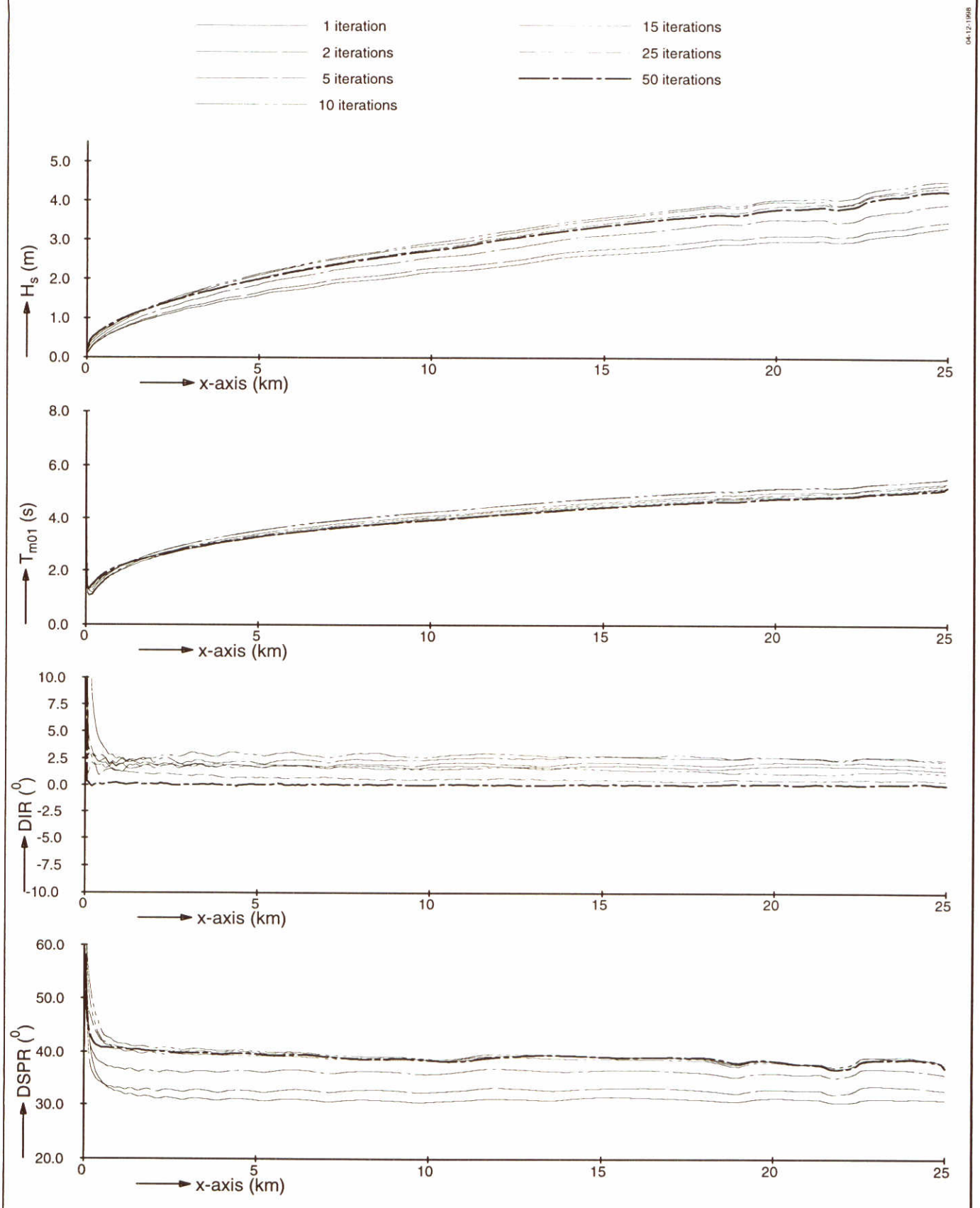

Model convergence behaviour using third-generation formulations Standard computation, bathymetry of Westerschelde Deactivated : BREAK, TRIAD and FRIC	SWAN-1D	U_{10}=30 m/s
WL | delft hydraulics	H3496	Fig. 3a

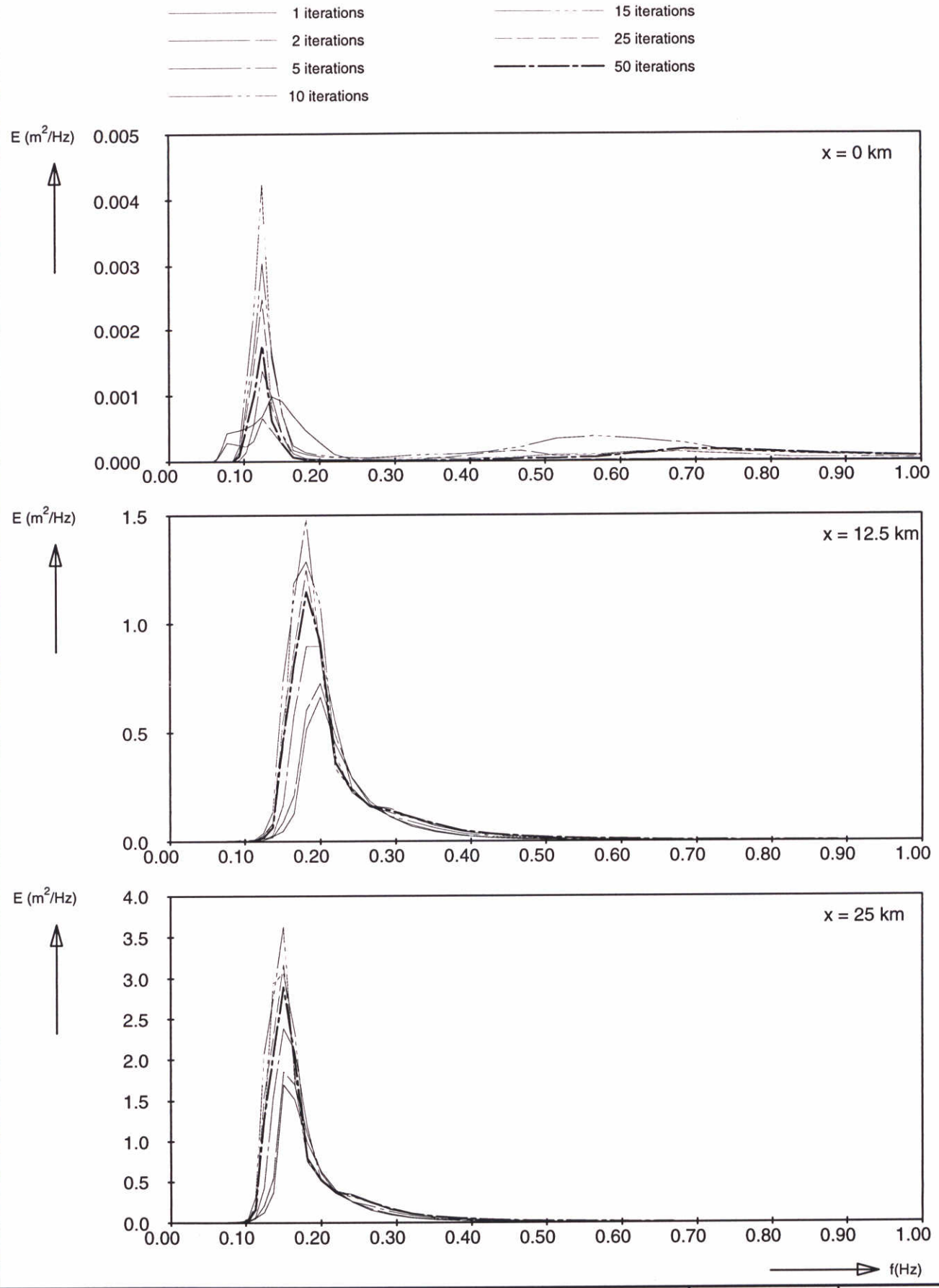

Frequency spectra at 3 locations Standard computation, bathymetry of Westerschelde Deactivated : BREAK, TRIAD and FRIC	SWAN-1D	U_{10}=30 m/s
WL | delft hydraulics	H3496	Fig. 3b

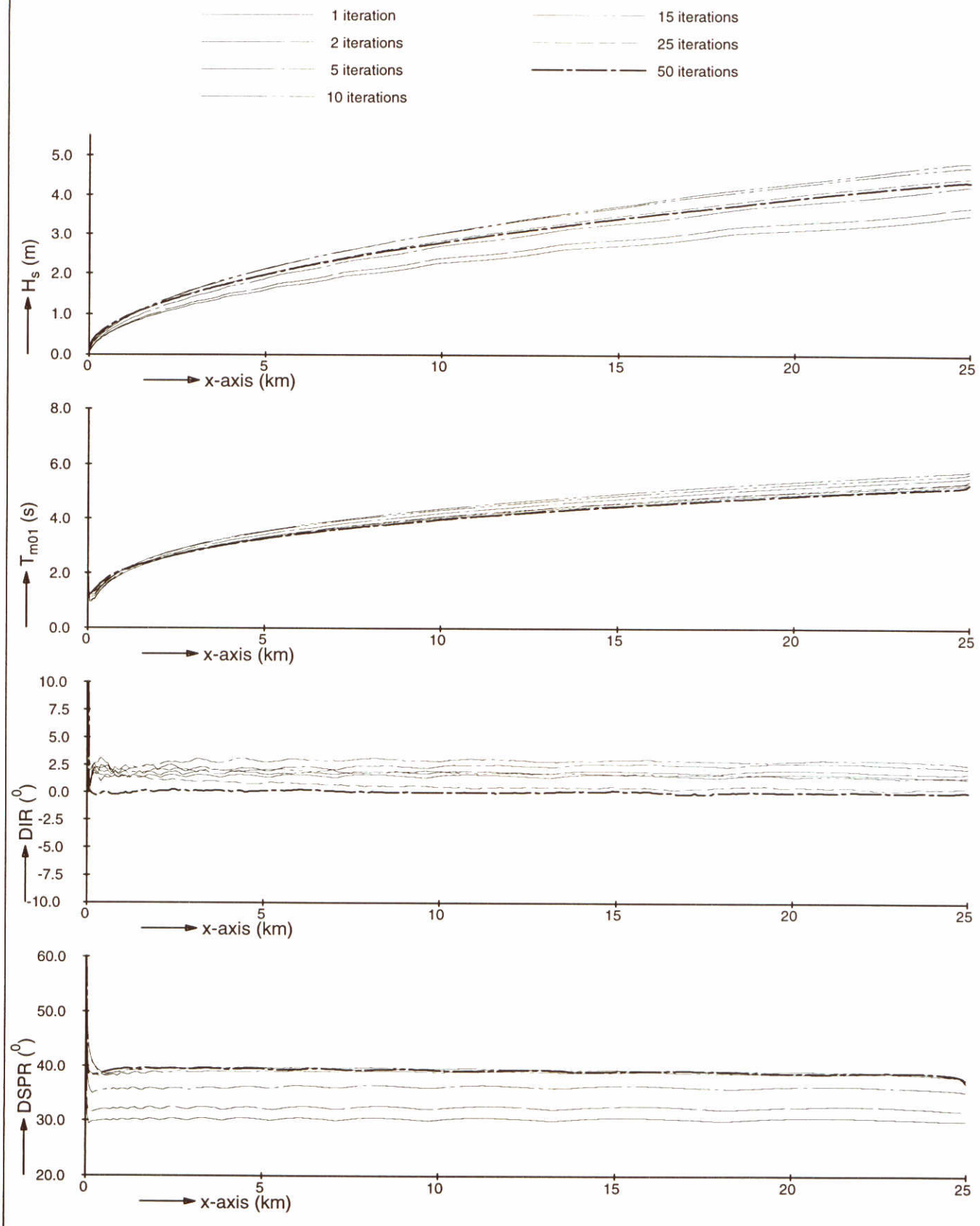

Model convergence behaviour using third-generation formulations
Standard computations (constant depth, deep water)

SWAN-1D

U_{10}=30 m/s

WL | delft hydraulics

H3496

Fig. 4a

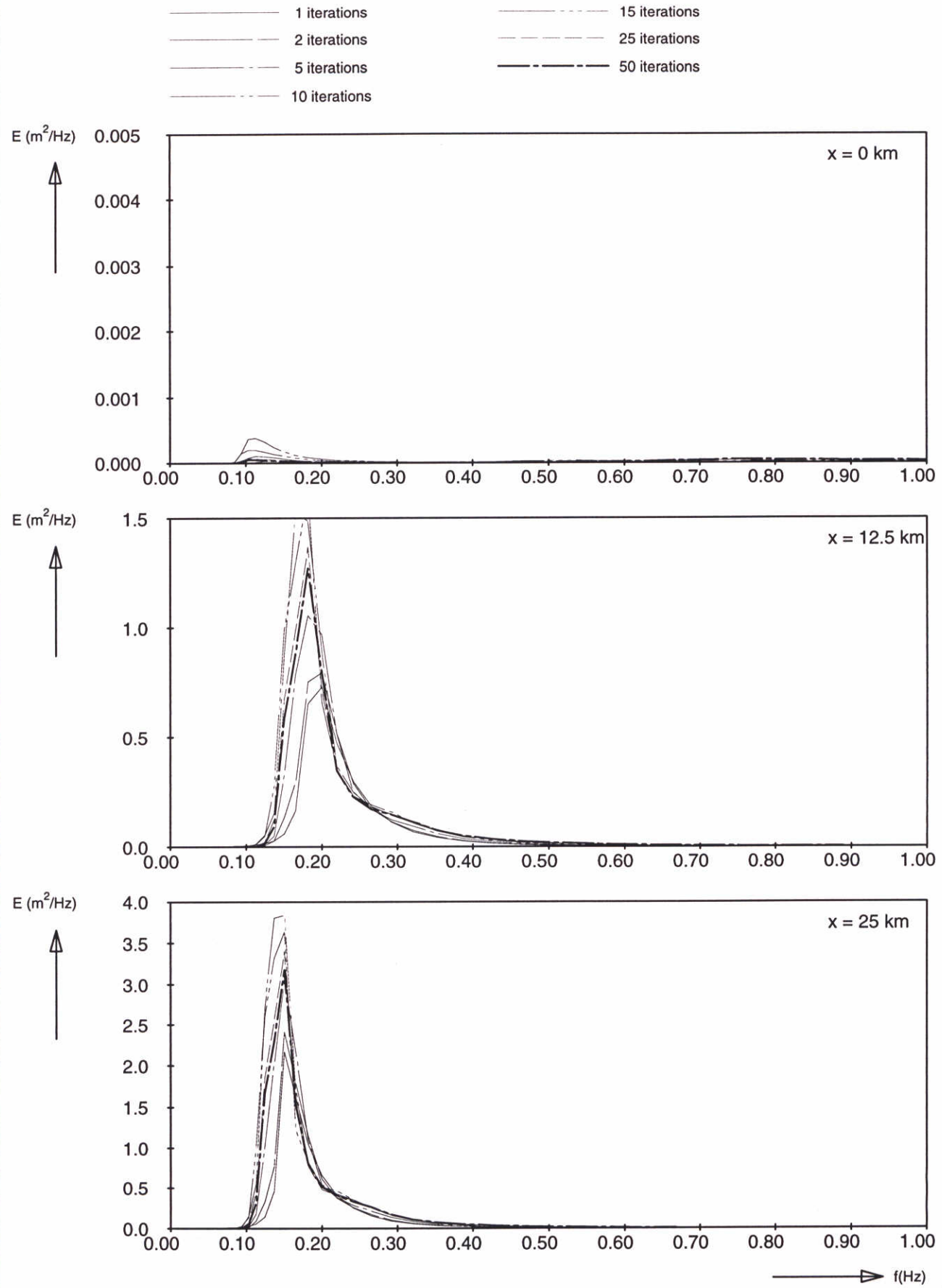

Frequency spectra at 3 locations Standard computations (constant depth, deep water)	SWAN-1D	U_{10}=30 m/s
WL | delft hydraulics	H3496	Fig. 4b

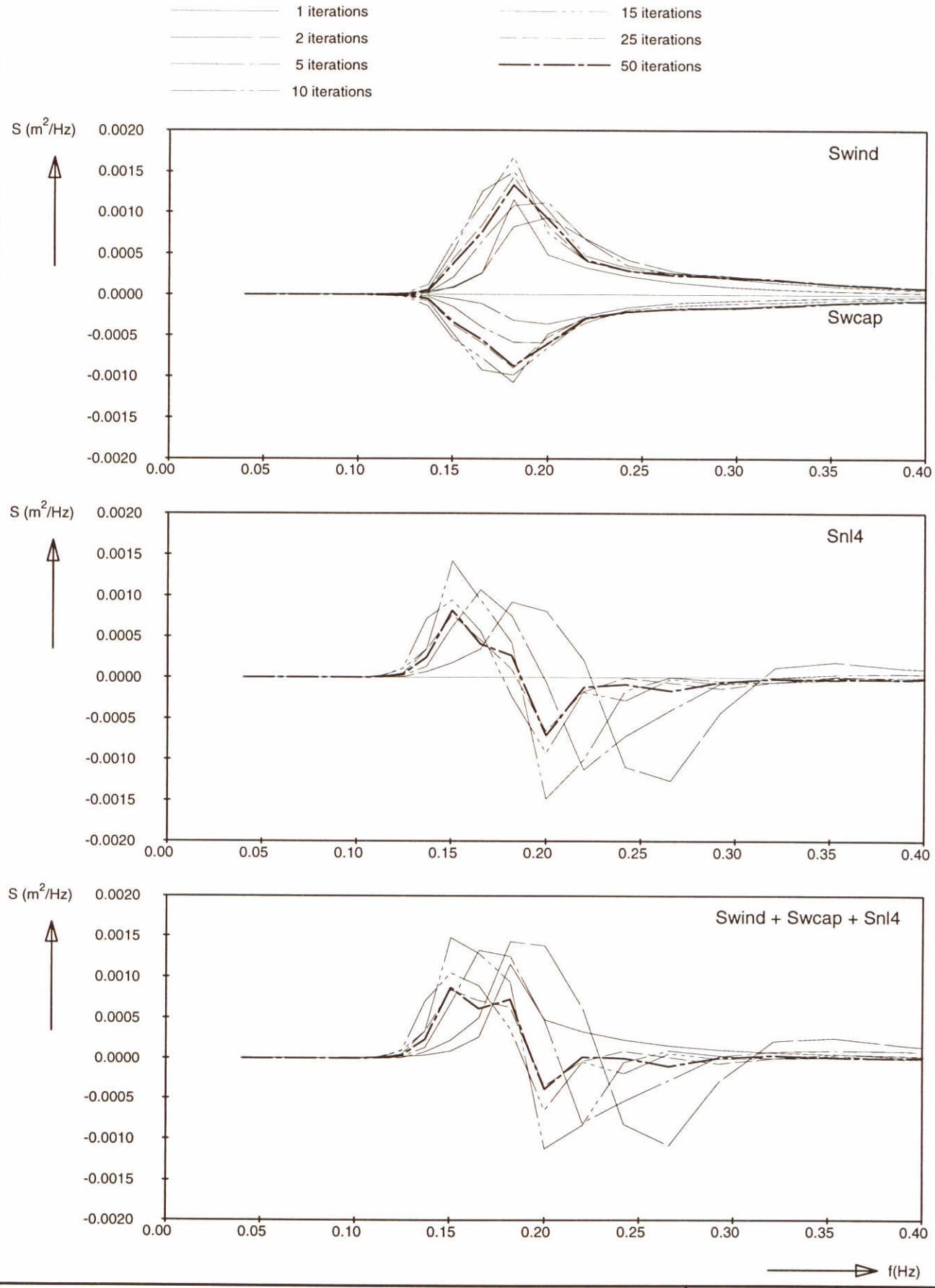

Source terms at x = 12.5 km Standard computations (constant depth, deep water)	SWAN-1D	U_{10}=30 m/s
WL | delft hydraulics	H3496	Fig. 4c

Significant wave height at 12.5 km Standard computations (constant depth, deep water)	SWAN-1D	U_{10}=30 m/s
WL | delft hydraulics	H3496	Fig. 4d

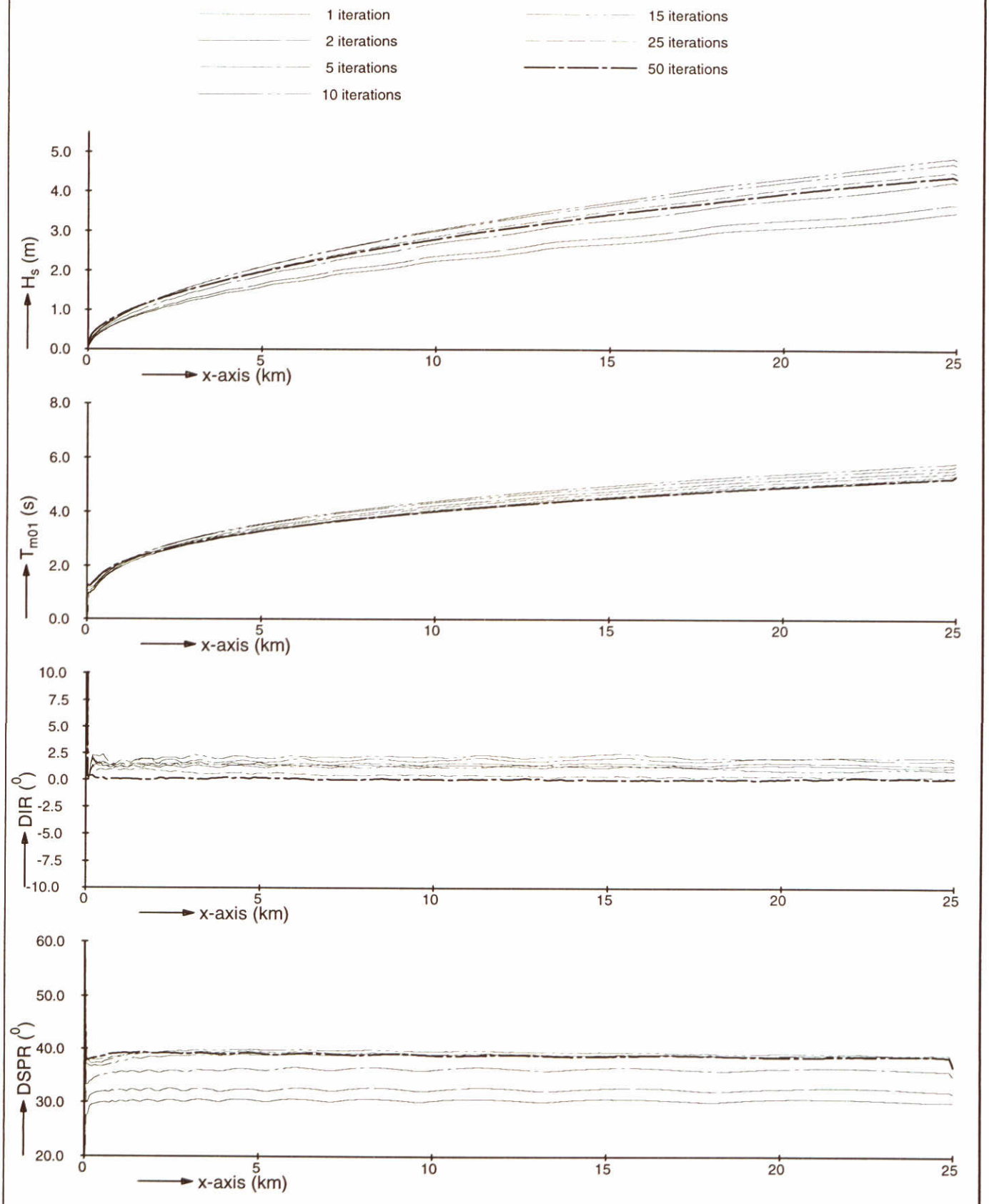

Model convergence behaviour using third-generation formulations
Adapted directional sector
dir1 = -90°, dir2 = +90°

SWAN-1D

U_{10}=30 m/s

WL | delft hydraulics

H3496

Fig. 5a

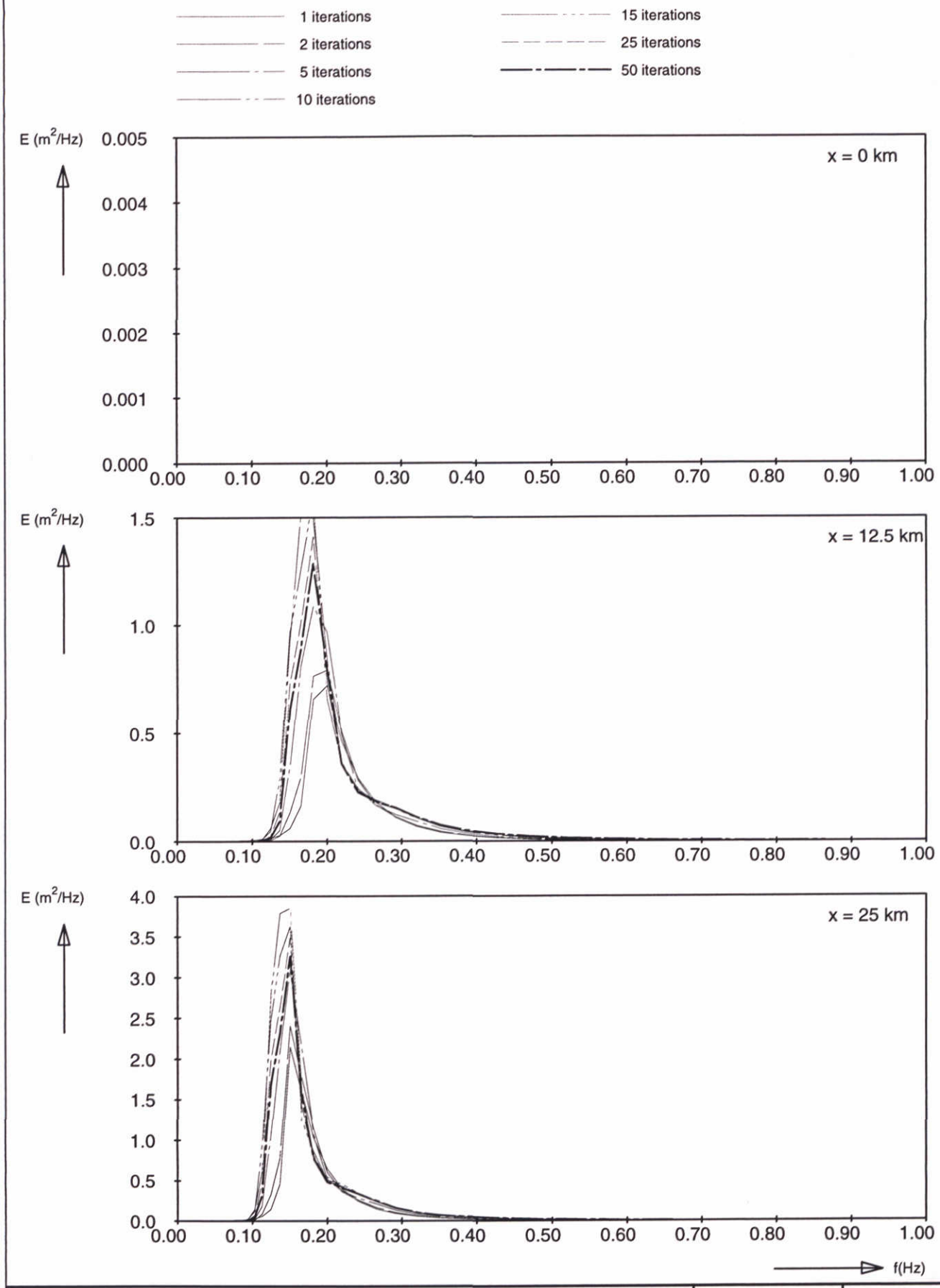

Frequency spectra at 3 locations Adapted directional sector dir1 = -90°, dir2 = +90°	SWAN-1D	U_{10}=30 m/s
WL | delft hydraulics	H3496	Fig. 5b

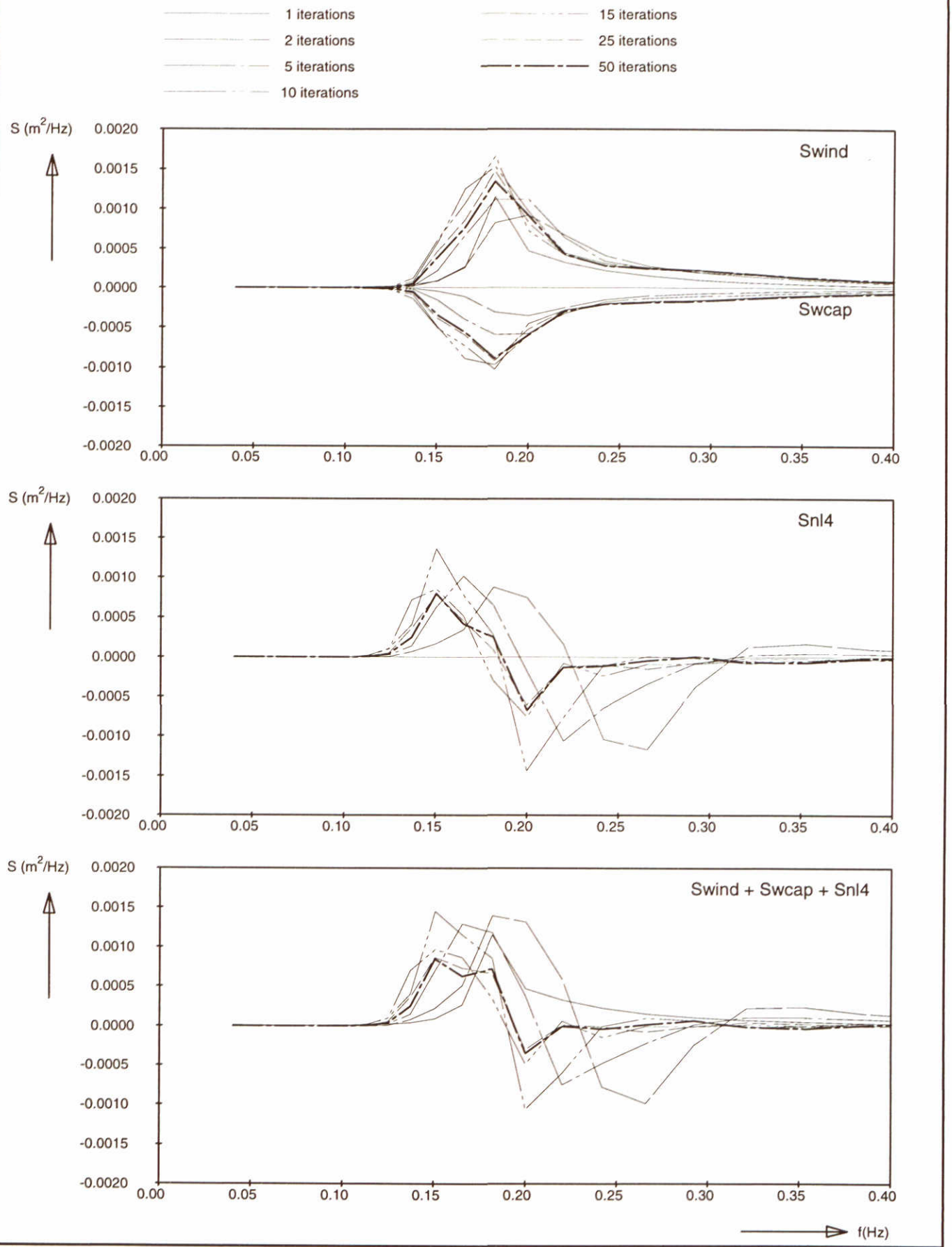

Source terms at x = 12.5 km Adapted directional sector dir1 = -90°, dir2 = +90°	SWAN-1D	U_{10}=30 m/s
WL | delft hydraulics	H3496	Fig. 5c

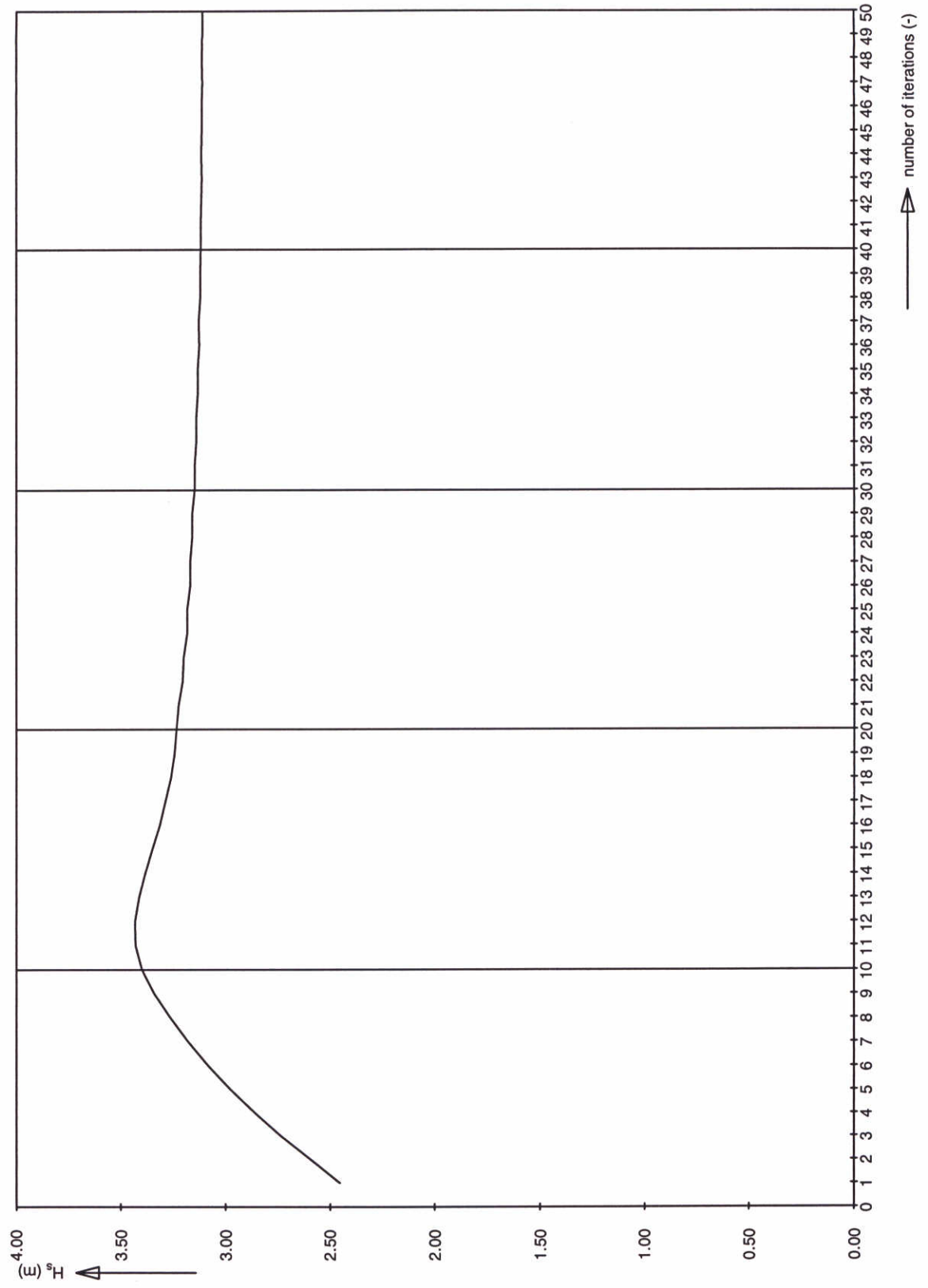

Significant wave height at 12.5 km Adapted directional sector dir1 = -90°, dir2 = +90°	SWAN-1D	U_{10}=30 m/s
WL | delft hydraulics	H3496	Fig. 5d

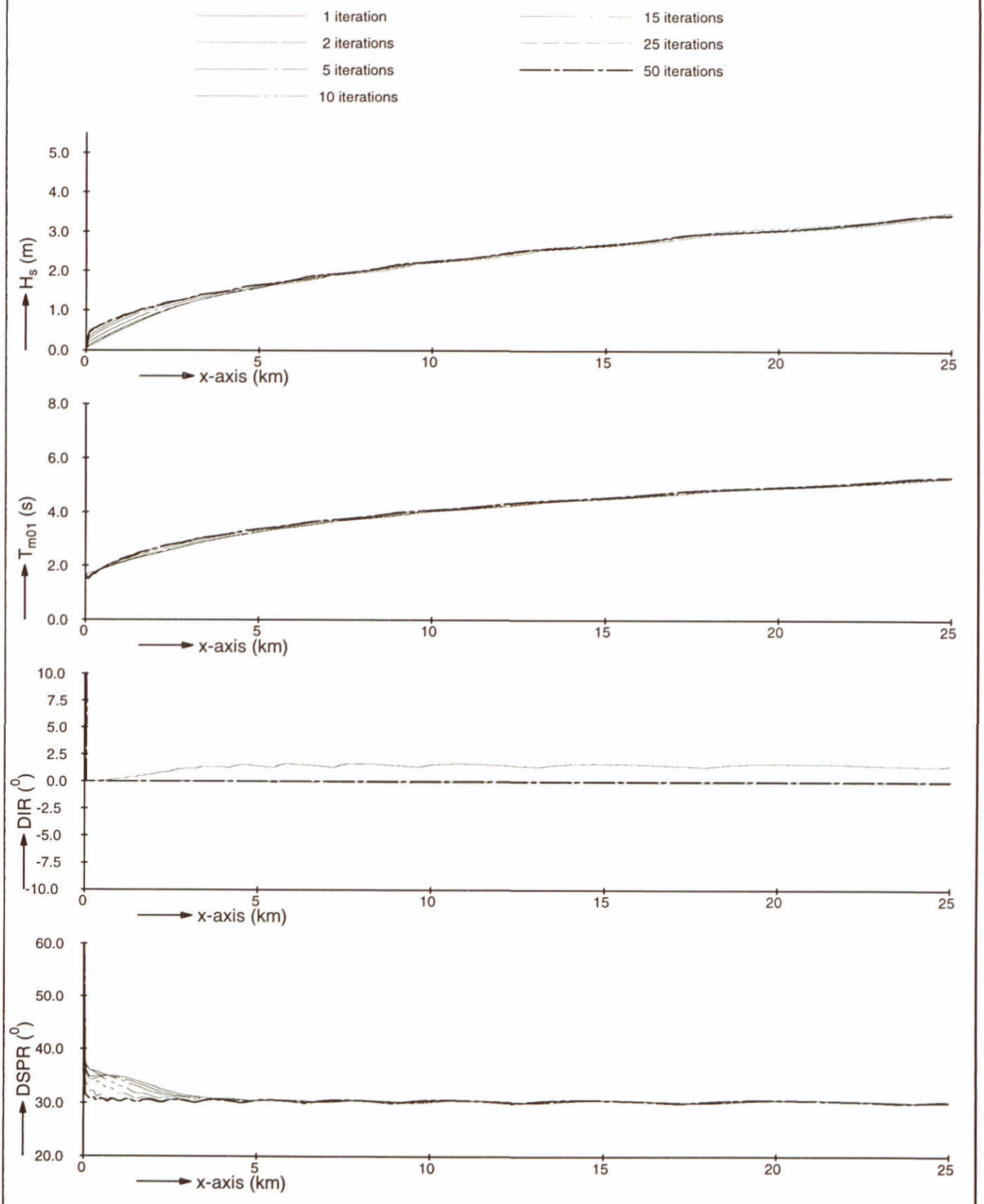

Model convergence behaviour using second-generation formulations
Deactivated: limiter

SWAN-1D

U_{10}=30 m/s

WL | delft hydraulics

H3496

Fig. 6a

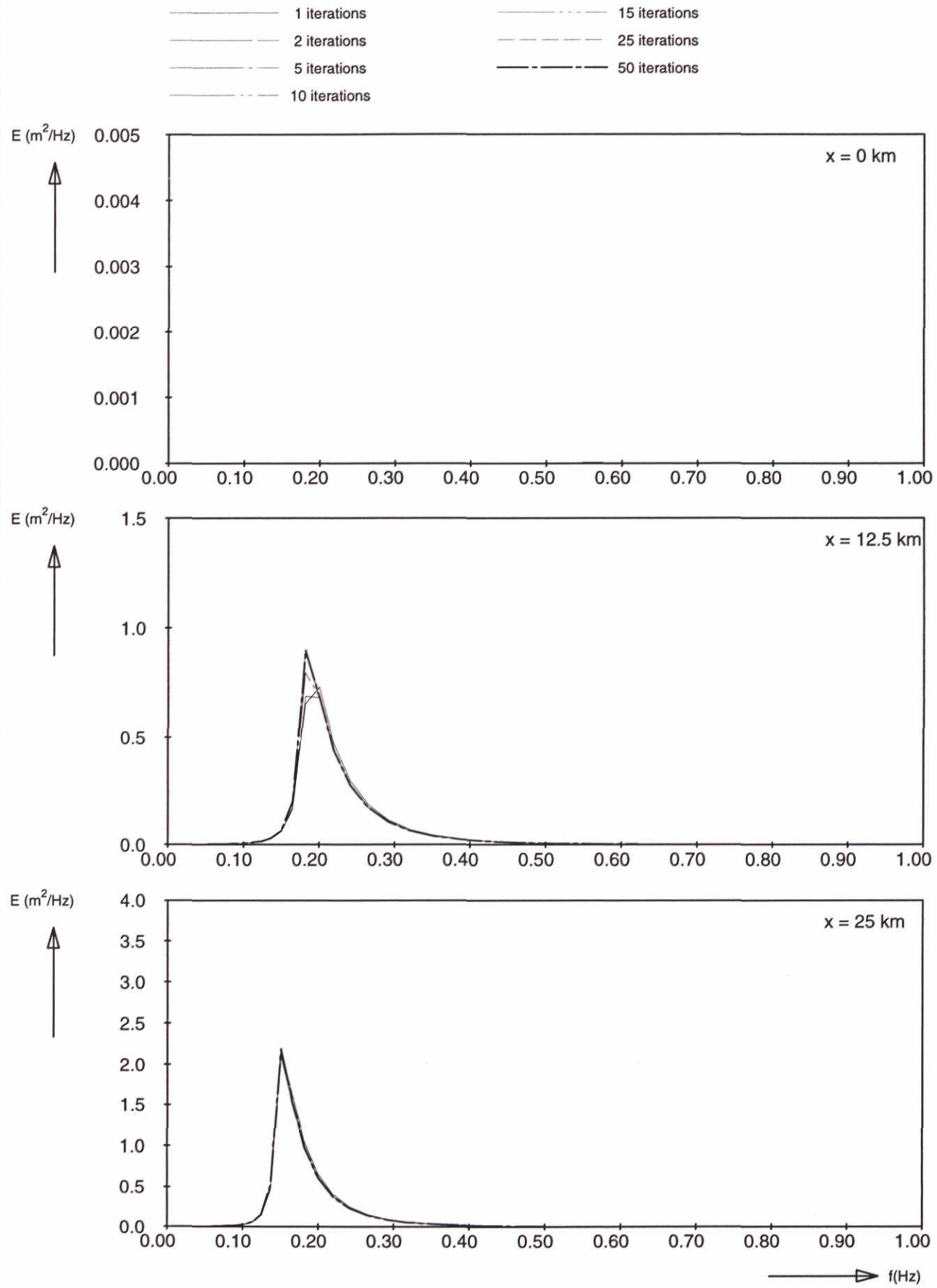

Frequency spectra at 3 locations Deactivated: limiter	SWAN-1D	U_{10}=30 m/s
WL | delft hydraulics	H3496	Fig. 6b

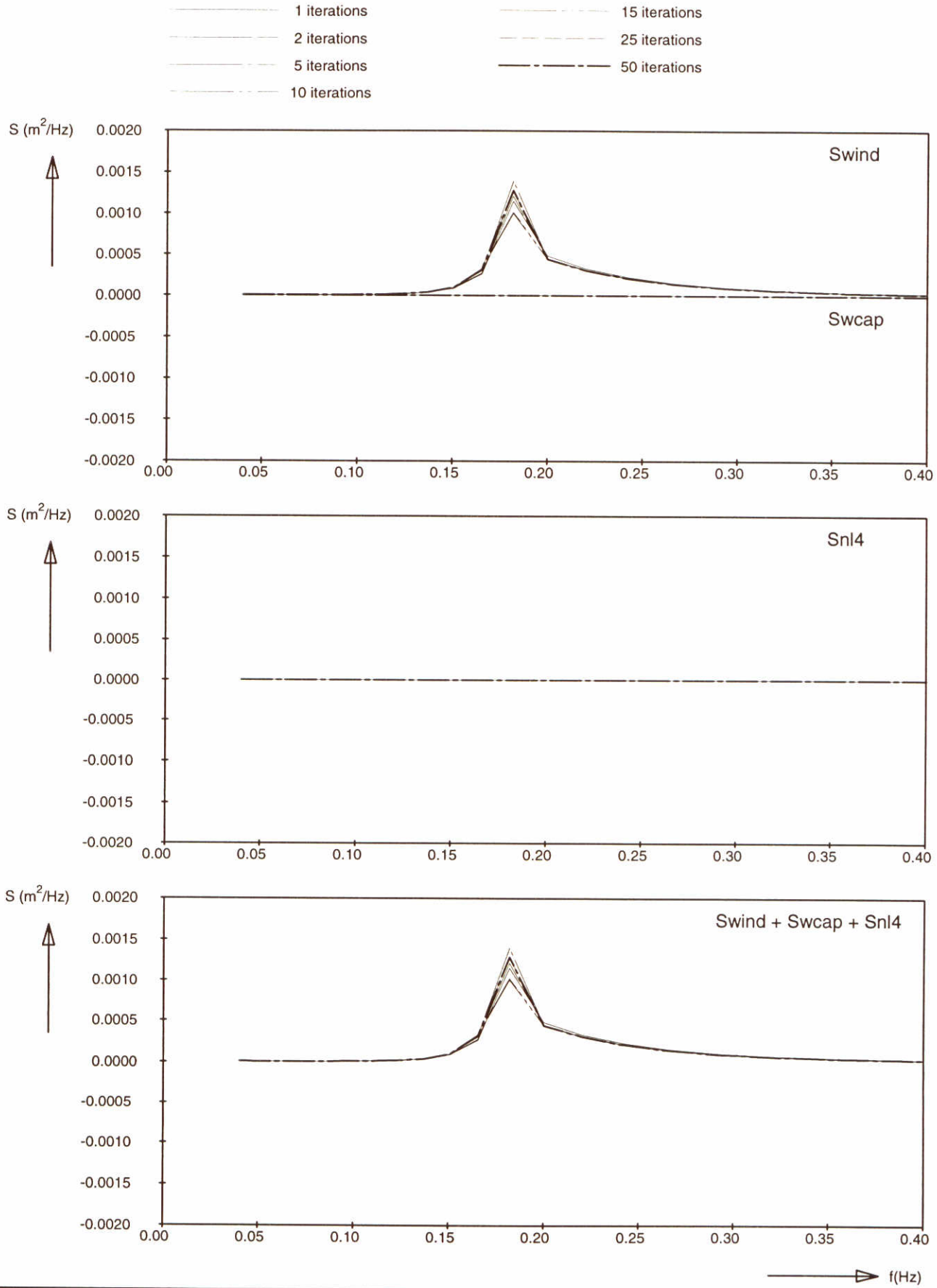

Source terms at x = 12.5 km
Deactivated: limiter

SWAN-1D

U_{10}=30 m/s

WL | delft hydraulics

H3496

Fig. 6c

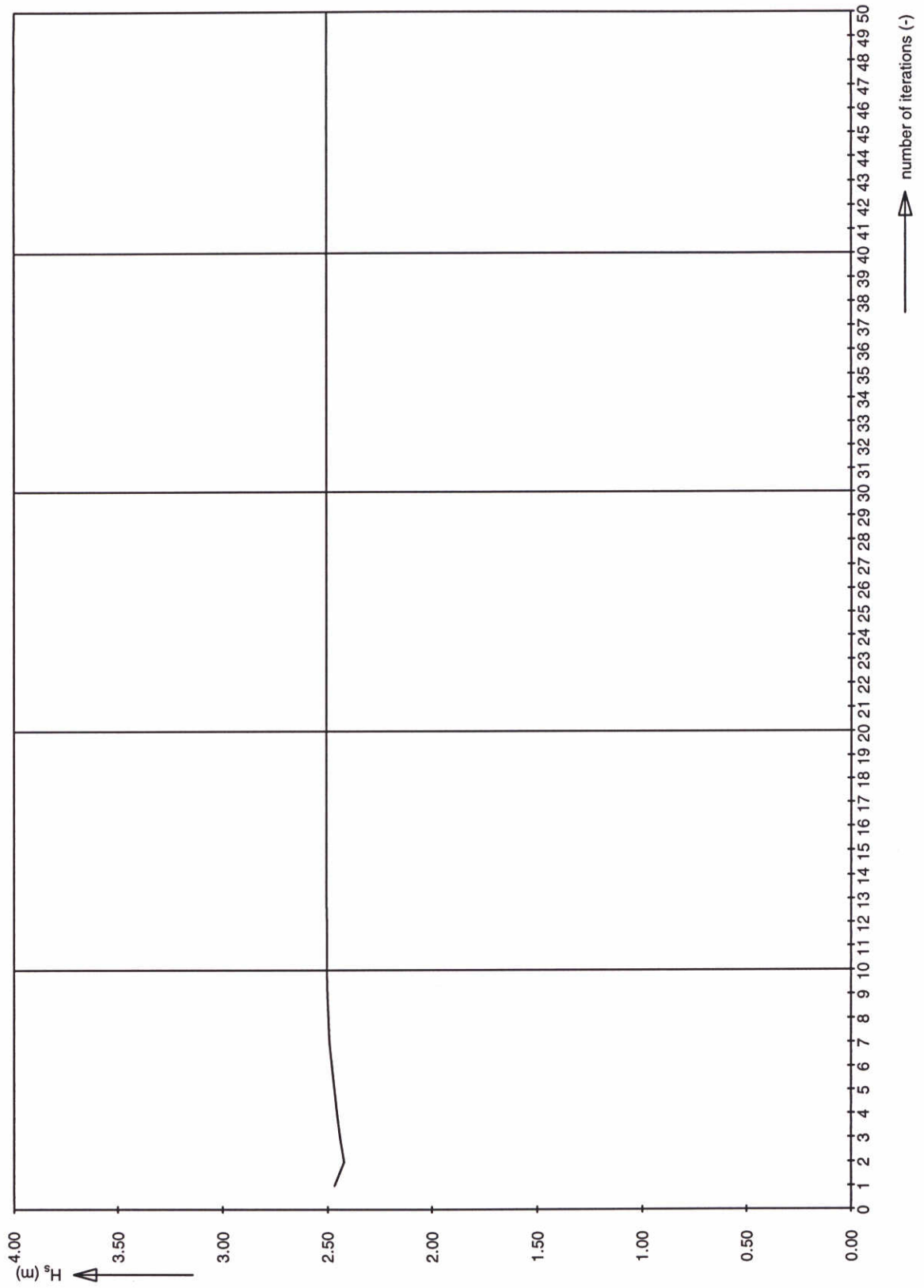

Significant wave height at 12.5 km Deactivated: limiter	SWAN-1D	U_{10}=30 m/s
WL | delft hydraulics	H3496	Fig. 6d

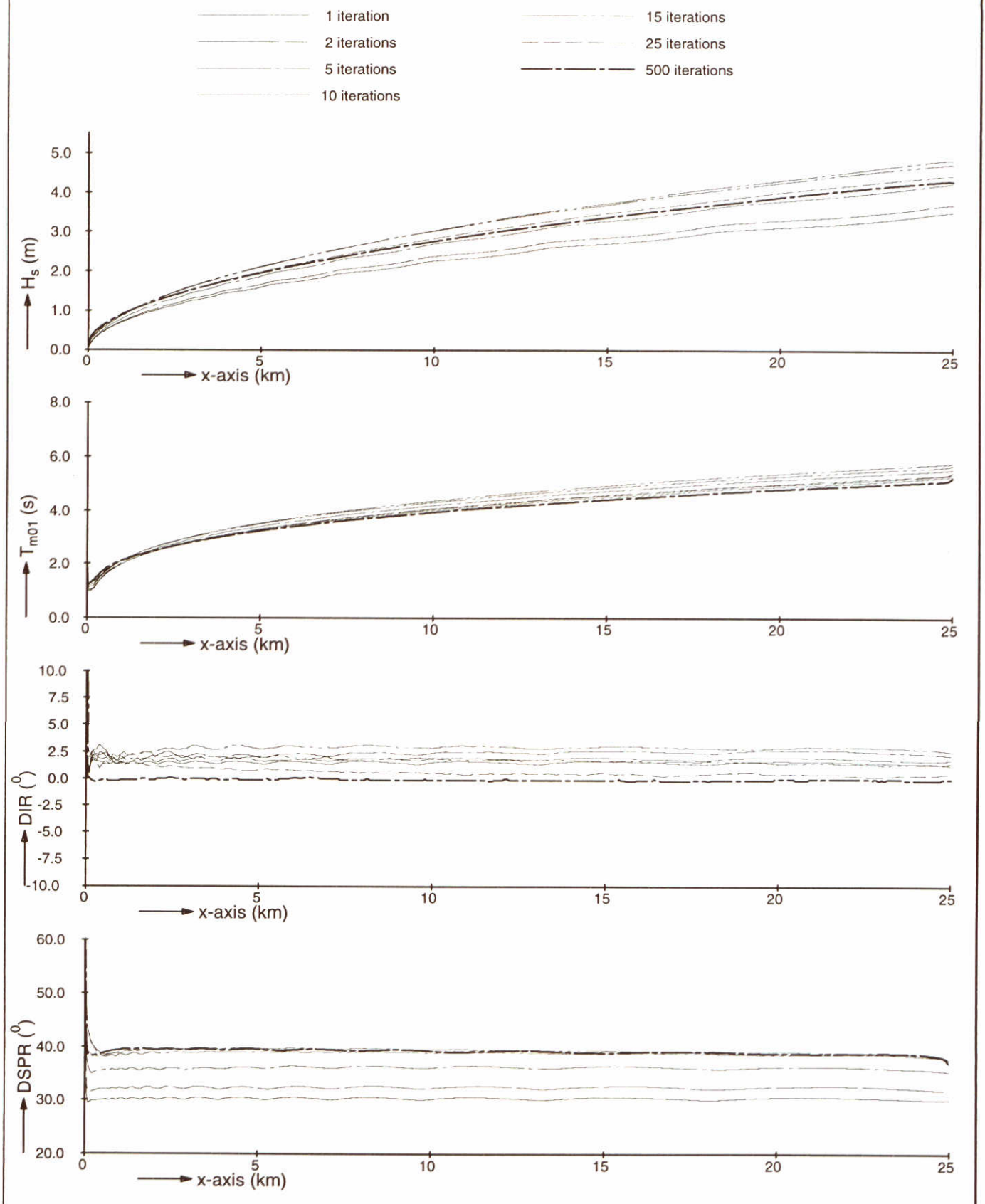

Model convergence behaviour using third-generation formulations
Adapted number of maximum iterations
Maximum number equal 500

SWAN-1D

U_{10}=30 m/s

WL | delft hydraulics

H3496

Fig. 7a

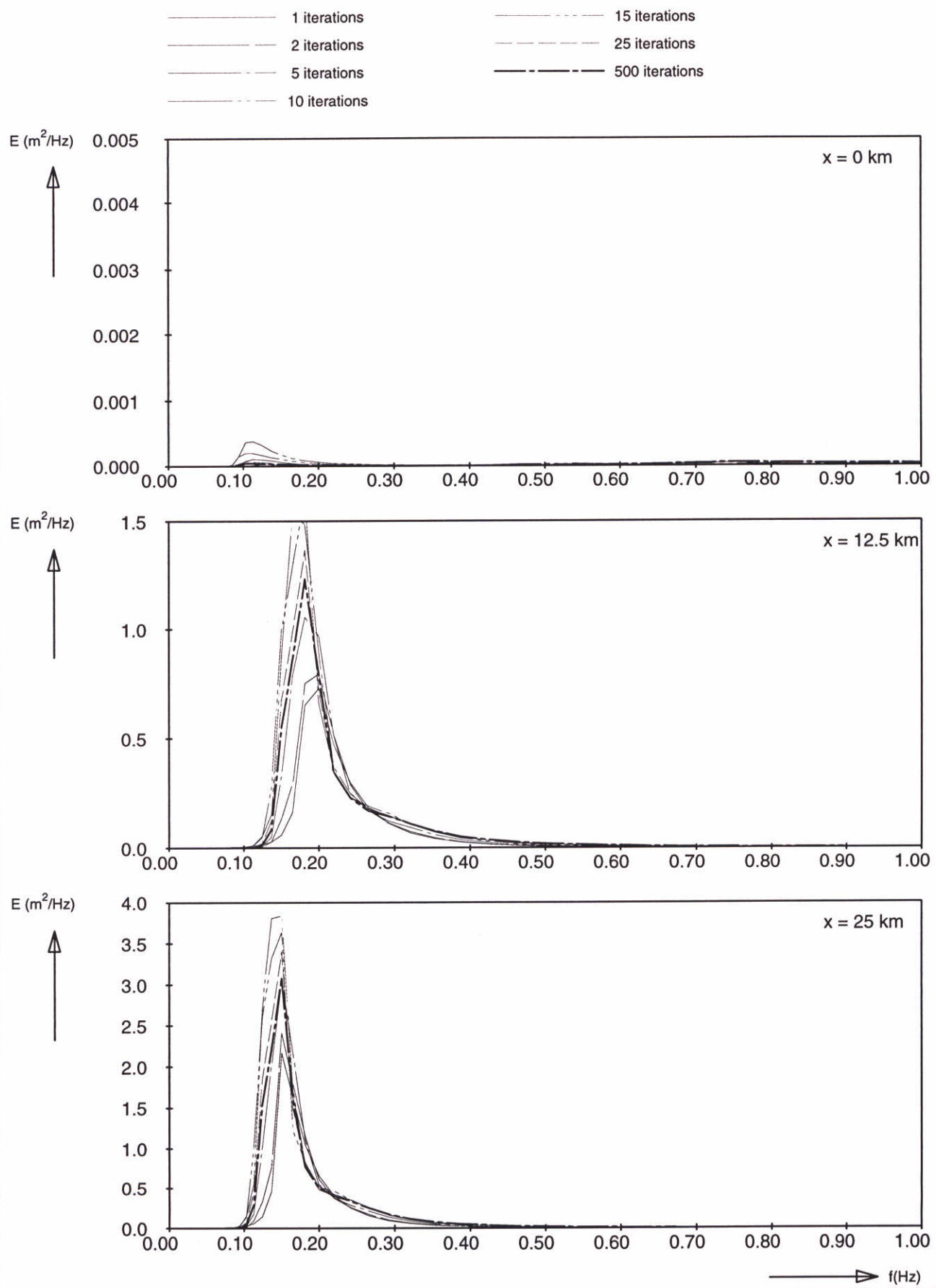

Frequency spectra at 3 locations Adapted number of maximum iterations Maximum number equal 500	SWAN-1D	U_{10}=30 m/s
WL | delft hydraulics	H3496	Fig. 7b

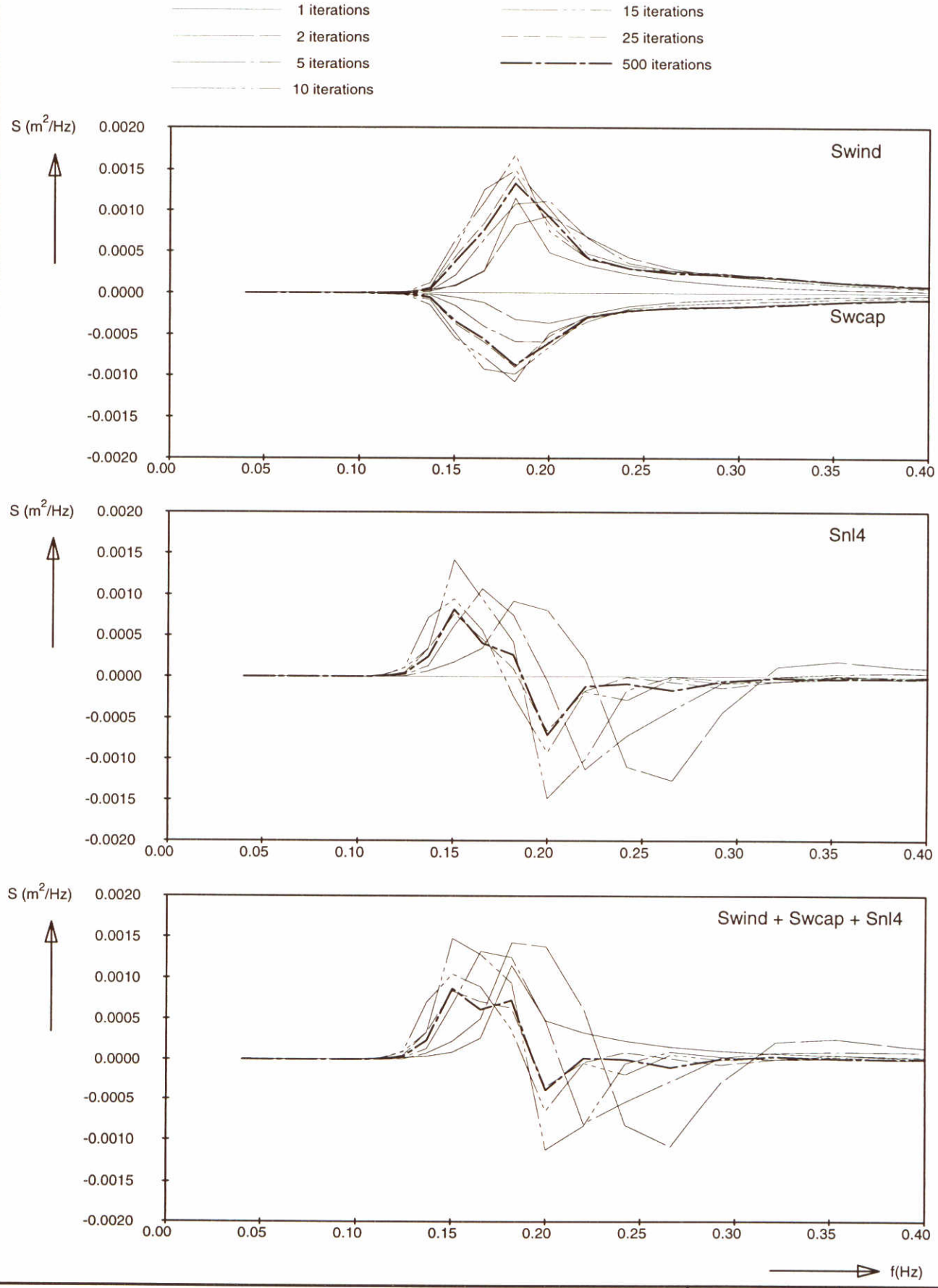

Source terms at x = 12.5 km
Adapted number of maximum iterations
Maximum number equal 500

SWAN-1D

U_{10}=30 m/s

WL | delft hydraulics

H3496

Fig. 7c

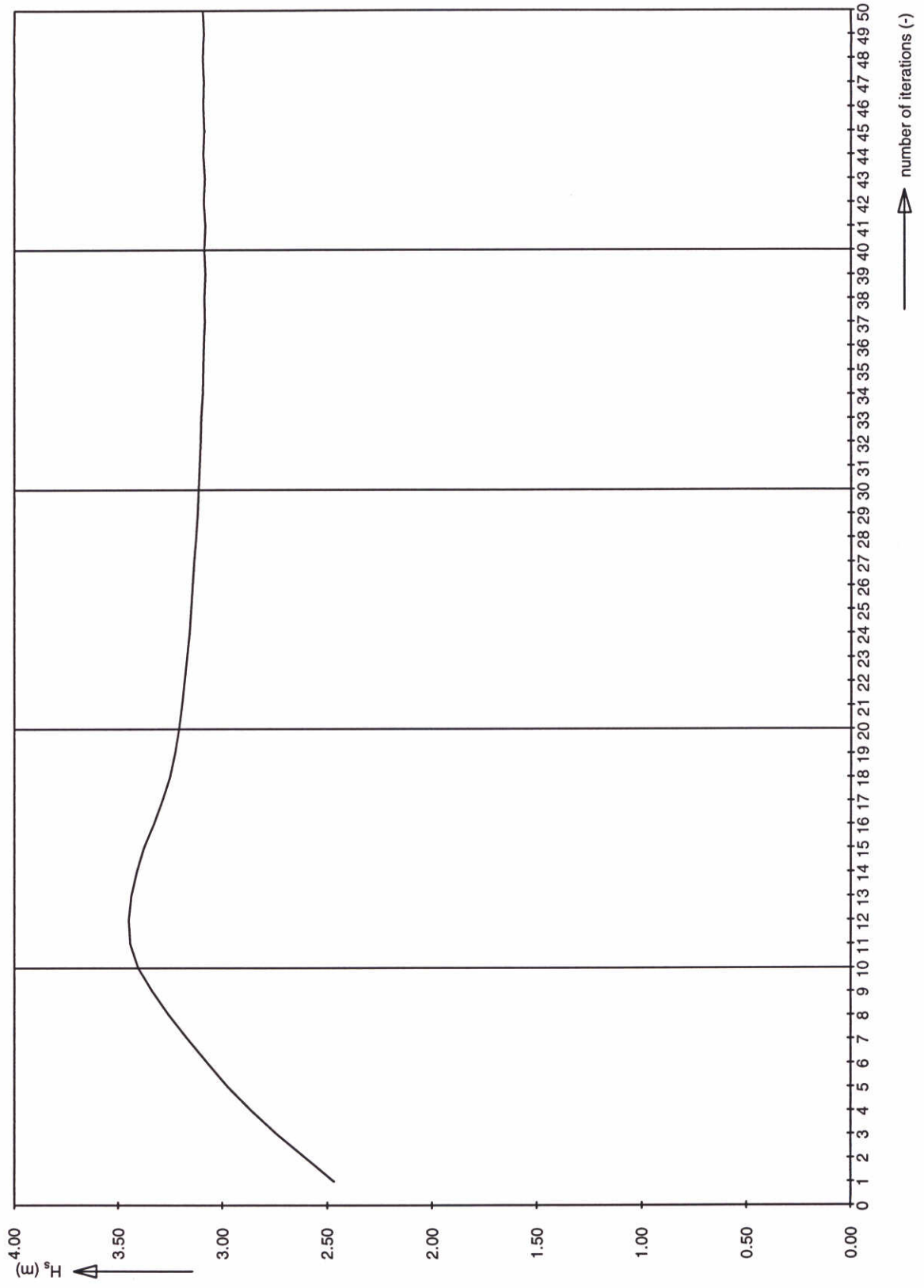

Significant wave height at 12.5 km Adapted number of maximum iterations Maximum number equal 500	SWAN-1D	U_{10}=30 m/s
WL | delft hydraulics	H3496	Fig. 7d

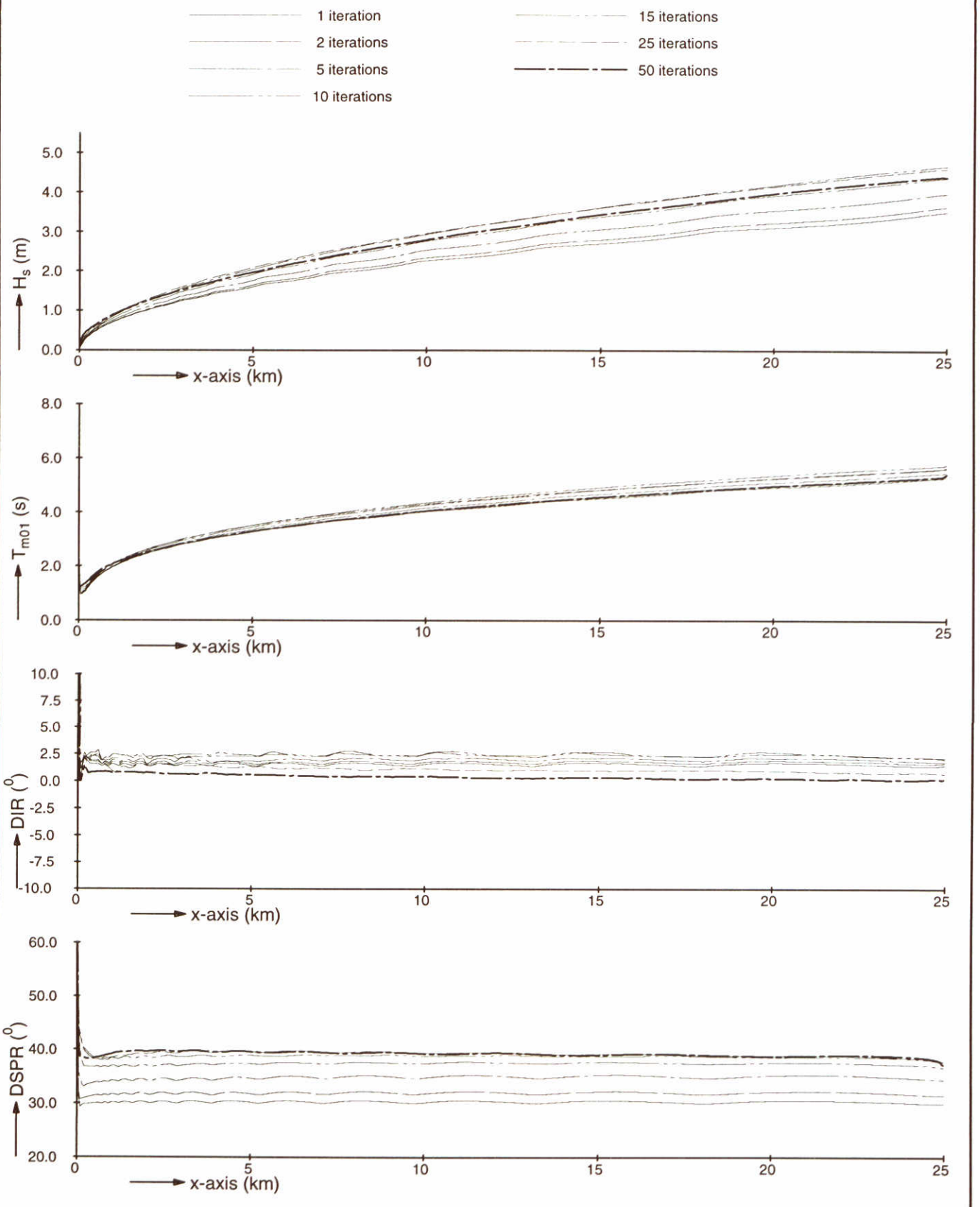

Model convergence behaviour using third-generation formulations Adapted limiter Limiter = 5%	SWAN-1D	U_{10}=30 m/s
WL | delft hydraulics	H3496	Fig. 8a

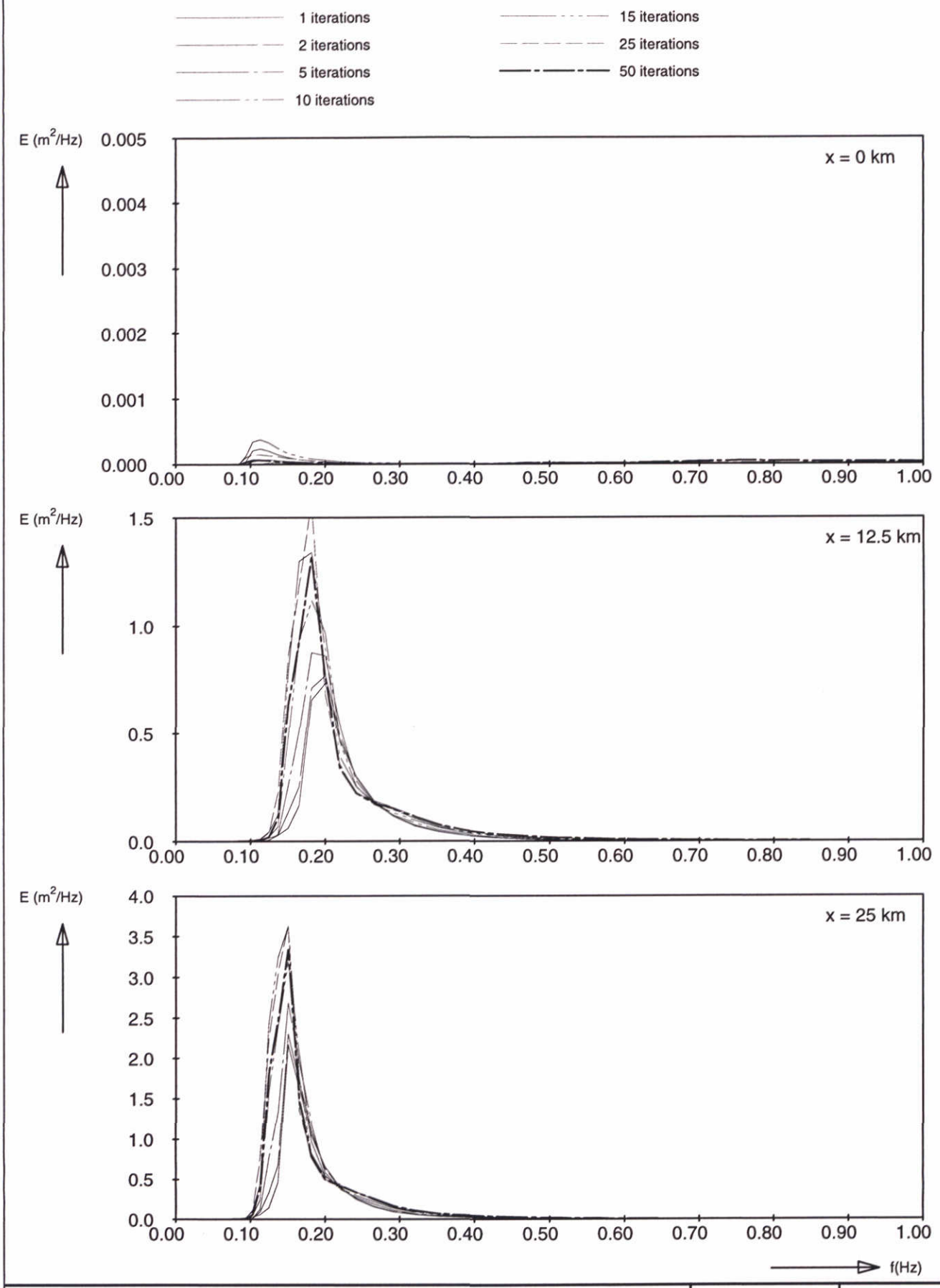

Frequency spectra at 3 locations Adapted limiter Limiter = 5%	SWAN-1D	U_{10}=30 m/s
WL | delft hydraulics	H3496	Fig. 8b

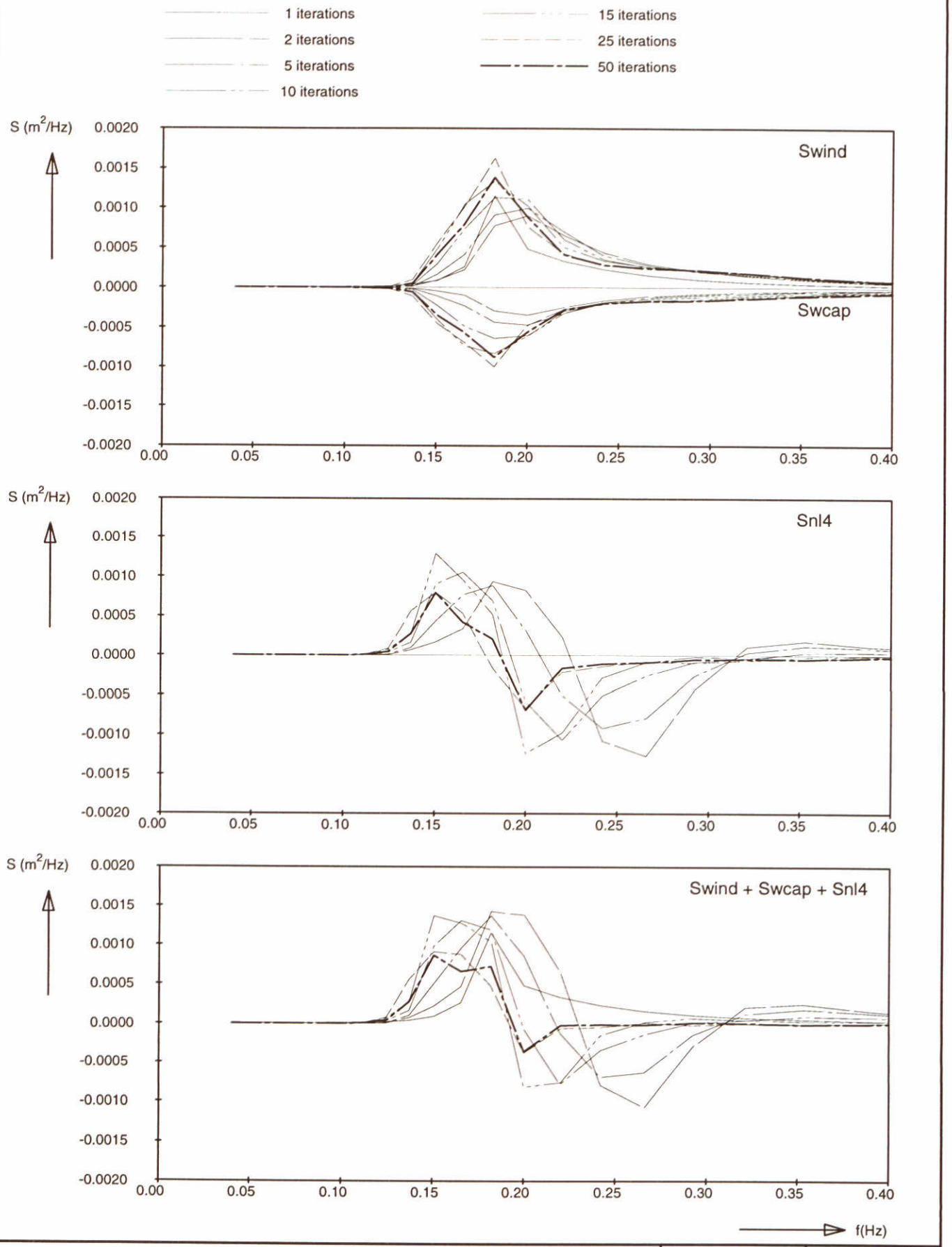

Source terms at x = 12.5 km Adapted limiter Limiter = 5%	SWAN-1D	U_{10}=30 m/s
WL | delft hydraulics	H3496	Fig. 8c

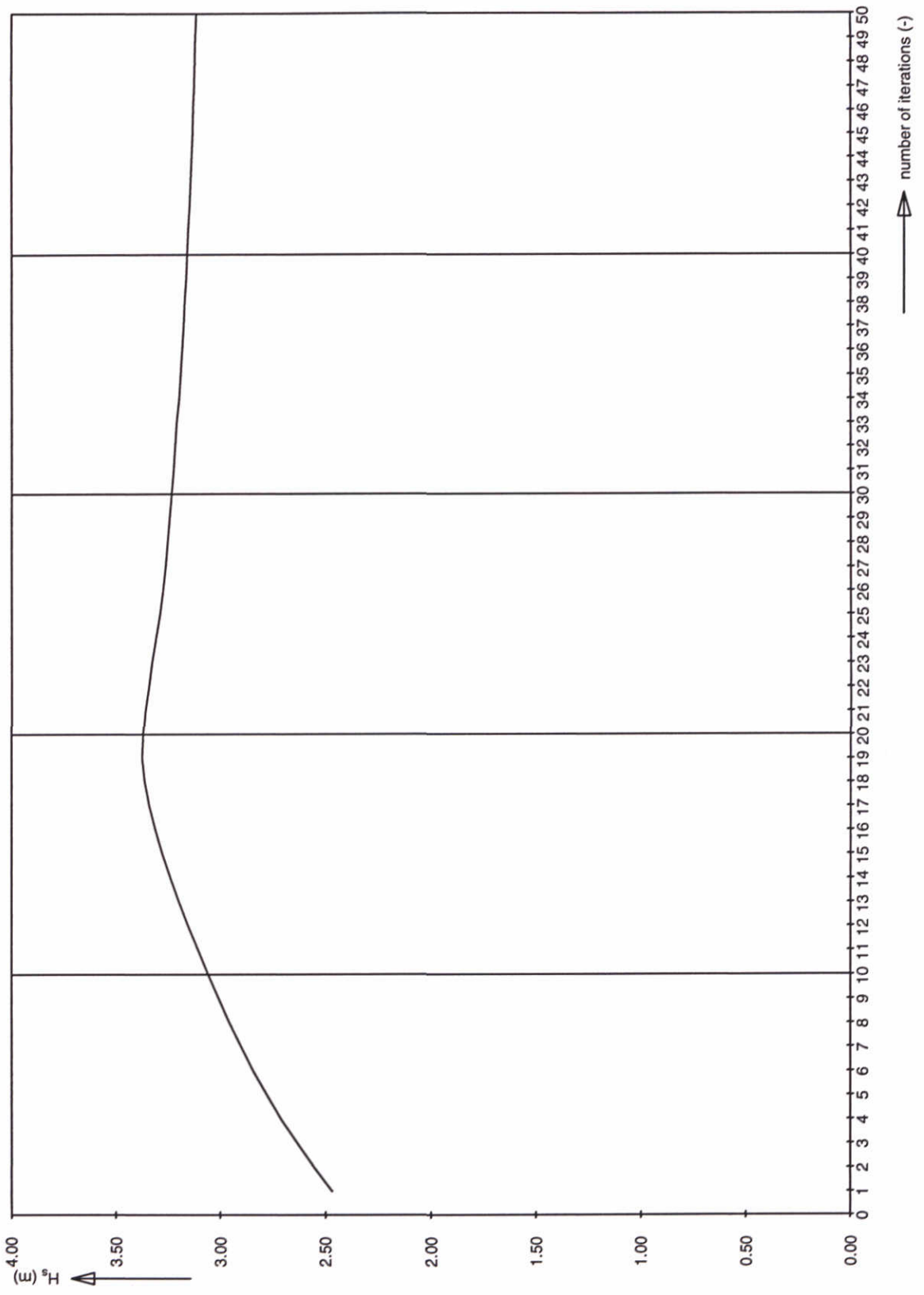

Significant wave height at 12.5 km Adapted limiter Limiter = 5%	SWAN-1D	U_{10}=30 m/s
WL | delft hydraulics	H3496	Fig. 8d

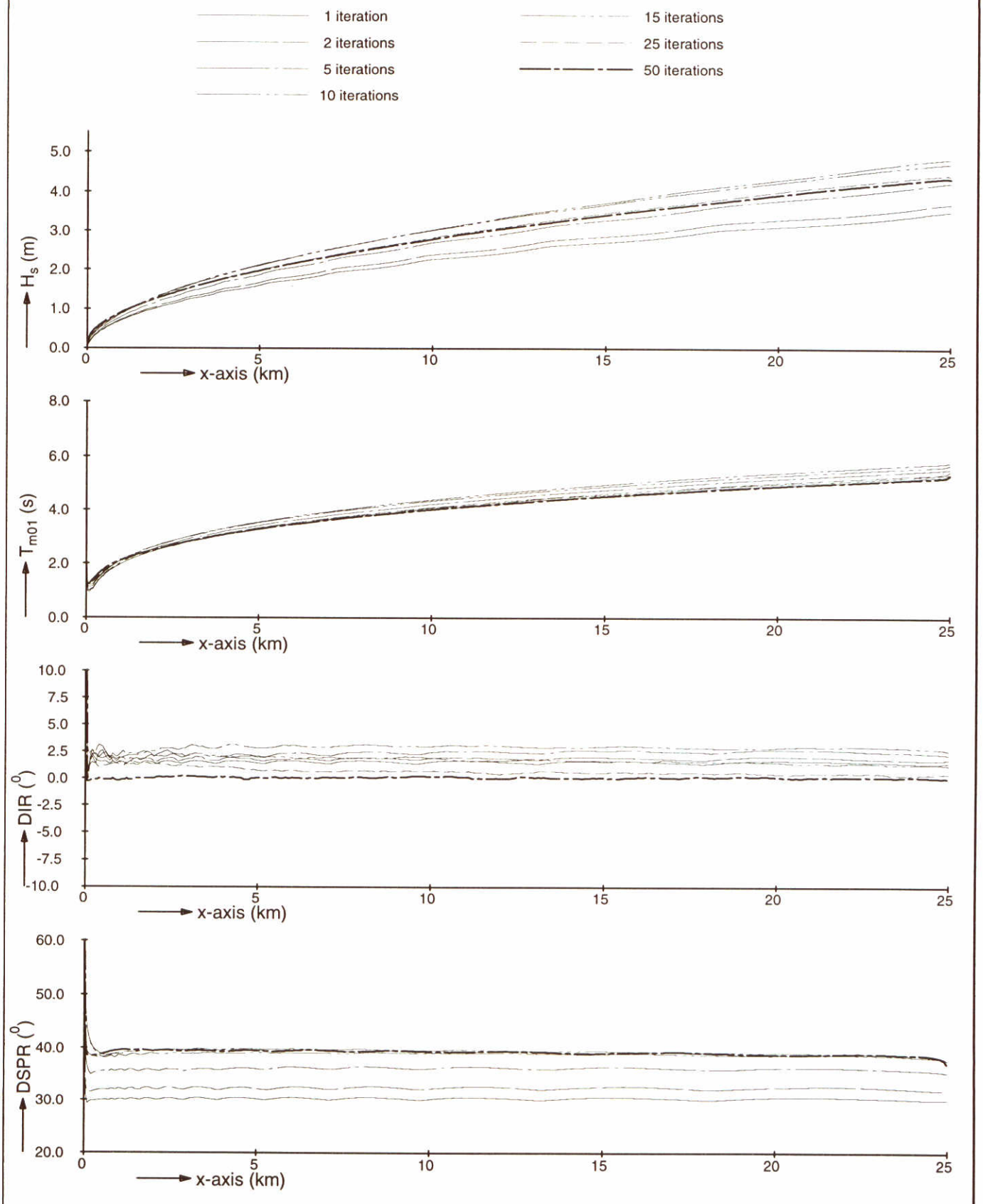

Model convergence behaviour using third-generation formulations Adapted computation of S_{nl4} Semi implicit method per sweep (IQUAD=1)	SWAN-1D	U_{10}=30 m/s
WL | delft hydraulics	H3496	Fig. 9a

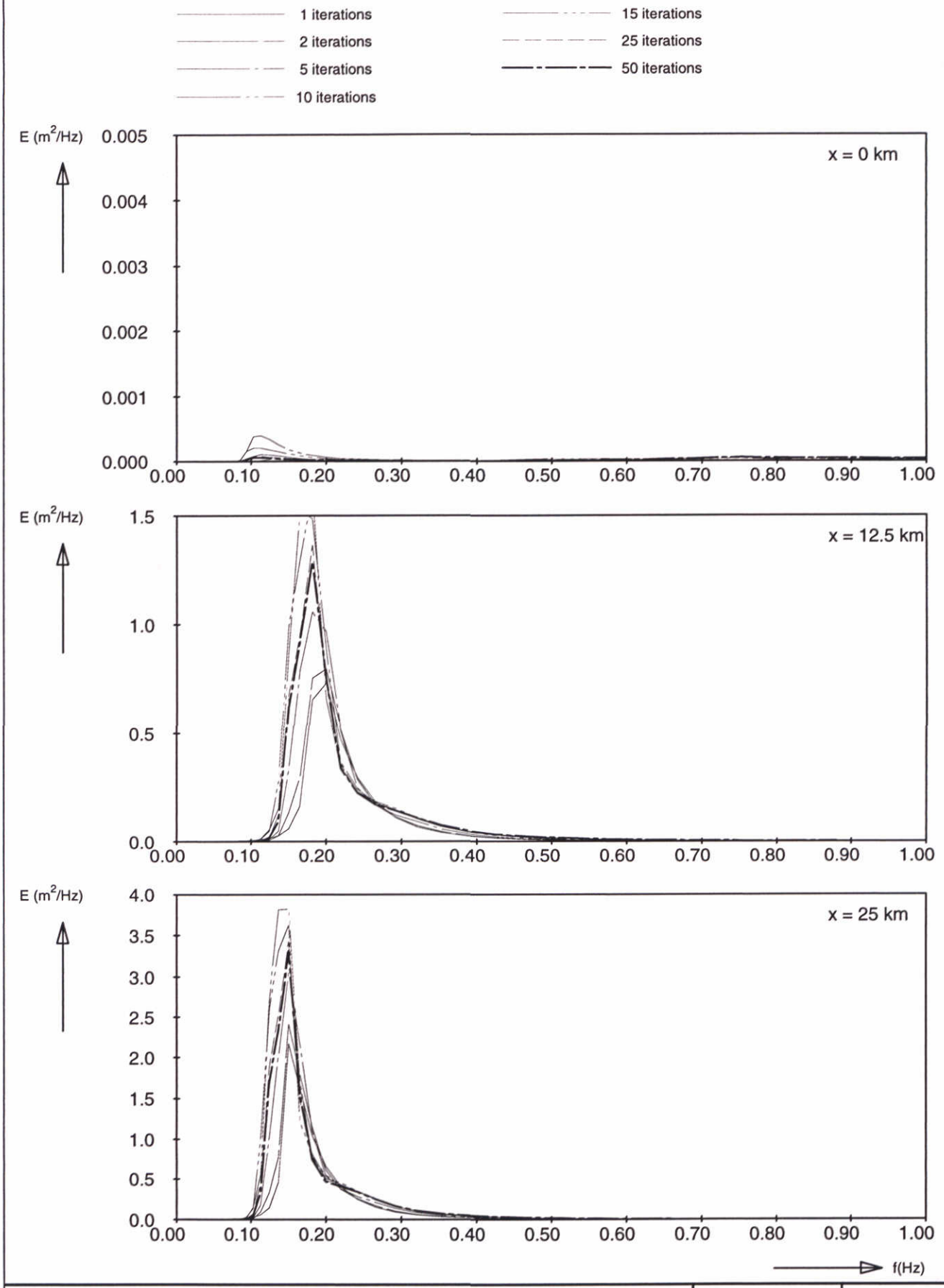

Frequency spectra at 3 locations Adapted computation of S_{nl4} Semi implicit method per sweep (IQUAD=1)	SWAN-1D	U_{10}=30 m/s
WL | delft hydraulics	H3496	Fig. 9b

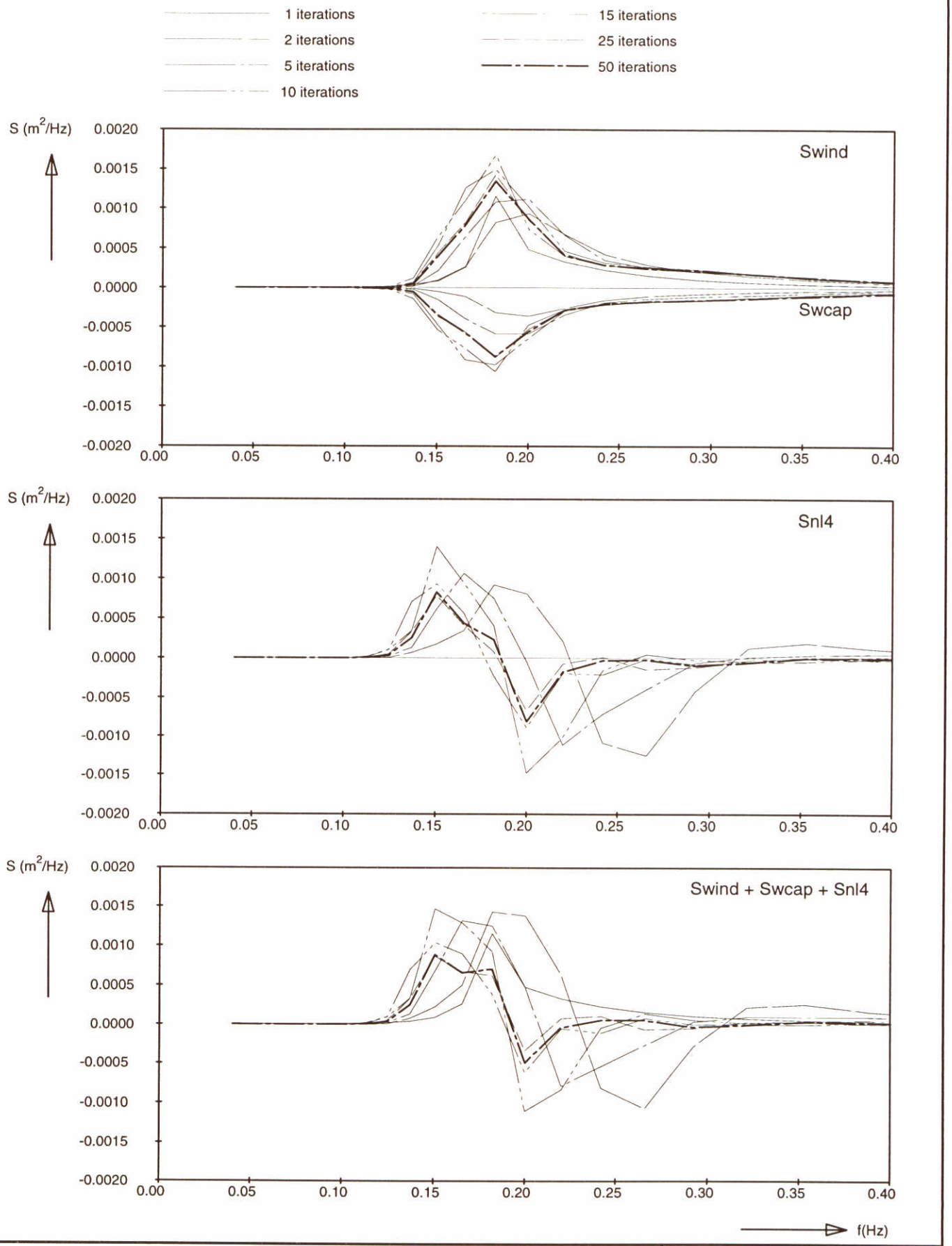

Source terms at x = 12.5 km Adapted computation of S_{nl4} Semi implicit method per sweep (IQUAD=1)	SWAN-1D	U_{10}=30 m/s
WL | delft hydraulics	H3496	Fig. 9c

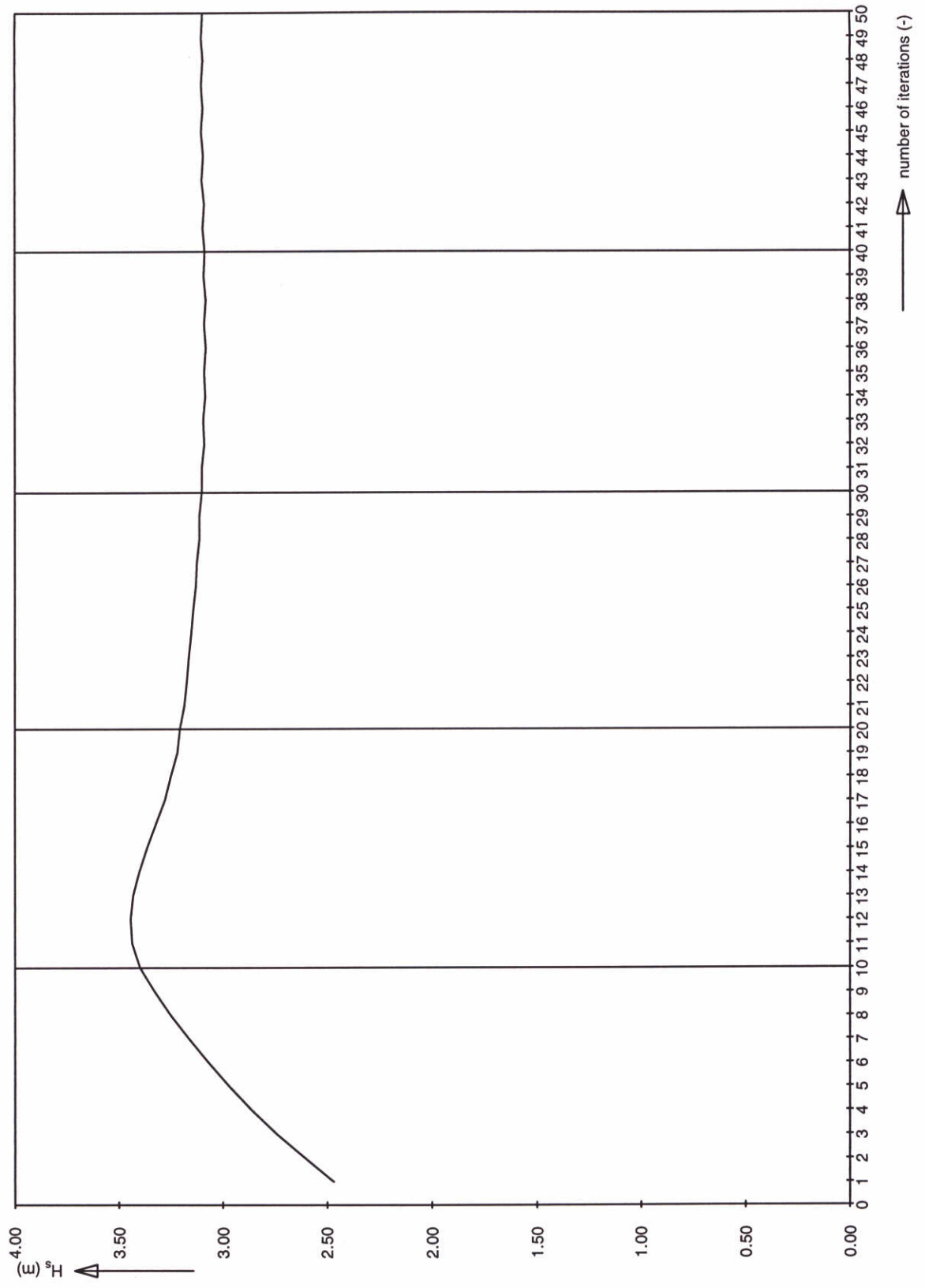

Significant wave height at 12.5 km Adapted computation of S_{nl4} Semi implicit method per sweep (IQUAD=1)	SWAN-1D	U_{10}=30 m/s
WL | delft hydraulics	H3496	Fig. 9d

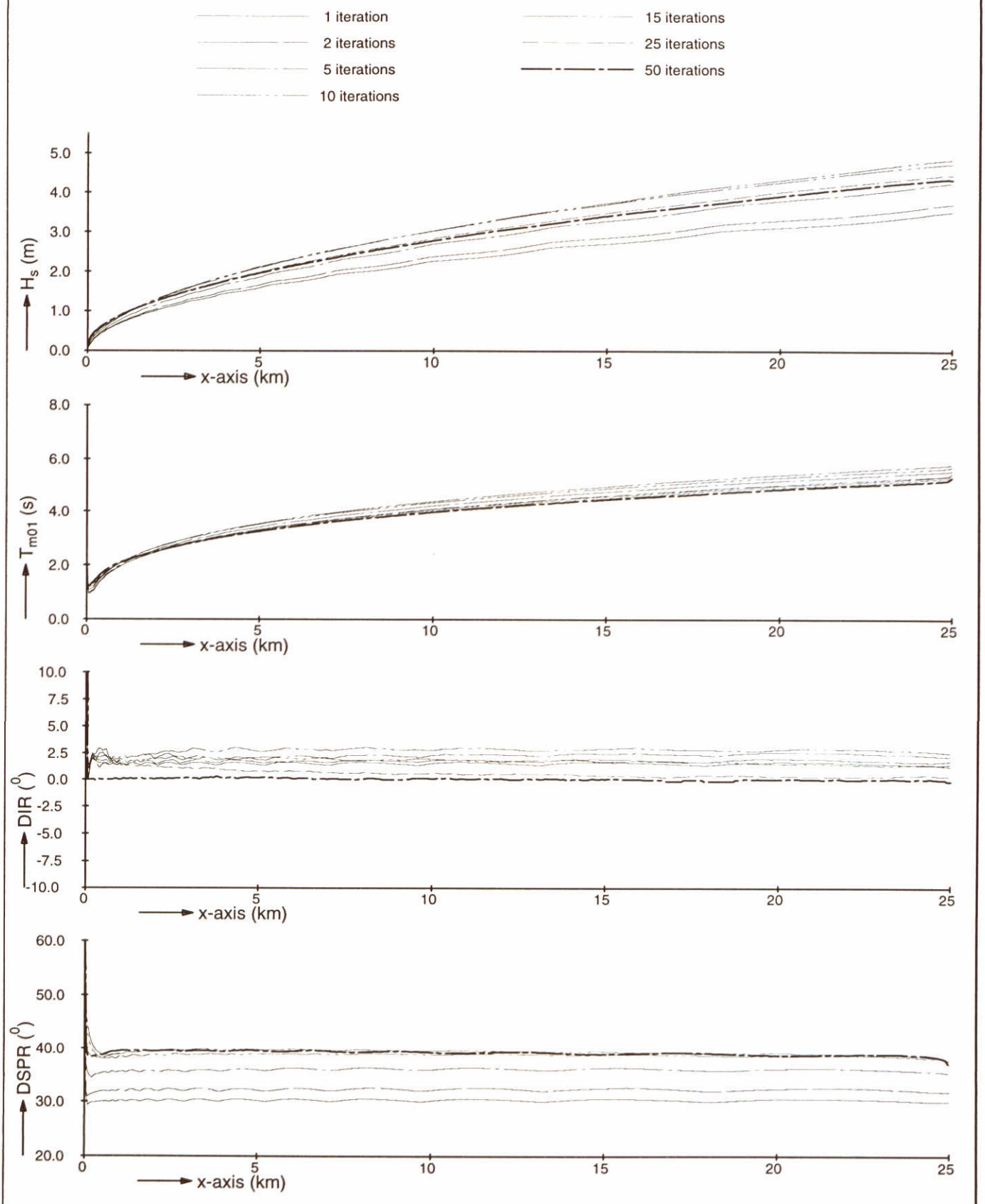

Model convergence behaviour using third-generation formulations Adapted computation of S_{nl4} Fully explicit method per iteration (IQUAD=3)	SWAN-1D	U_{10}=30 m/s
WL | delft hydraulics	H3496	Fig. 10a

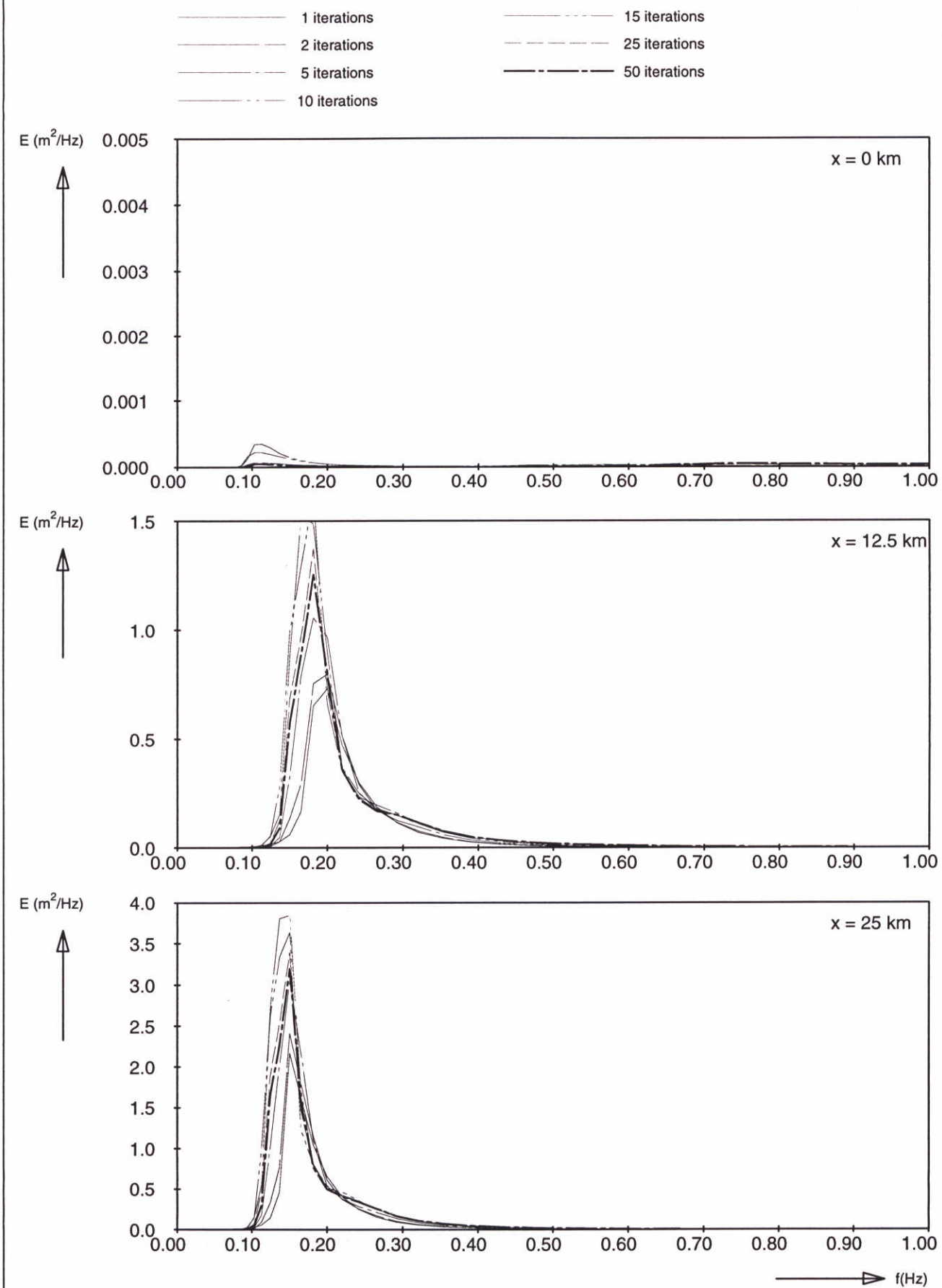

Frequency spectra at 3 locations Adapted computation of S_{nl4} Fully explicit method per iteration (IQUAD=3)	SWAN-1D	U_{10}=30 m/s
WL | delft hydraulics	H3496	Fig. 10b

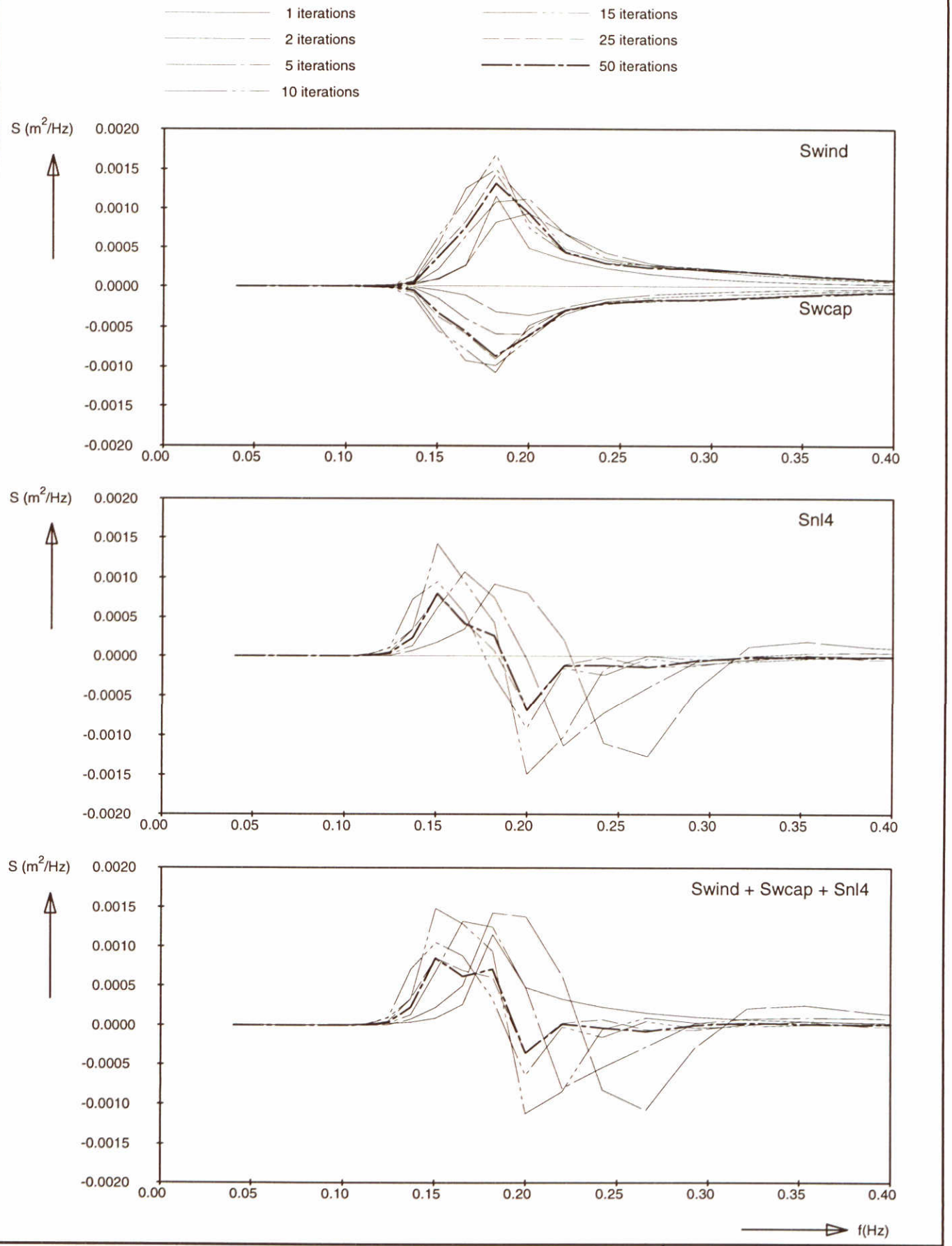

Source terms at x = 12.5 km Adapted computation of S_{nl4} Fully explicit method per iteration (IQUAD=3)	SWAN-1D	U_{10}=30 m/s
WL | delft hydraulics	H3496	Fig. 10c

Significant wave height at 12.5 km Adapted computation of S_{nl4} Fully explicit method per iteration (IQUAD=3)	SWAN-1D	U_{10}=30 m/s
WL | delft hydraulics	H3496	Fig. 10d

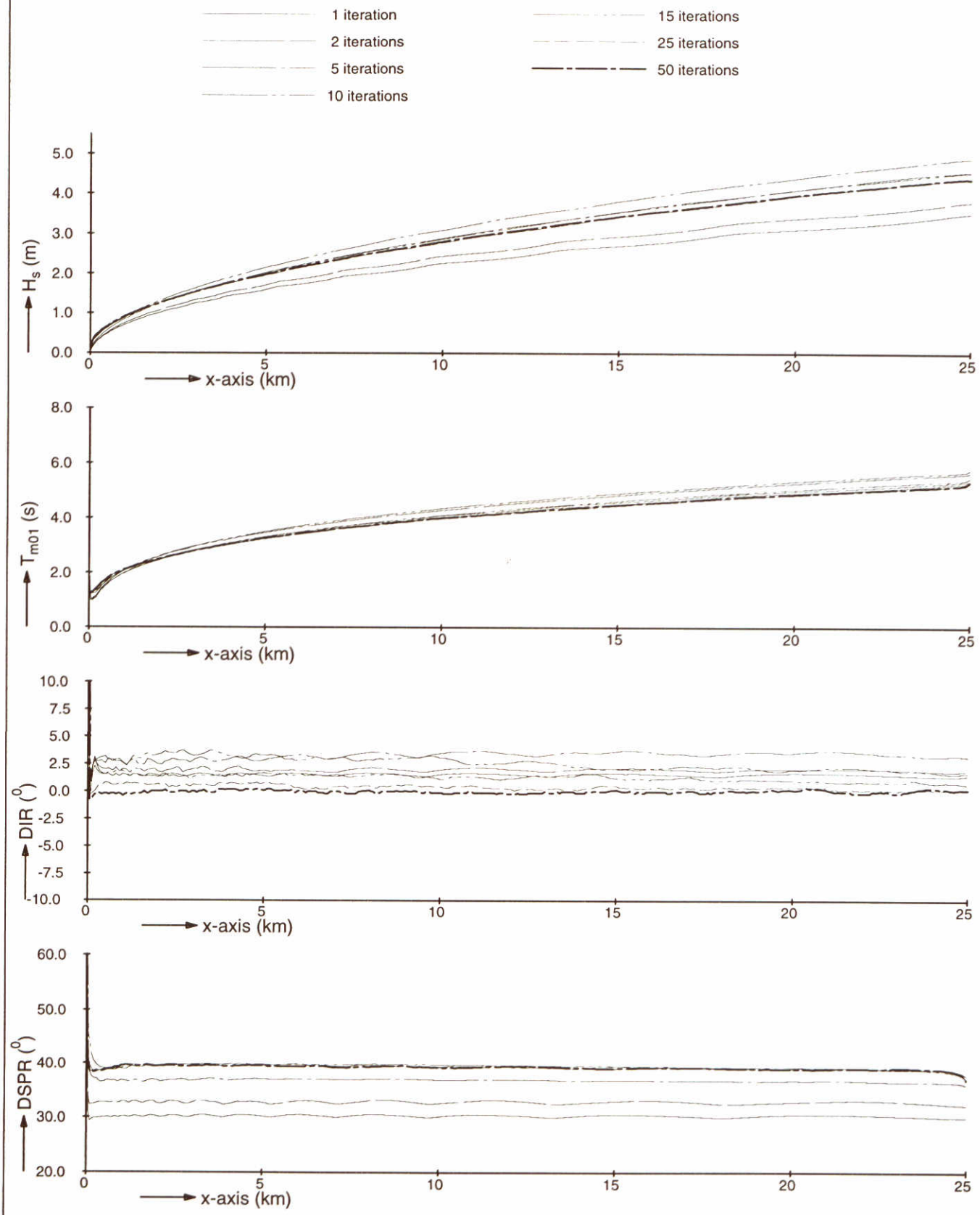

Model convergence behaviour using third-generation formulations
Adapted limiter
Limiter = 20%

SWAN-1D

U_{10}=30 m/s

WL | delft hydraulics

H3496

Fig. 11a

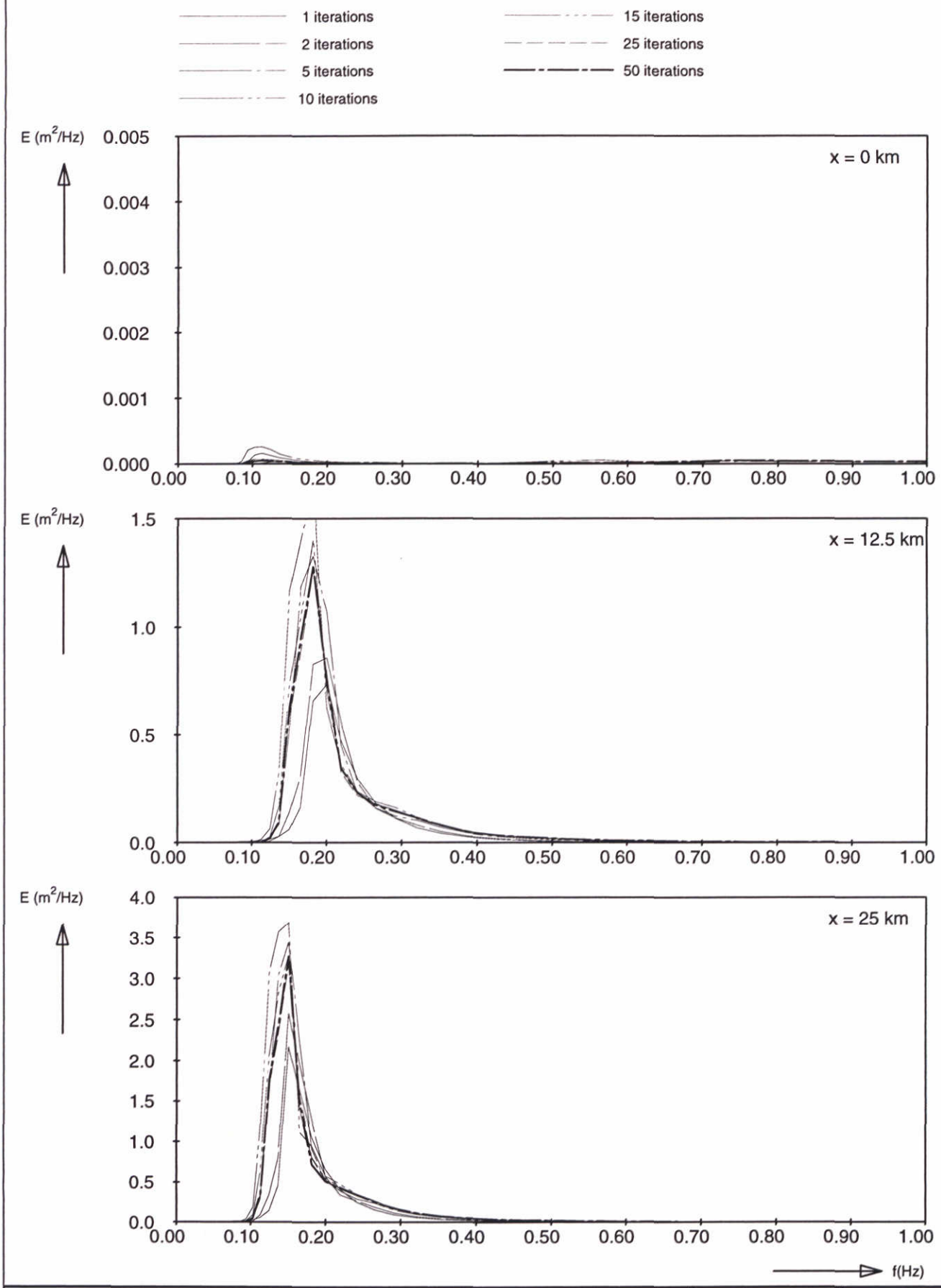

Frequency spectra at 3 locations Adapted limiter Limiter = 20%	SWAN-1D	U_{10}=30 m/s
WL | delft hydraulics	H3496	Fig. 11b

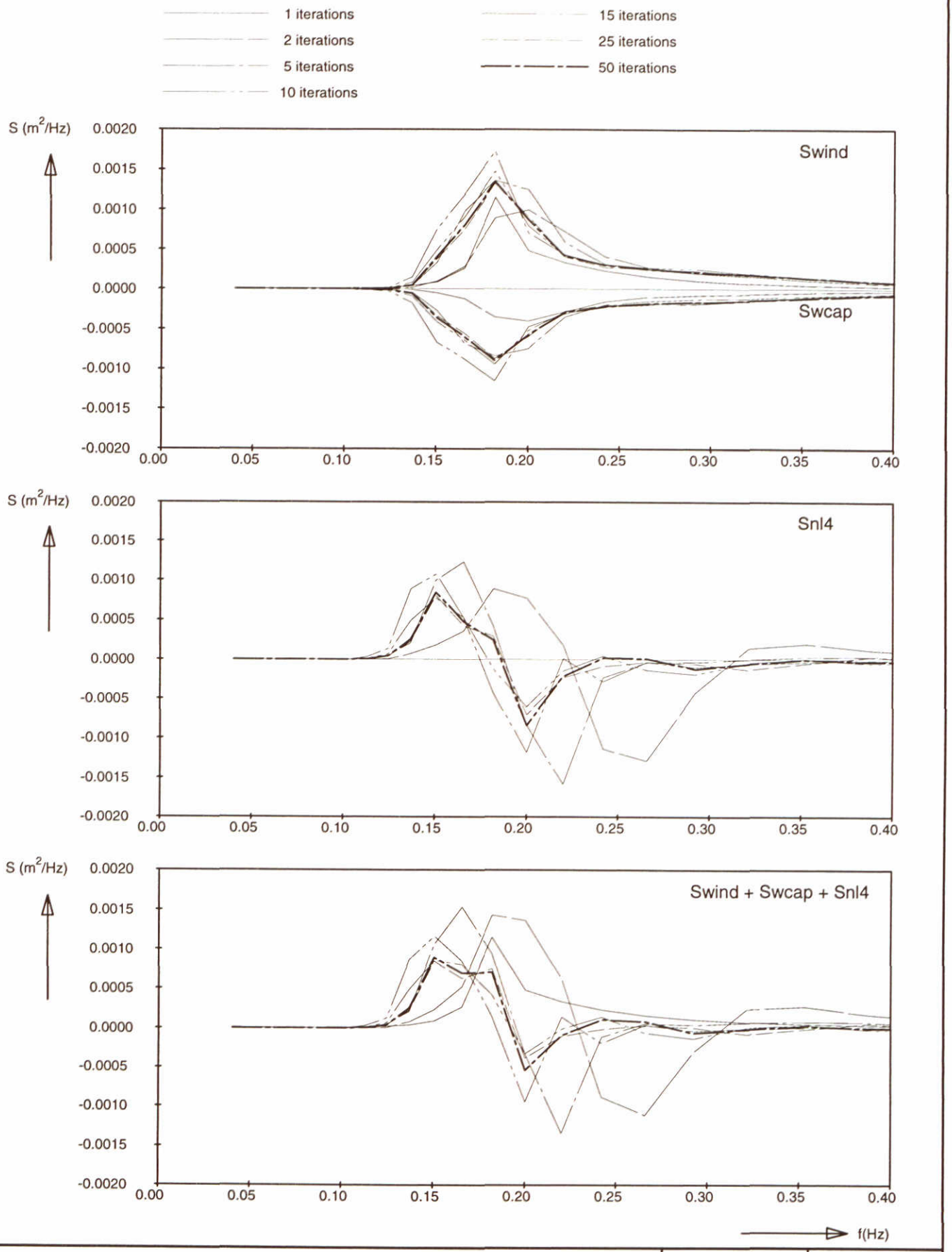

Source terms at x = 12.5 km Adapted limiter Limiter = 20%	SWAN-1D	U_{10}=30 m/s
WL | delft hydraulics	H3496	Fig. 11c

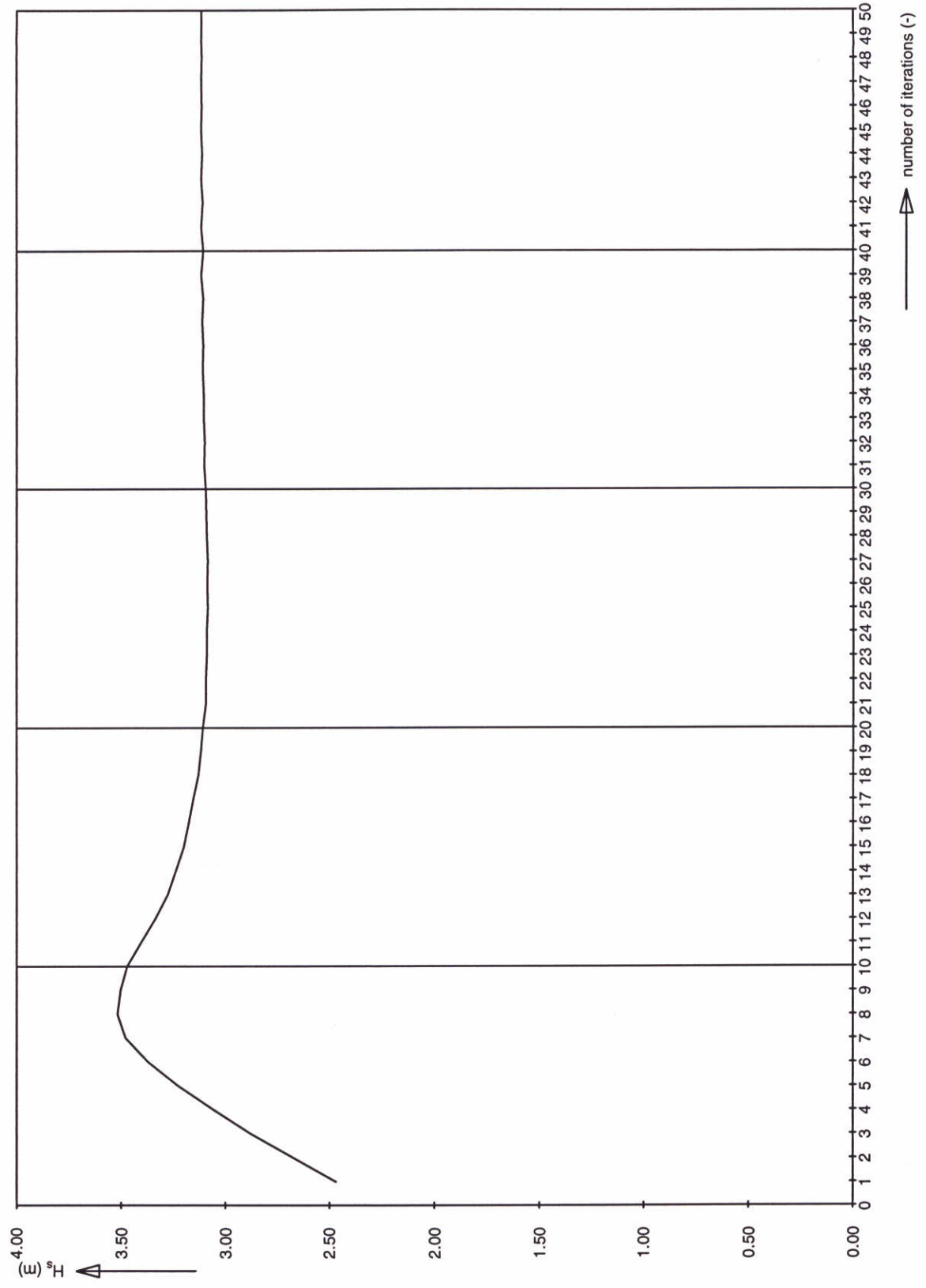

Significant wave height at 12.5 km Adapted limiter Limiter = 20%	SWAN-1D	U_{10}=30 m/s
WL | delft hydraulics	H3496	Fig. 11d

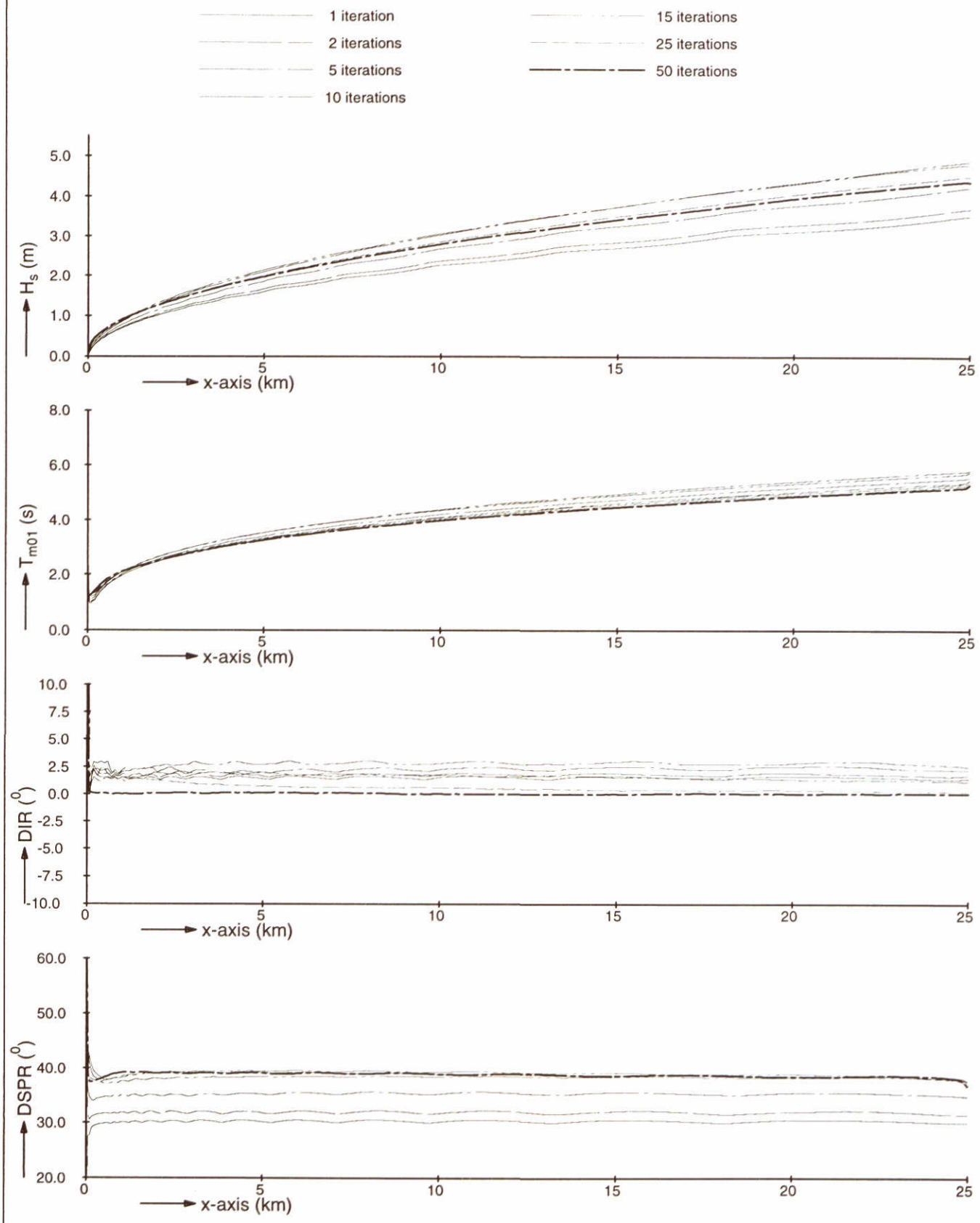

Model convergence behaviour using third-generation formulations Adapted directional resolution Directional increment = 2^o	SWAN-1D	U_{10}=30 m/s
WL | delft hydraulics	H3496	Fig. 12a

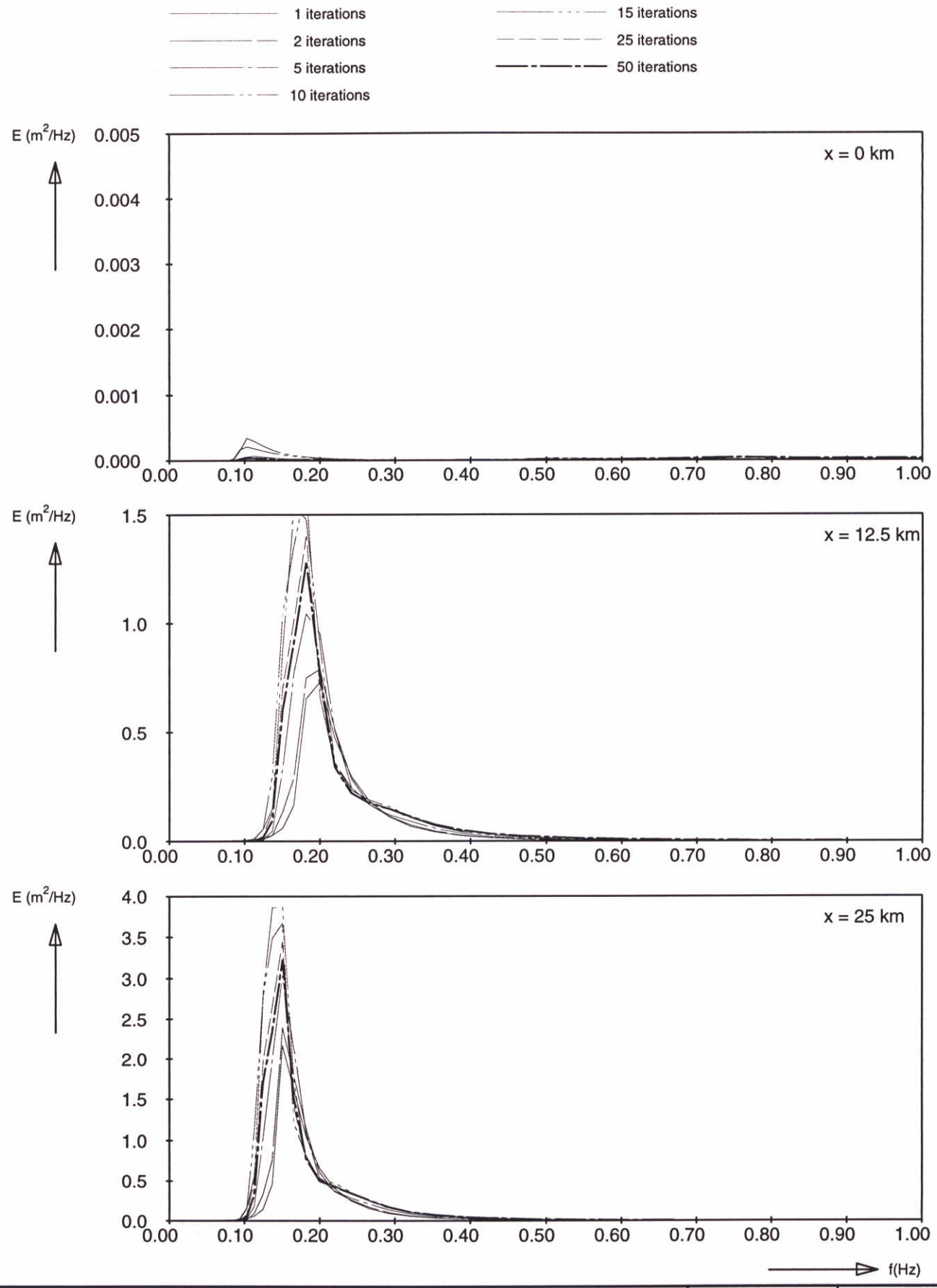

Frequency spectra at 3 locations Adapted directional resolution Directional increment = 2°	SWAN-1D	U_{10}=30 m/s
WL | delft hydraulics	H3496	Fig. 12b

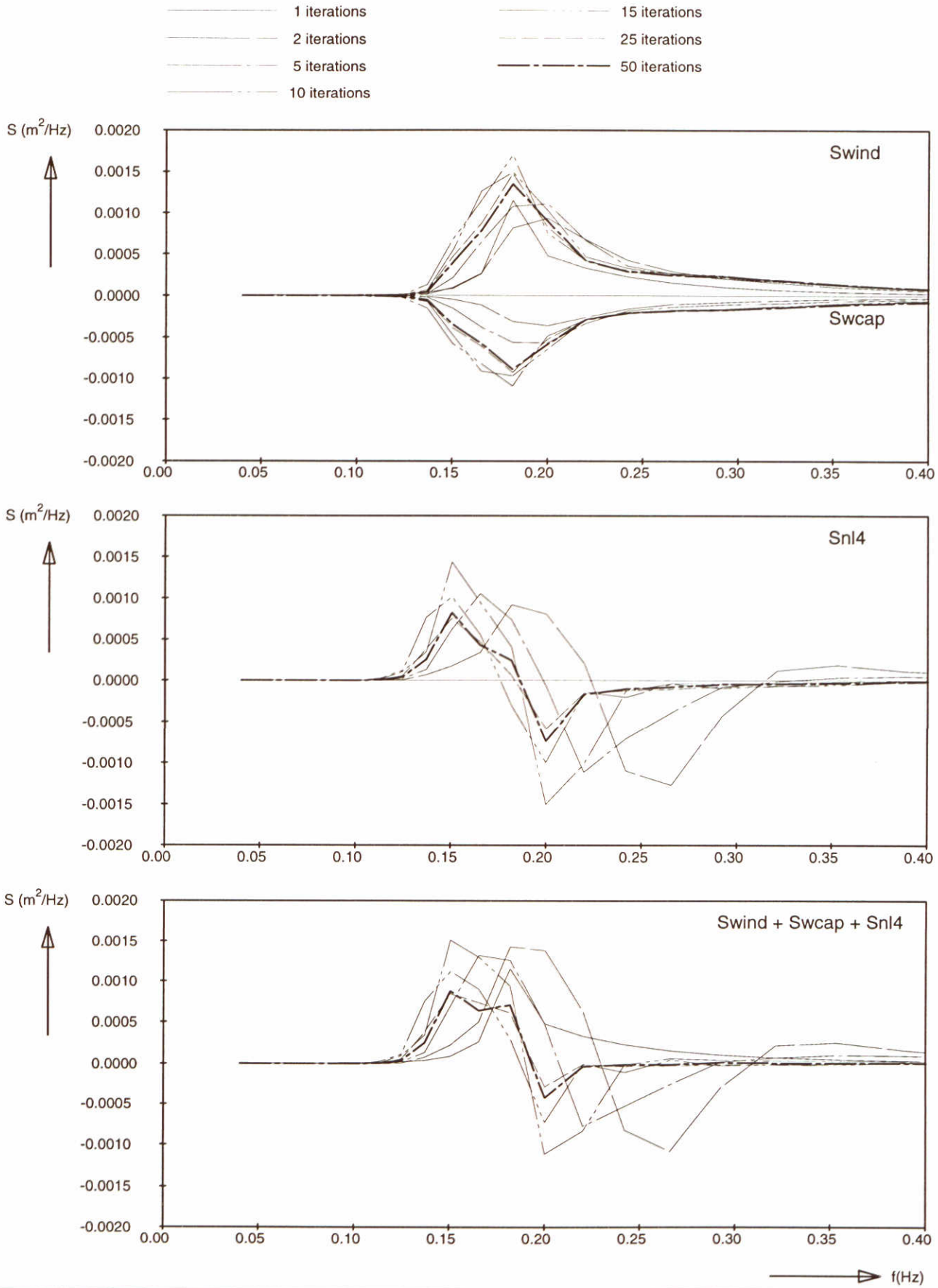

Source terms at x = 12.5 km Adapted directional resolution Directional increment = 2°	SWAN-1D	U_{10}=30 m/s
WL | delft hydraulics	H3496	Fig. 12c

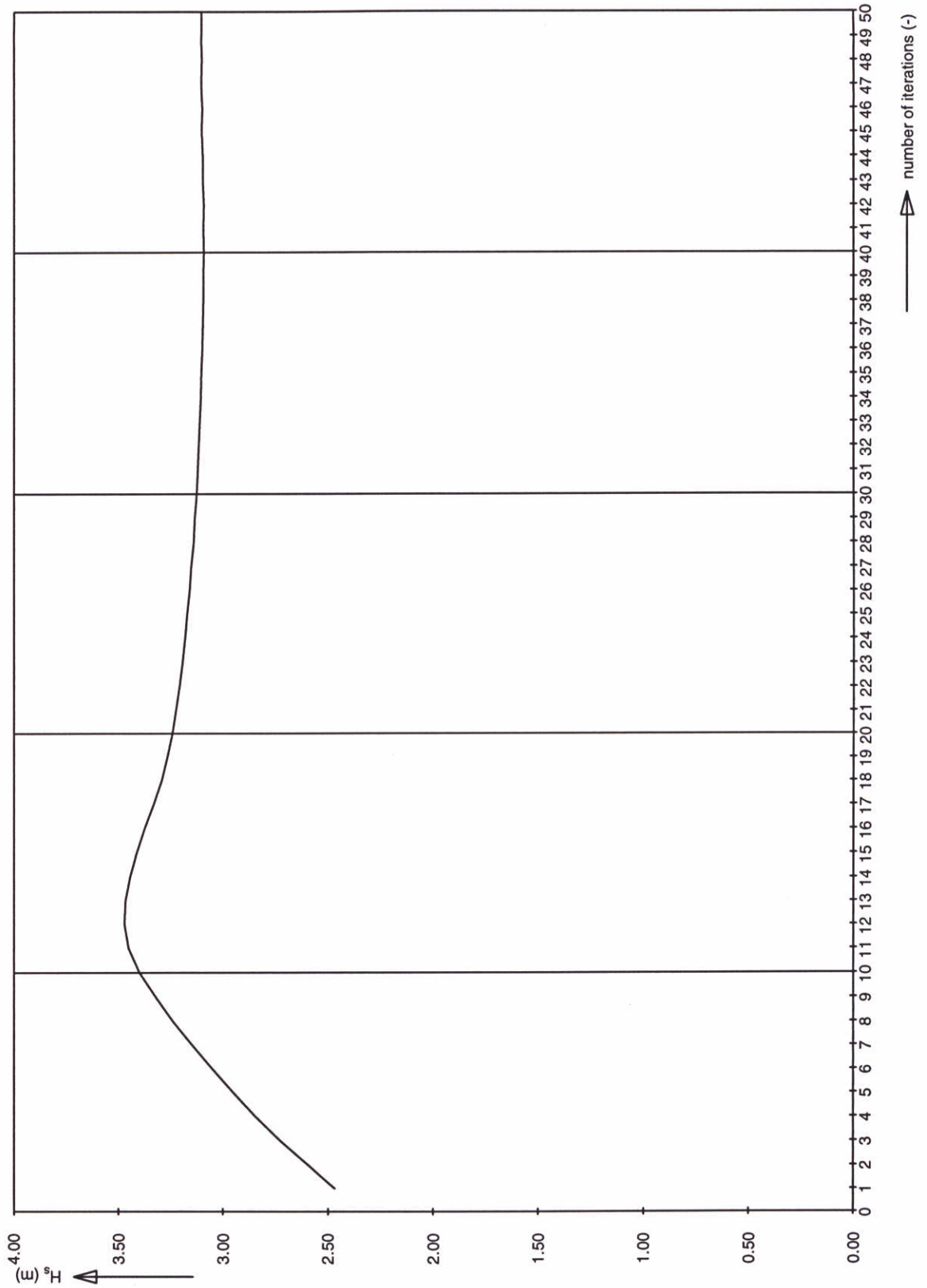

Significant wave height at 12.5 km Adapted directional resolution Directional increment = 2^{o}	SWAN-1D	U_{10}=30 m/s
WL | delft hydraulics	H3496	Fig. 12d

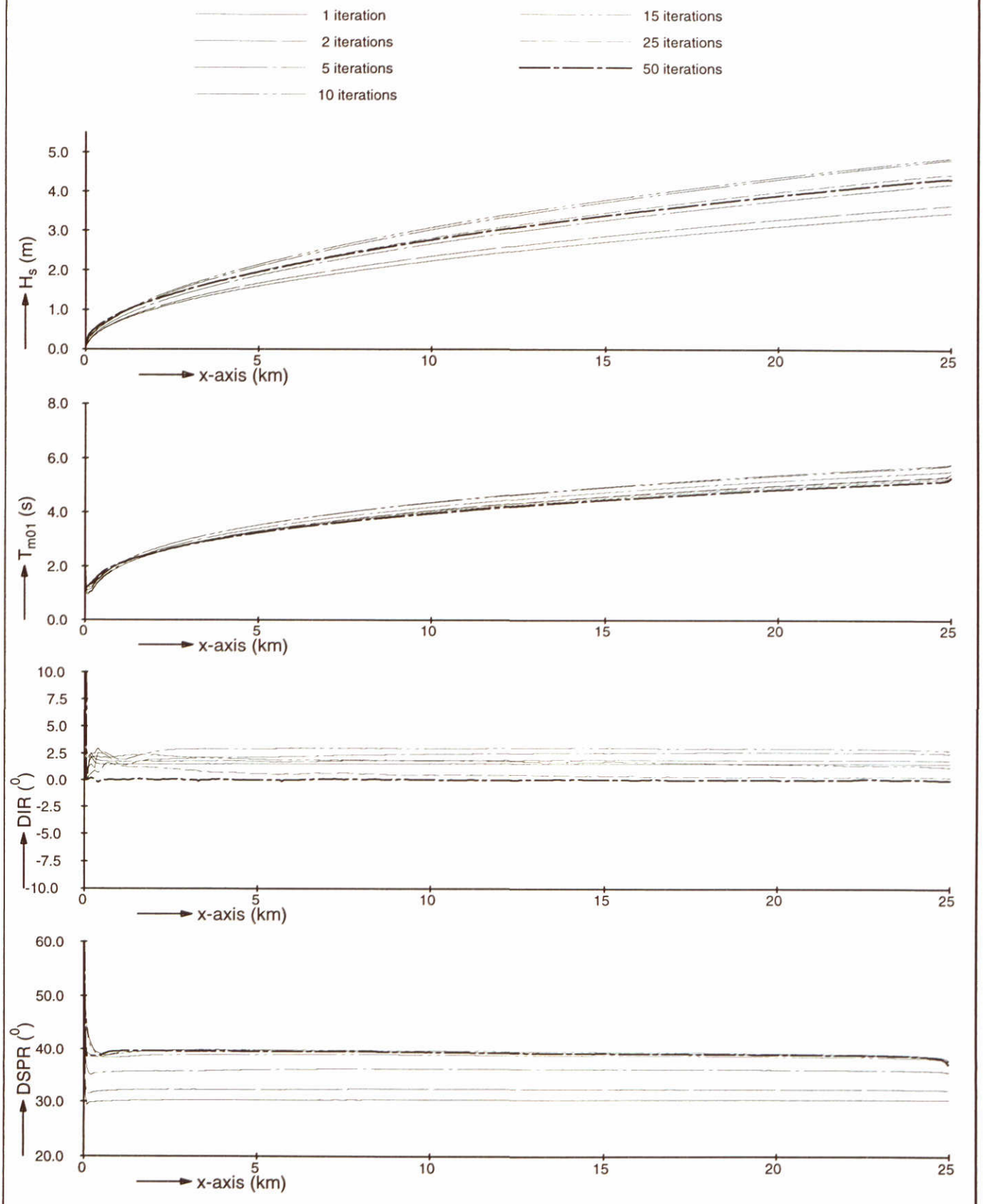

Model convergence behaviour using third-generation formulations Adapted frequency resolution f_{i+1}= 1.01 * f_i	SWAN-1D	U_{10}=30 m/s
WL | delft hydraulics	H3496	Fig. 13a

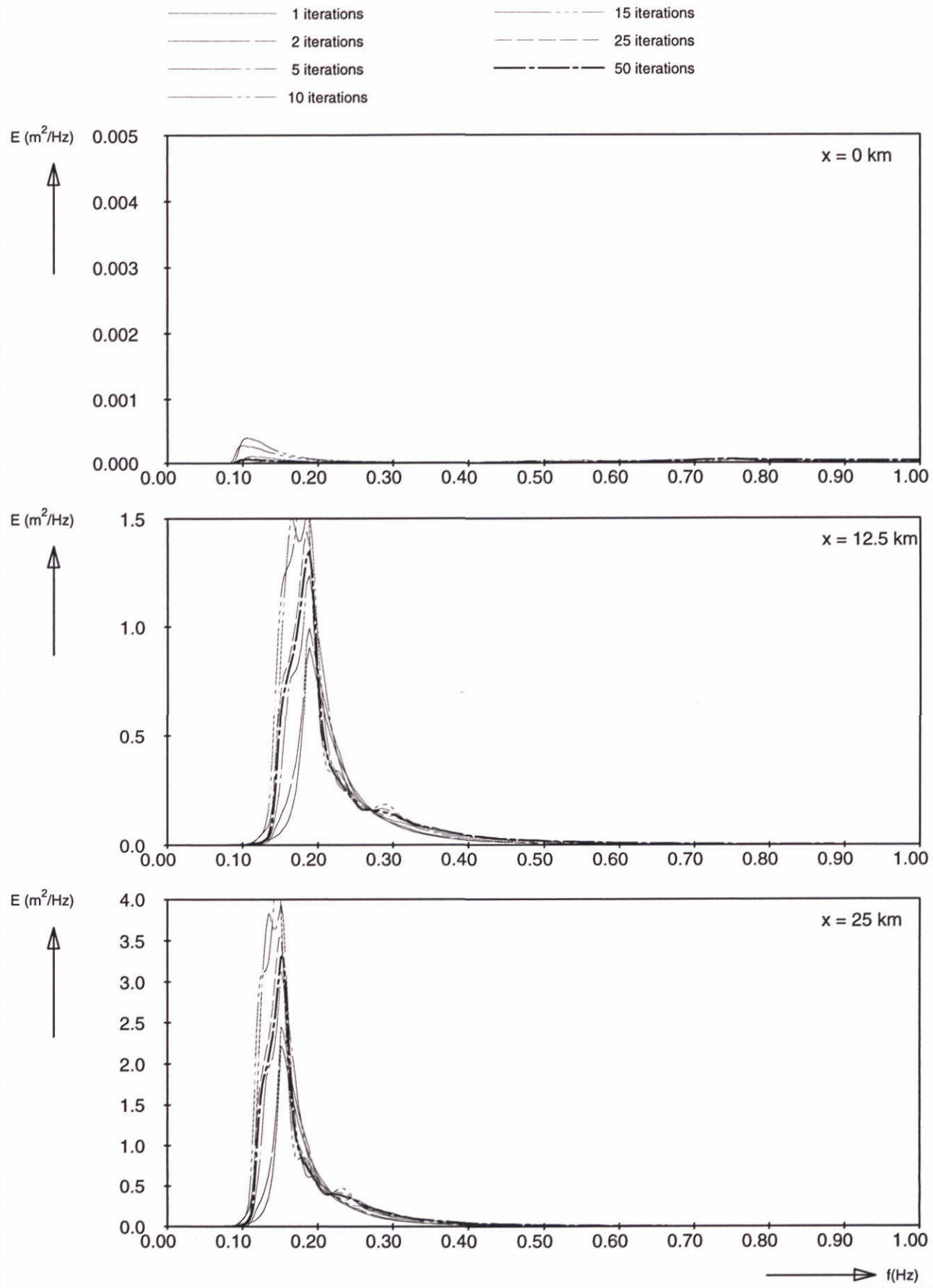

Frequency spectra at 3 locations Adapted frequency resolution $f_{i+1} = 1.01 * f_i$	SWAN-1D	U_{10}=30 m/s
WL | delft hydraulics	H3496	Fig. 13b

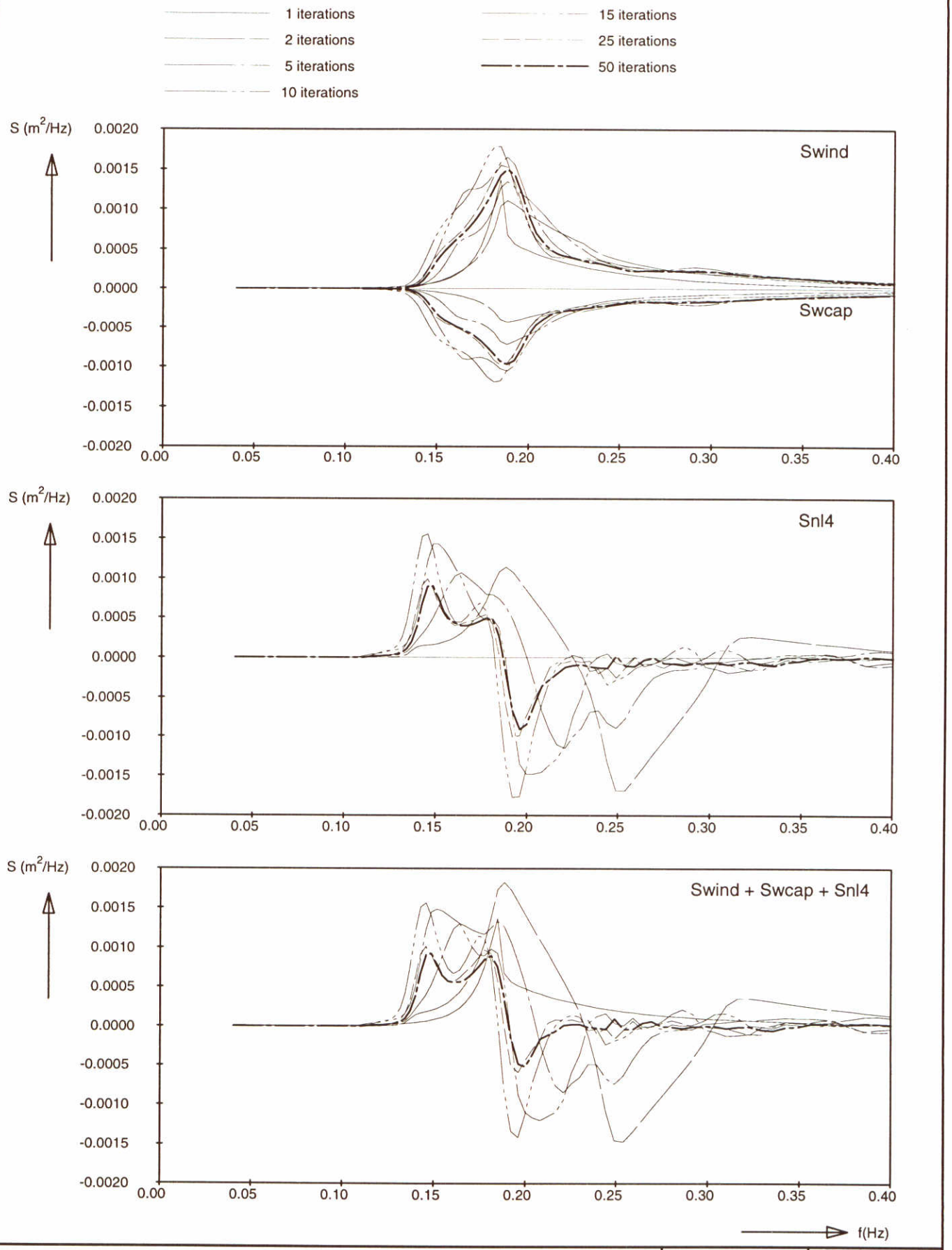

Source terms at x = 12.5 km Adapted frequency resolution $f_{i+1} = 1.01 * f_i$	SWAN-1D	U_{10}=30 m/s
WL | delft hydraulics	H3496	Fig. 13c

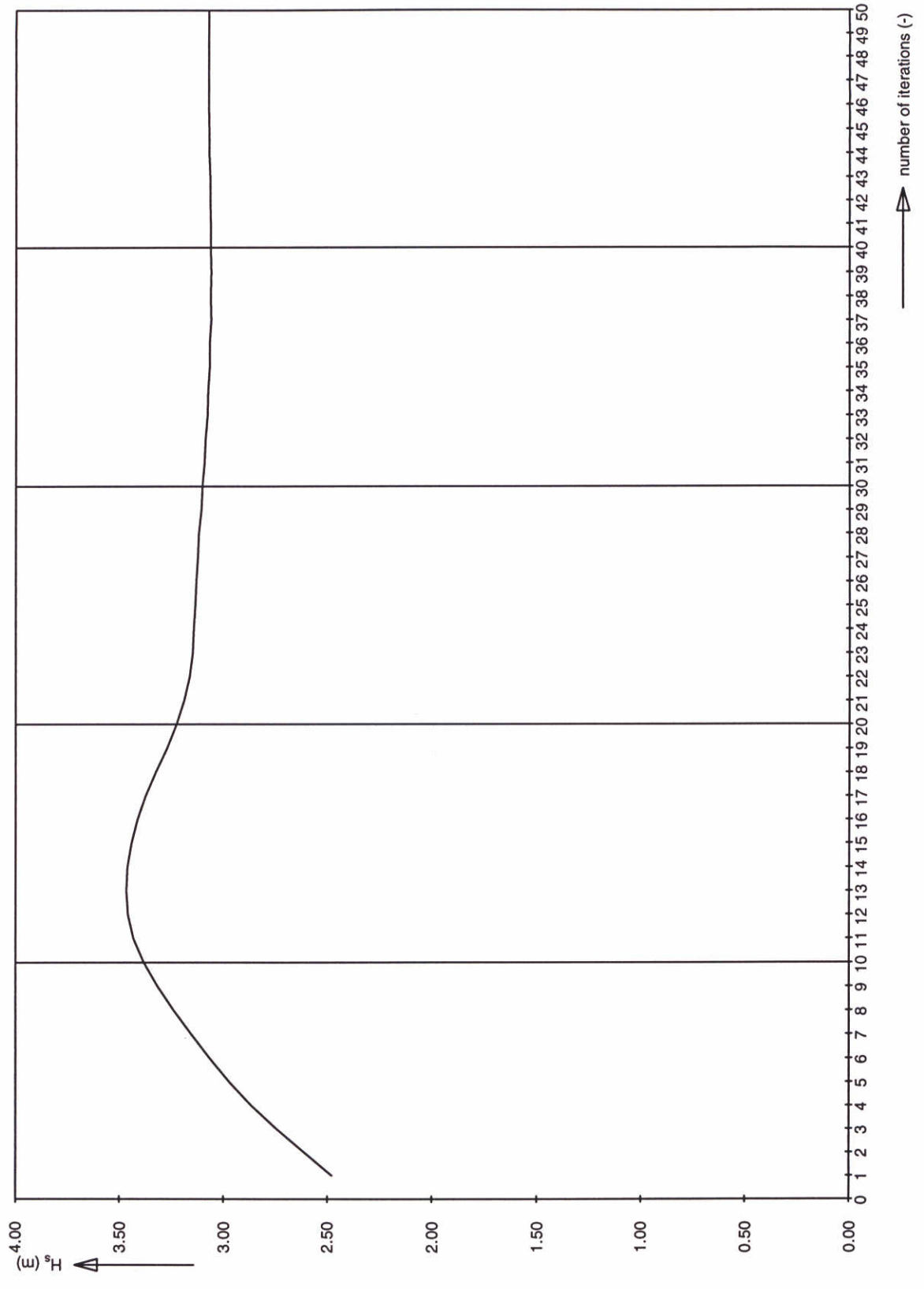

Significant wave height at 12.5 km Adapted frequency resolution $f_{i+1} = 1.01 * f_i$	SWAN-1D	U_{10}=30 m/s
WL | delft hydraulics	H3496	Fig. 13d

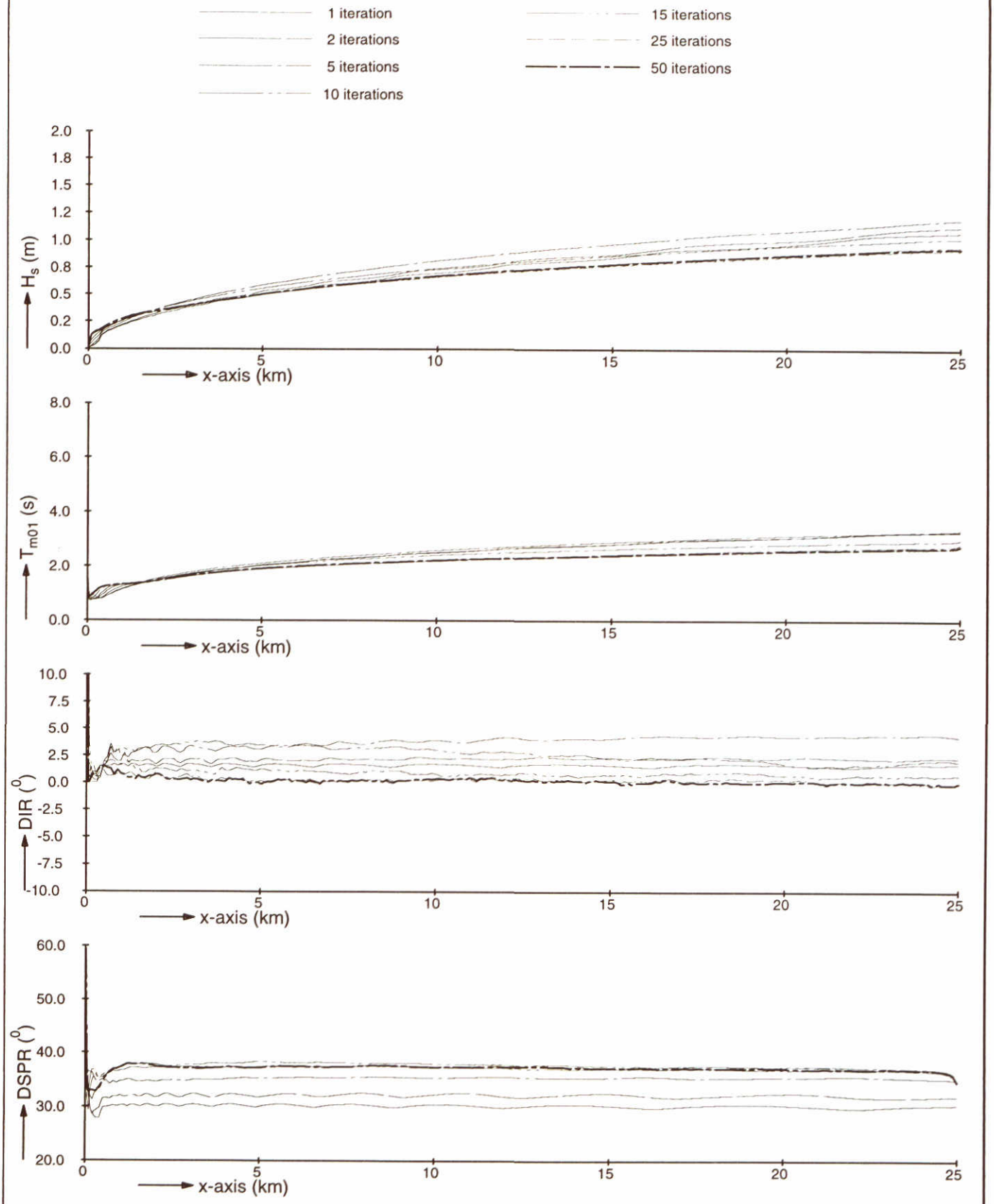

Model convergence behaviour using third-generation formulations
Adapted wind speed: U_{10} = 10 m/s

SWAN-1D | U_{10}=10 m/s

WL | delft hydraulics | H3496 | Fig. 14a

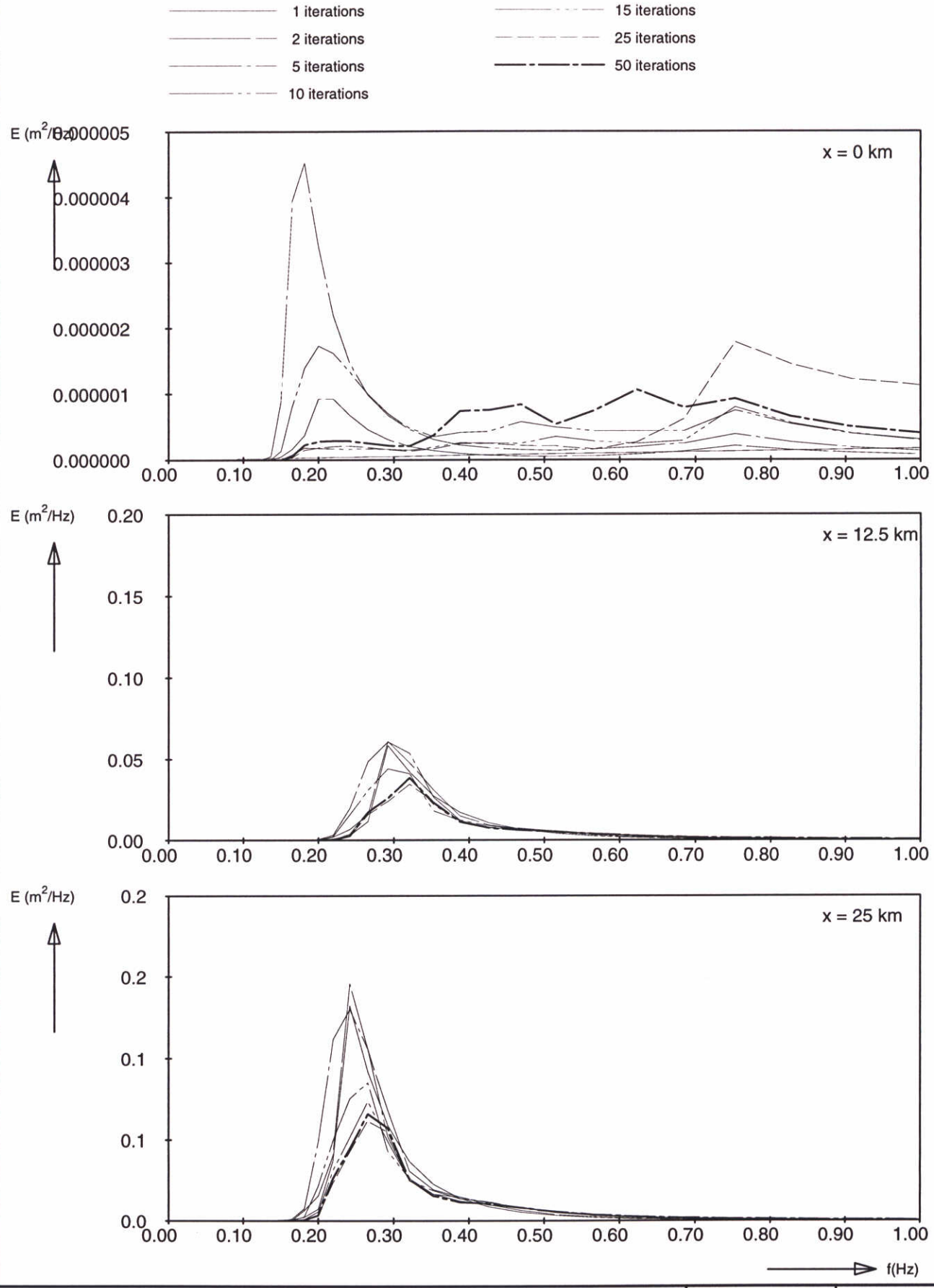

Frequency spectra at 3 locations
Adapted wind speed: U_{10} = 10 m/s

SWAN-1D	U_{10}=10 m/s

WL | delft hydraulics

H3496	Fig. 14b

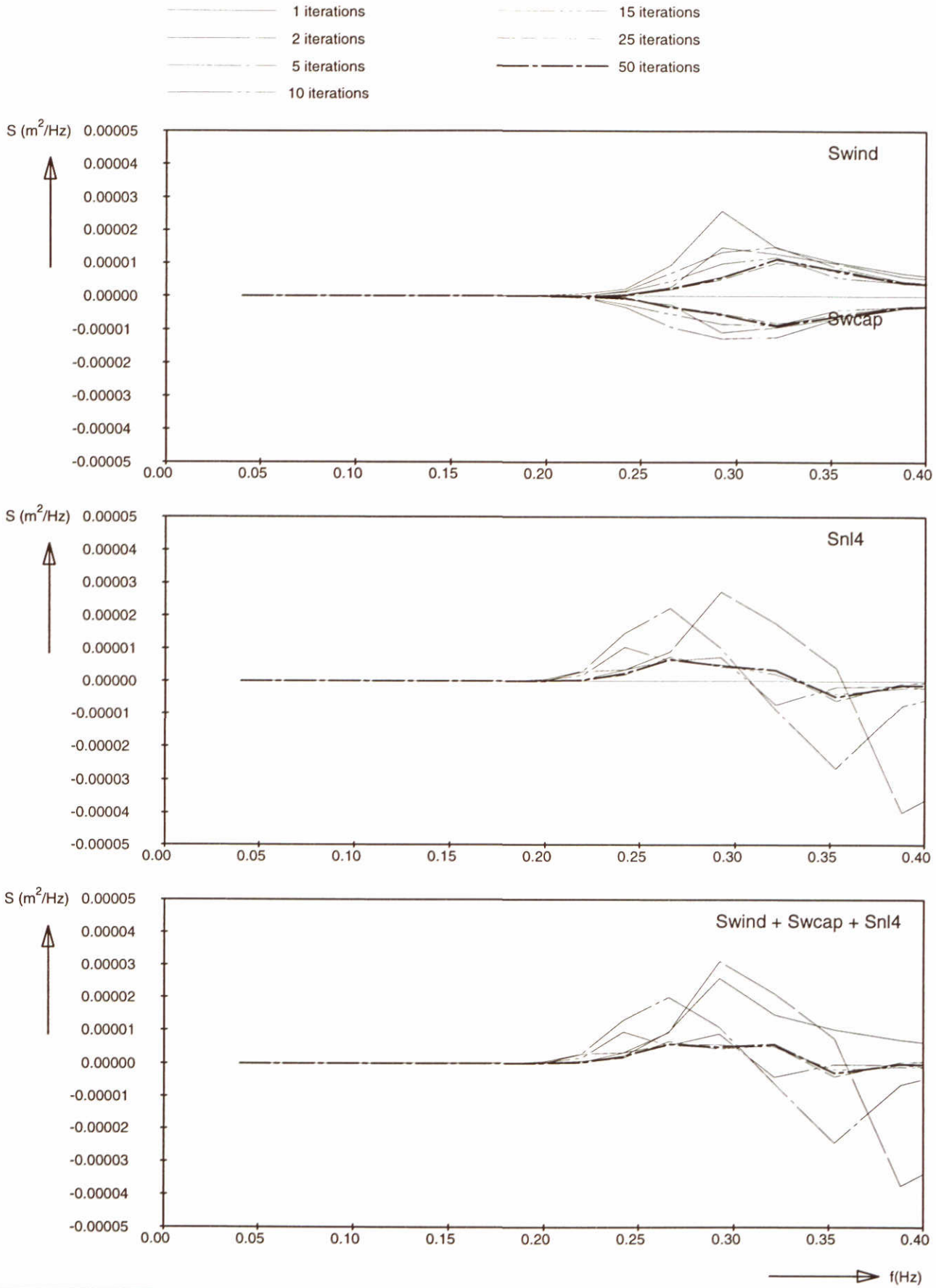

Source terms at x = 12.5 km Adapted wind speed: U_{10} = 10 m/s	SWAN-1D	U_{10}=10 m/s
WL | delft hydraulics	H3496	Fig. 14c

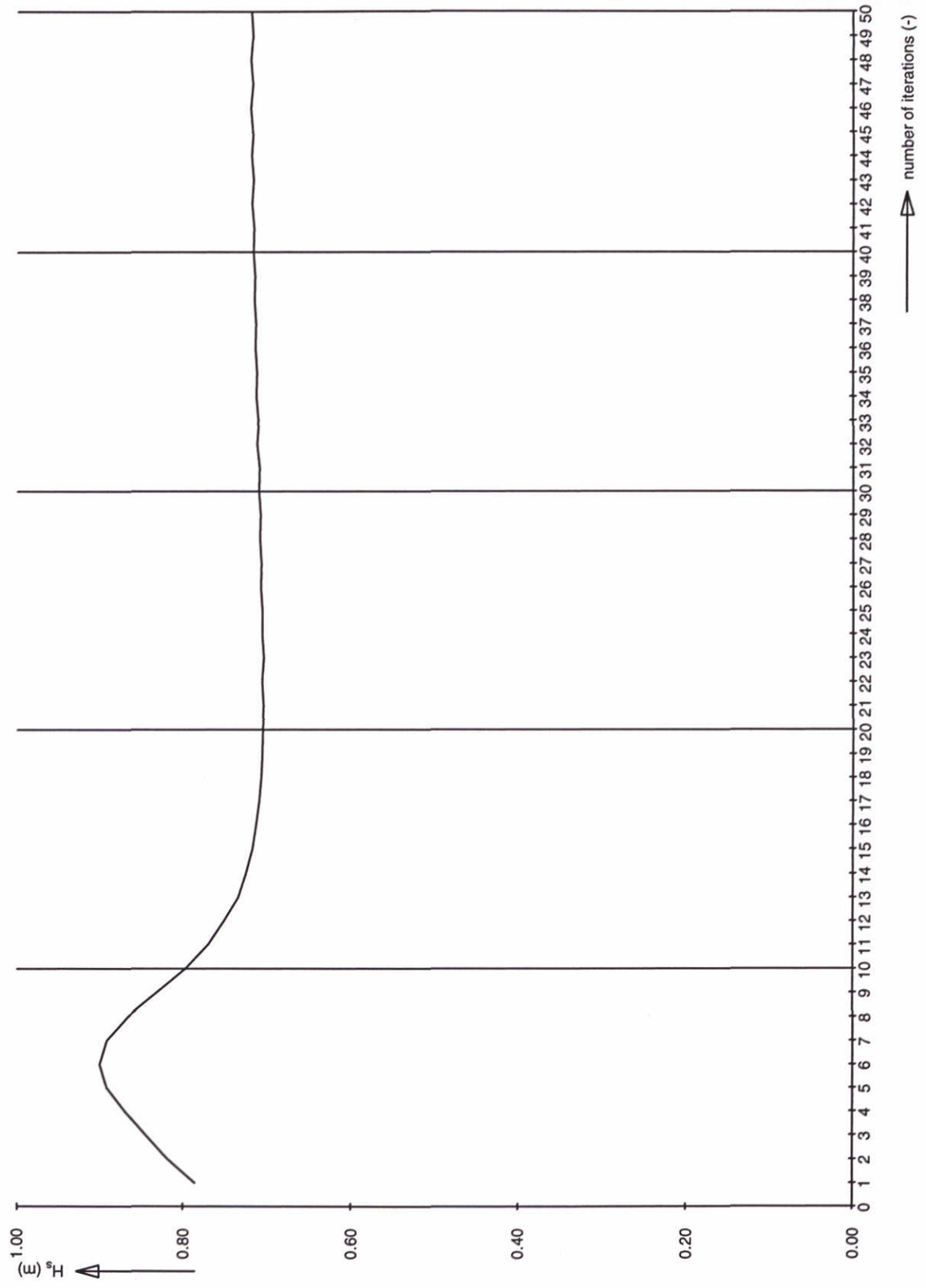

Significant wave height at 12.5 km Adapted wind speed: U_{10} = 10 m/s	SWAN-1D	U_{10}=10 m/s
WL | delft hydraulics	H3496	Fig. 14d

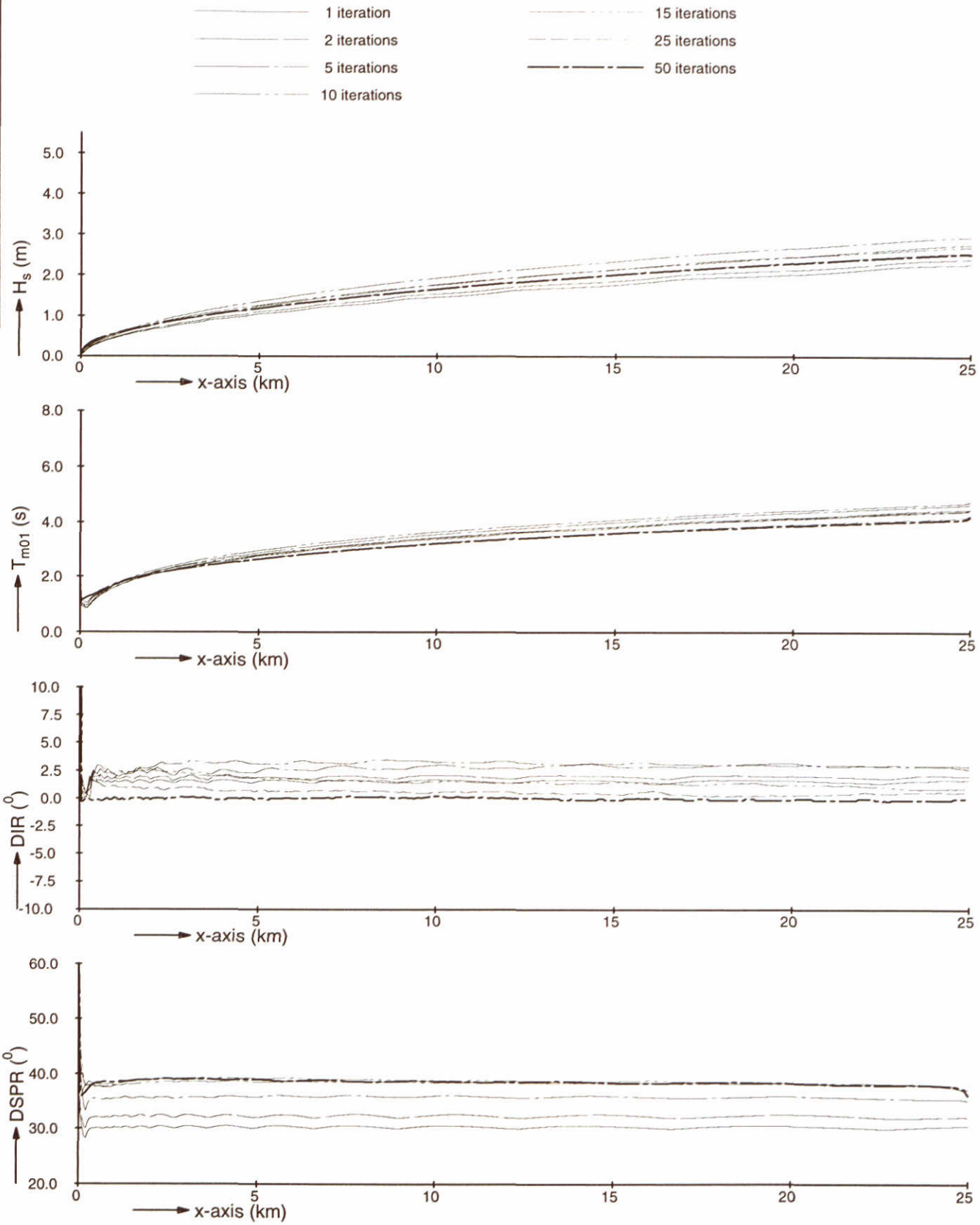

Model convergence behaviour using third-generation formulations
Adapted wind speed: U_{10} = 20 m/s

SWAN-1D	U_{10}=20 m/s

WL | delft hydraulics

H3496	Fig. 15a

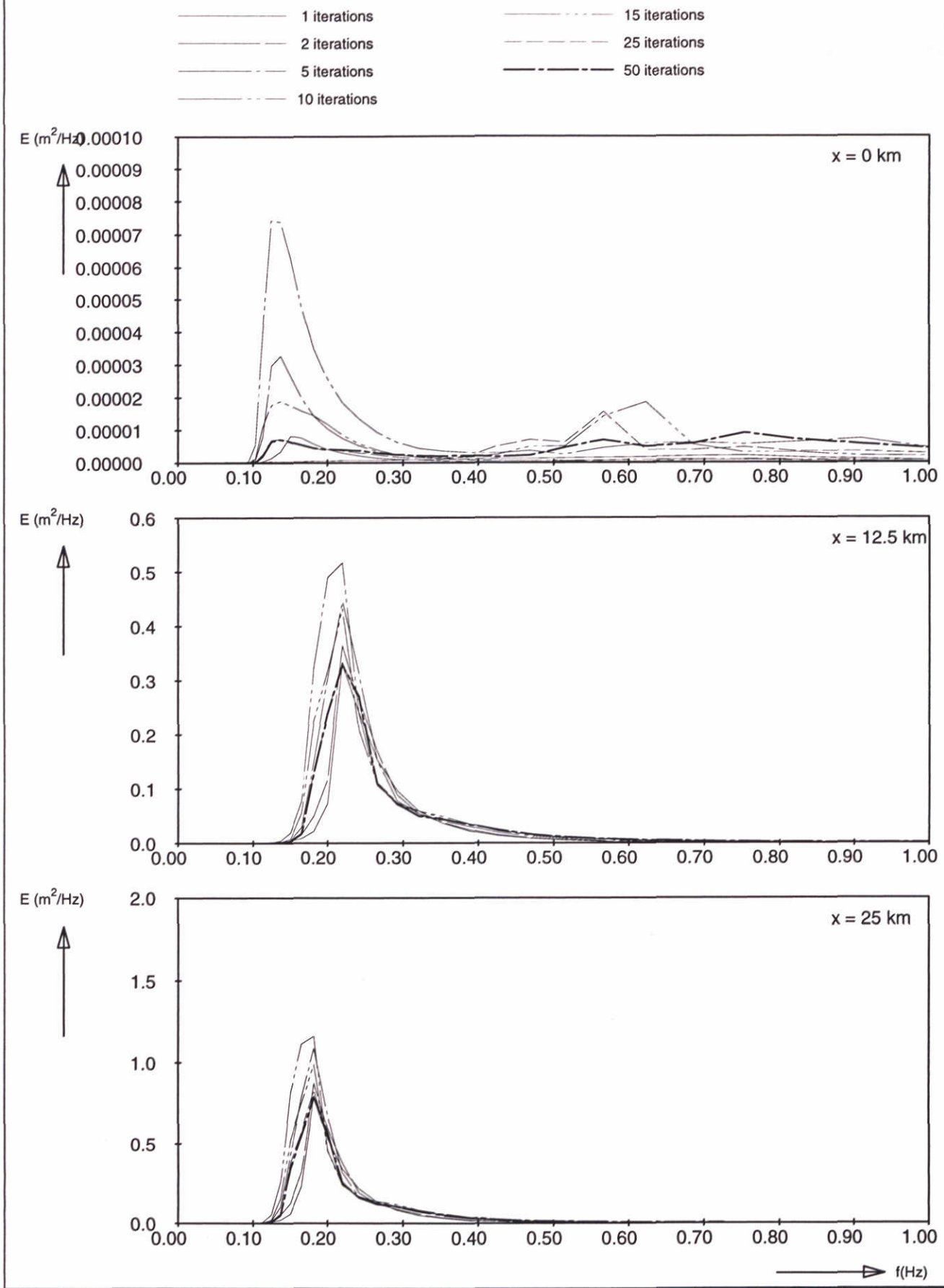

Frequency spectra at 3 locations Adapted wind speed: U_{10} = 20 m/s	SWAN-1D	U_{10}=20 m/s
WL | delft hydraulics	H3496	Fig. 15b

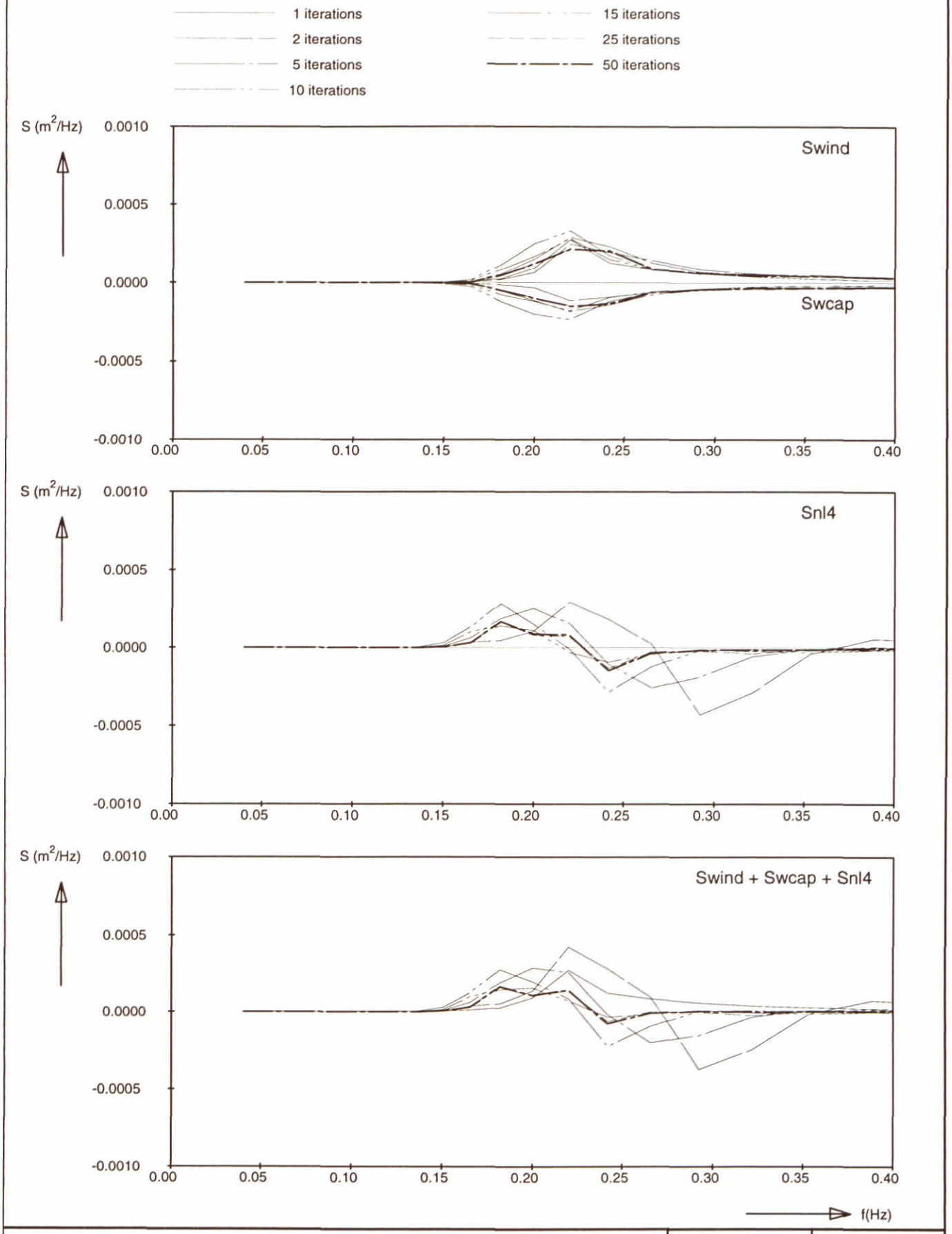

Source terms at x = 12.5 km
Adapted wind speed: U_{10} = 20 m/s

SWAN-1D	U_{10}=20 m/s

WL | delft hydraulics

H3496	Fig. 15c

Significant wave height at 12.5 km
Adapted wind speed: U_{10} = 20 m/s

SWAN-1D	U_{10}=20 m/s

WL | delft hydraulics

H3496	Fig. 15d

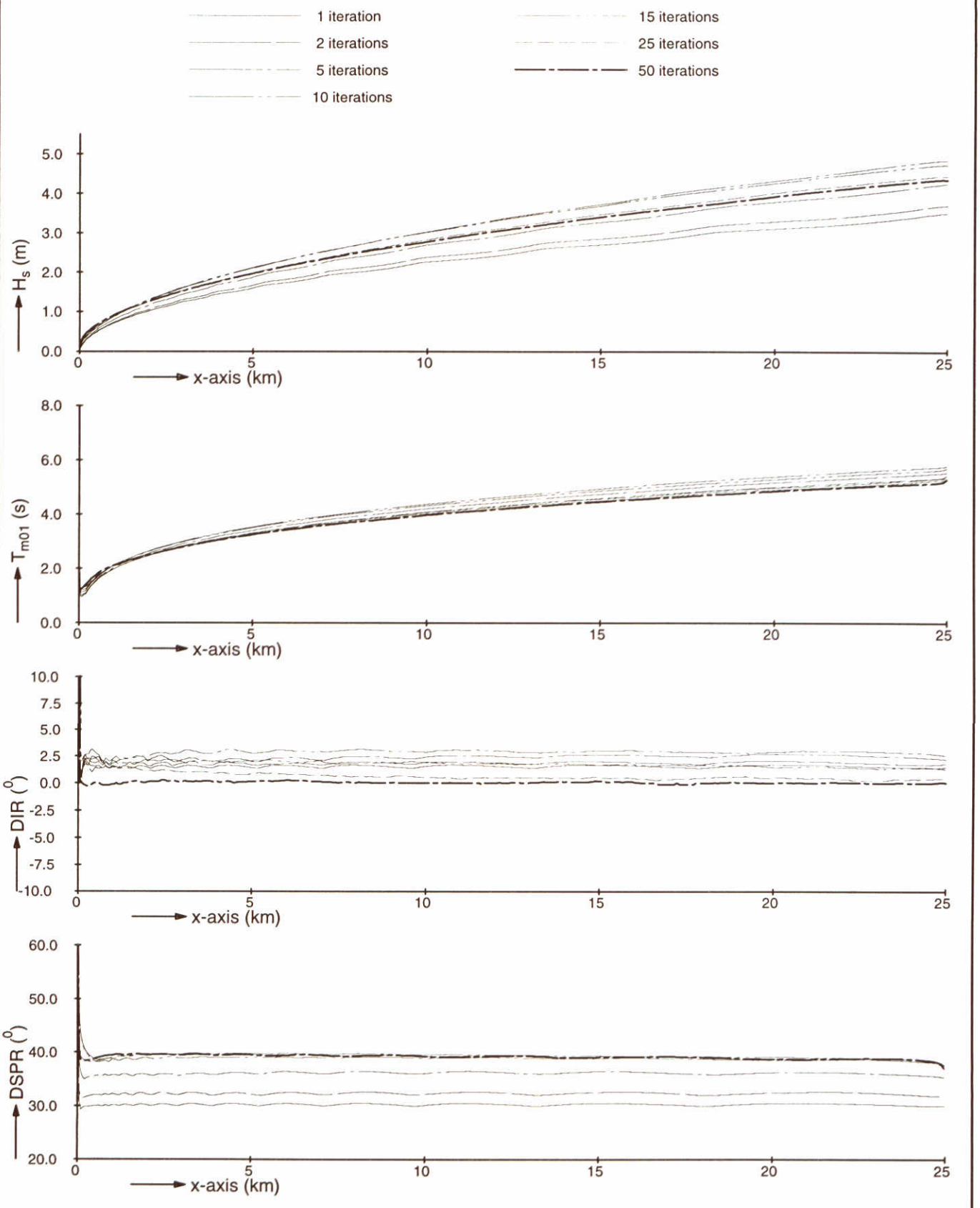

Model convergence behaviour using third-generation formulations
Standard computation (as case 4)

SWAN-1D	U_{10}=30 m/s

WL | delft hydraulics

H3496

Fig. 16a

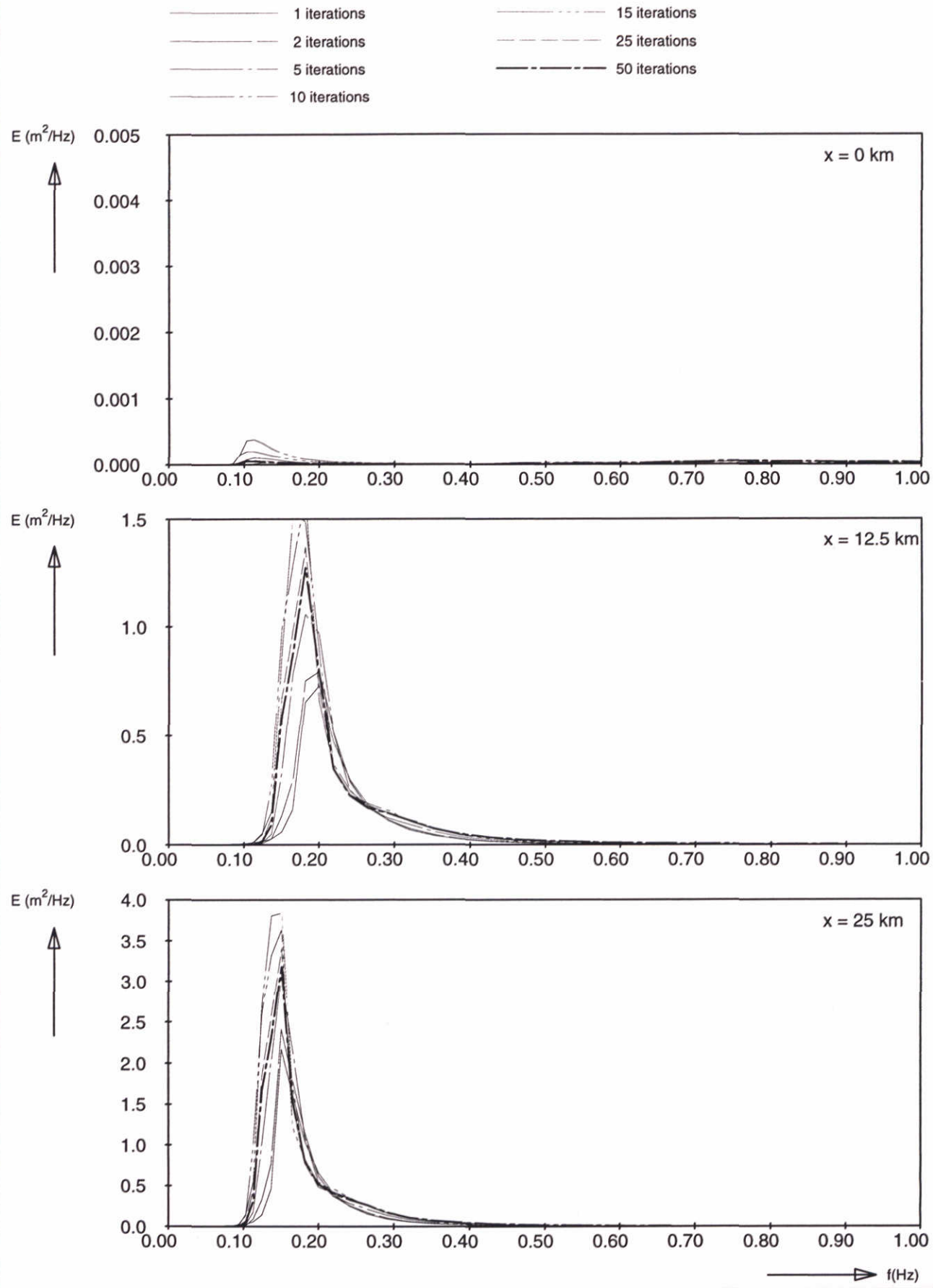

Frequency spectra at 3 locations Standard computation (as case 4)	SWAN-1D	U_{10}=30 m/s
WL | delft hydraulics	H3496	Fig. 16b

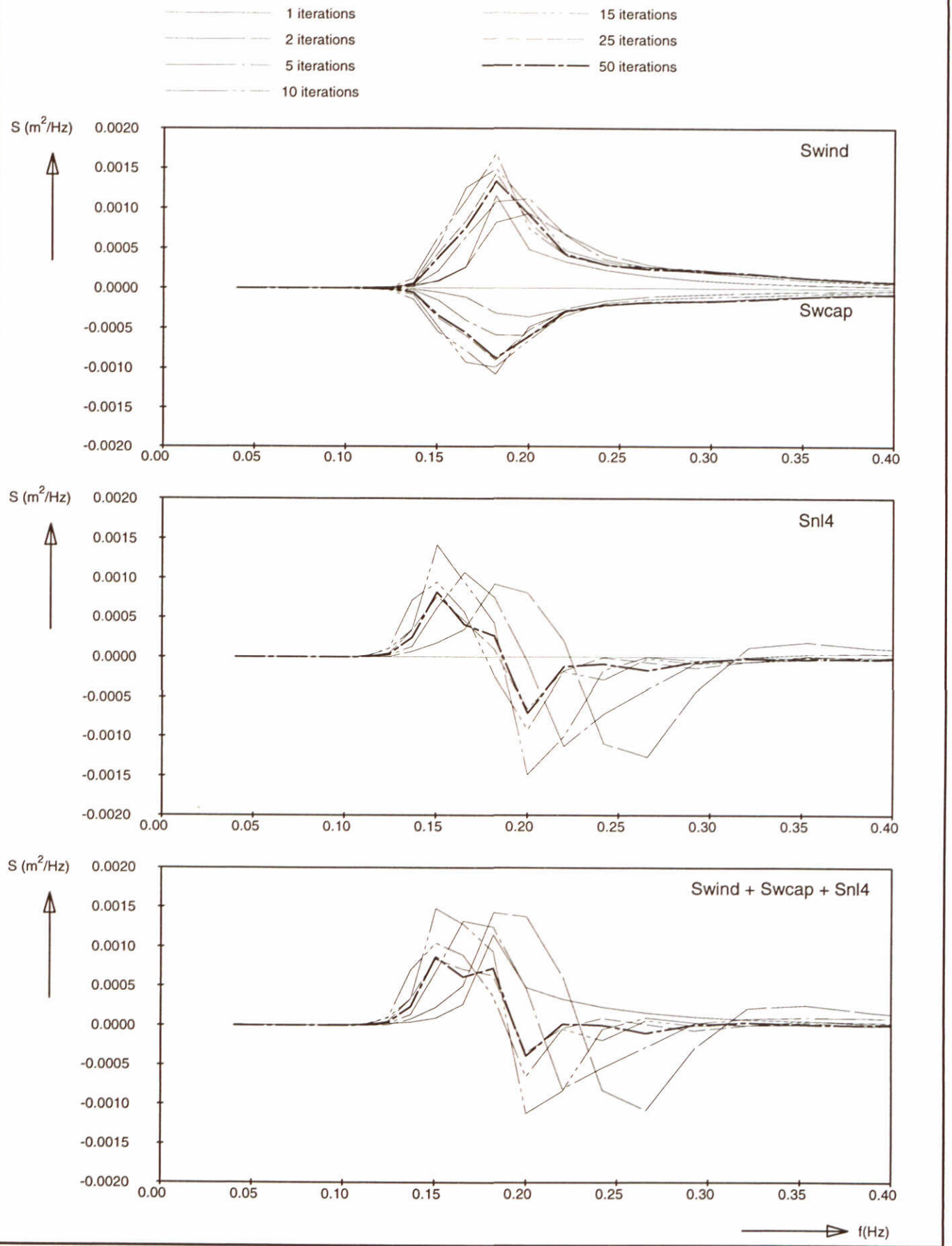

Source terms at x = 12.5 km
Standard computation (as case 4)

SWAN-1D

U_{10}=30 m/s

WL | delft hydraulics

H3496

Fig. 16c

Significant wave height at 12.5 km Standard computation (as case 4)	SWAN-1D	U_{10}=30 m/s
WL | delft hydraulics	H3496	Fig. 16d

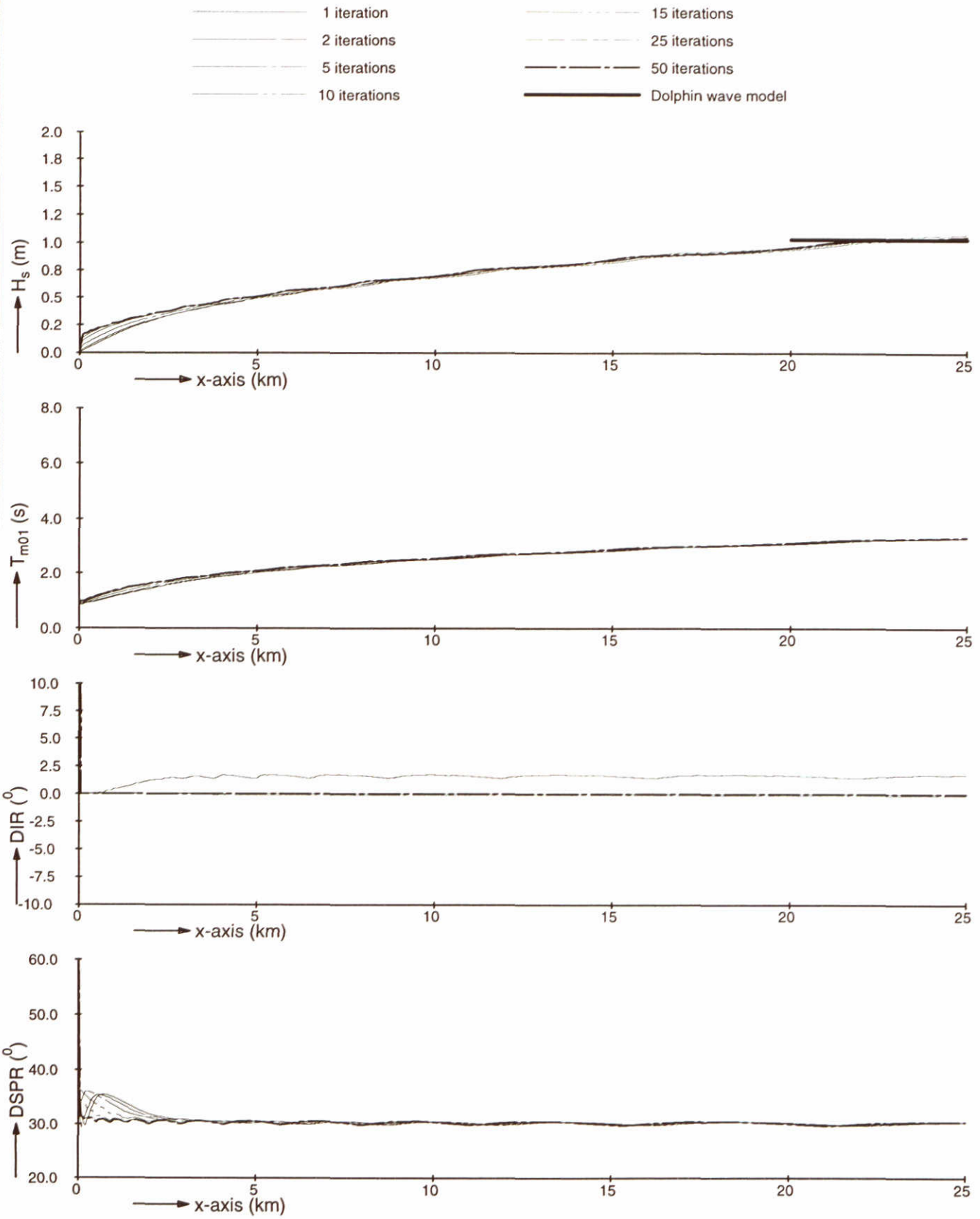

Model convergence behaviour using second-generation formulations
Adapted mode of SWAN (GEN2)

SWAN-1D

U_{10}=10 m/s

WL | delft hydraulics

H3496

Fig. 17a

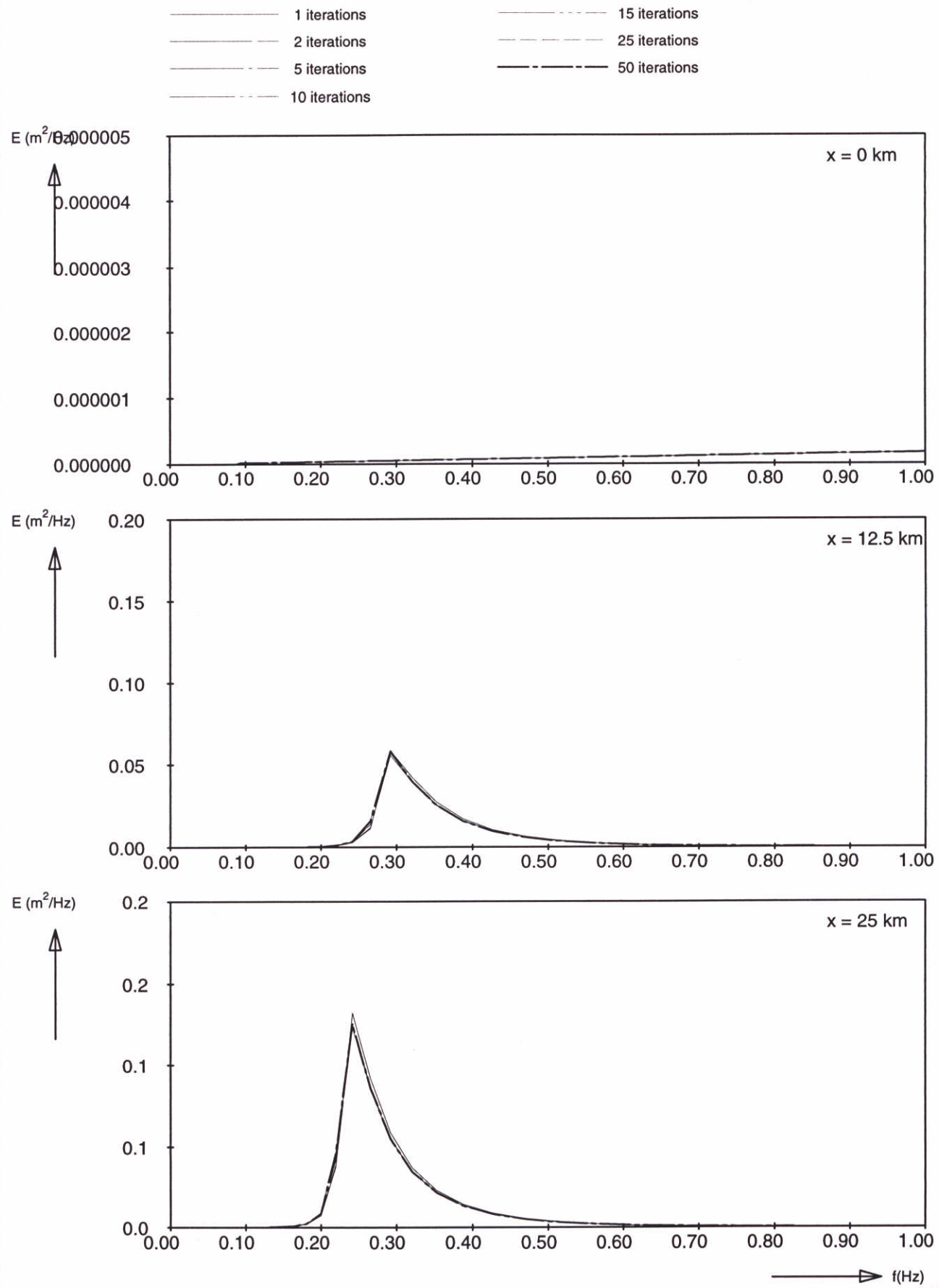

Frequency spectra at 3 locations Adapted mode of SWAN (GEN2)	SWAN-1D	U_{10}=10 m/s
WL | delft hydraulics	H3496	Fig. 17b

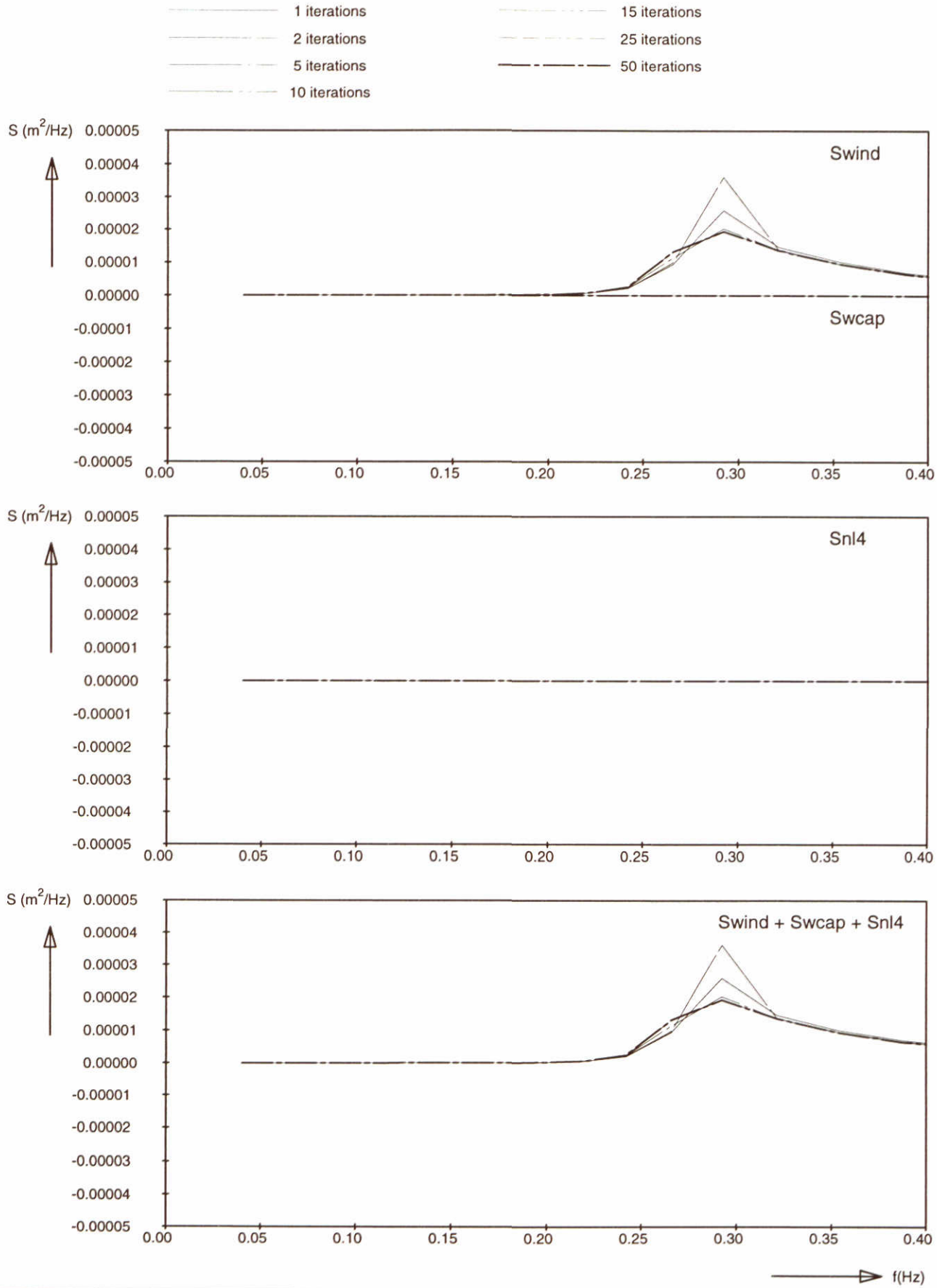

Source terms at x = 12.5 km Adapted mode of SWAN (GEN2)	SWAN-1D	U_{10}=10 m/s
WL | delft hydraulics	H3496	Fig. 17c

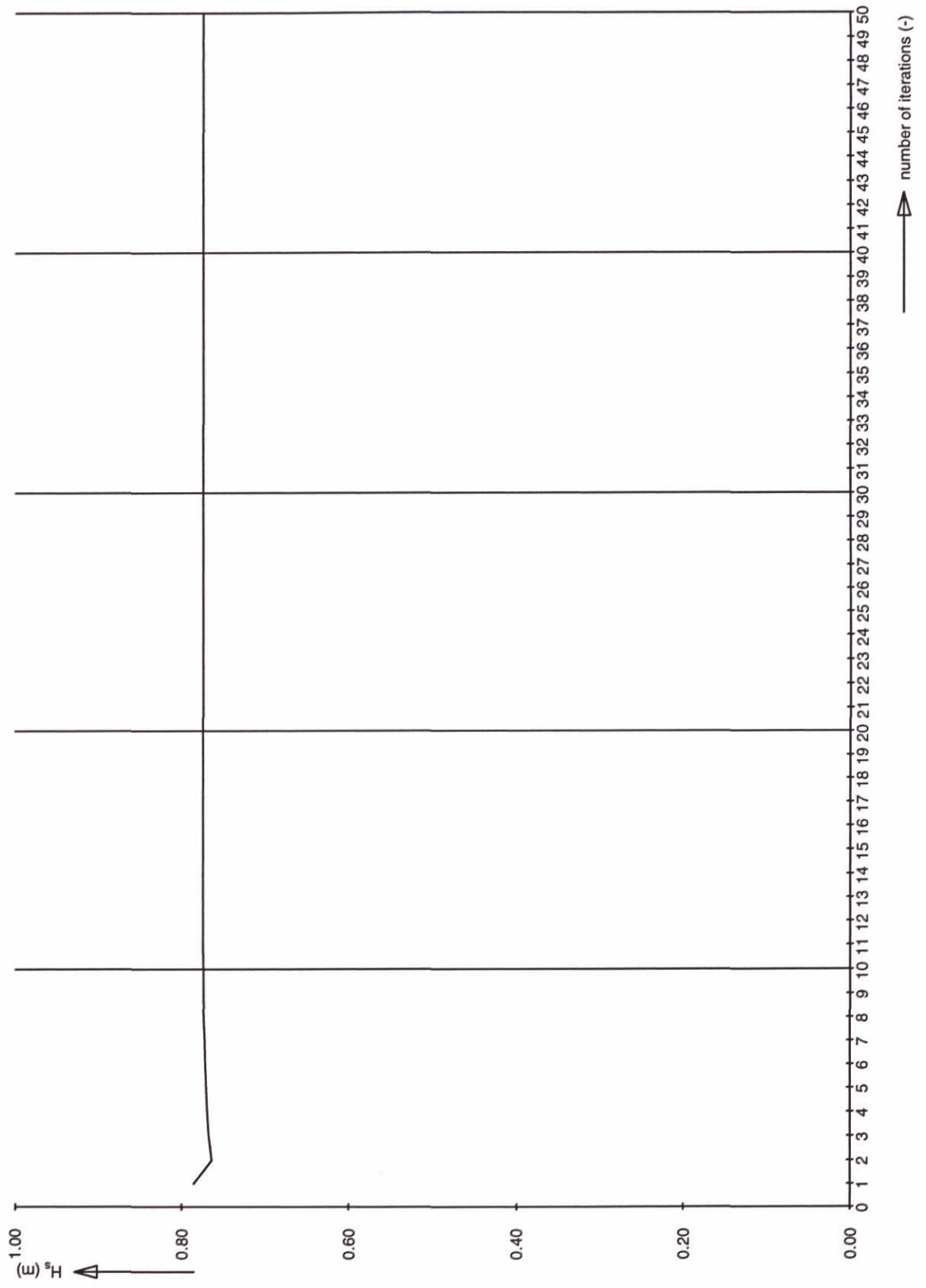

Significant wave height at 12.5 km Adapted mode of SWAN (GEN2)	SWAN-1D	U_{10}=10 m/s
WL | delft hydraulics	H3496	Fig. 17d

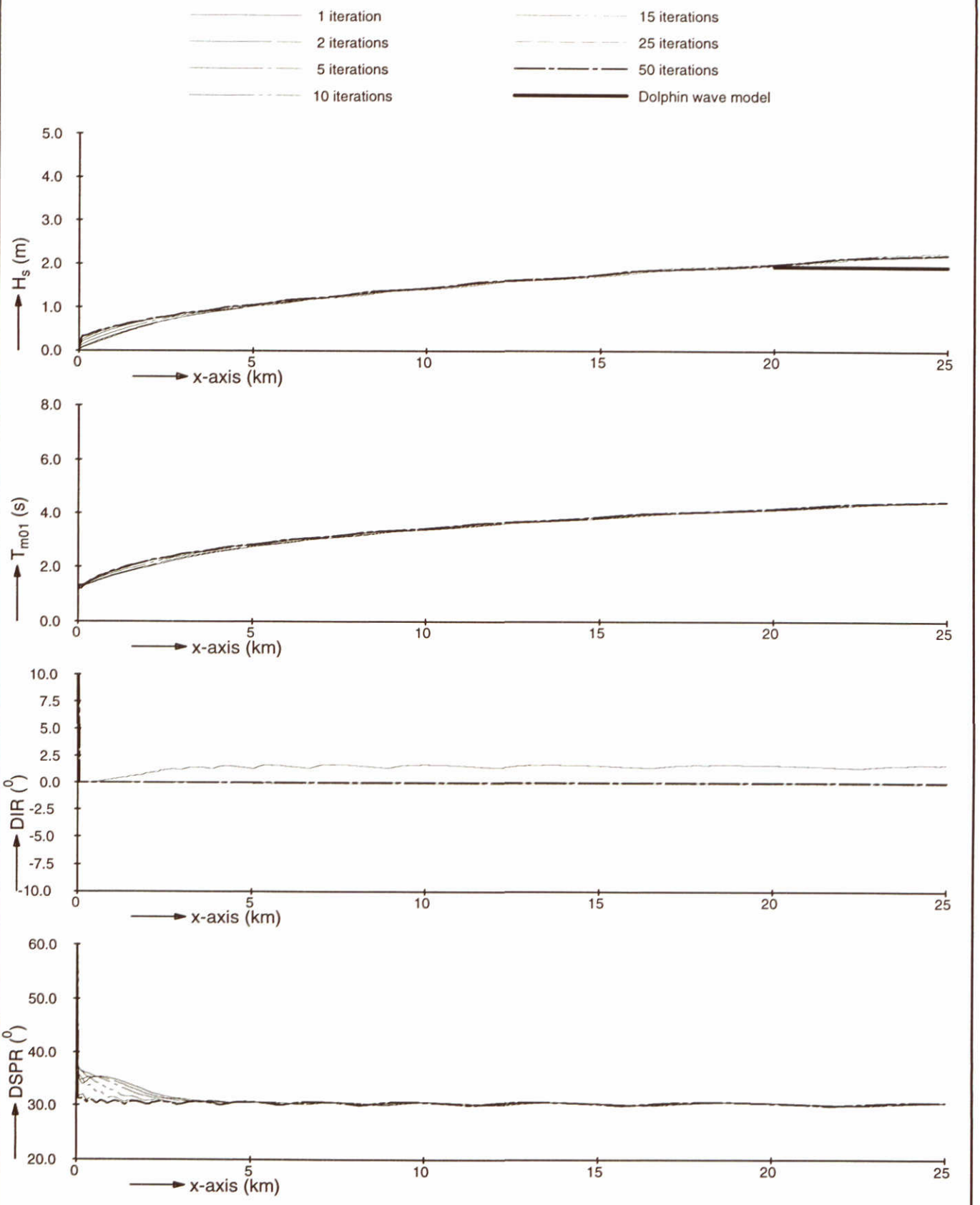

Model convergence behaviour using second-generation formulations
Adapted mode of SWAN (GEN2)

SWAN-1D

U_{10}=20 m/s

WL | delft hydraulics

H3496

Fig. 18a

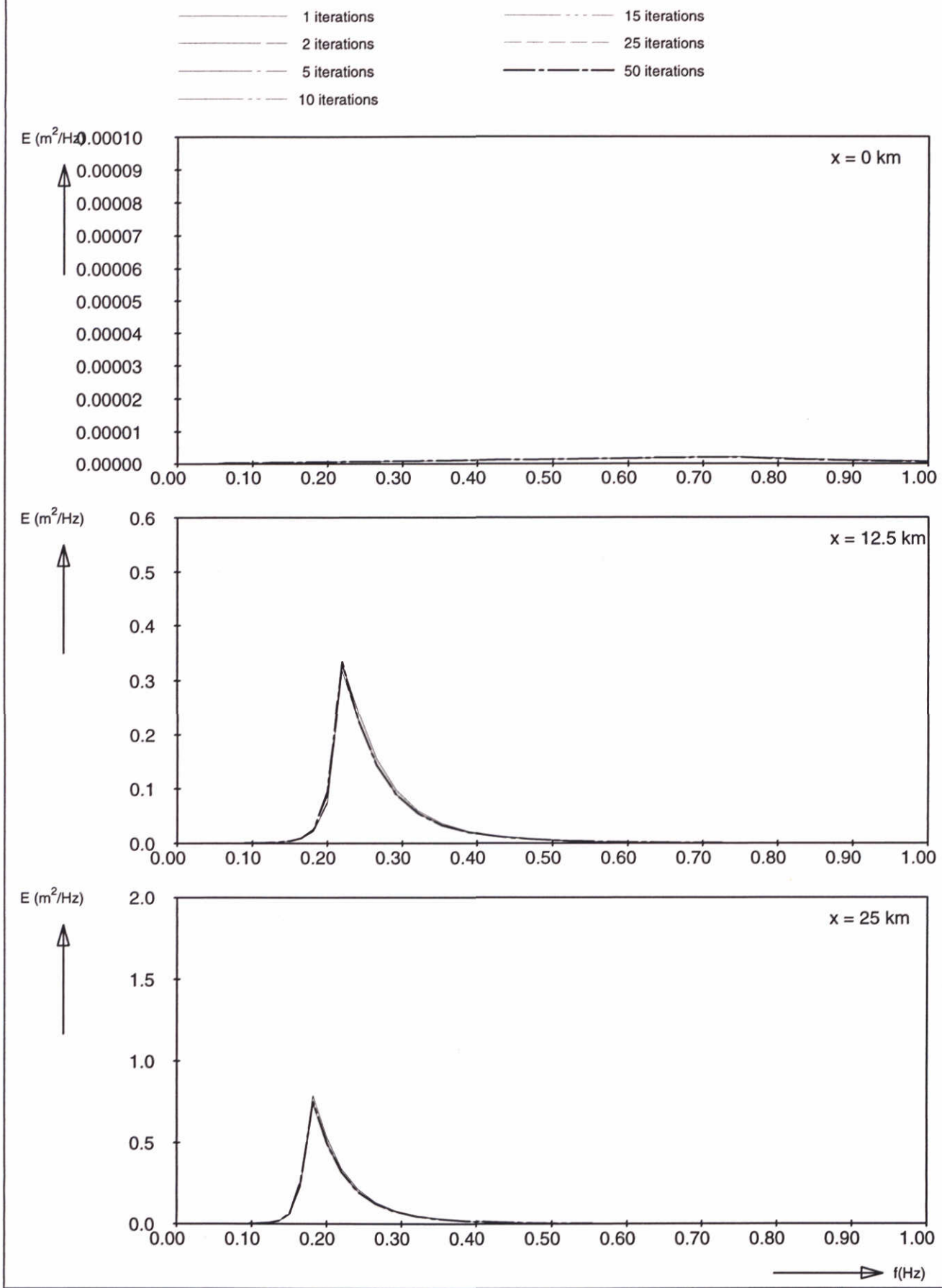

Frequency spectra at 3 locations Adapted mode of SWAN (GEN2)	SWAN-1D	U_{10}=20 m/s
WL | delft hydraulics	H3496	Fig. 18b

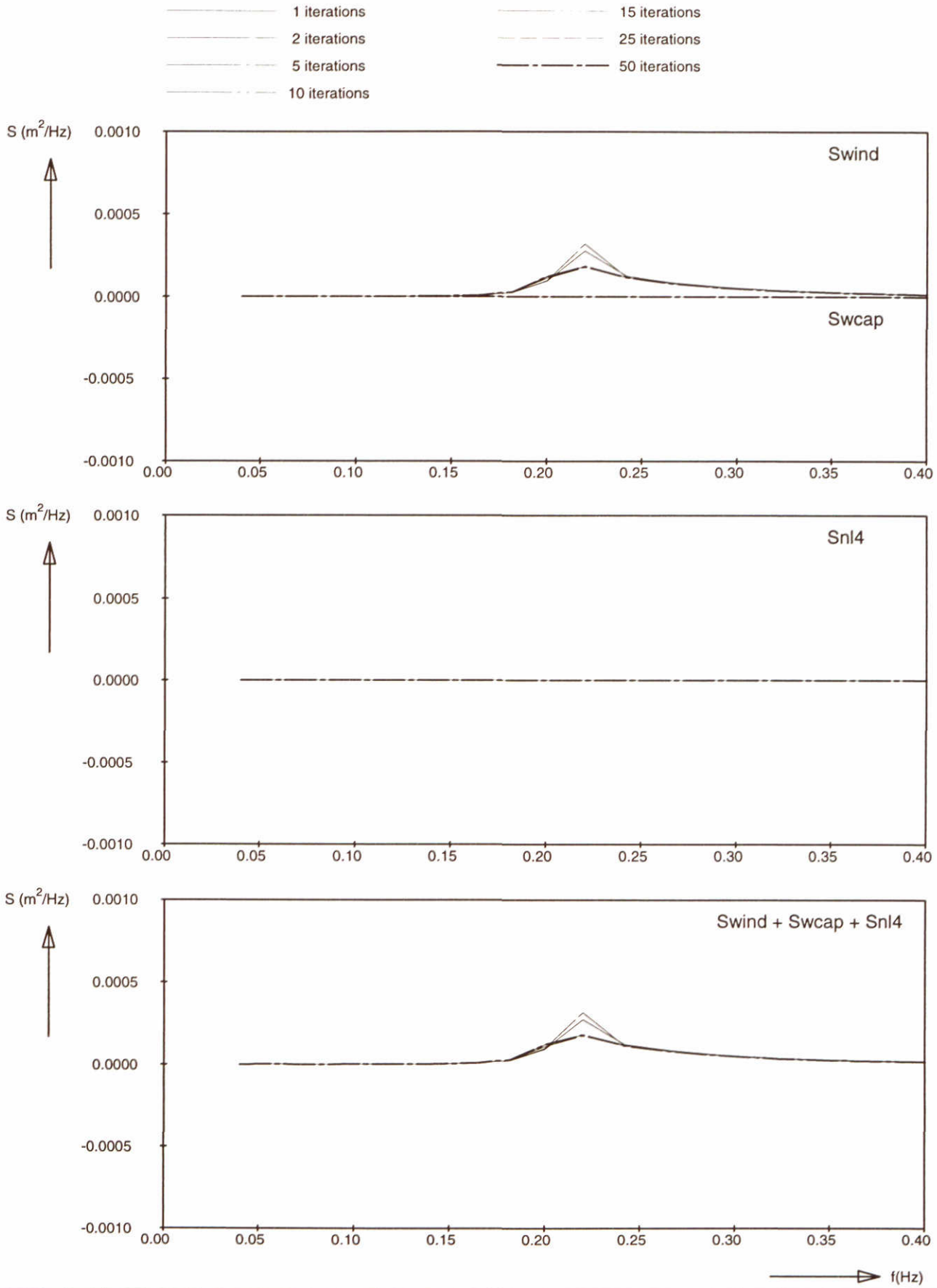

Source terms at x = 12.5 km Adapted mode of SWAN (GEN2)	SWAN-1D	U_{10}=20 m/s
WL | delft hydraulics	H3496	Fig. 18c

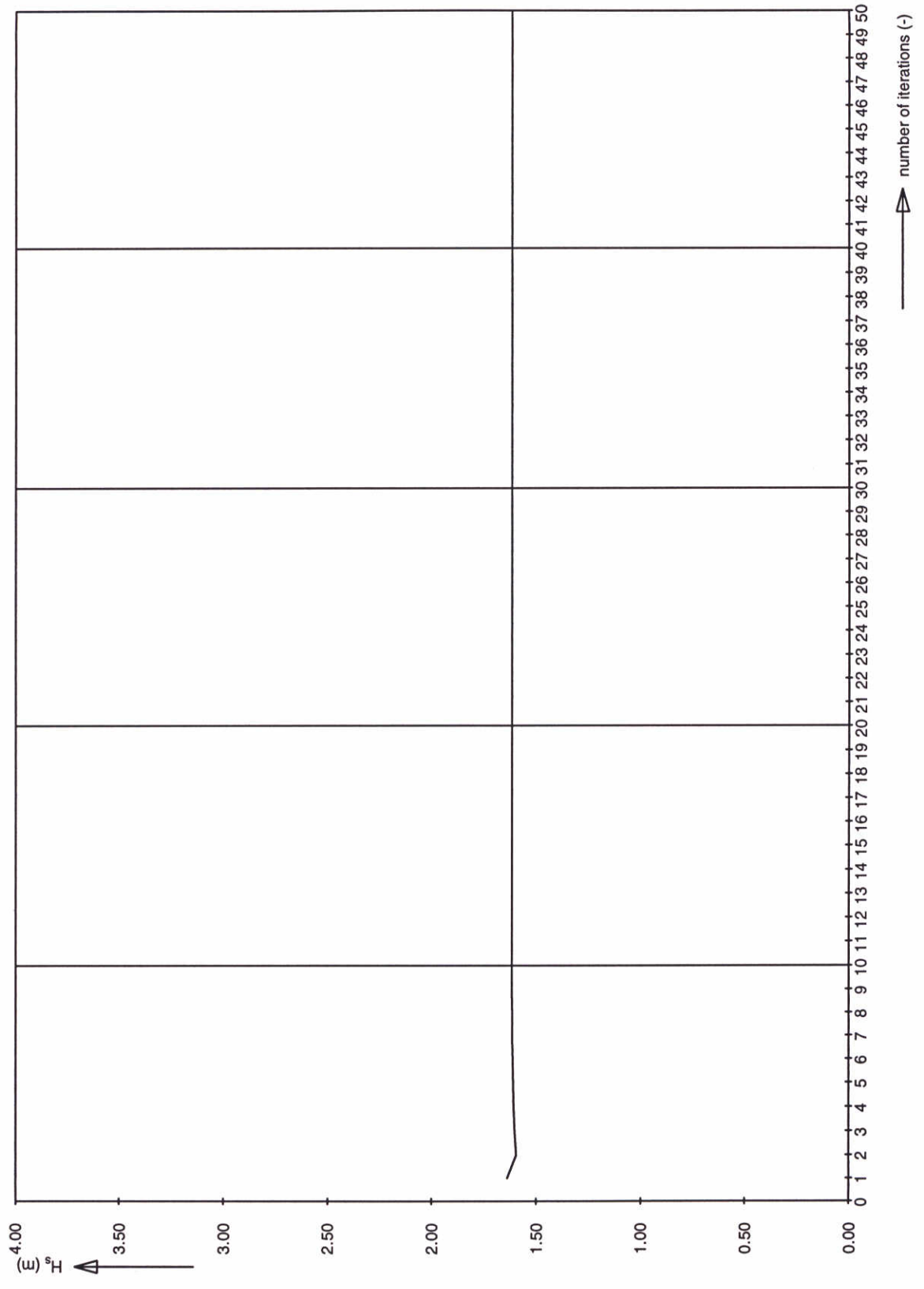

Significant wave height at 12.5 km Adapted mode of SWAN (GEN2)	SWAN-1D	U_{10}=20 m/s
WL | delft hydraulics	H3496	Fig. 18d

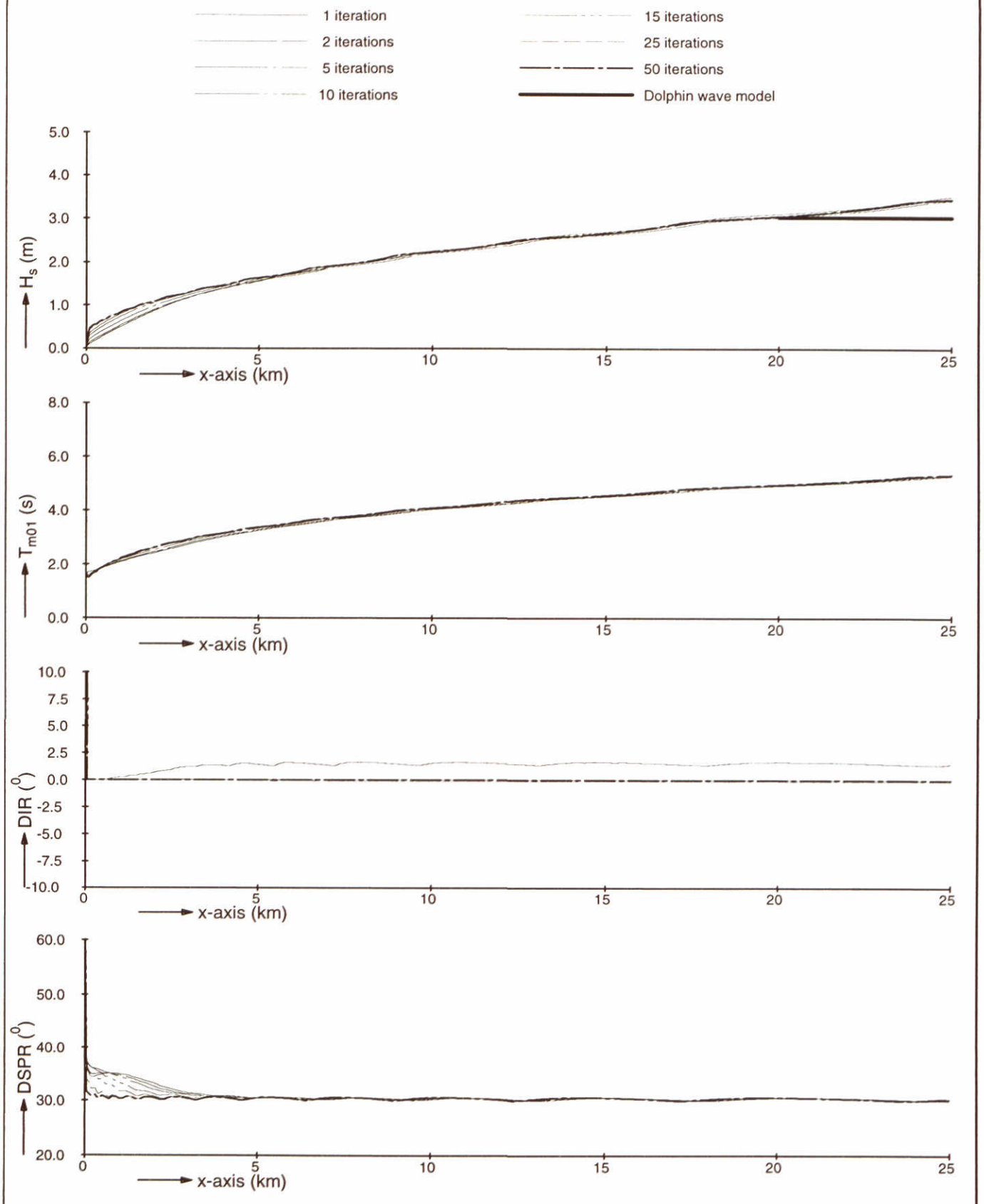

Model convergence behaviour using second-generation formulations
Adapted mode of SWAN (GEN2)

SWAN-1D

U_{10}=30 m/s

WL | delft hydraulics

H3496

Fig. 19a

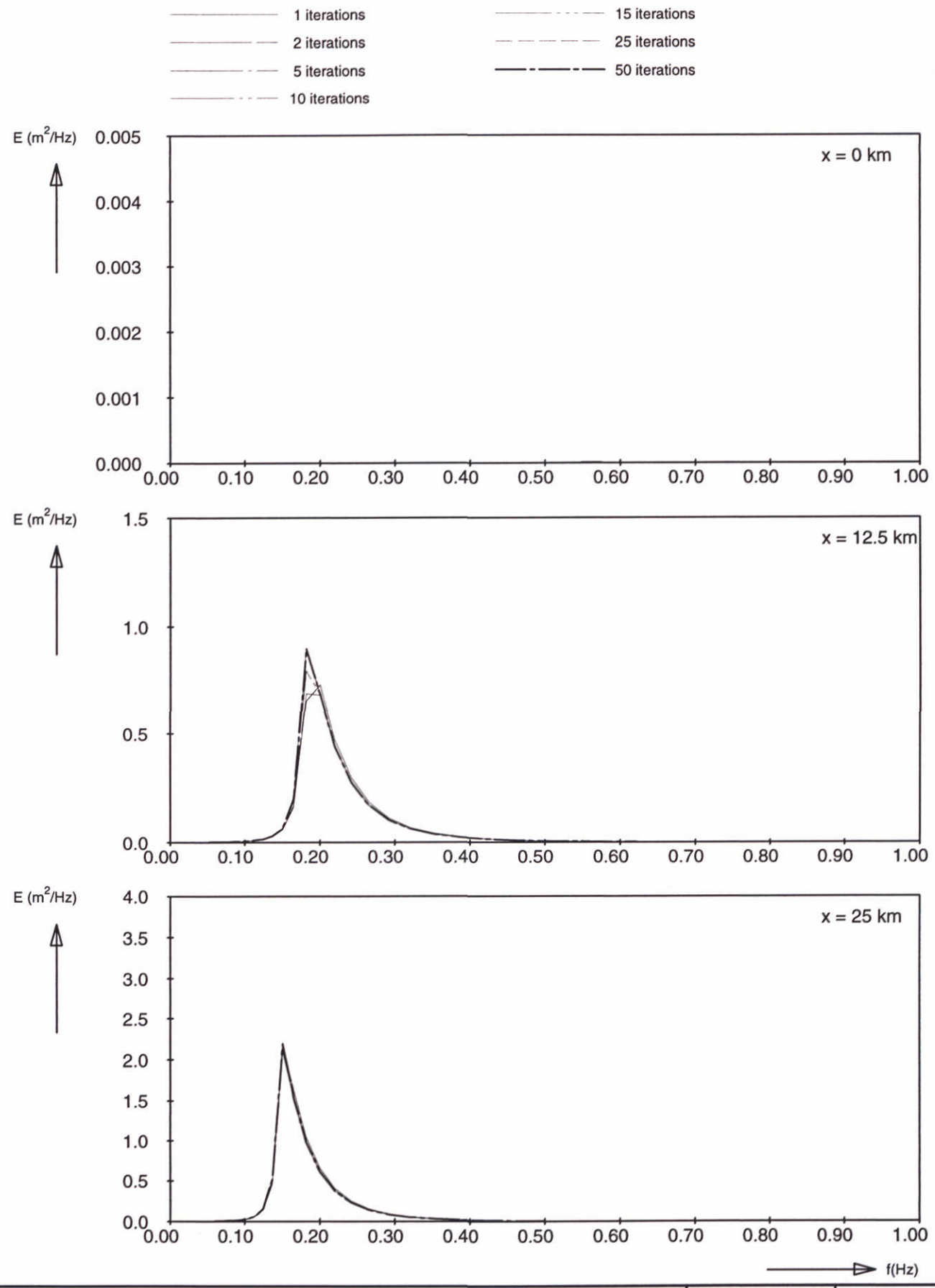

Frequency spectra at 3 locations Adapted mode of SWAN (GEN2)	SWAN-1D	U_{10}=30 m/s
WL | delft hydraulics	H3496	Fig. 19b

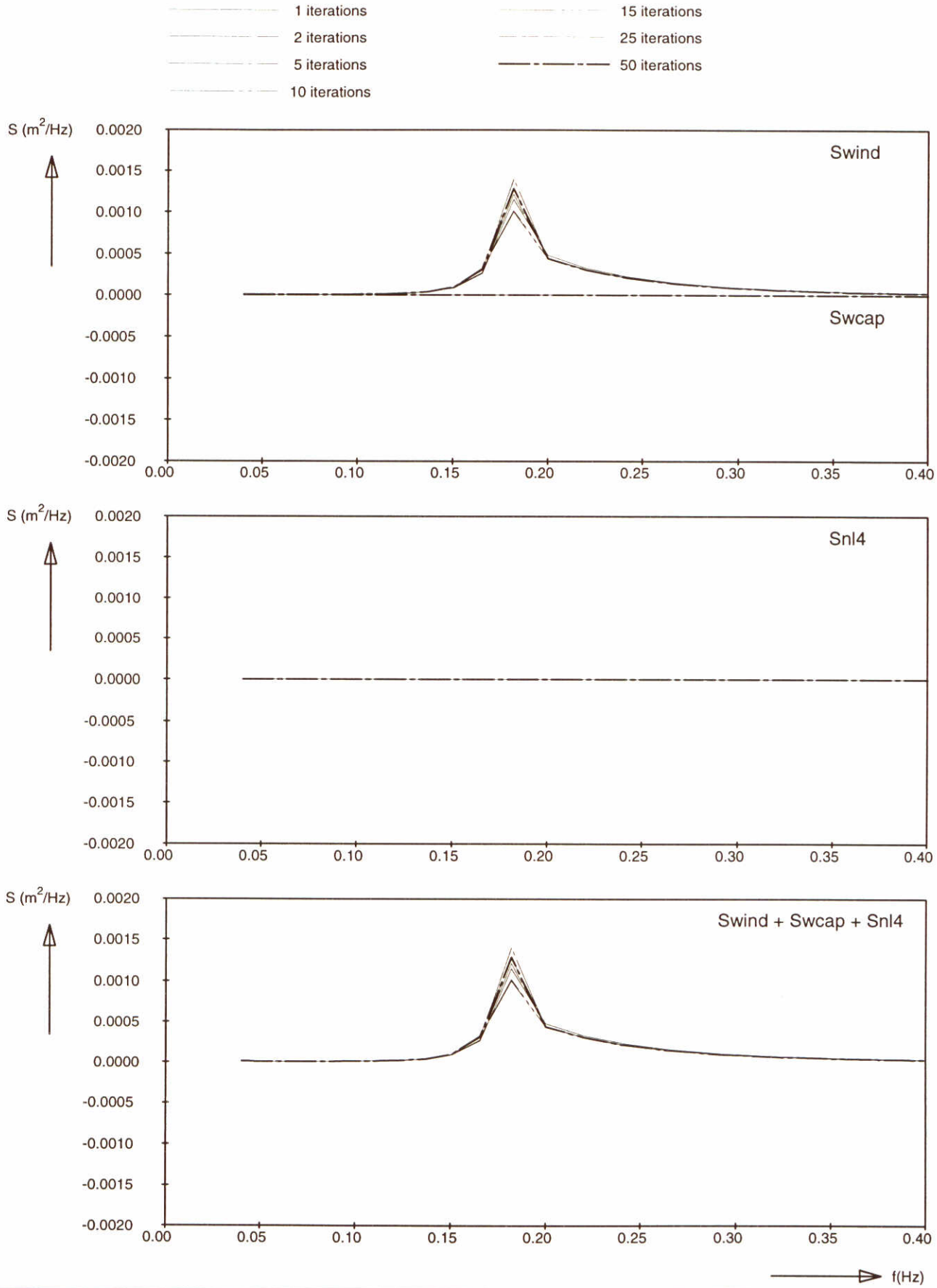

Source terms at x = 12.5 km
Adapted mode of SWAN (GEN2)

SWAN-1D

U_{10}=30 m/s

WL | delft hydraulics

H3496

Fig. 19c

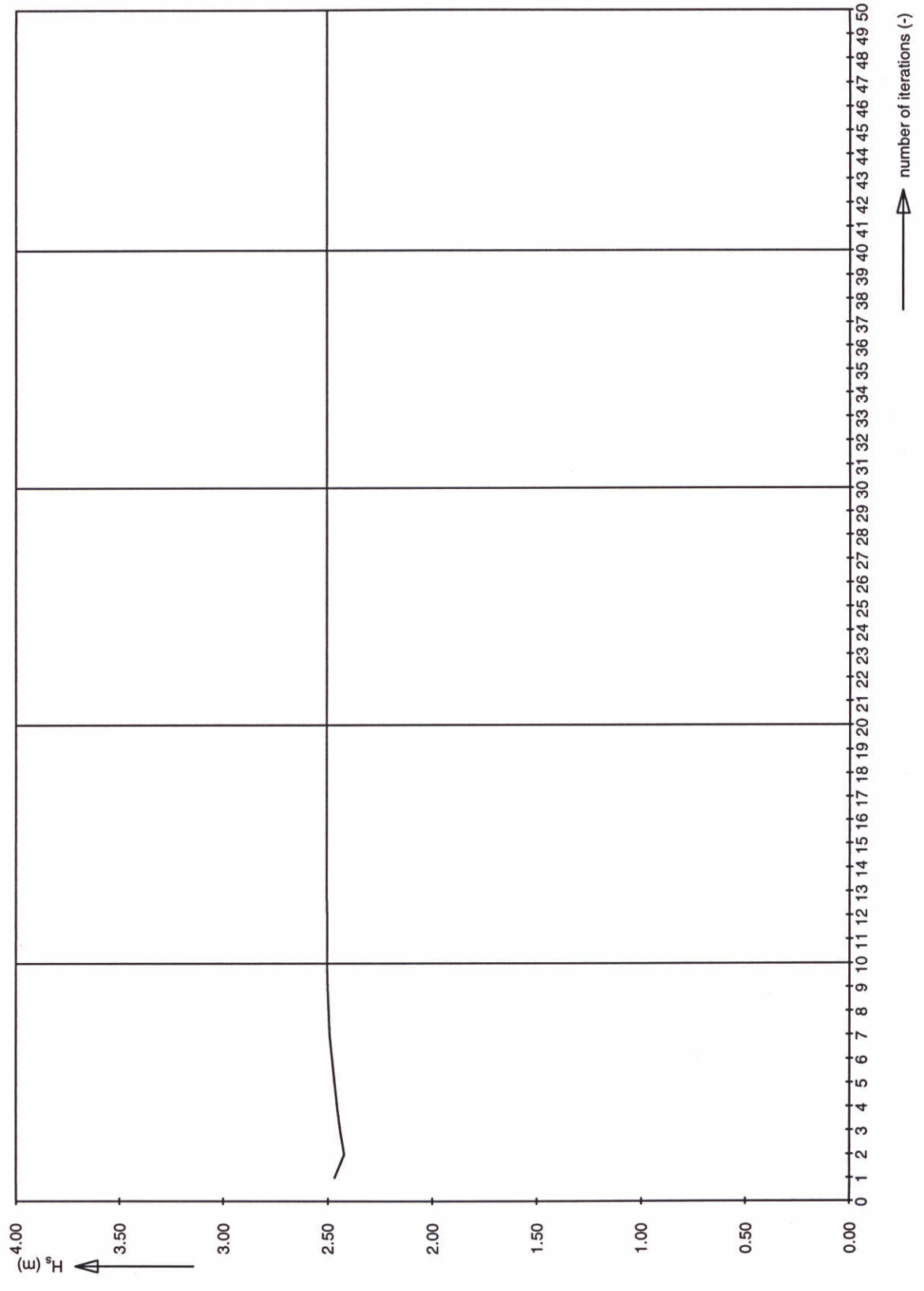

Significant wave height at 12.5 km Adapted mode of SWAN (GEN2)	SWAN-1D	U_{10}=30 m/s
WL | delft hydraulics	H3496	Fig. 19d

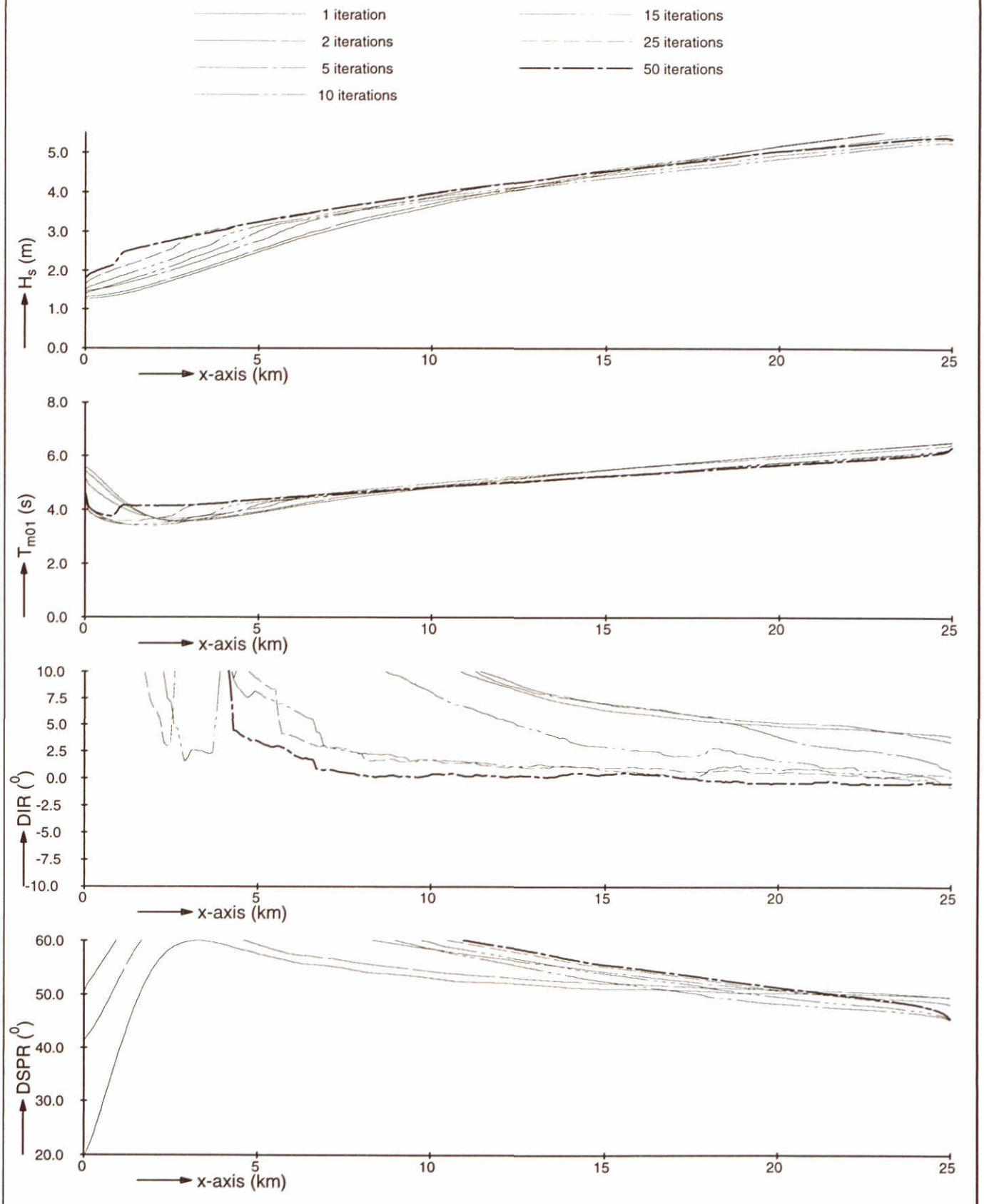

Model convergence behaviour using second-generation formulations
Second generation mode of SWAN but with
quadruplets activated (limiter = 10%)

SWAN-1D

U_{10}=30 m/s

WL | delft hydraulics

H3496

Fig. 20a

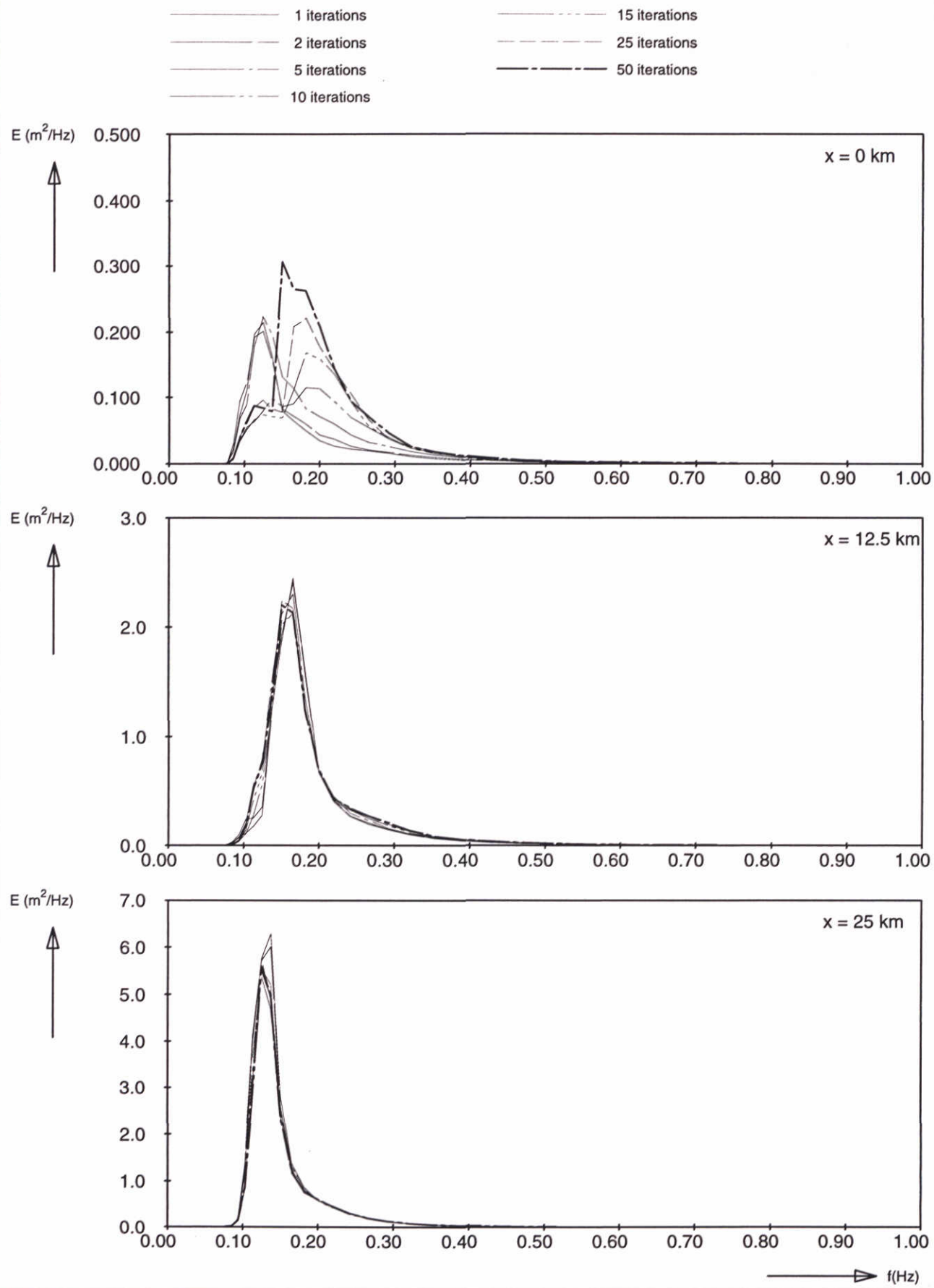

Frequency spectra at 3 locations Second generation mode of SWAN but with quadruplets activated (limiter = 10%)	SWAN-1D	U_{10}=30 m/s
WL | delft hydraulics	H3496	Fig. 20b

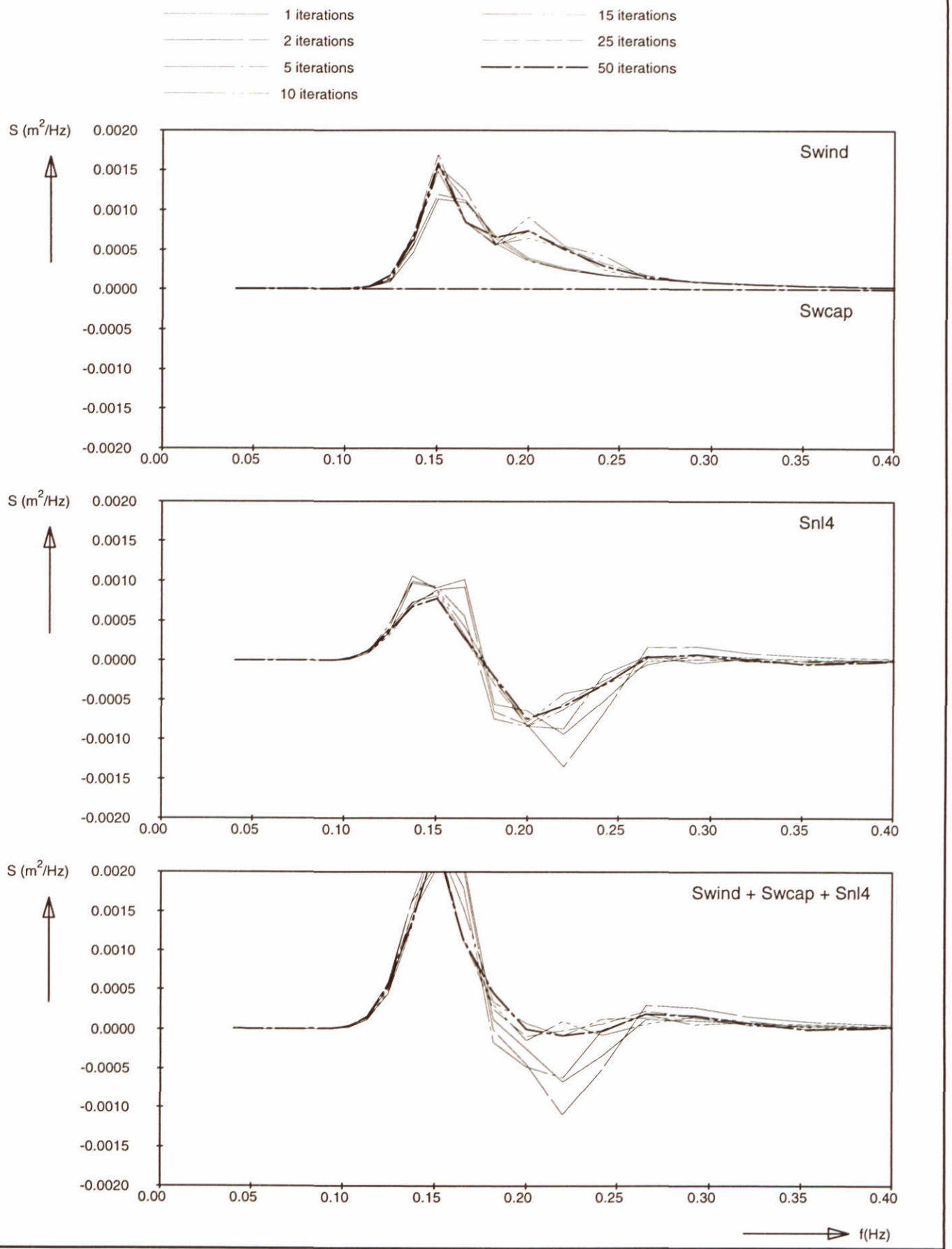

Source terms at x = 12.5 km
Second generation mode of SWAN but with
quadruplets activated (limiter = 10%)

SWAN-1D

U_{10}=30 m/s

WL | delft hydraulics

H3496

Fig. 20c

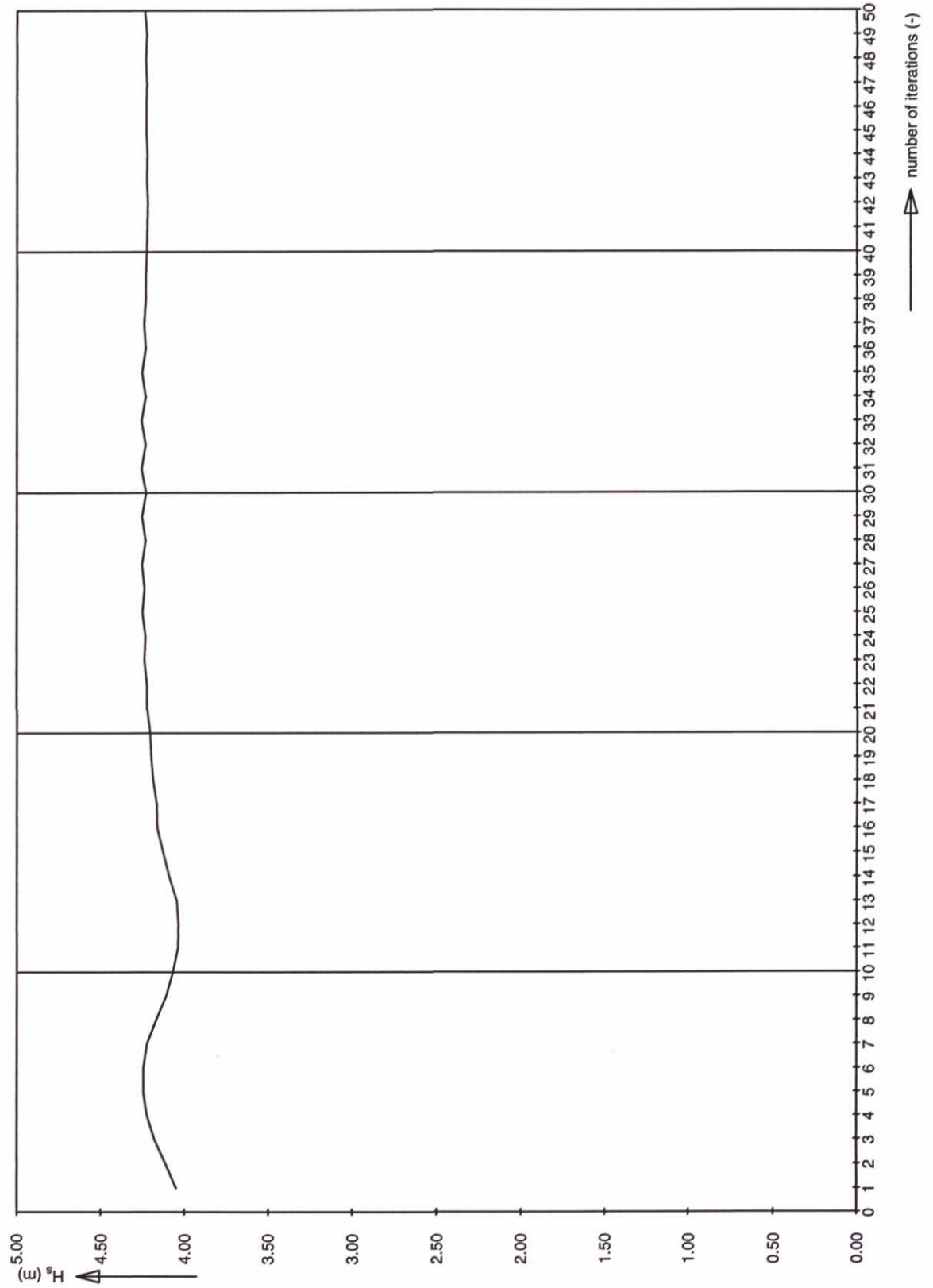

Significant wave height at 12.5 km Second generation mode of SWAN but with quadruplets activated (limiter = 10%)	SWAN-1D	U_{10}=30 m/s
WL | delft hydraulics	H3496	Fig. 20d

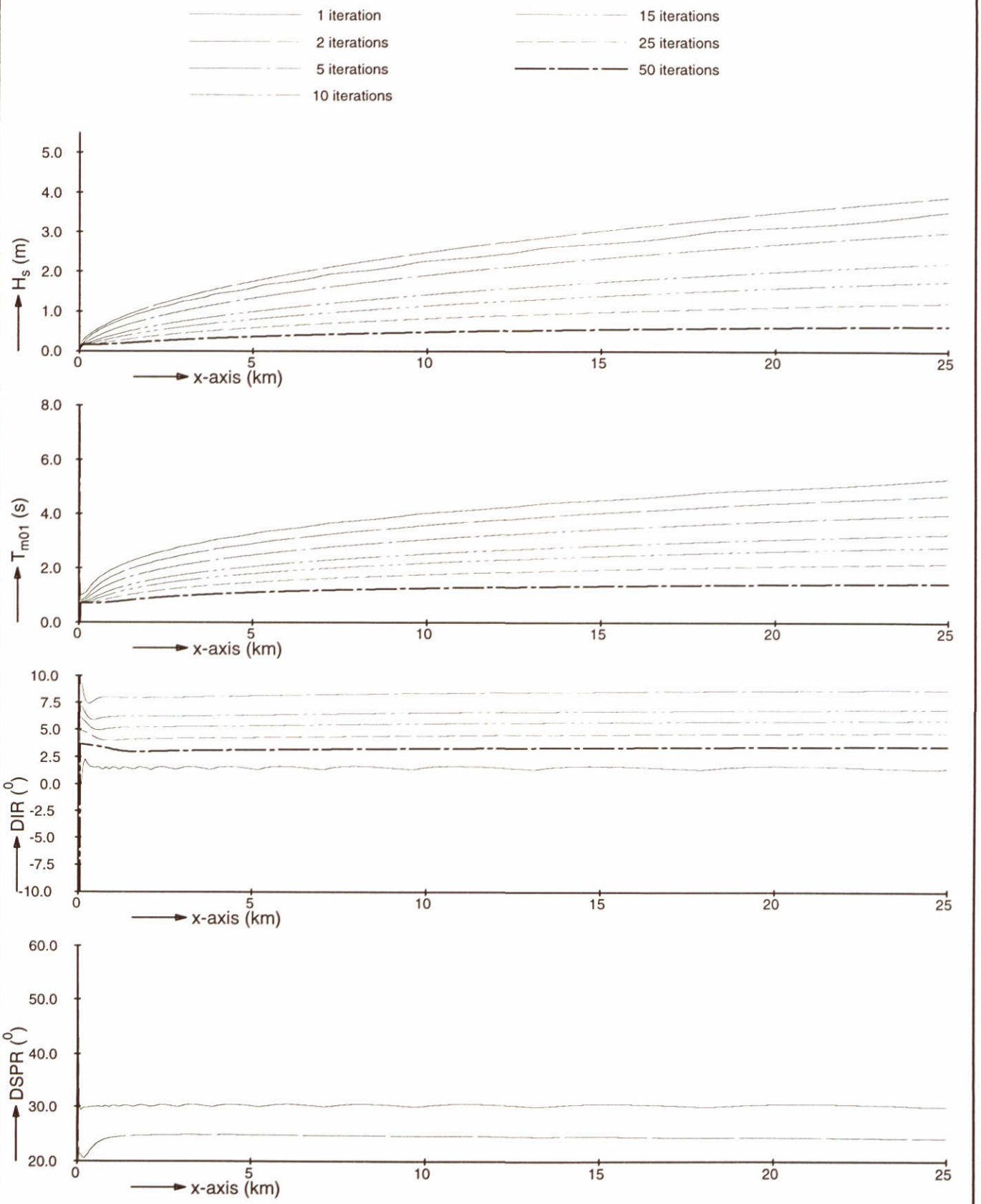

Model convergence behaviour using third-generation formulations Deactivated: Quadruplets Limiter = 10%	SWAN-1D	U_{10}=30 m/s
WL | delft hydraulics	H3496	Fig. 21a

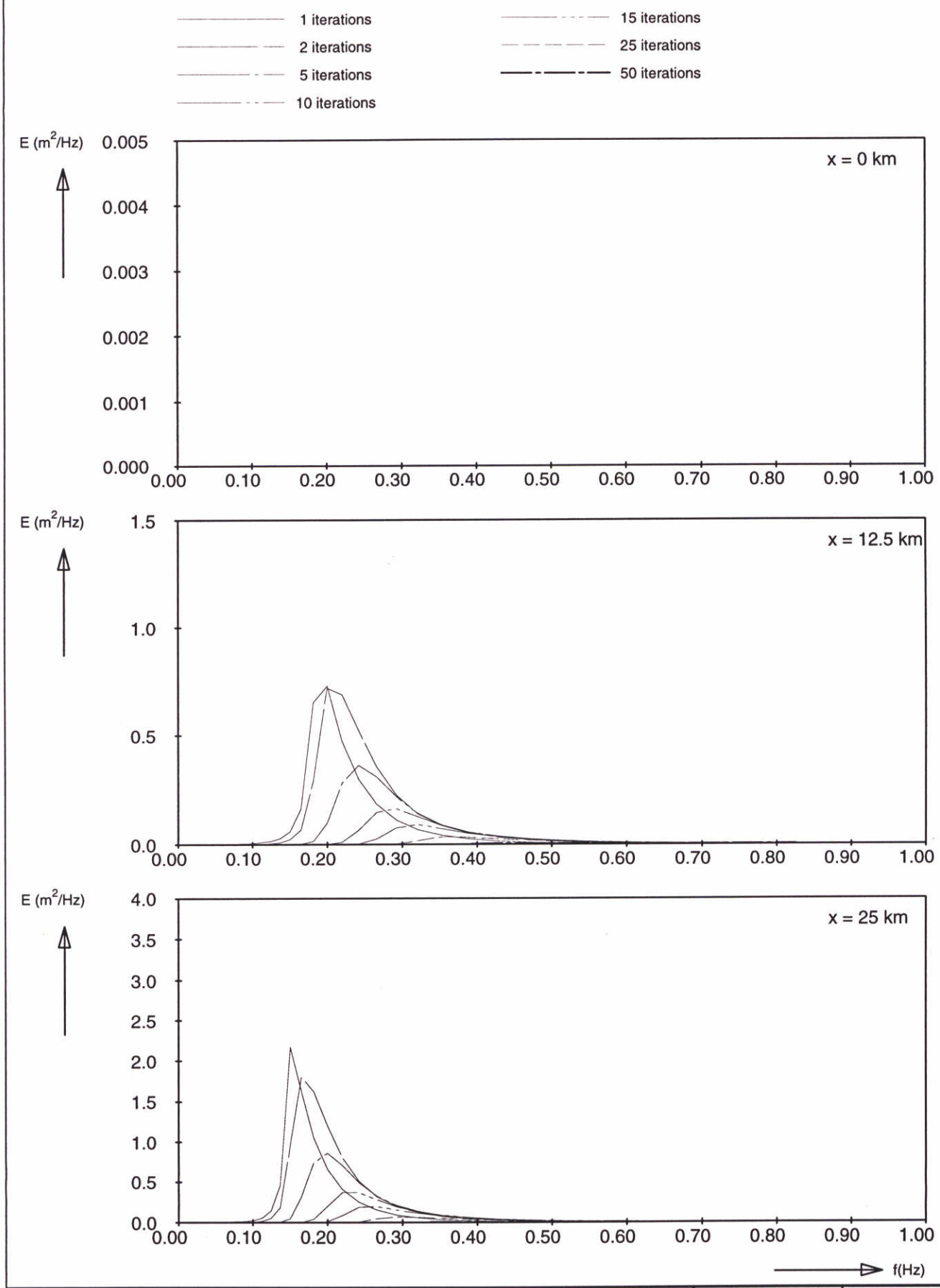

Frequency spectra at 3 locations Deactivated: Quadruplets Limiter = 10%	SWAN-1D	U_{10}=30 m/s
WL | delft hydraulics	H3496	Fig. 21b

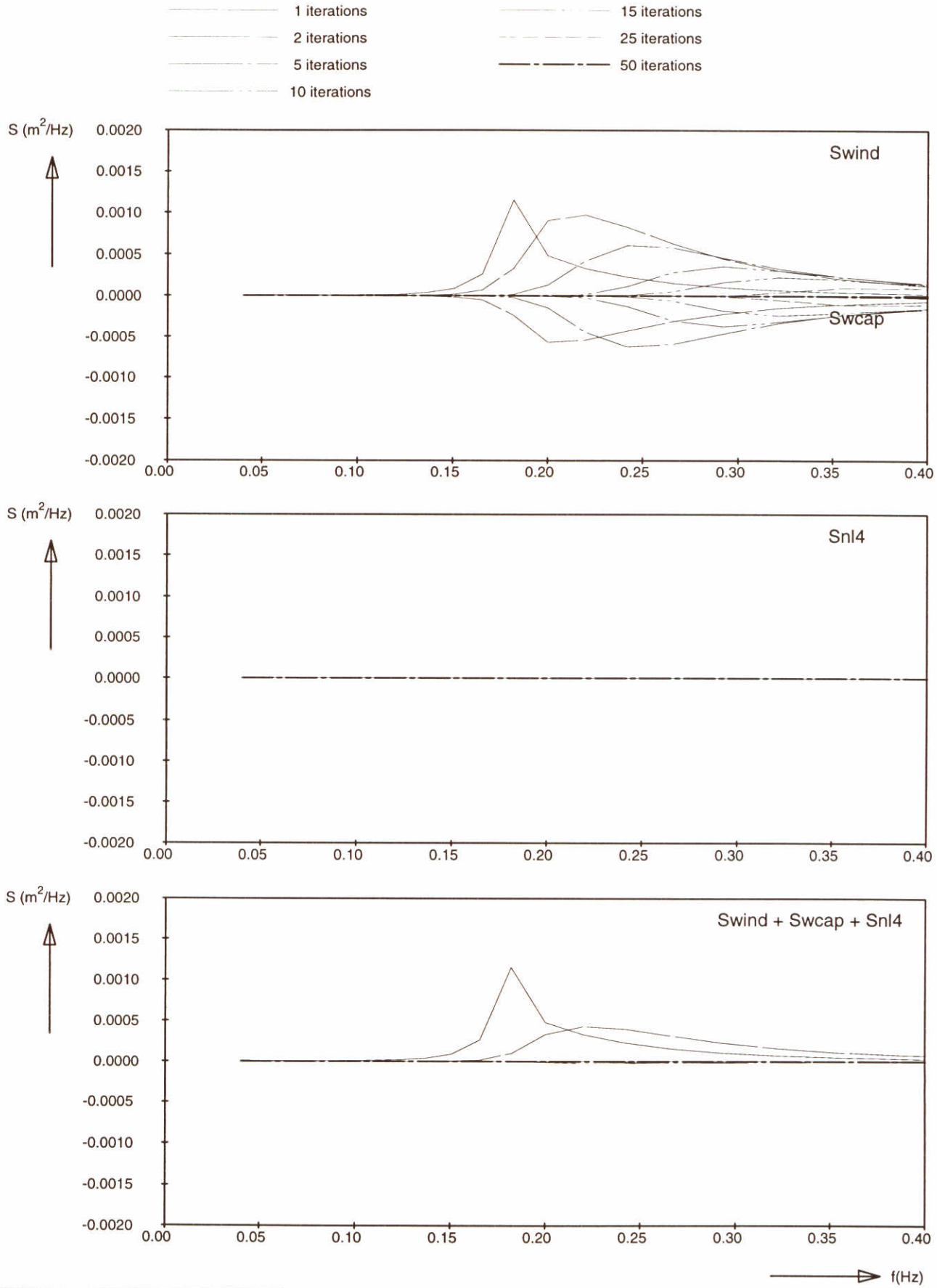

Source terms at x = 12.5 km Deactivated: Quadruplets Limiter = 10%	SWAN-1D	U_{10}=30 m/s
WL | delft hydraulics	H3496	Fig. 21c

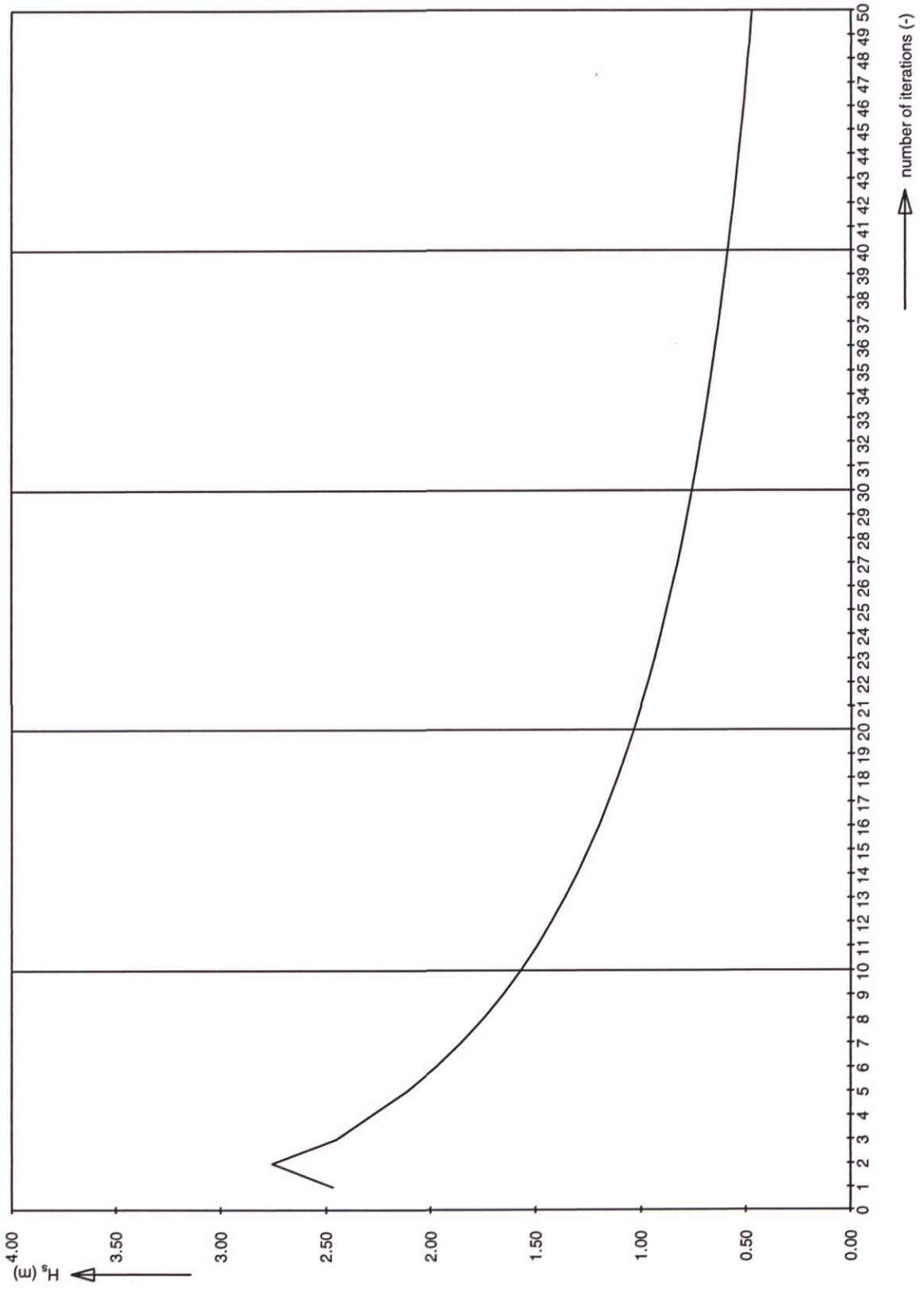

Significant wave height at 12.5 km Deactivated: Quadruplets Limiter = 10%	SWAN-1D	U_{10}=30 m/s
WL | delft hydraulics	H3496	Fig. 21d

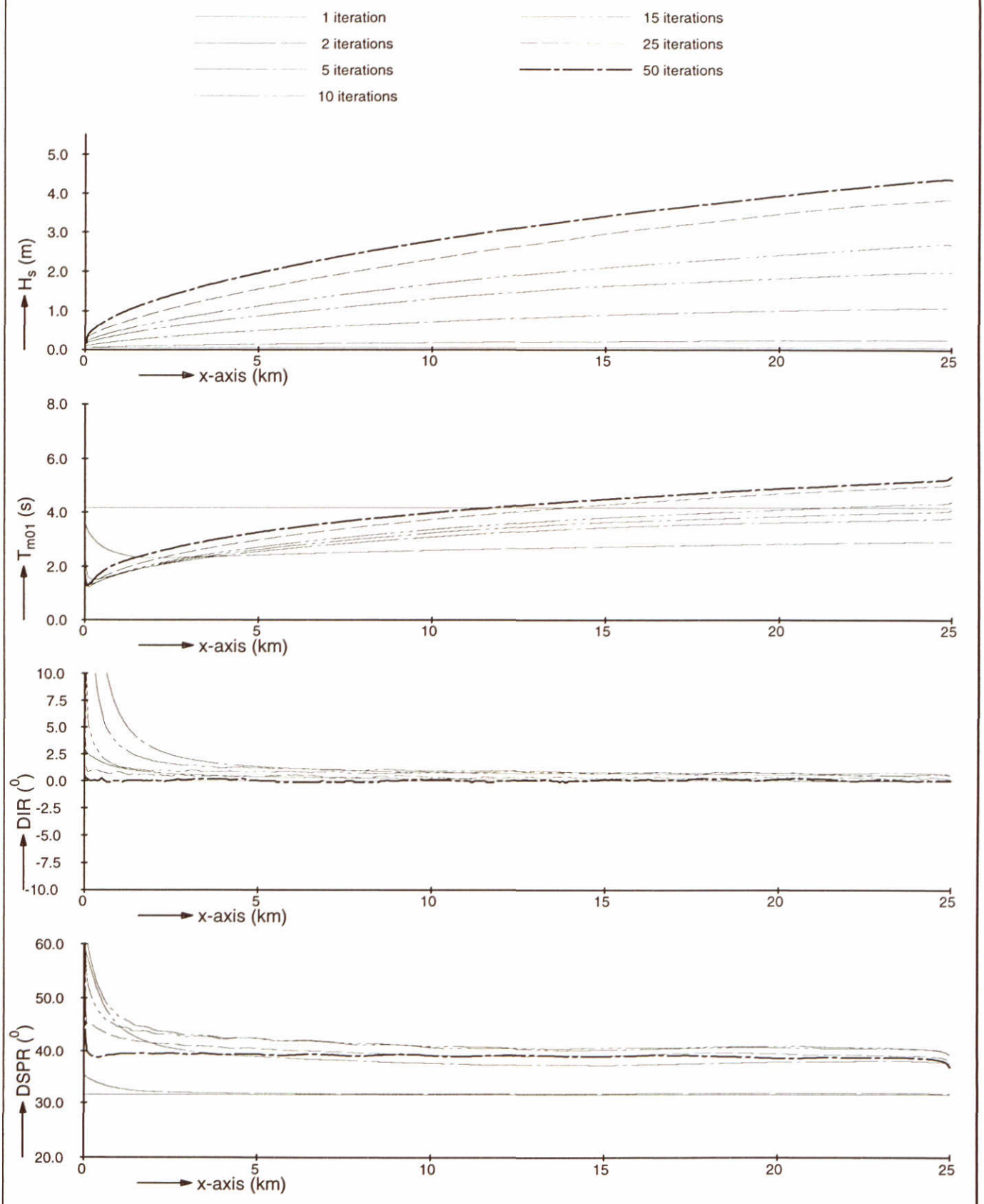

Model convergence behaviour using third-generation formulations
No pre-conditioner (i.e. no first guess)
Boundary condition: H_s=0.05 m, T_p=5 s

SWAN-1D | U_{10}=30 m/s

WL | delft hydraulics

H3496 | Fig. 22a

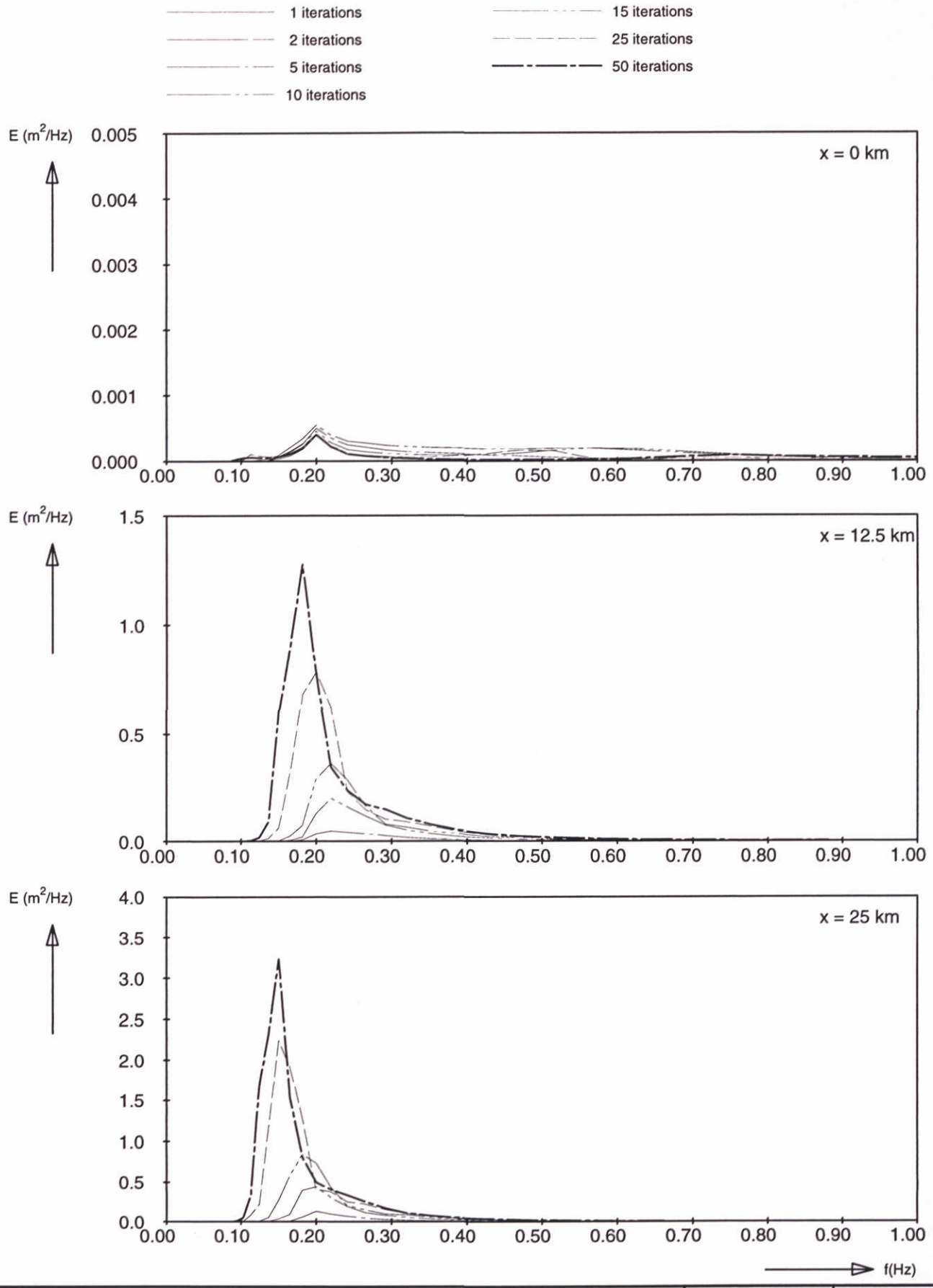

Frequency spectra at 3 locations No pre-conditioner (i.e. no first guess) Boundary condition: H_s=0.05 m, T_p=5 s	SWAN-1D	U_{10}=30 m/s
WL | delft hydraulics	H3496	Fig. 22b

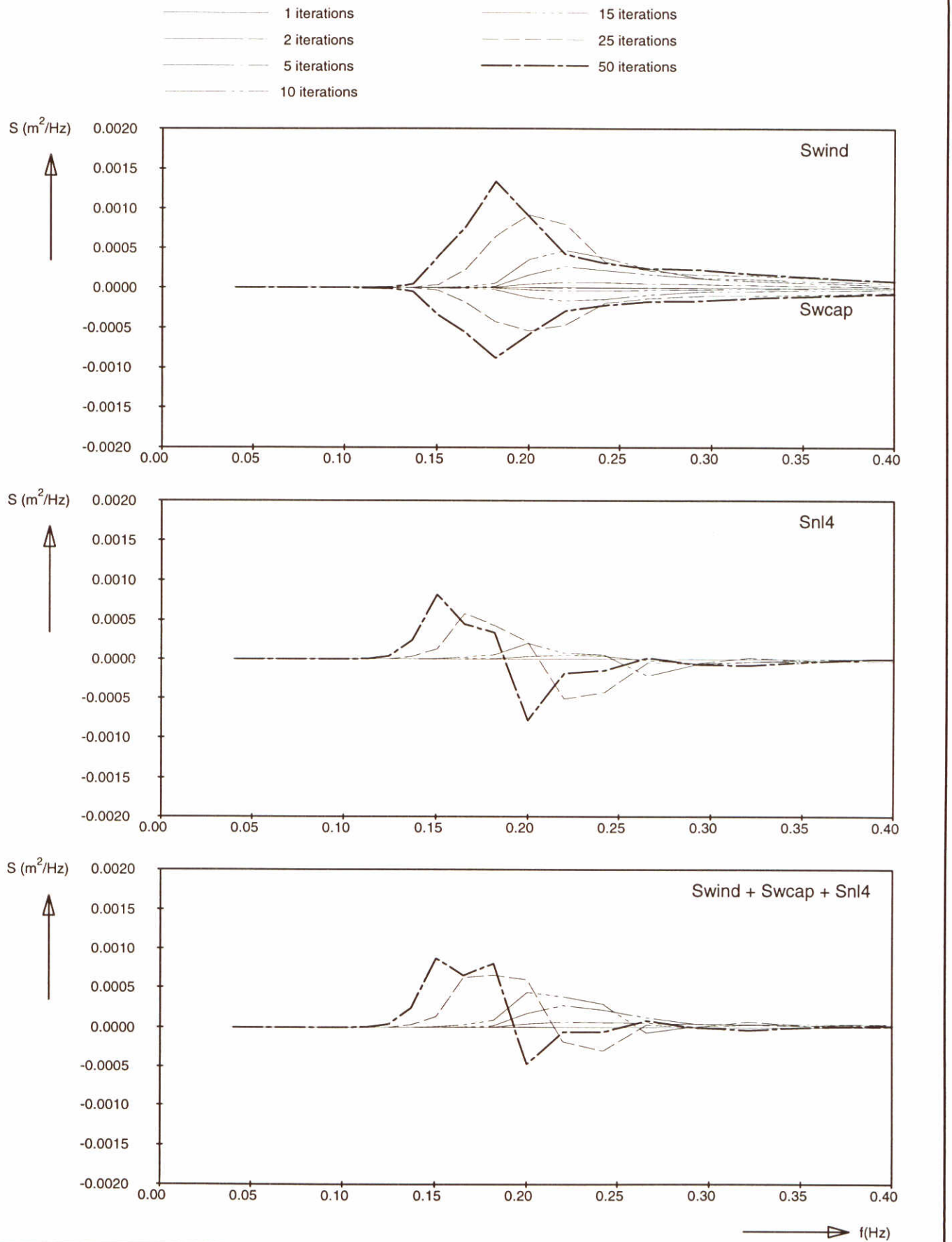

Source terms at x = 12.5 km
No pre-conditioner (i.e. no first guess)
Boundary condition: H_s=0.05 m, T_p=5 s

SWAN-1D | U_{10}=30 m/s

WL | delft hydraulics

H3496 | Fig. 22c

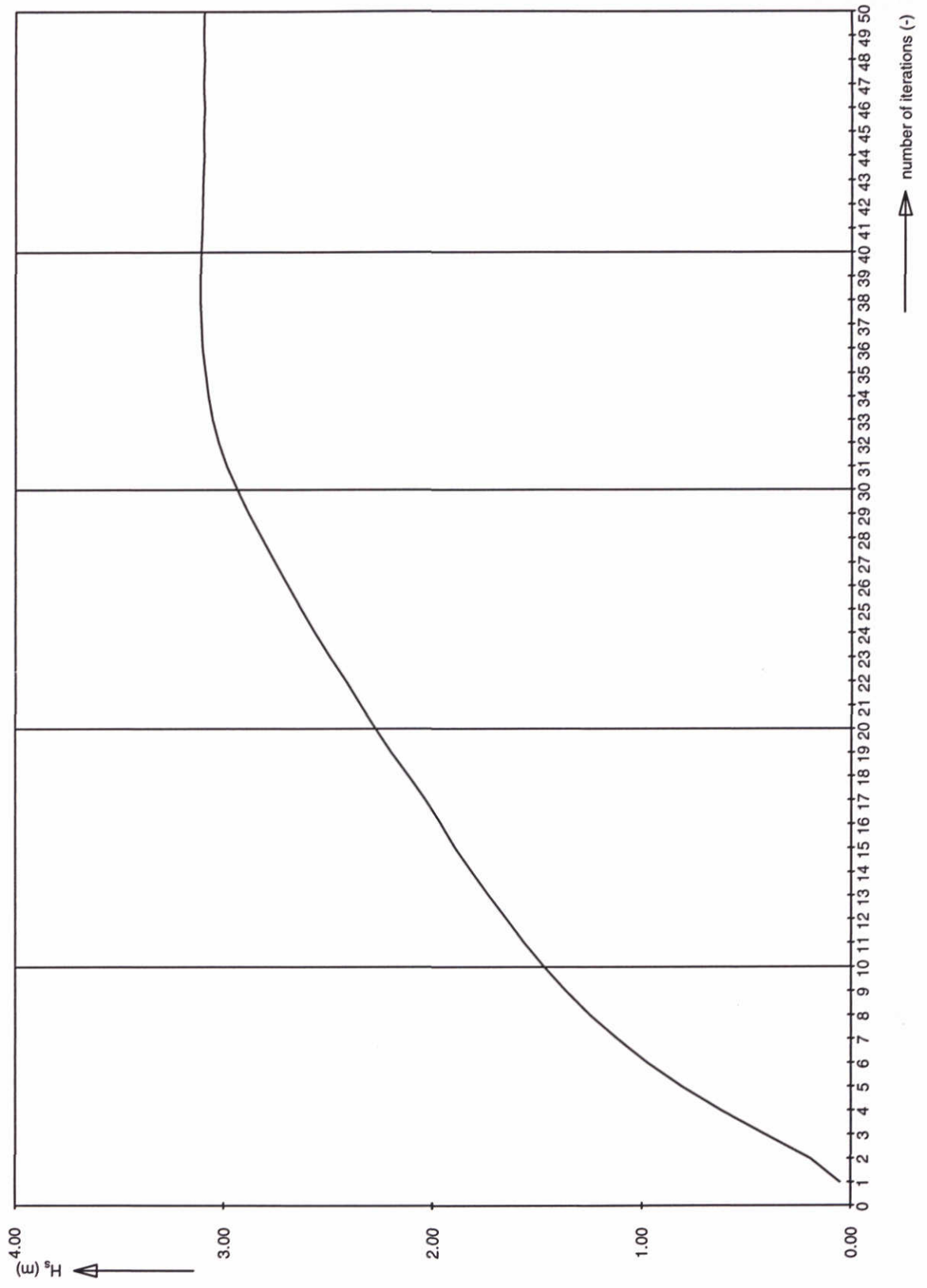

Significant wave height at 12.5 km No pre-conditioner (i.e. no first guess) Boundary condition: H_s=0.05 m, T_p=5 s	SWAN-1D	U_{10}=30 m/s
WL | delft hydraulics	H3496	Fig. 22d

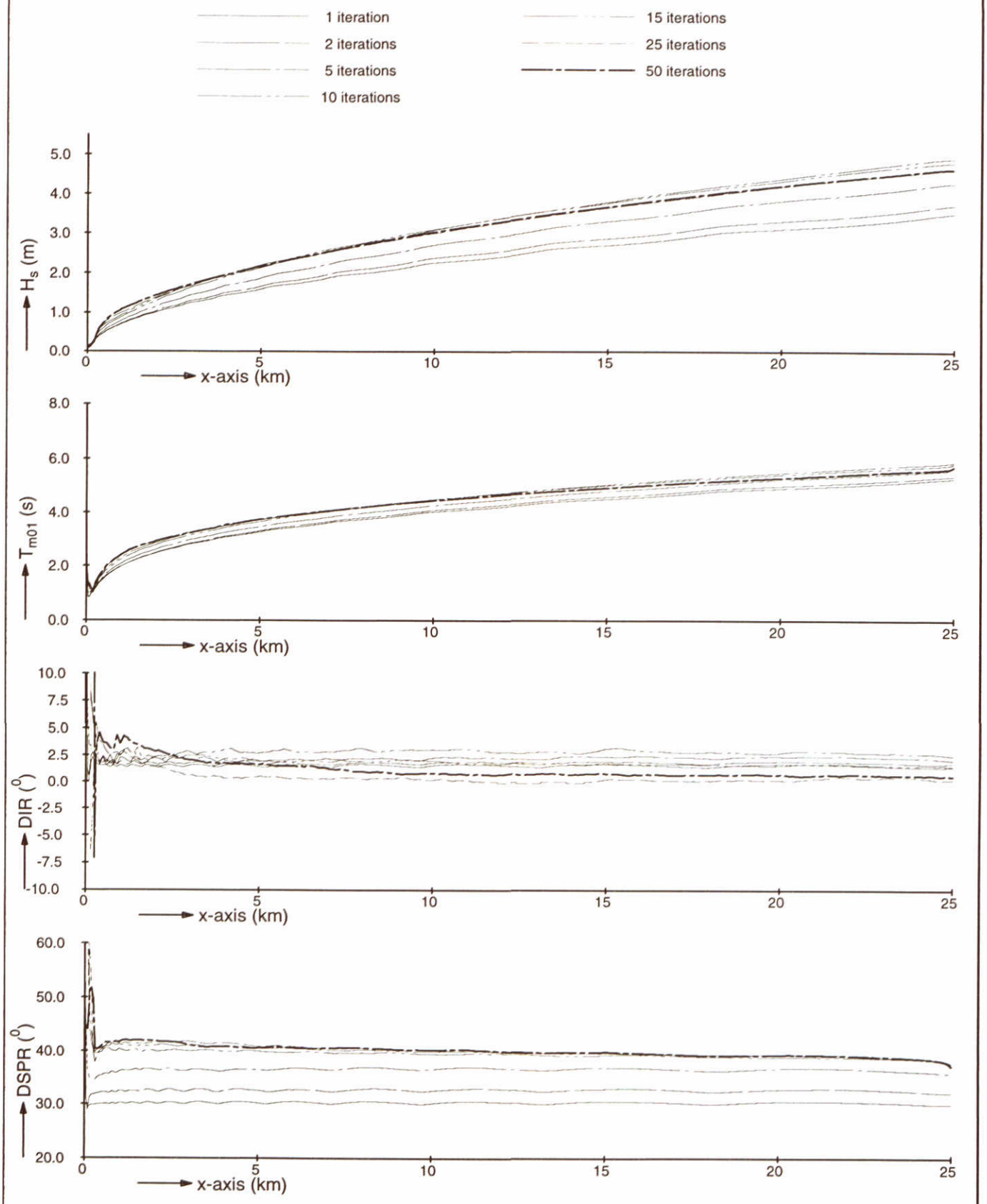

Model convergence behaviour using third-generation formulations
Implicit computation of Swind

SWAN-1D

U_{10}=30 m/s

WL | delft hydraulics

H3496

Fig. 23a

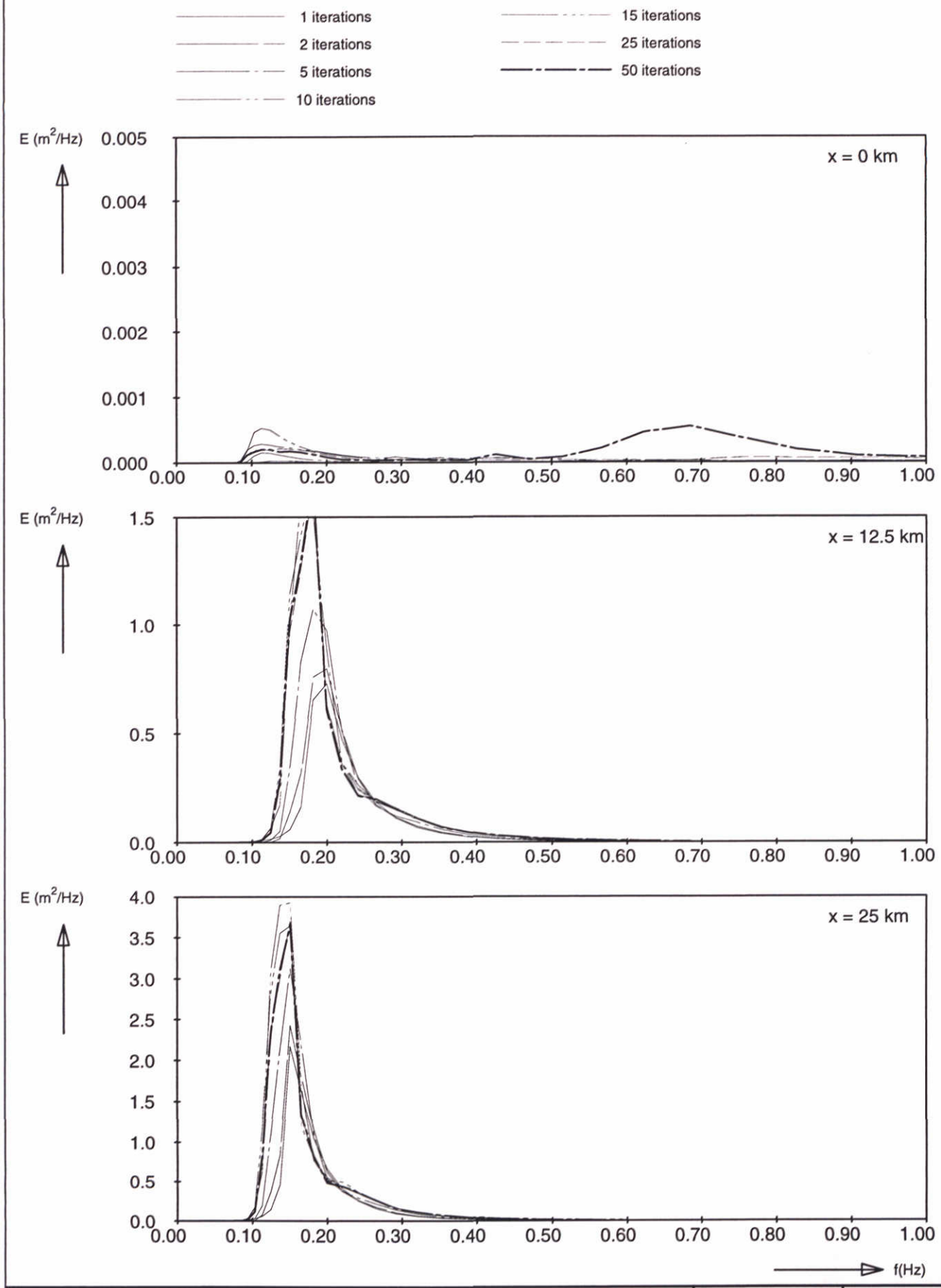

Frequency spectra at 3 locations Implicit computation of Swind	SWAN-1D	U_{10}=30 m/s
WL | delft hydraulics	H3496	Fig. 23b

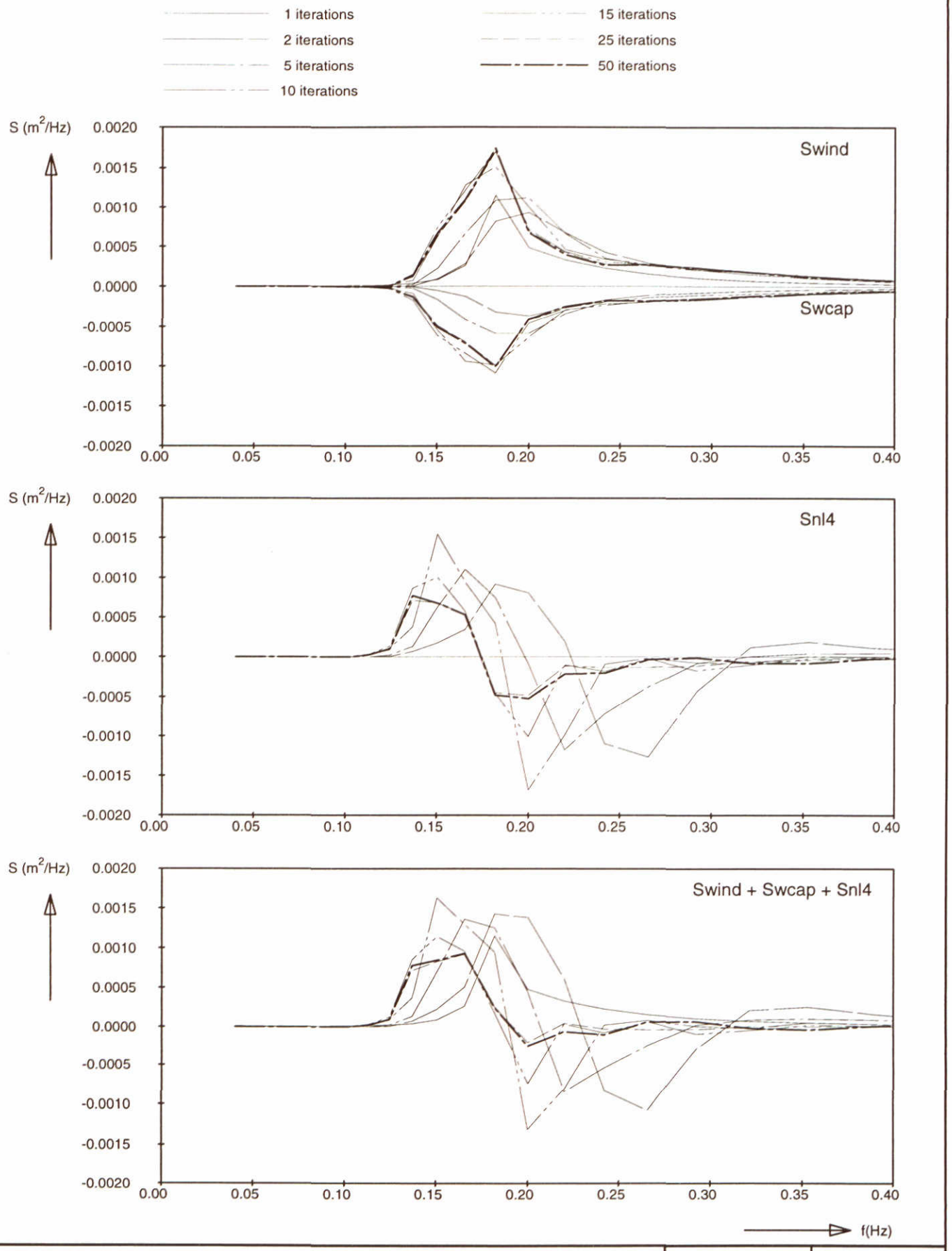

Source terms at x = 12.5 km
Implicit computation of Swind

SWAN-1D

U_{10}=30 m/s

WL | delft hydraulics

H3496

Fig. 23c

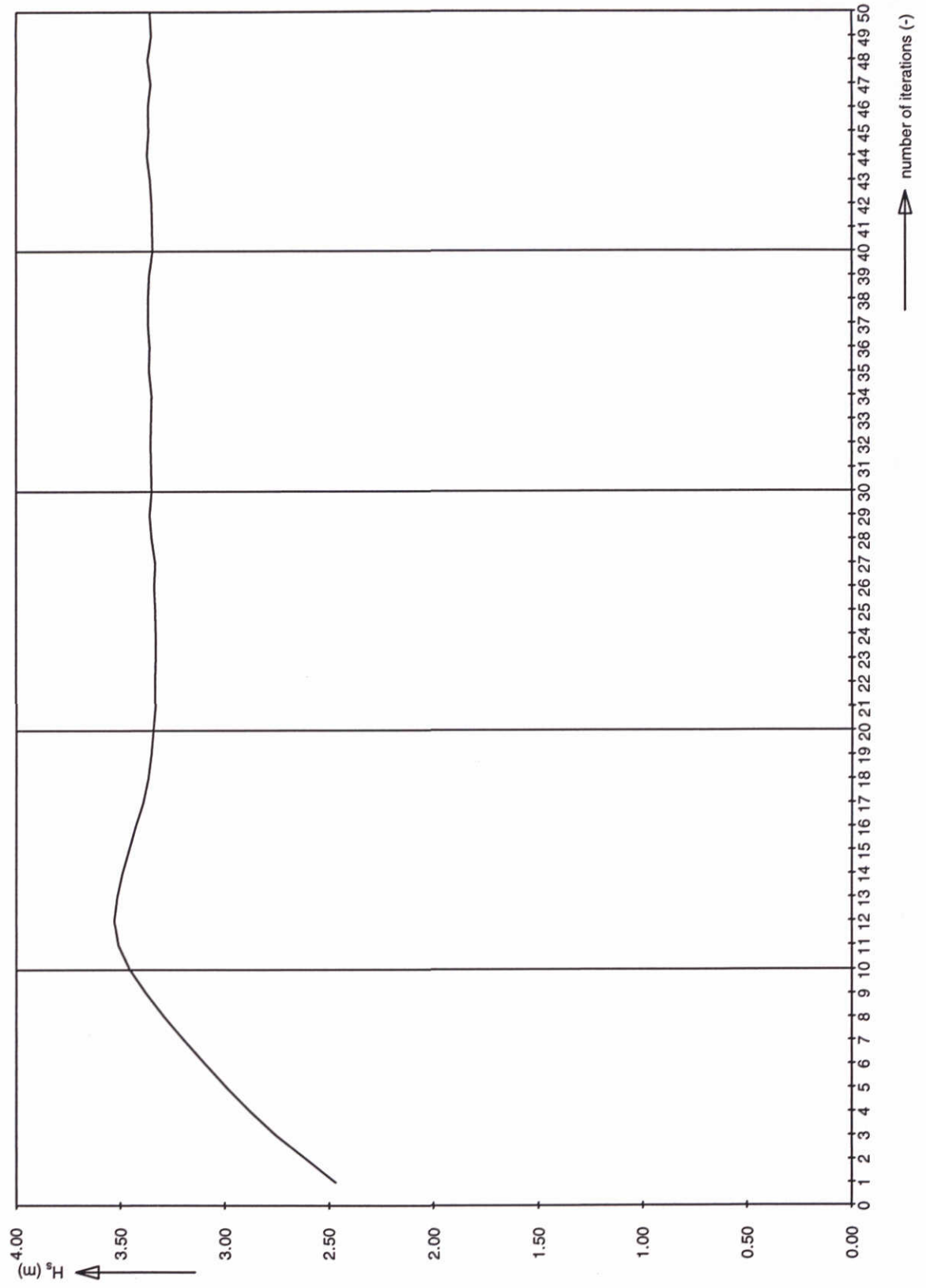

Significant wave height at 12.5 km Implicit computation of Swind	SWAN-1D	U_{10}=30 m/s
WL | delft hydraulics	H3496	Fig. 23d

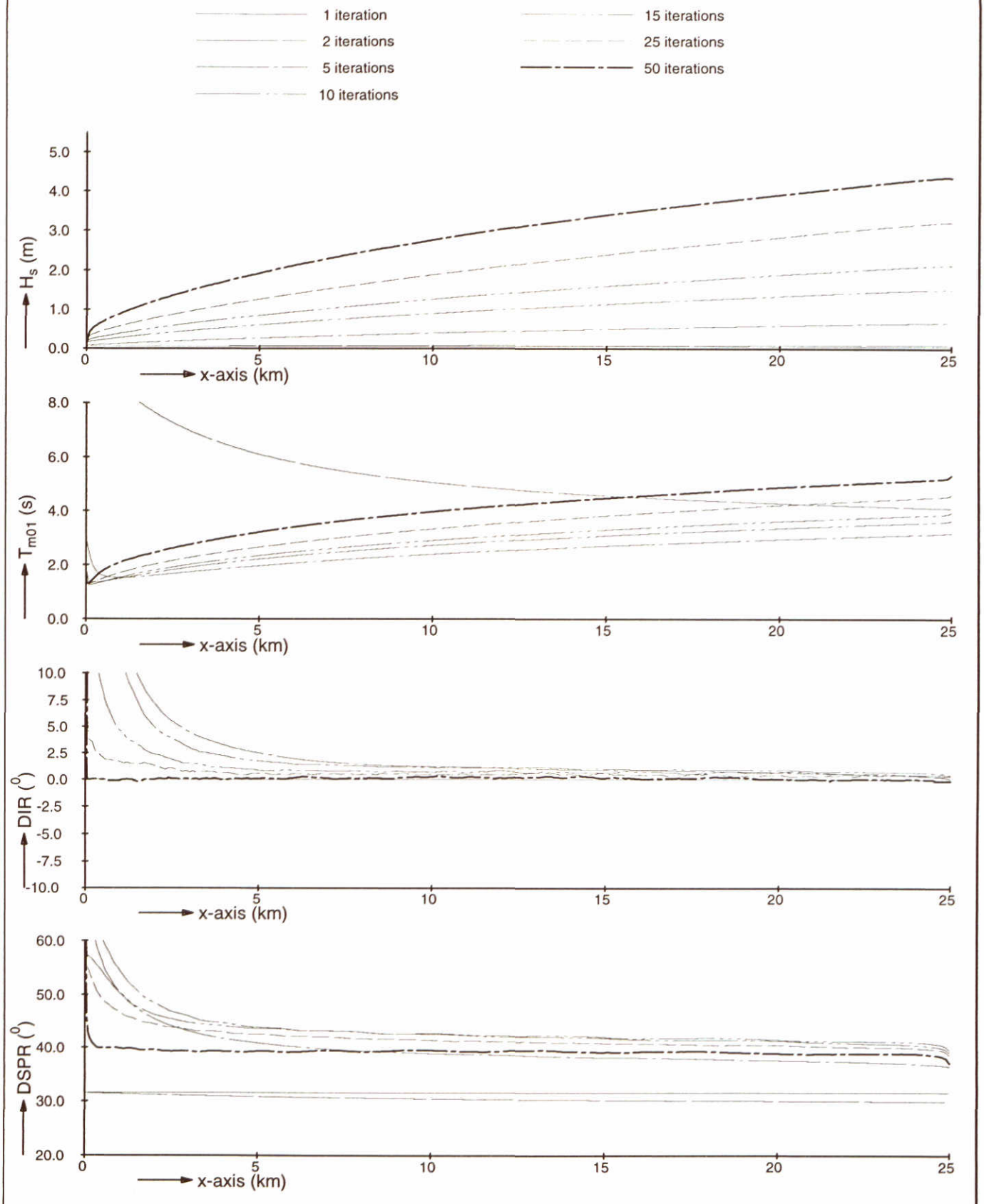

Model convergence behaviour using third-generation formulations
No pre-conditioner (i.e. no first guess)
Boundary condition: H_s=0.05 m, T_p=12 s

SWAN-1D | U_{10}=30 m/s

WL | delft hydraulics | H3496 | Fig. 24a

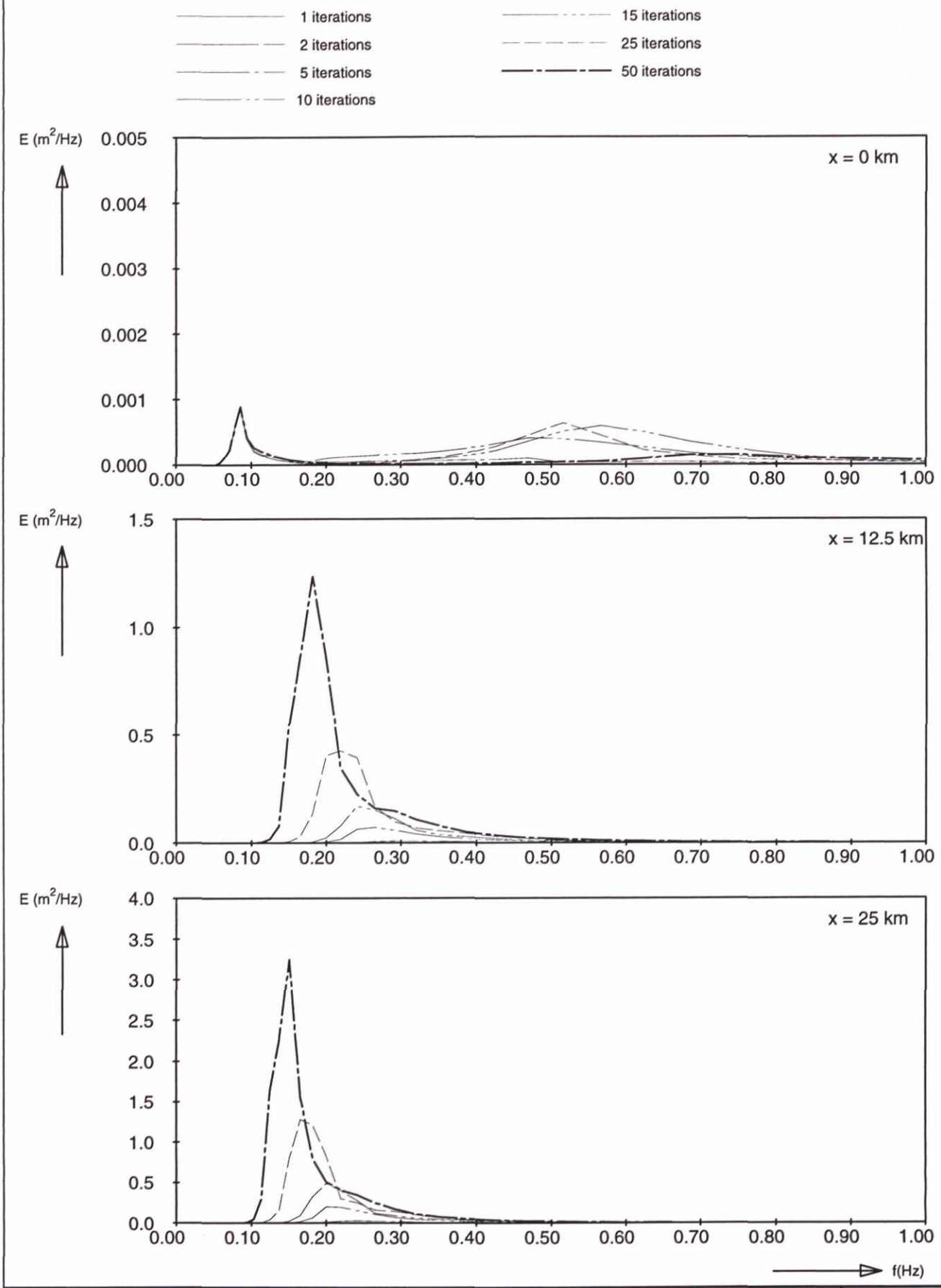

Frequency spectra at 3 locations No pre-conditioner (i.e. no first guess) Boundary condition: H_s=0.05 m, T_p=12 s	SWAN-1D	U_{10}=30 m/s
WL | delft hydraulics	H3496	Fig. 24b

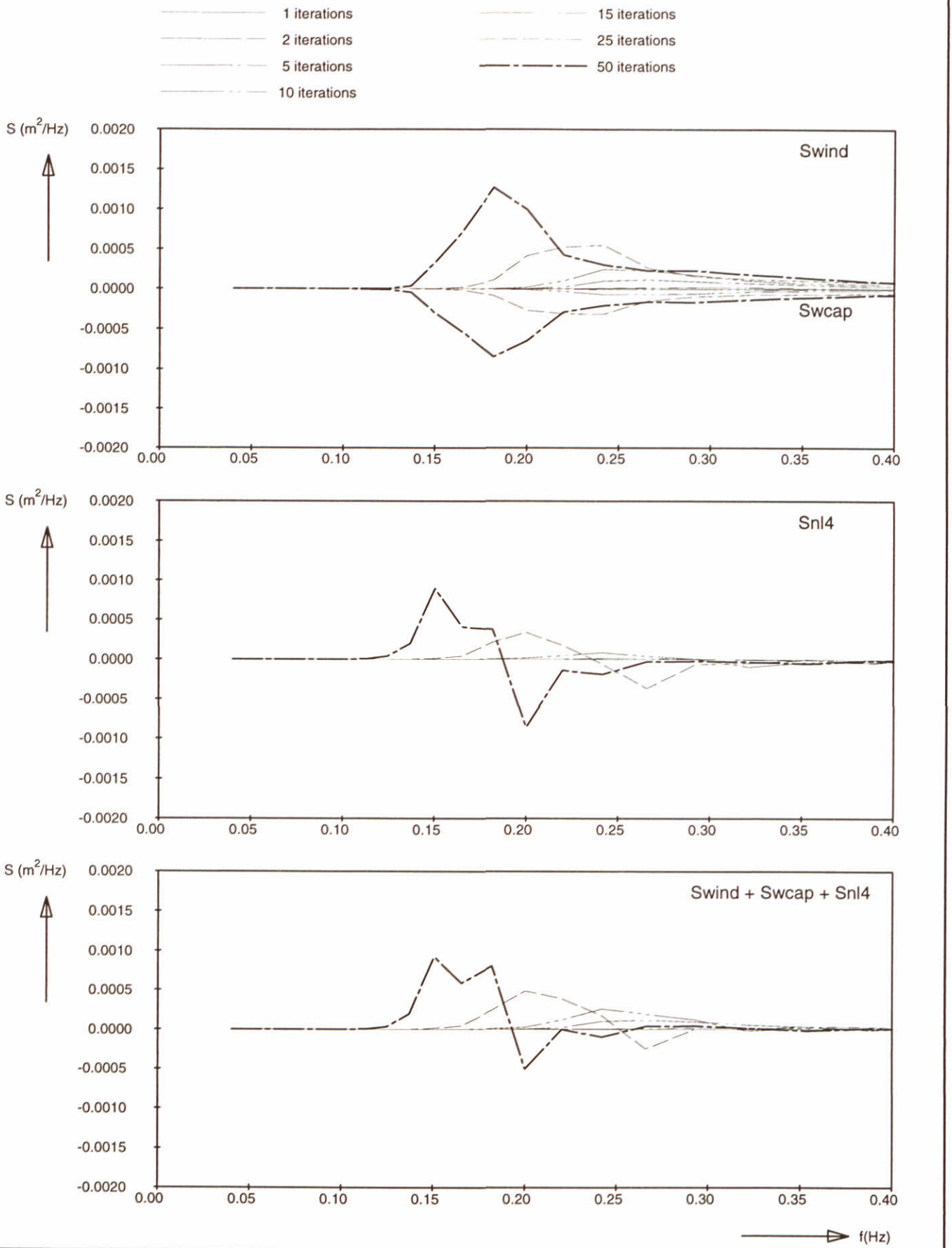

Source terms at x = 12.5 km No pre-conditioner (i.e. no first guess) Boundary condition: H_s=0.05 m, T_p=12 s	SWAN-1D	U_{10}=30 m/s
WL | delft hydraulics	H3496	Fig. 24c

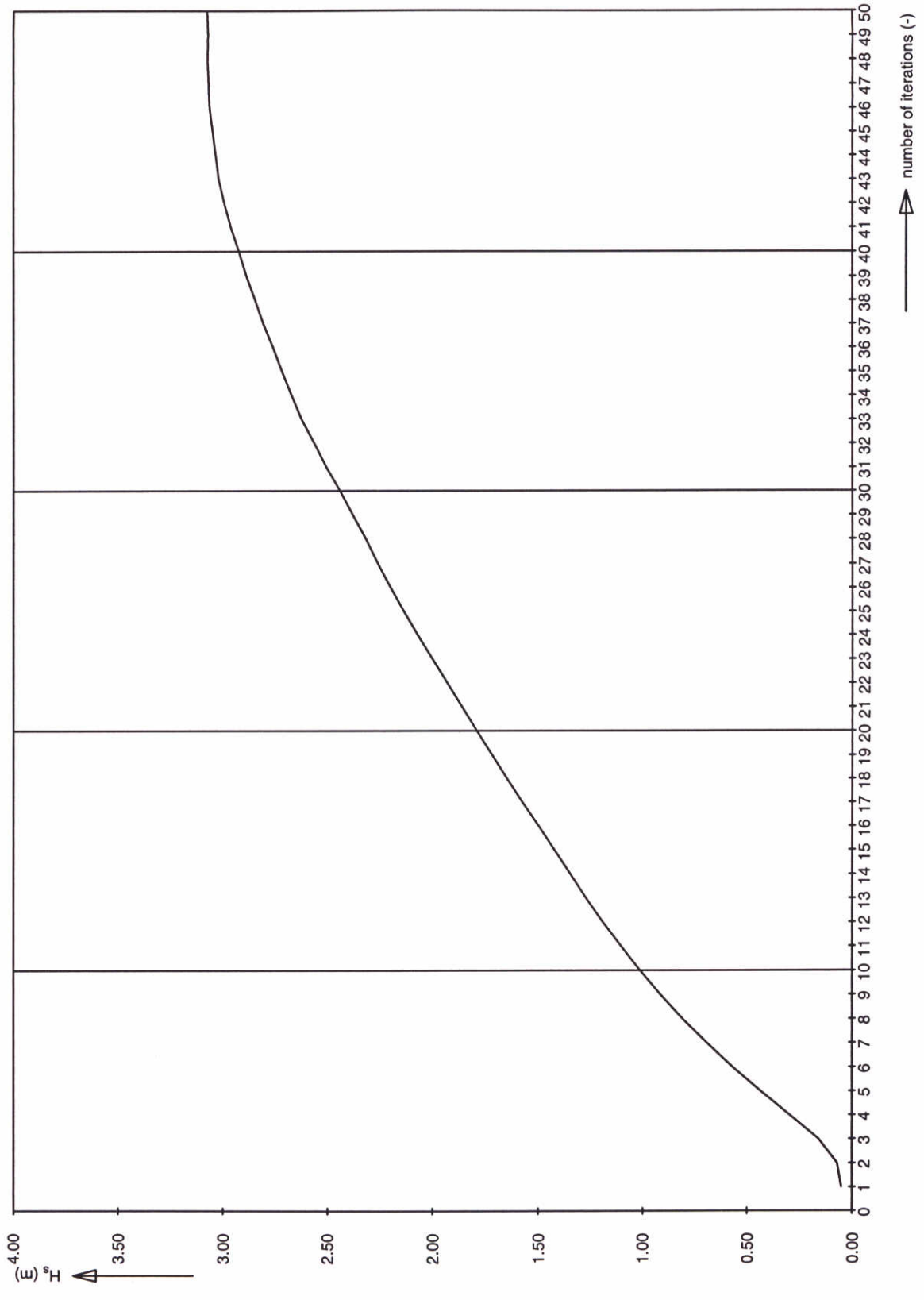

Significant wave height at 12.5 km No pre-conditioner (i.e. no first guess) Boundary condition: H_s=0.05 m, T_p=12 s	SWAN-1D	U_{10}=30 m/s
WL | delft hydraulics	H3496	Fig. 24d

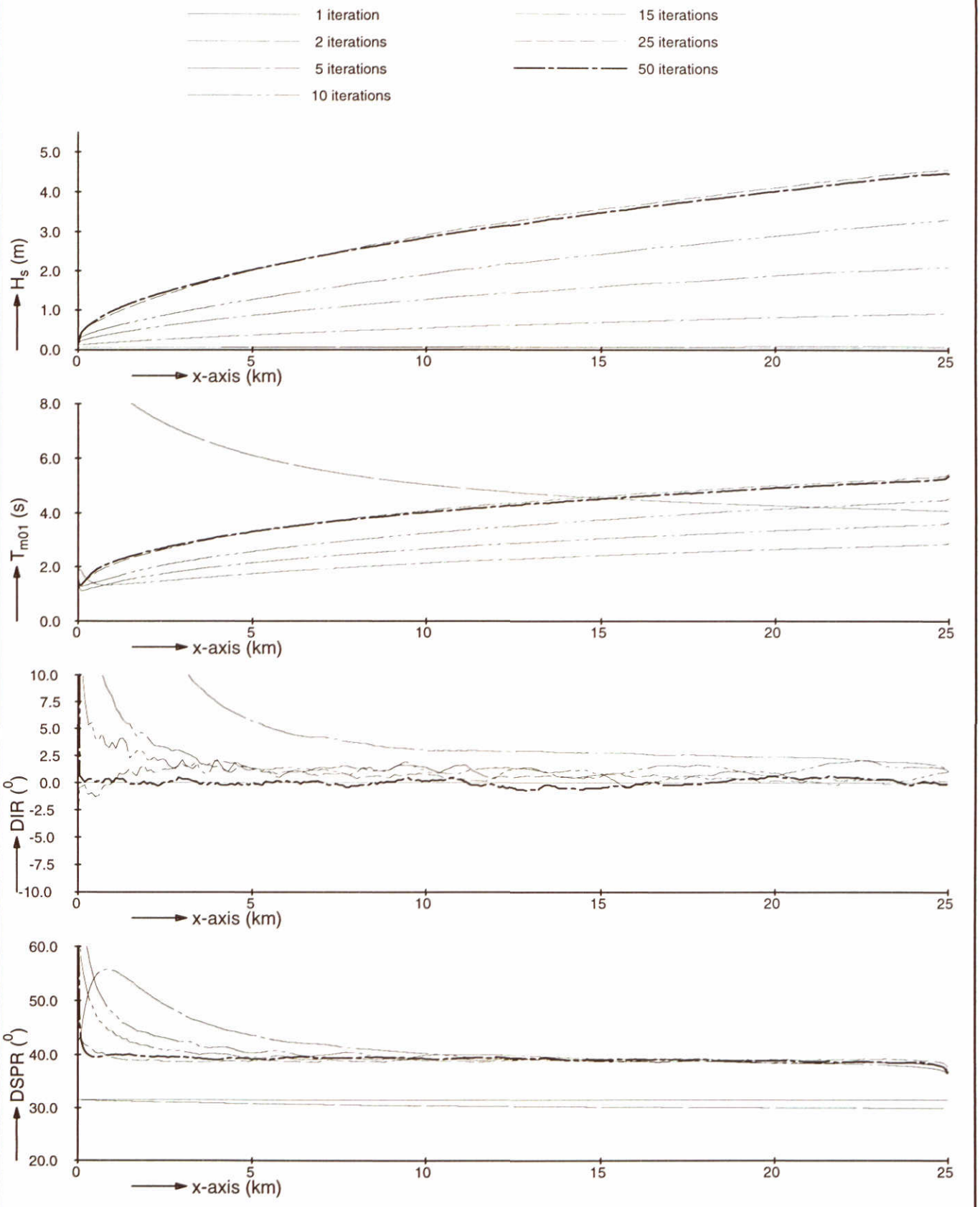

Model convergence behaviour using third-generation formulations
No pre-conditioner (i.e. no first guess)
Boundary condition: H_s=0.05 m, T_p=12 s, limiter=30%

SWAN-1D | U_{10}=30 m/s

WL | delft hydraulics

H3496 | Fig. 25a

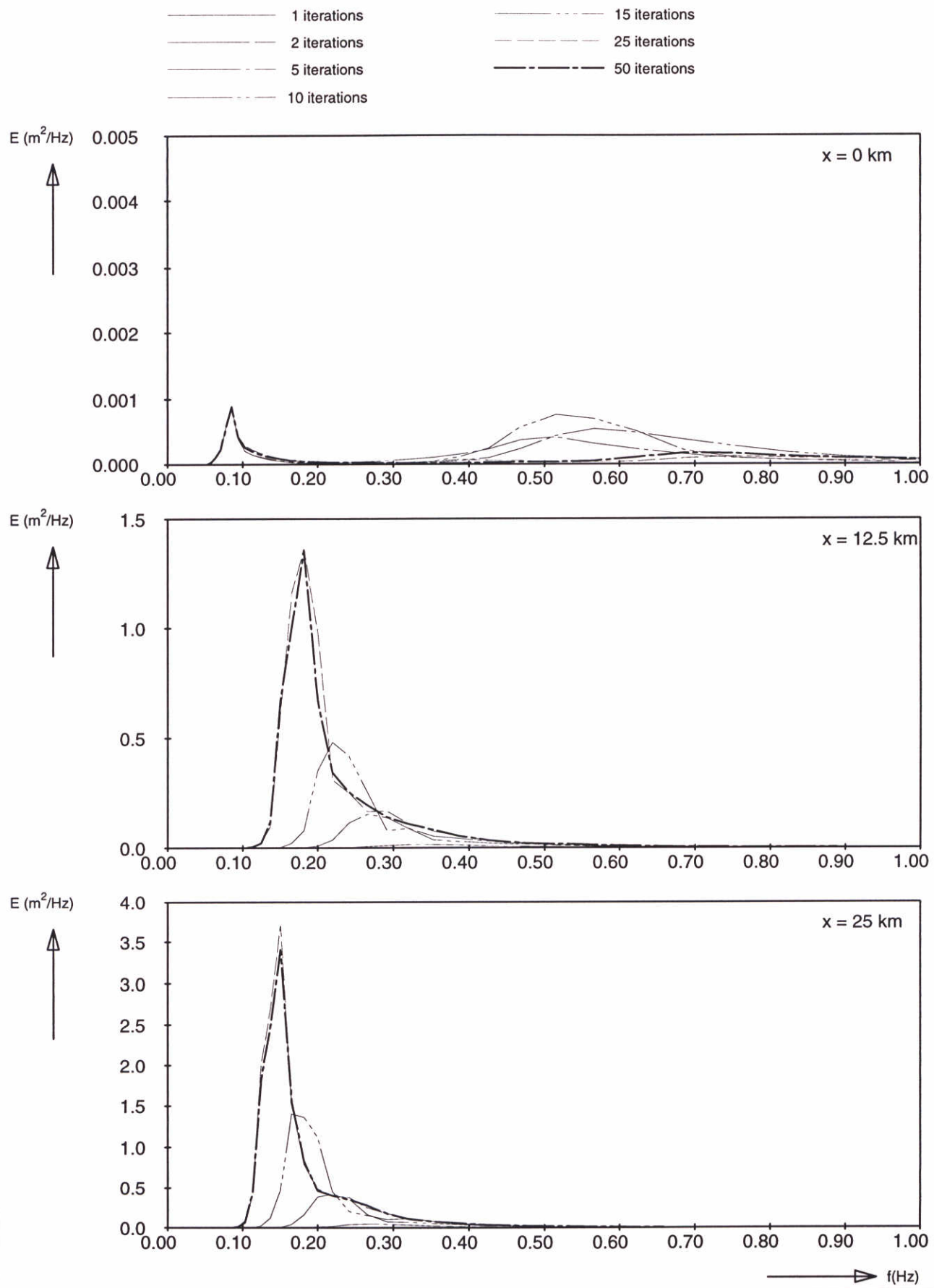

Frequency spectra at 3 locations No pre-conditioner (i.e. no first guess) Boundary condition: H_s=0.05 m, T_p=12 s, limiter=30%	SWAN-1D	U_{10}=30 m/s
WL | delft hydraulics	H3496	Fig. 25b

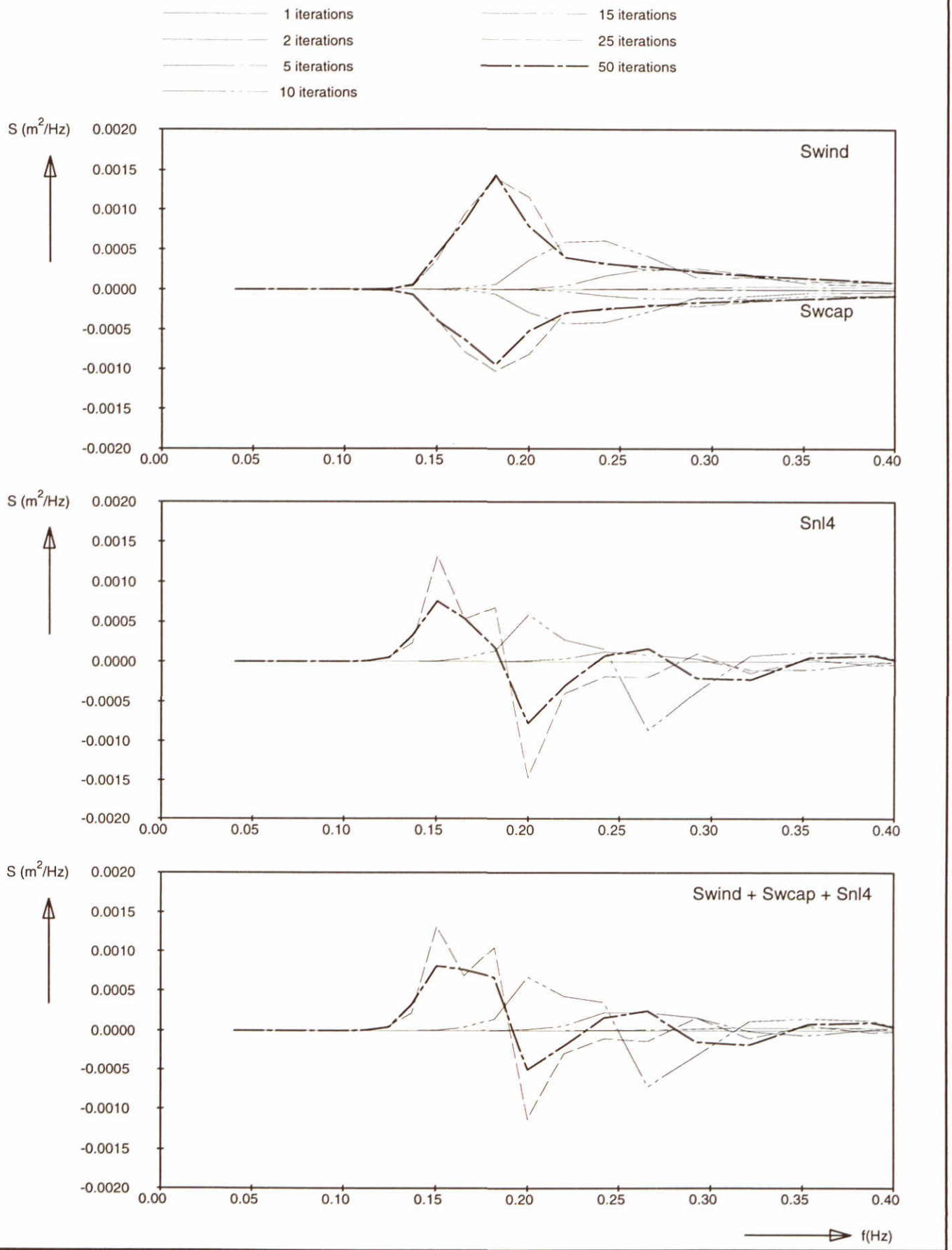

Source terms at x = 12.5 km No pre-conditioner (i.e. no first guess) Boundary condition: H_s=0.05 m, T_p=12 s, limiter=30%	SWAN-1D	U_{10}=30 m/s
WL | delft hydraulics	H3496	Fig. 25c

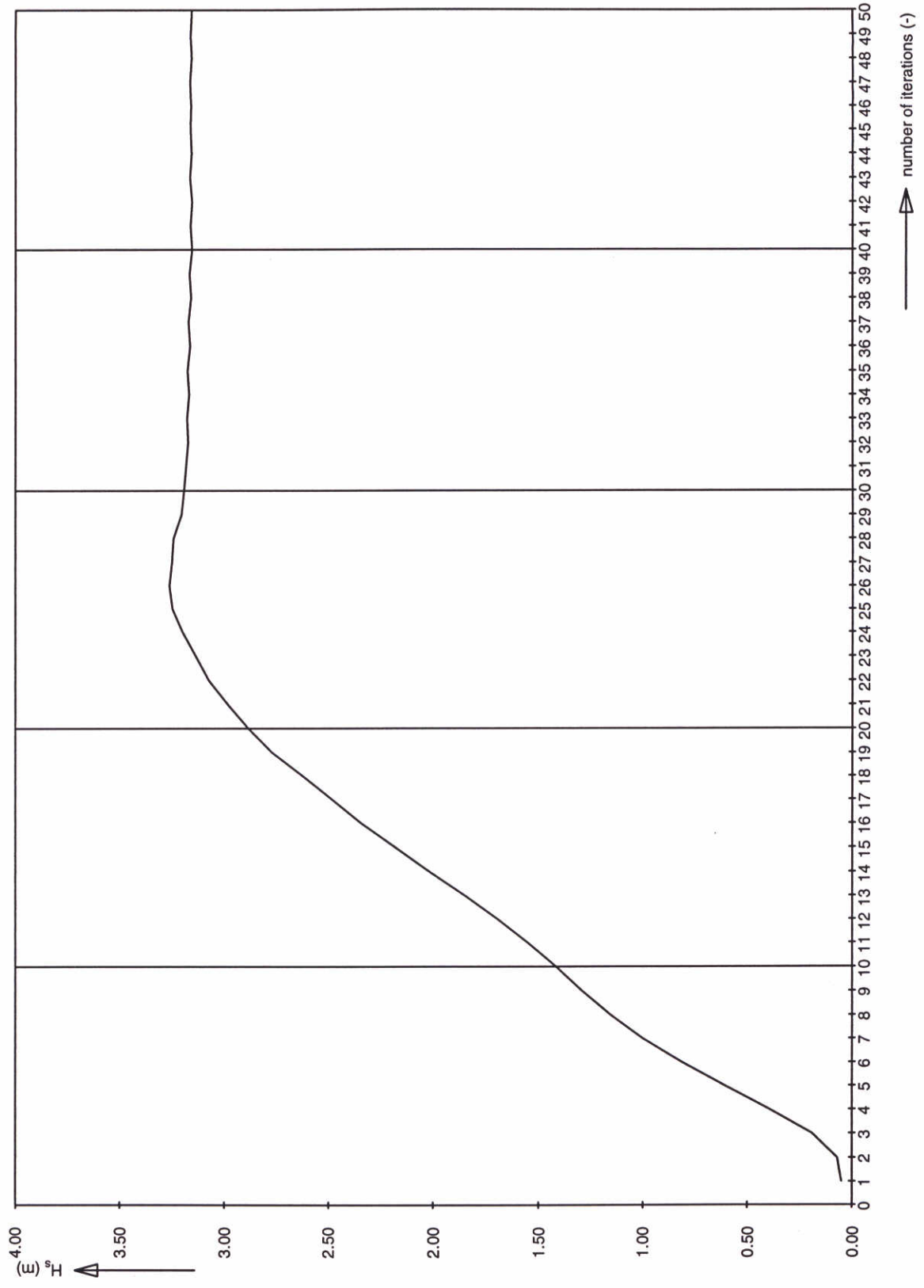

Significant wave height at 12.5 km No pre-conditioner (i.e. no first guess) Boundary condition: H_s=0.05 m, T_p=12 s, limiter=30%	SWAN-1D	U_{10}=30 m/s
WL | delft hydraulics	H3496	Fig. 25d

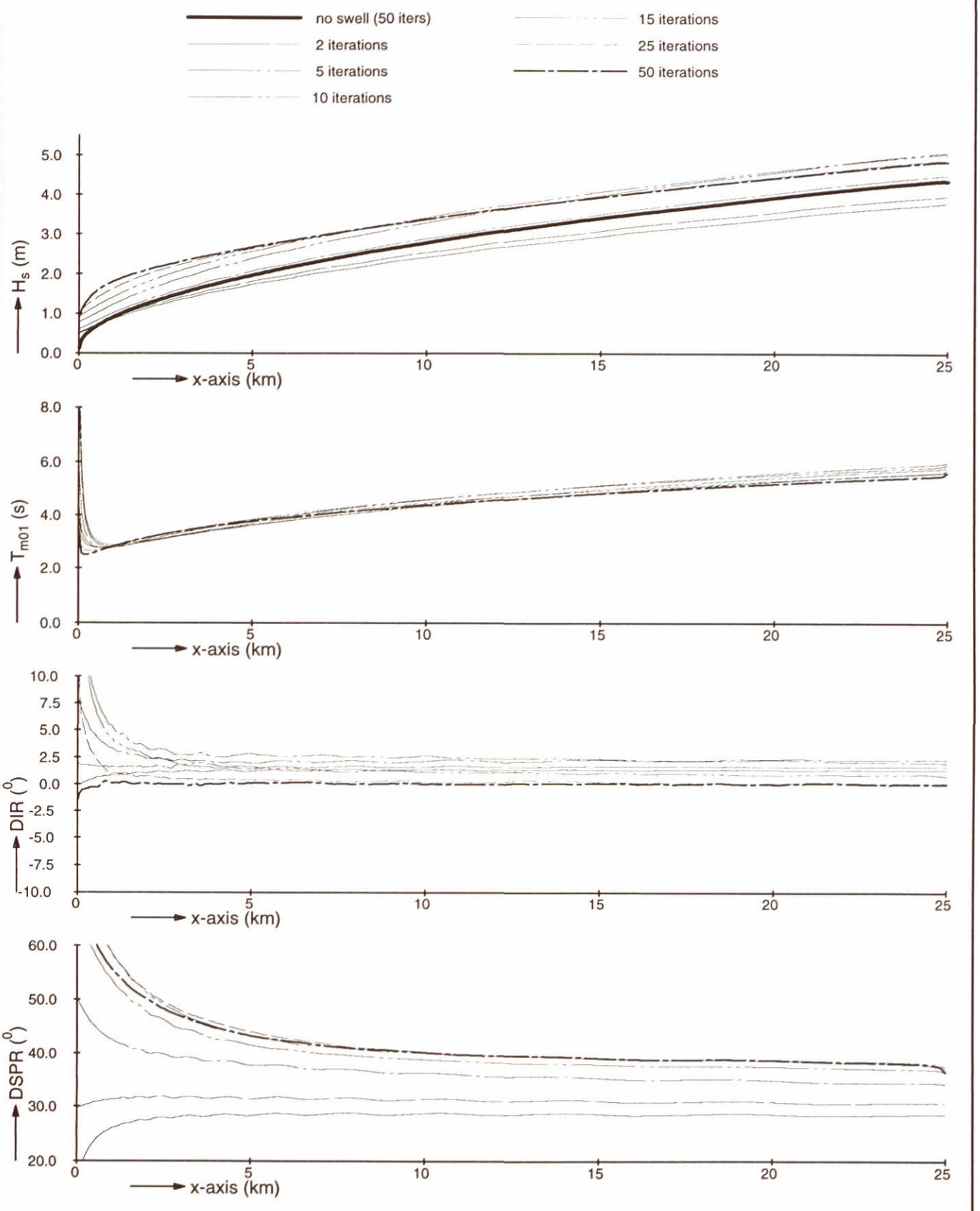

Model convergence behaviour using third-generation formulations Effect of incident swell on wave growth Swell: H_s=0.5 m, T_p=15 s, ms = 10	SWAN-1D	U_{10}=30 m/s
WL | delft hydraulics	H3496	Fig. 26a

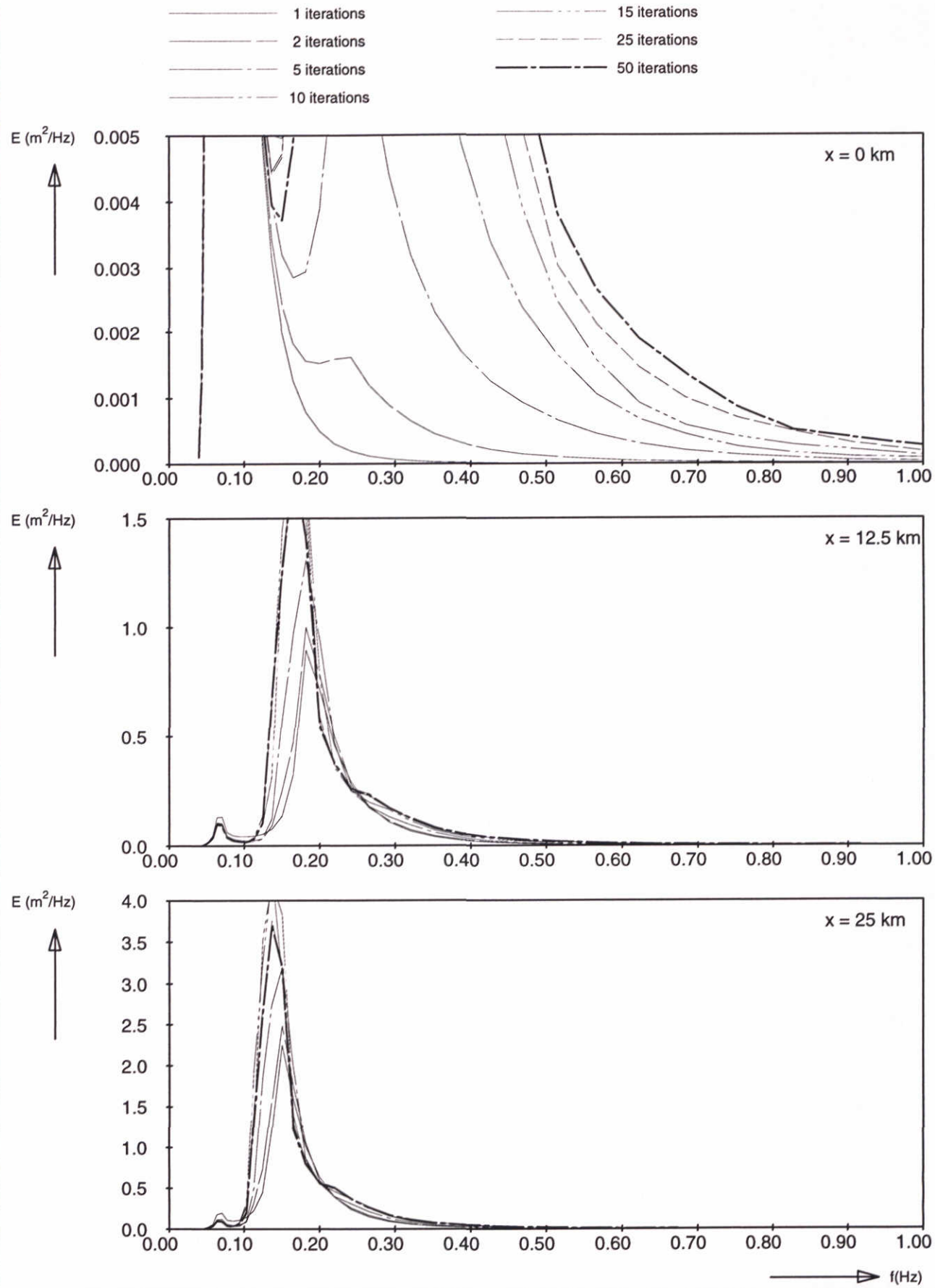

Frequency spectra at 3 locations Effect of incident swell on wave growth Swell: H_s=0.5 m, T_p=15 s, ms = 10	SWAN-1D	U_{10}=30 m/s
WL | delft hydraulics	H3496	Fig. 26b

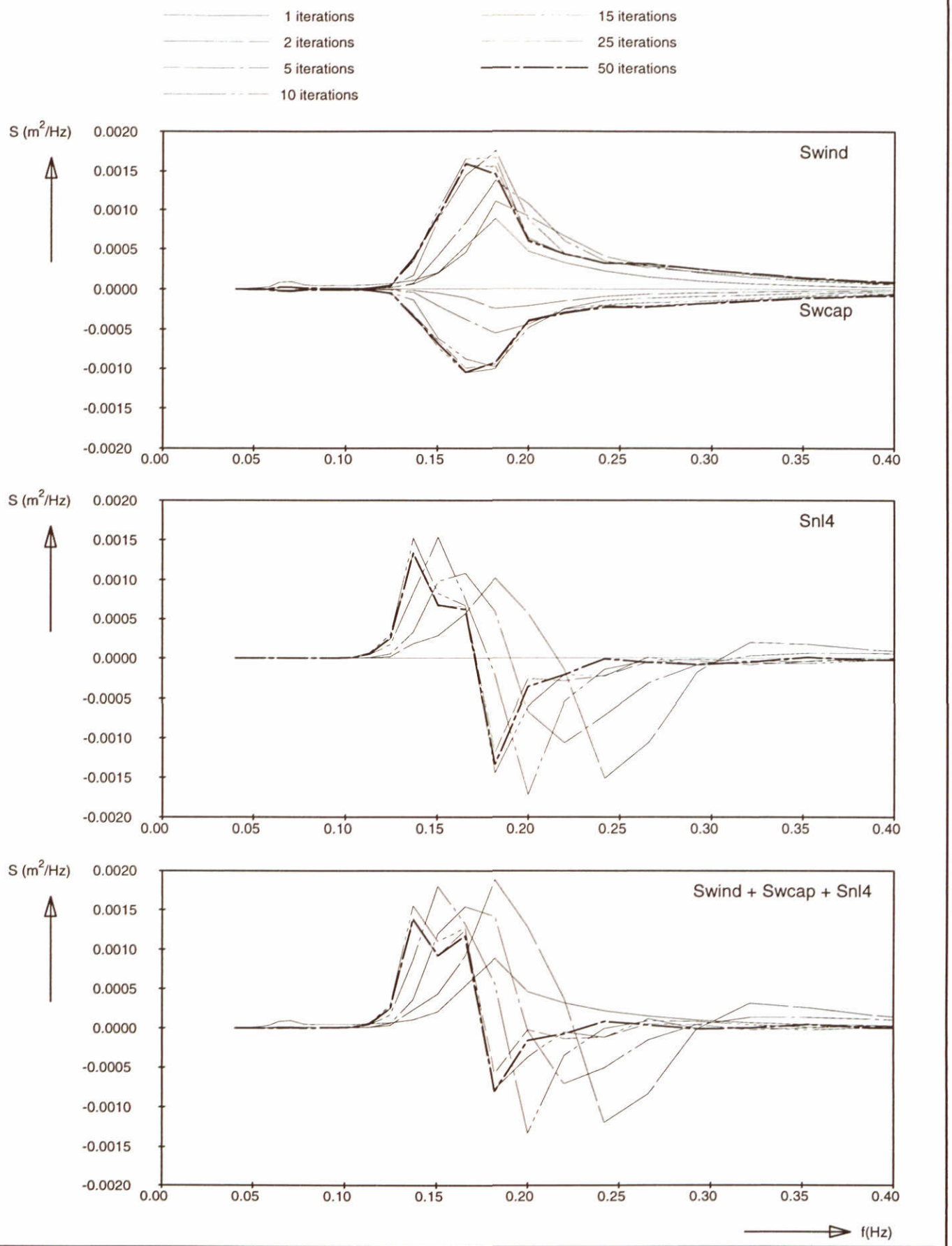

Source terms at x = 12.5 km
Effect of incident swell on wave growth
Swell: H_s=0.5 m, T_p=15 s, ms = 10

SWAN-1D | U_{10}=30 m/s

WL | delft hydraulics | H3496 | Fig. 26c

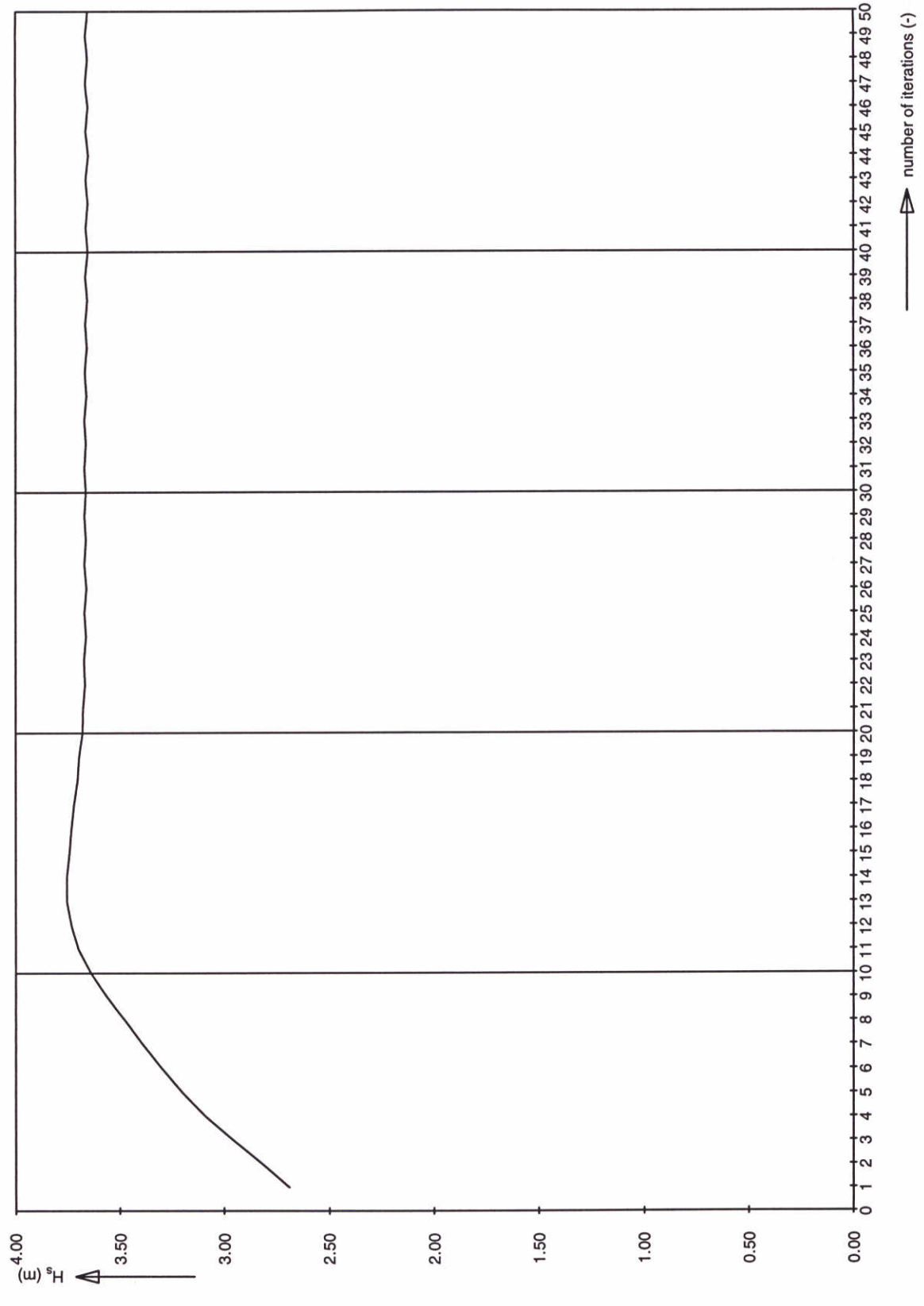

Significant wave height at 12.5 km Effect of incident swell on wave growth Swell: H_s=0.5 m, T_p=15 s, ms = 10	SWAN-1D	U_{10}=30 m/s
WL | delft hydraulics	H3496	Fig. 26d

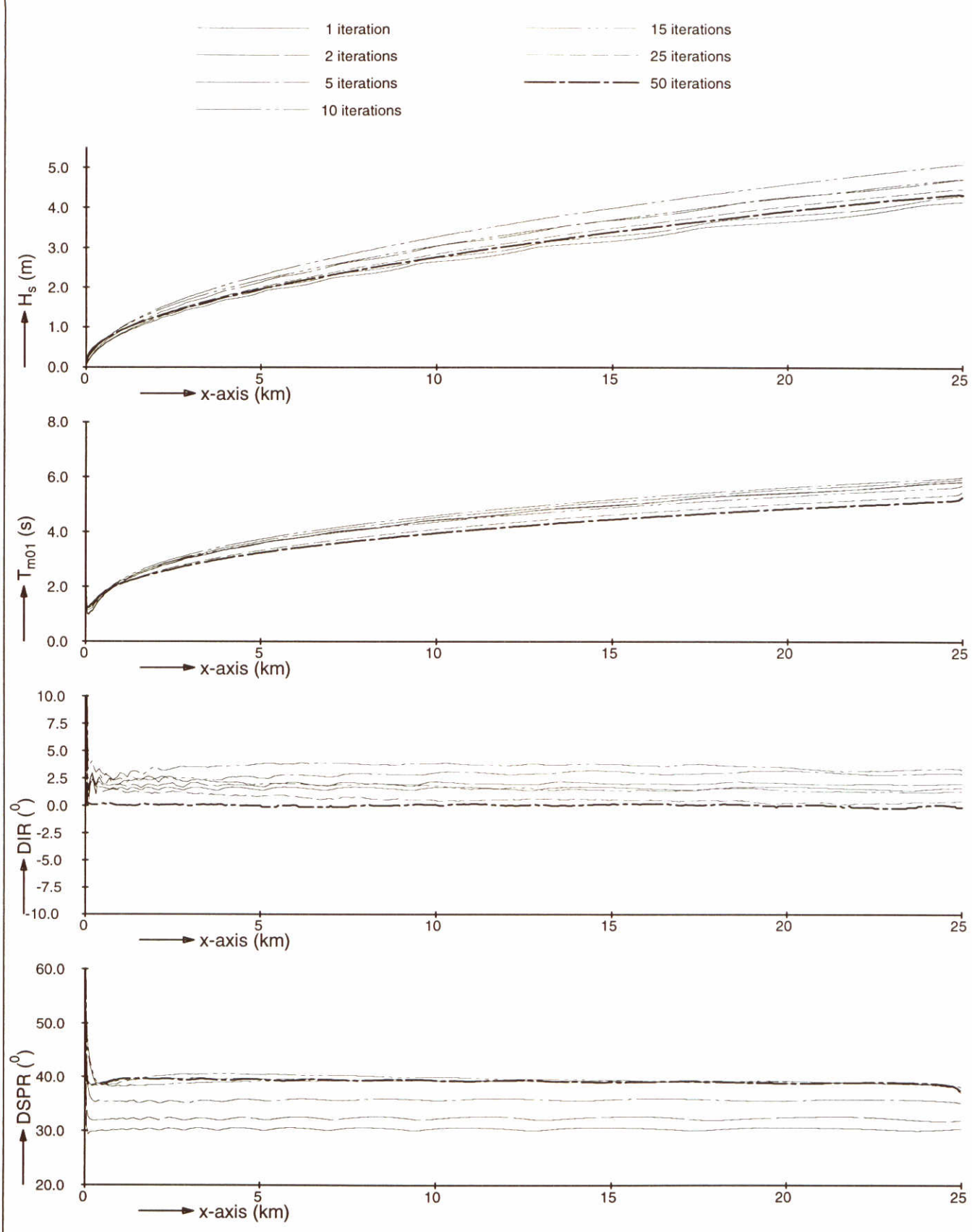

Model convergence behaviour using third-generation formulations
Enhanced first-guess by changing coefficients GEN2 mode
Adapted coefficients: cf20 = 0.885, cf30 = 0.1, cfpm=0.1

SWAN-1D | U_{10}=30 m/s

WL | delft hydraulics | H3496 | Fig. 27a

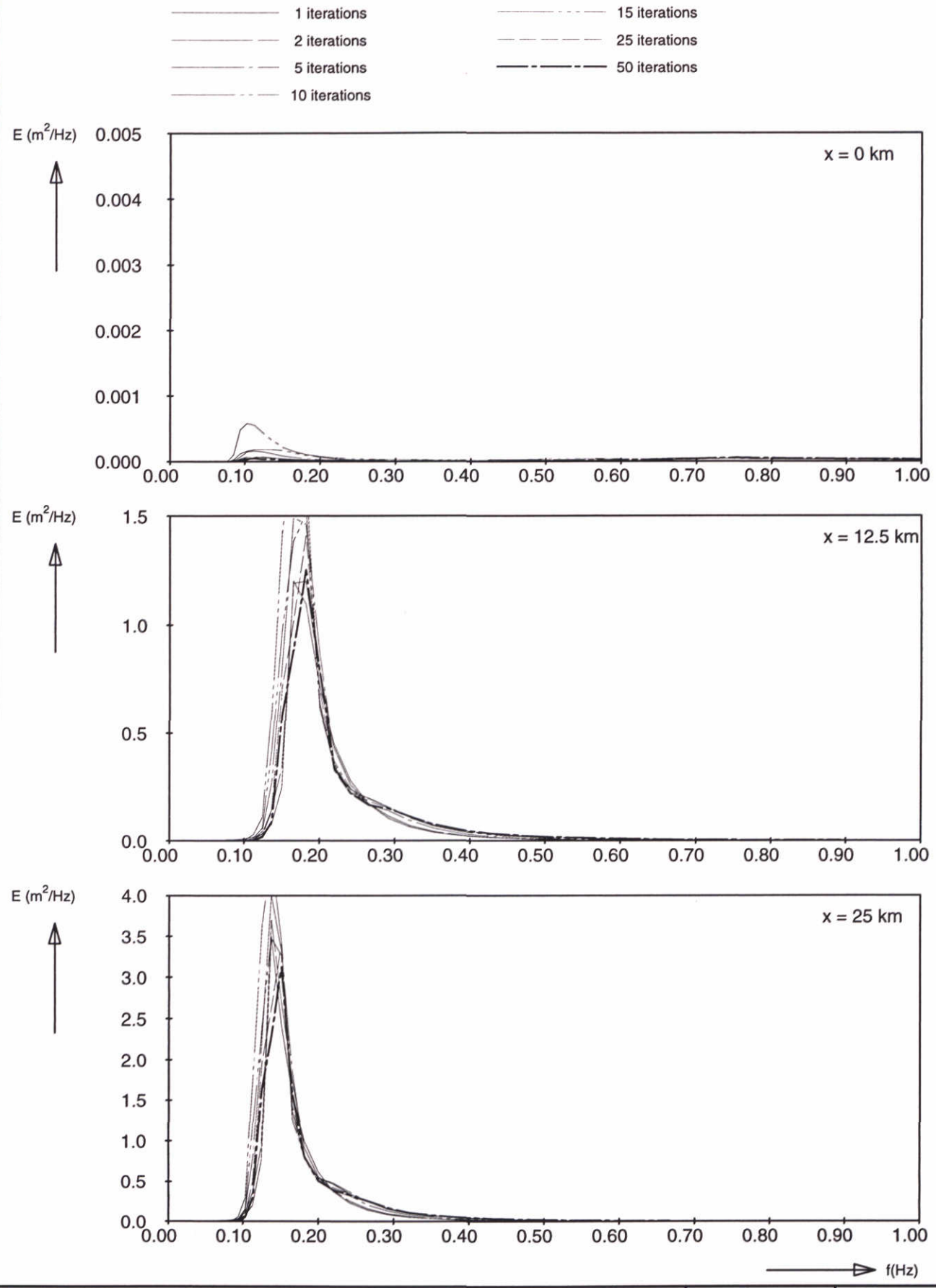

Frequency spectra at 3 locations
Enhanced first-guess by changing coefficients GEN2 mode
Adapted coefficients: cf20 = 0.885, cf30 = 0.1, cfpm=0.1

SWAN-1D

U_{10}=30 m/s

WL | delft hydraulics

H3496

Fig. 27b

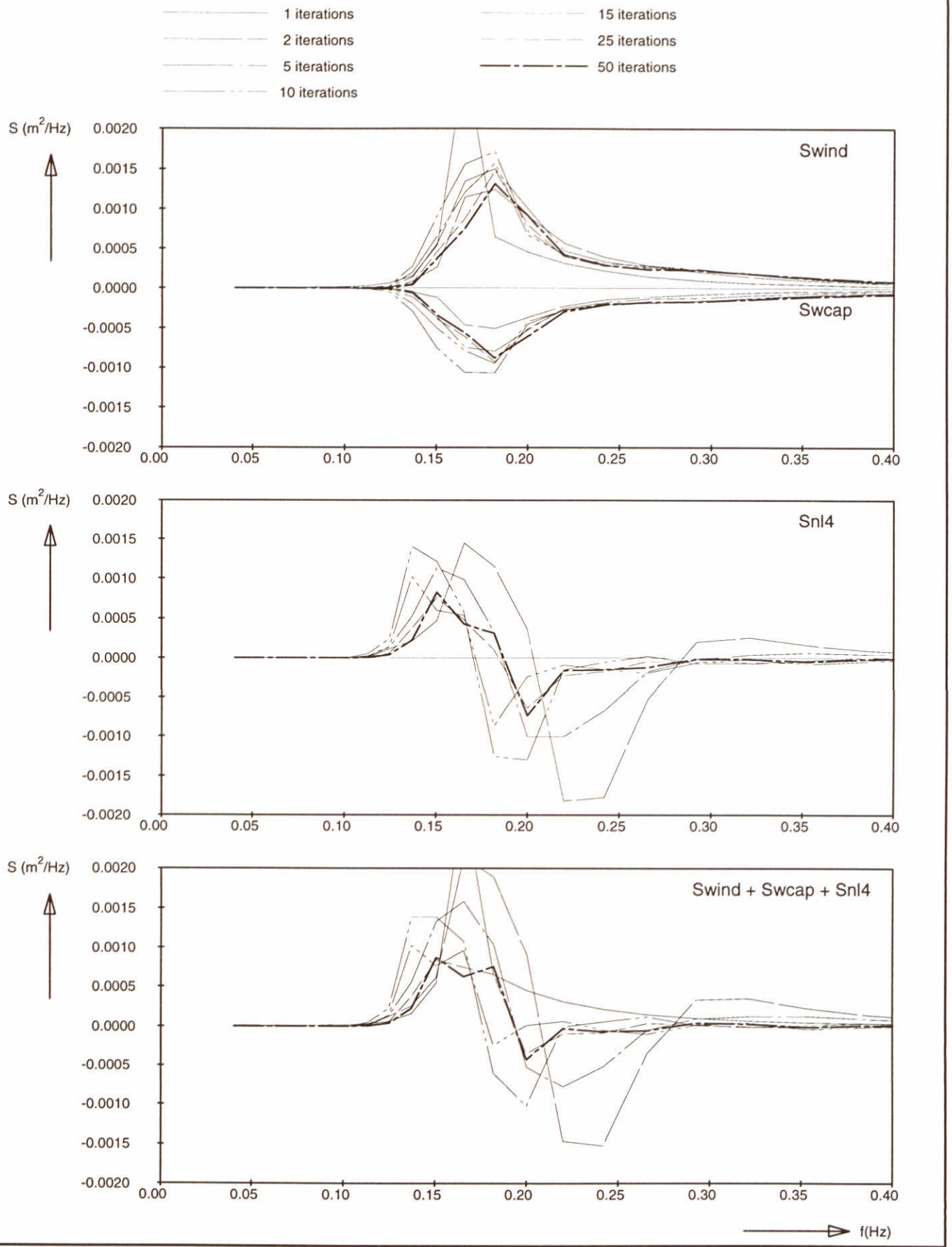

Source terms at x = 12.5 km
Enhanced first-guess by changing coefficients GEN2 mode
Adapted coefficients: cf20 = 0.885, cf30 = 0.1, cfpm=0.1

SWAN-1D | U_{10}=30 m/s

WL | delft hydraulics | H3496 | Fig. 27c

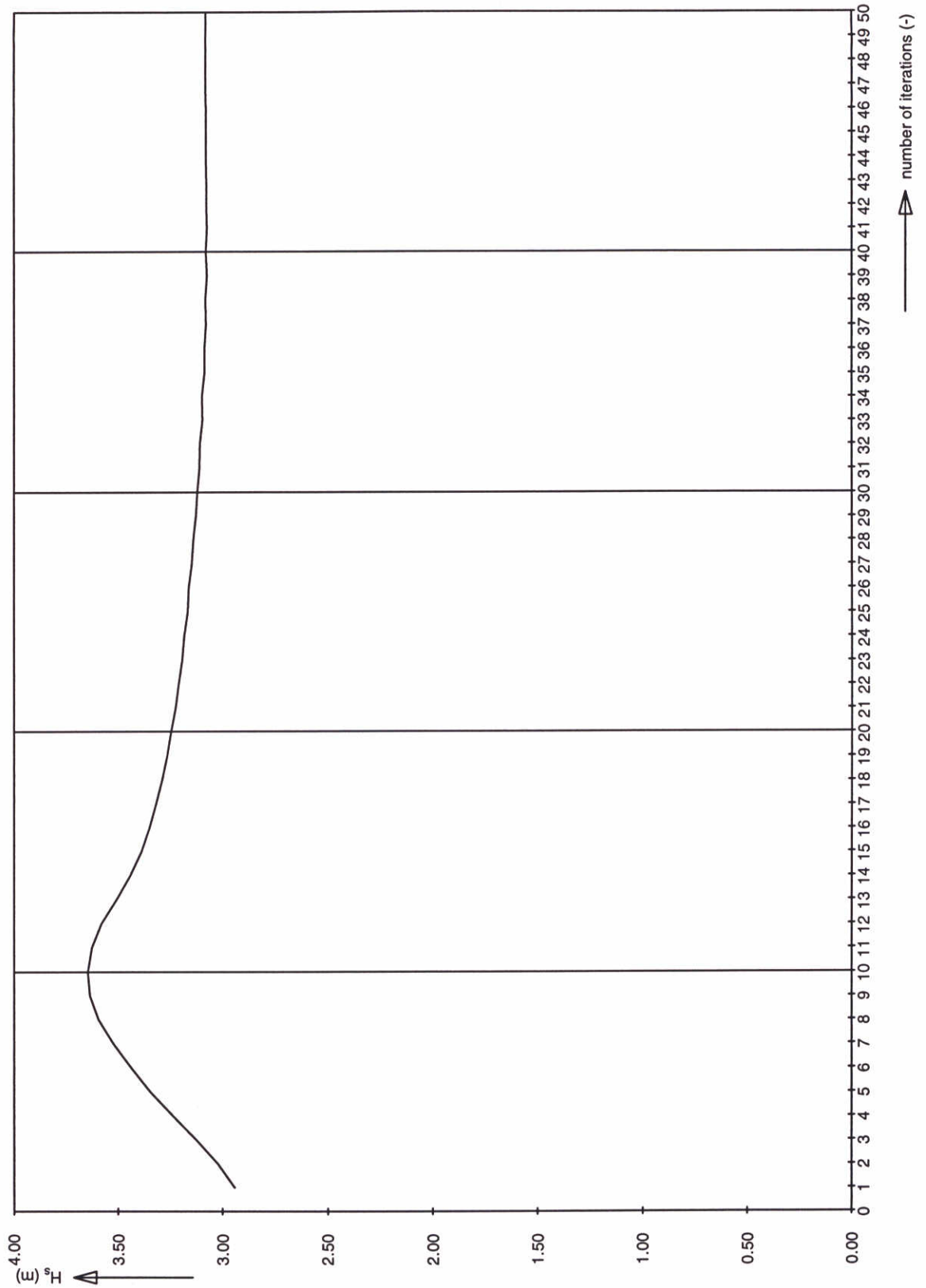

Significant wave height at 12.5 km Enhanced first-guess by changing coefficients GEN2 mode Adapted coefficients: cf20 = 0.885, cf30 = 0.1, cfpm=0.1	SWAN-1D	U_{10}=30 m/s
WL I delft hydraulics	H3496	Fig. 27d

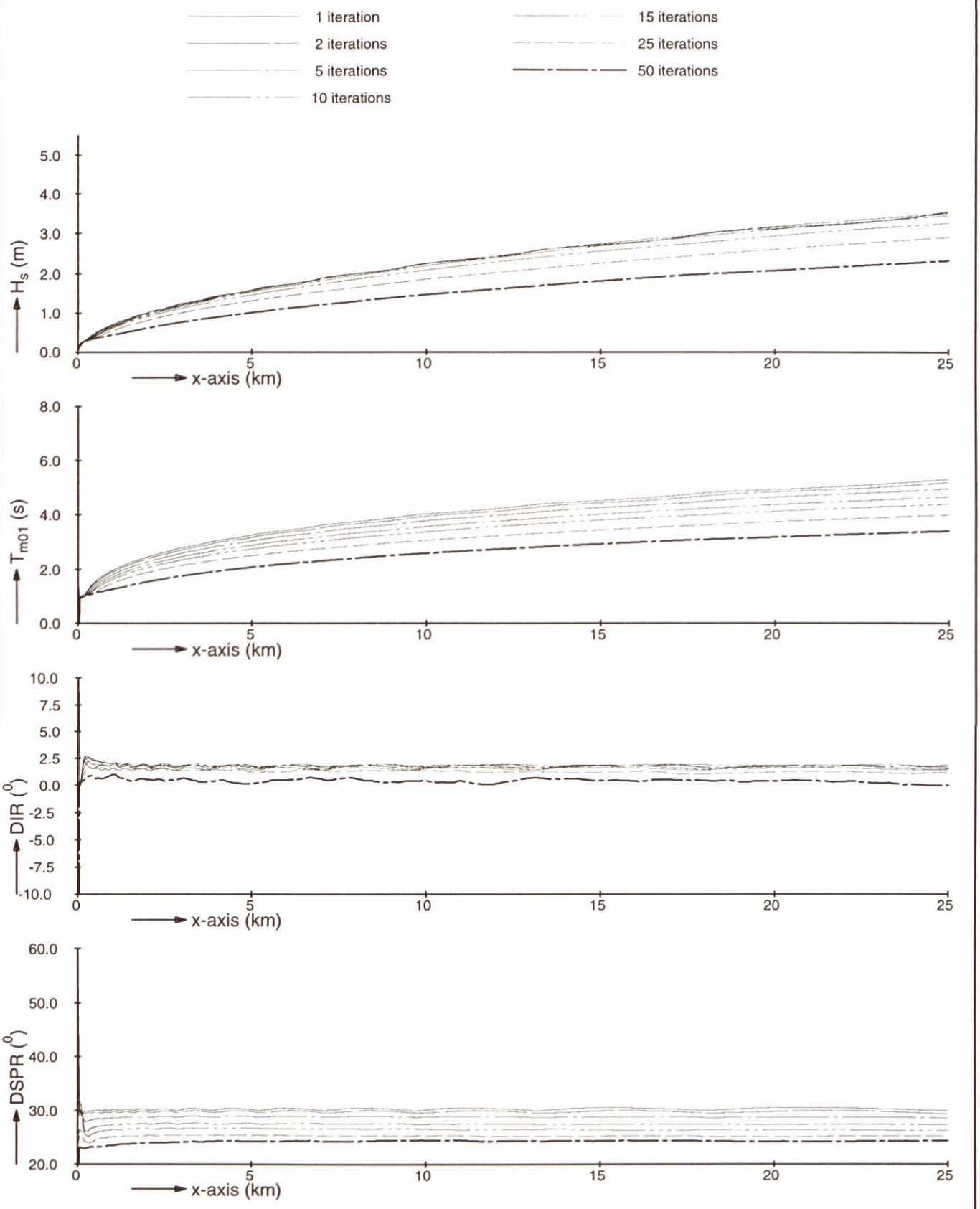

Model convergence behaviour using third-generation formulations
Adapted coefficient for quadruplets
Lambda = 0.1

SWAN-1D | U_{10}=30 m/s

WL | delft hydraulics | H3496 | Fig. 28a

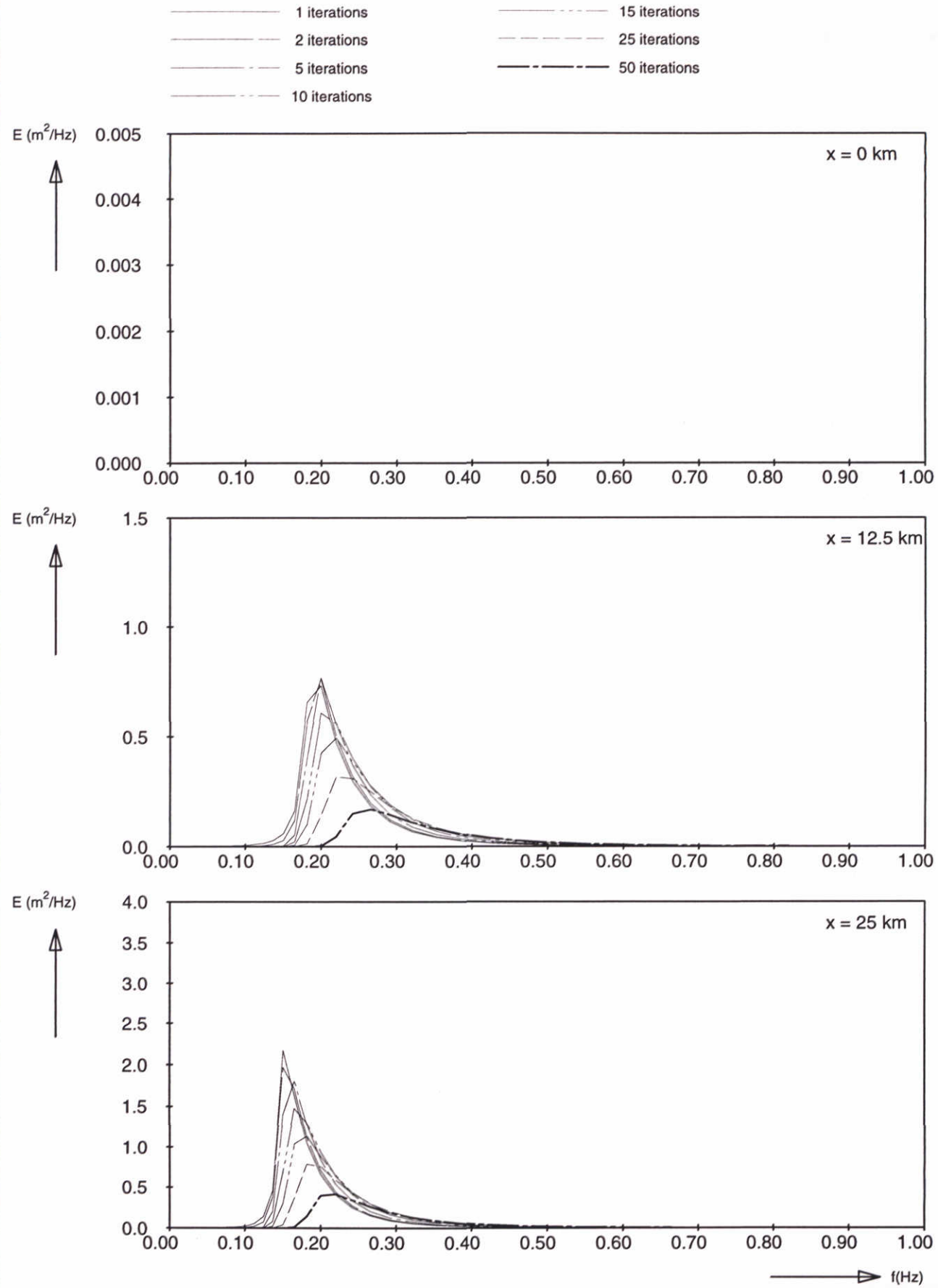

Frequency spectra at 3 locations Adapted coefficient for quadruplets Lambda = 0.1	SWAN-1D	U_{10}=30 m/s
WL | delft hydraulics	H3496	Fig. 28b

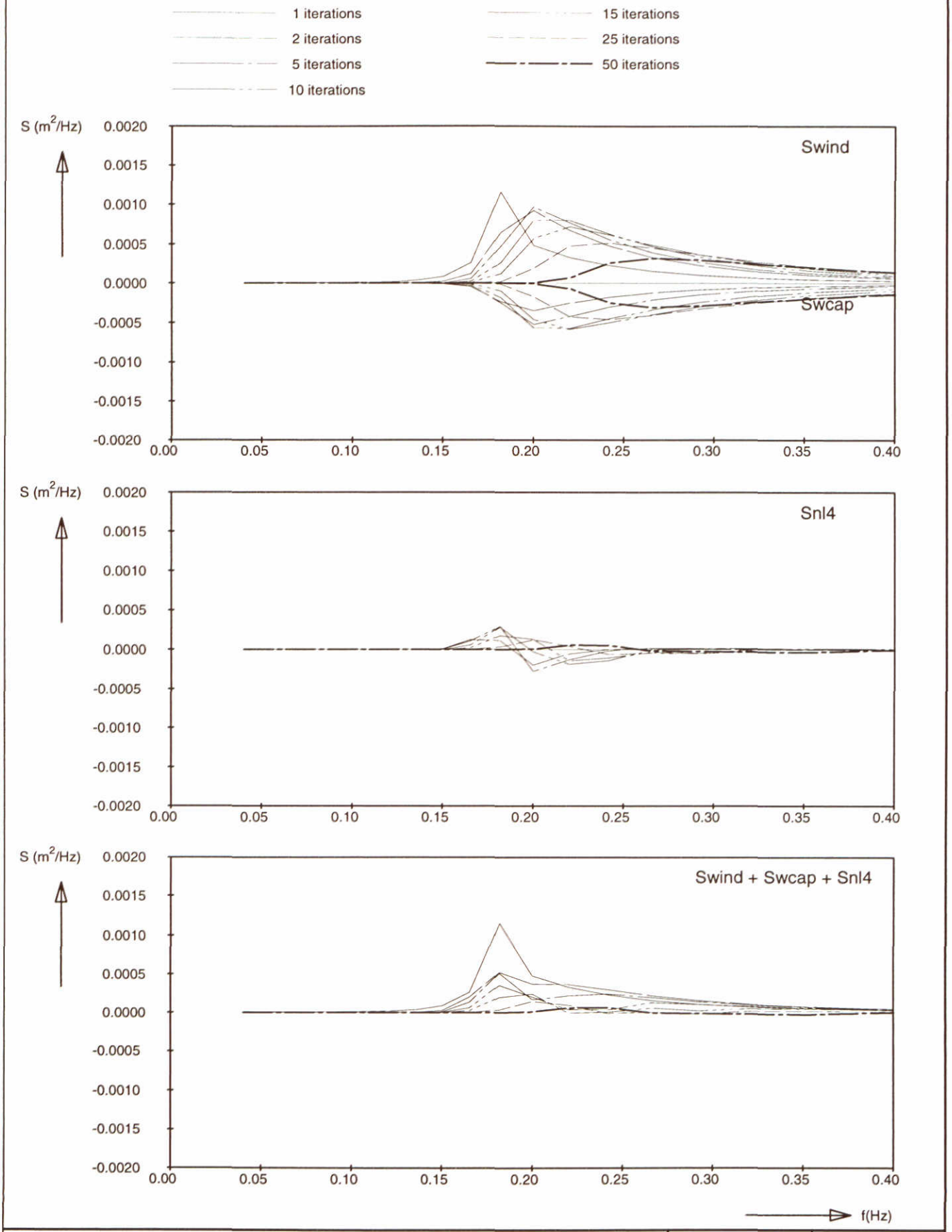

Source terms at x = 12.5 km Adapted coefficient for quadruplets Lambda = 0.1	SWAN-1D	U_{10}=30 m/s
WL | delft hydraulics	H3496	Fig. 28c

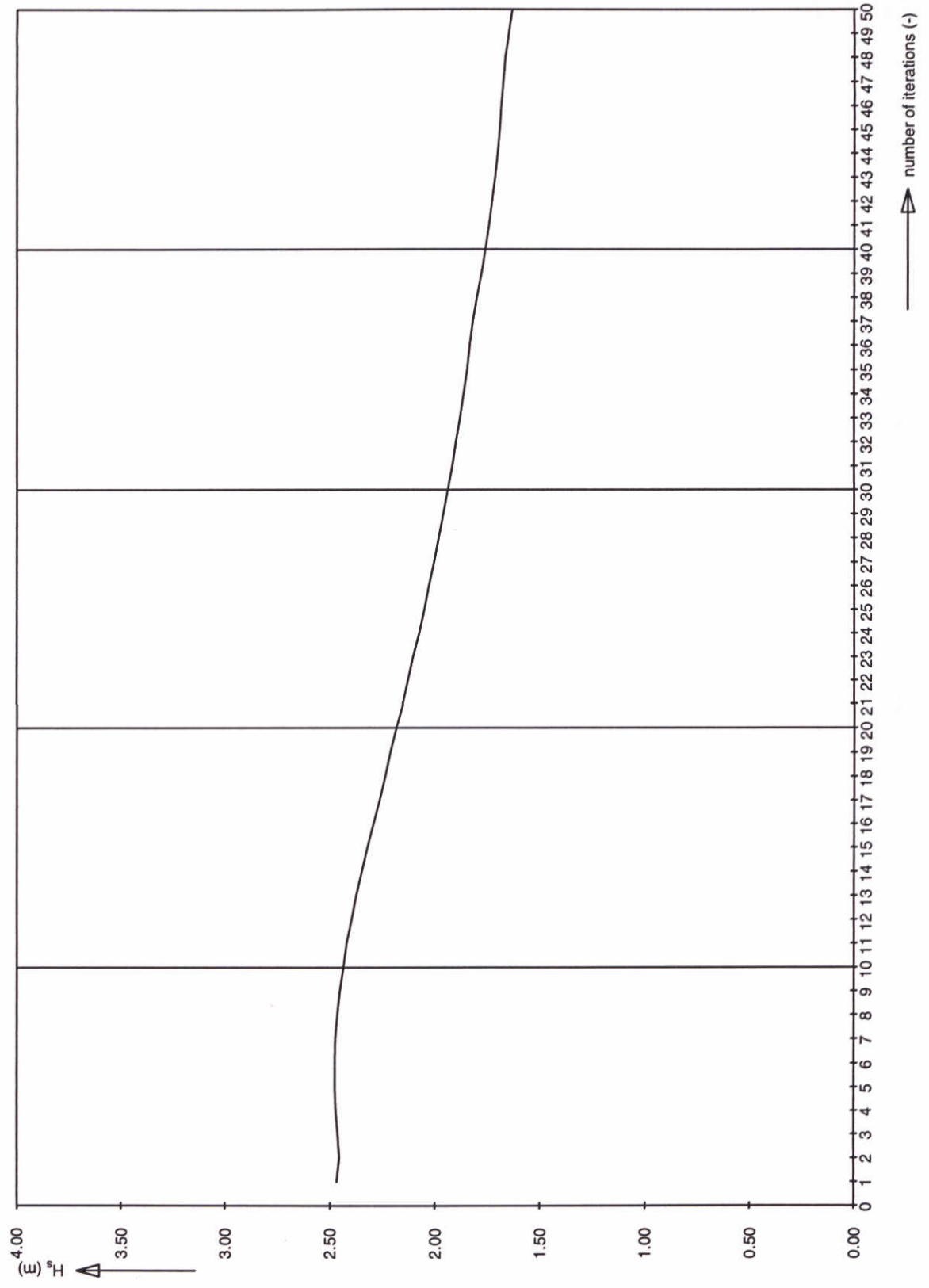

Significant wave height at 12.5 km Adapted coefficient for quadruplets Lambda = 0.1	SWAN-1D	U_{10}=30 m/s
WL | delft hydraulics	H3496	Fig. 28d

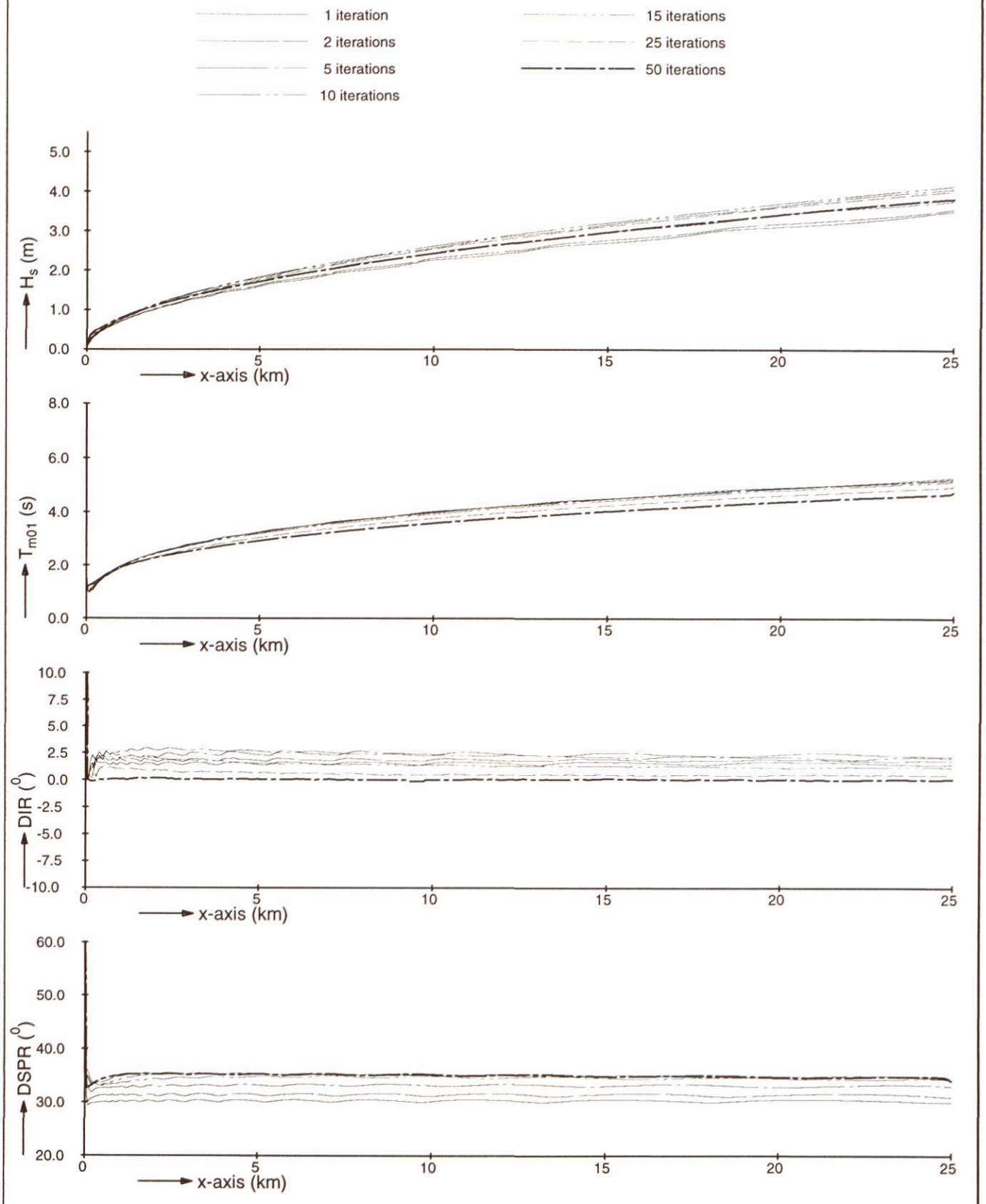

Model convergence behaviour using third-generation formulations Adapted coefficients for quadruplets C_{nl4} = 1.5e7	SWAN-1D	U_{10}=30 m/s
WL | delft hydraulics	H3496	Fig. 29a

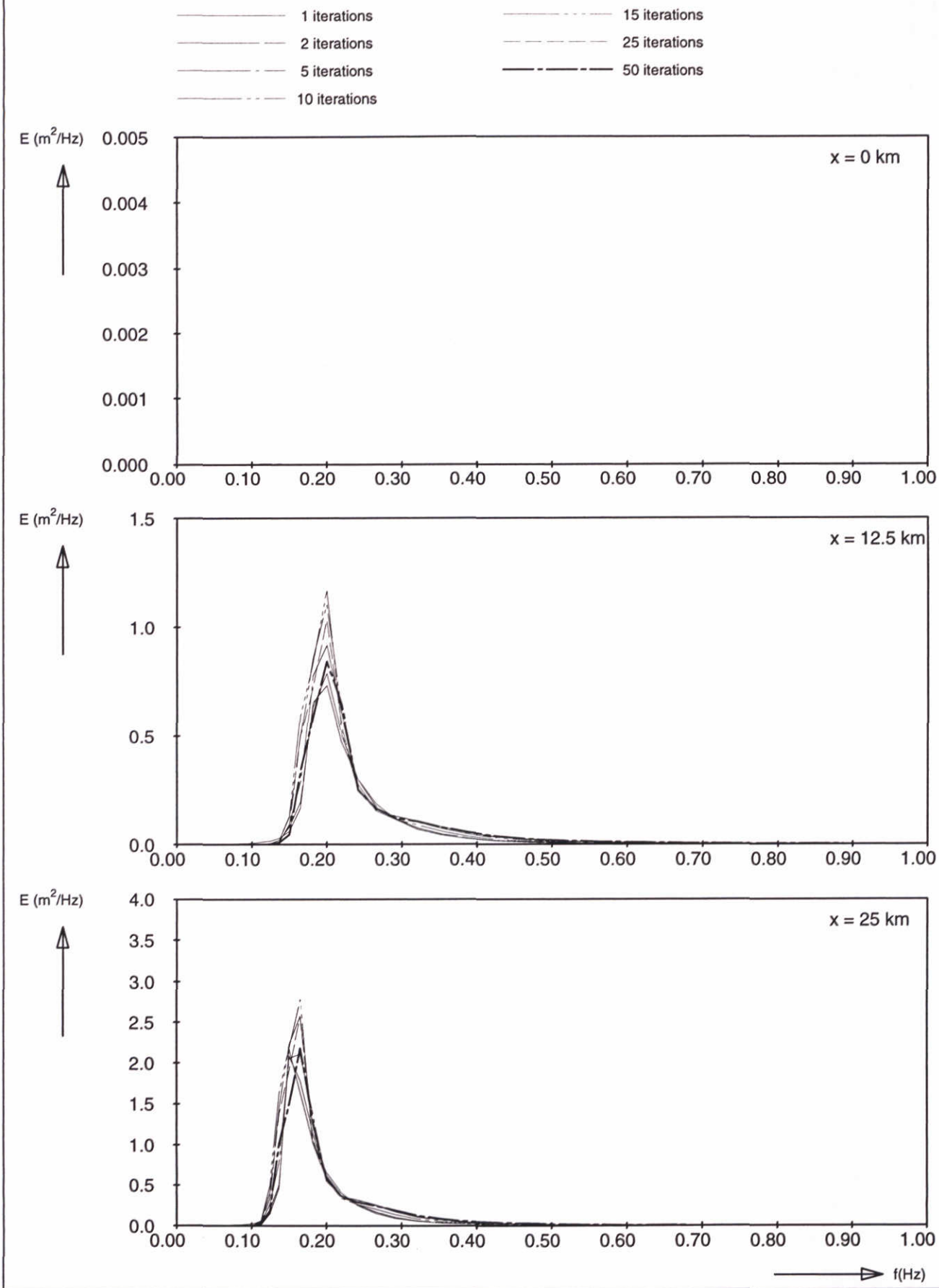

Frequency spectra at 3 locations Adapted coefficients for quadruplets C_{nl4} = 1.5e7	SWAN-1D	U_{10}=30 m/s
WL | delft hydraulics	H3496	Fig. 29b

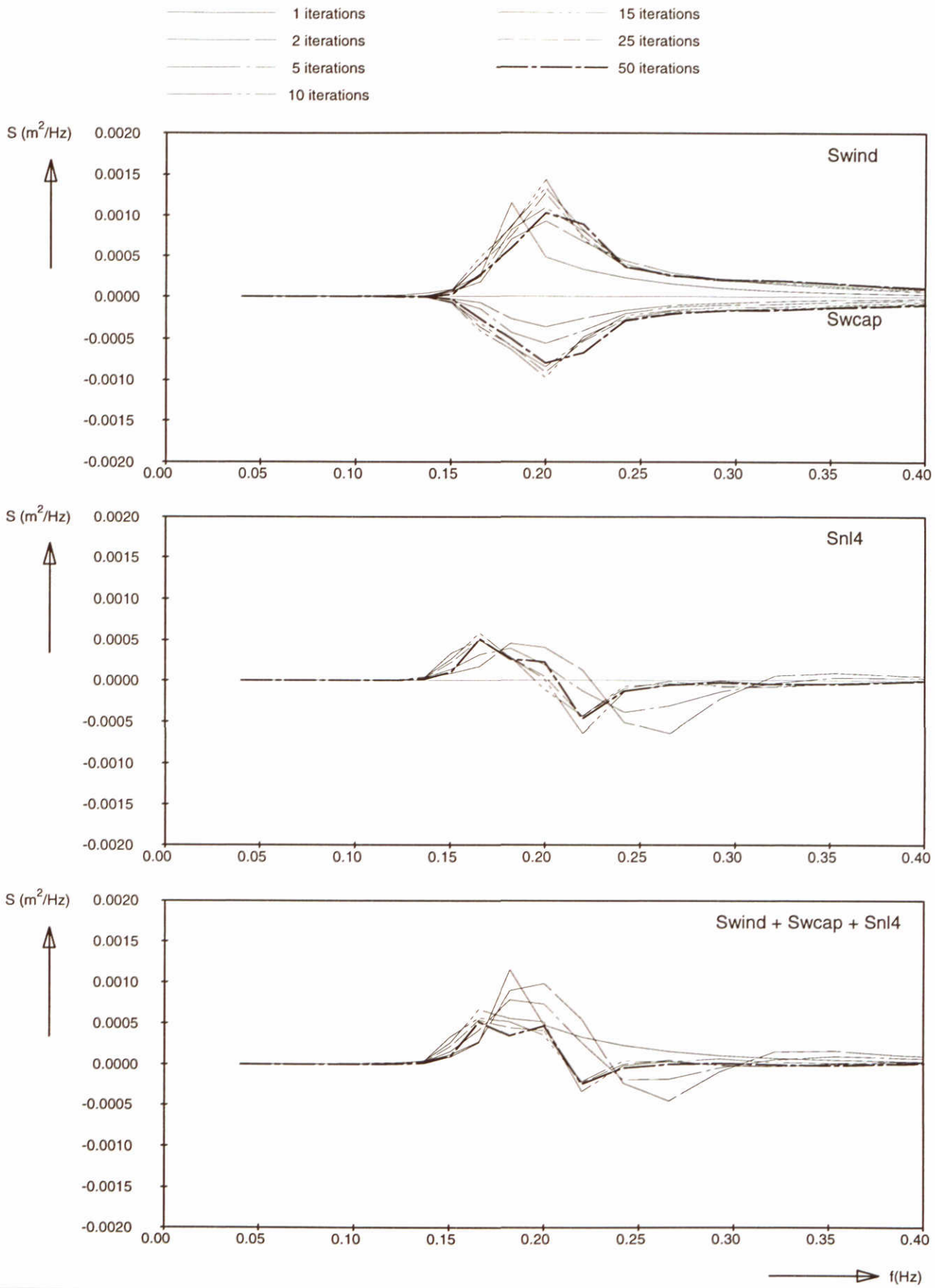

Source terms at x = 12.5 km Adapted coefficients for quadruplets C_{nl4} = 1.5e7	SWAN-1D	U_{10}=30 m/s
WL | delft hydraulics	H3496	Fig. 29c

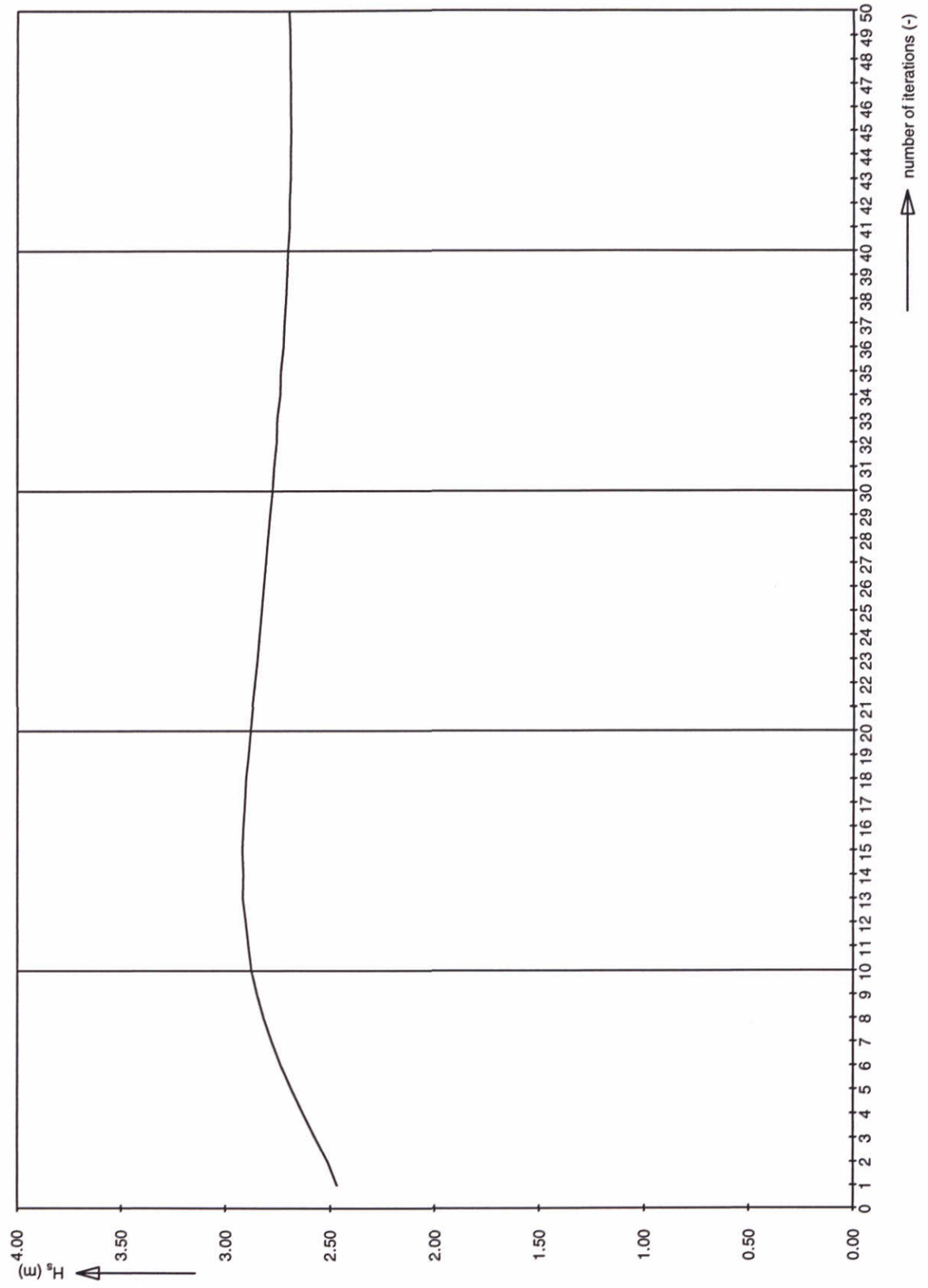

Significant wave height at 12.5 km Adapted coefficients for quadruplets C_{nl4} = 1.5e7	SWAN-1D	U_{10}=30 m/s
WL | delft hydraulics	H3496	Fig. 29d

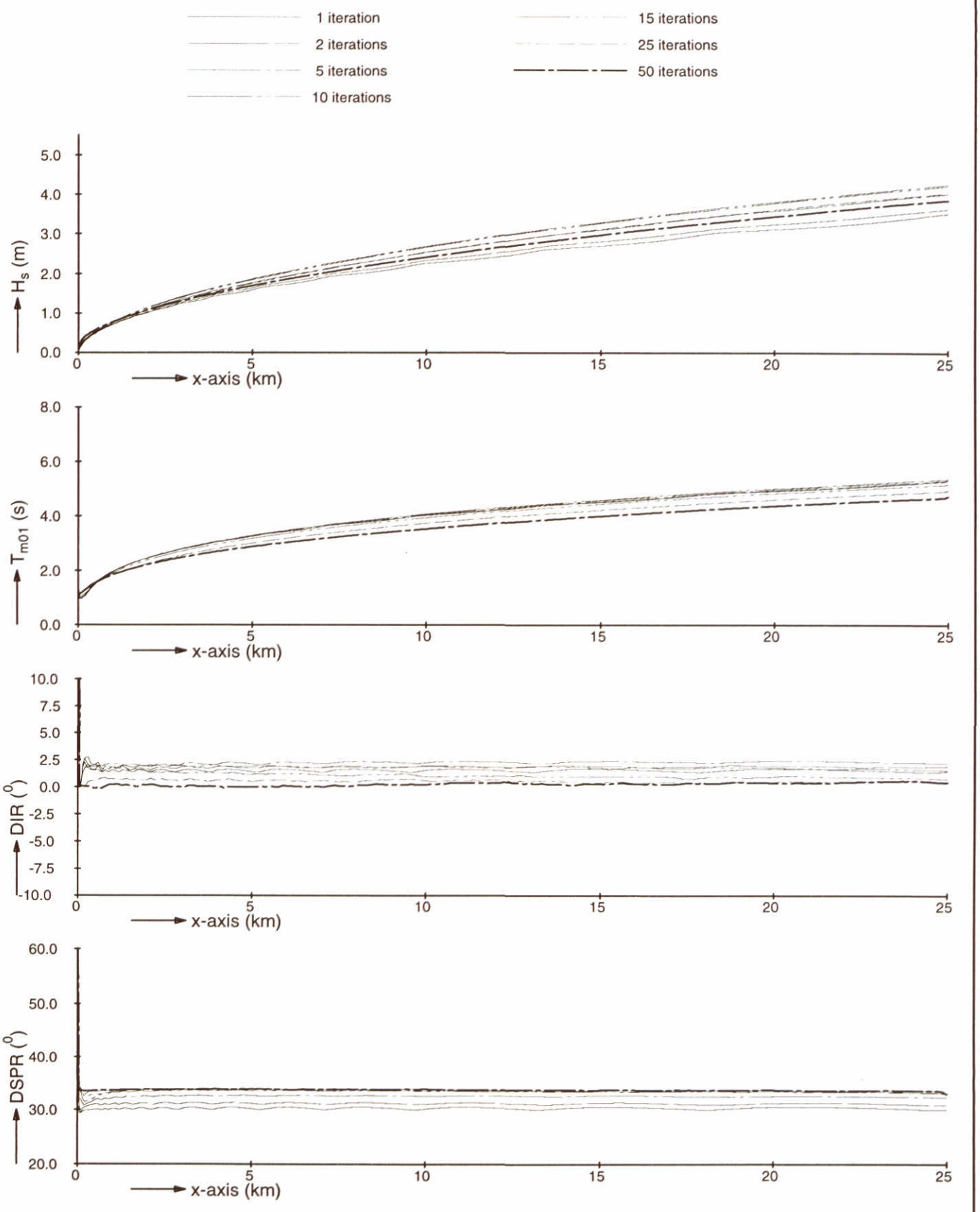

Model convergence behaviour using third-generation formulations
Adapted coefficient for quadruplets
Lambda = 0.2

SWAN-1D

U_{10}=30 m/s

WL | delft hydraulics

H3496

Fig. 30a

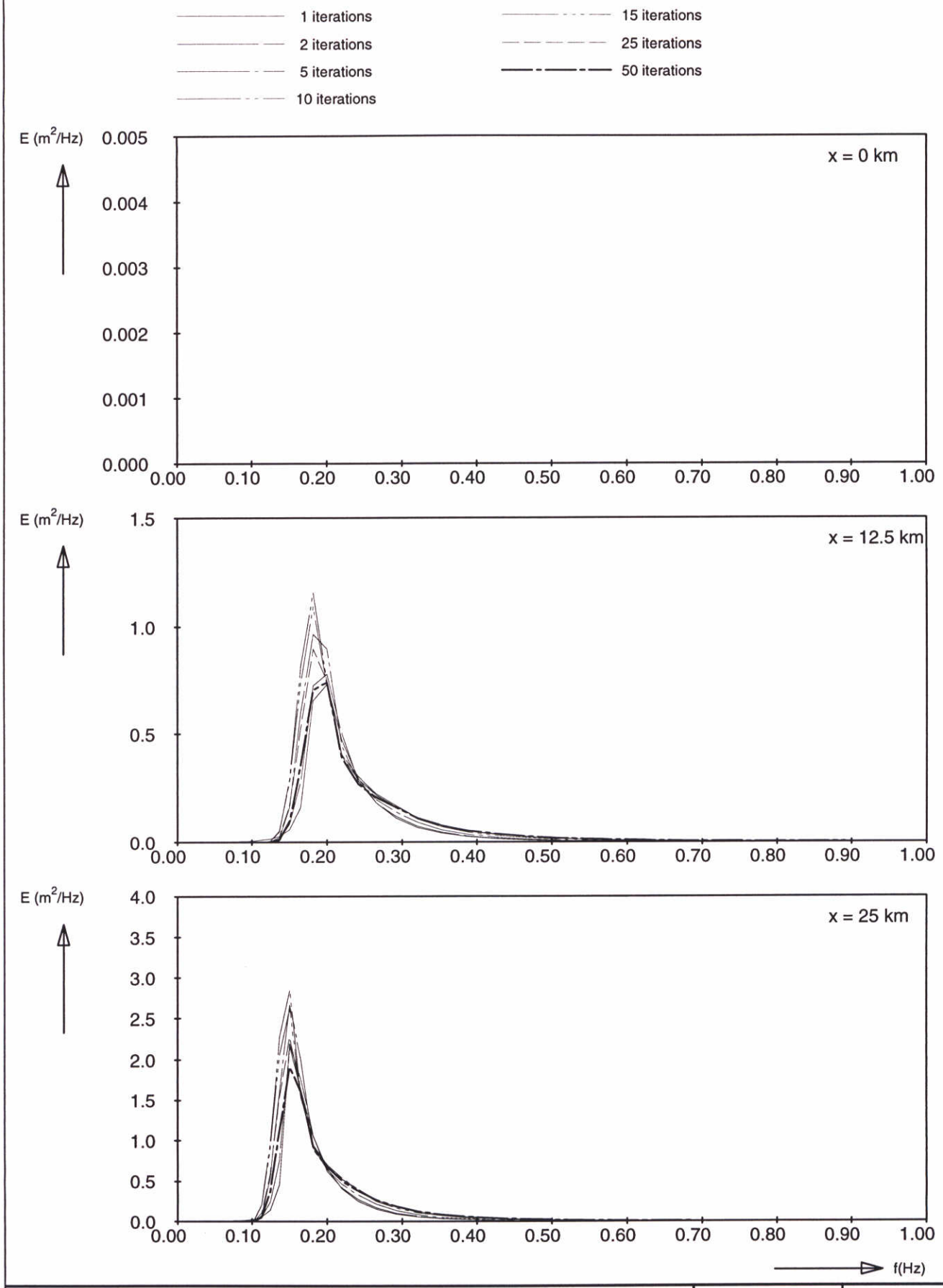

Frequency spectra at 3 locations Adapted coefficient for quadruplets Lambda = 0.2	SWAN-1D	U_{10}=30 m/s
WL | delft hydraulics	H3496	Fig. 30b

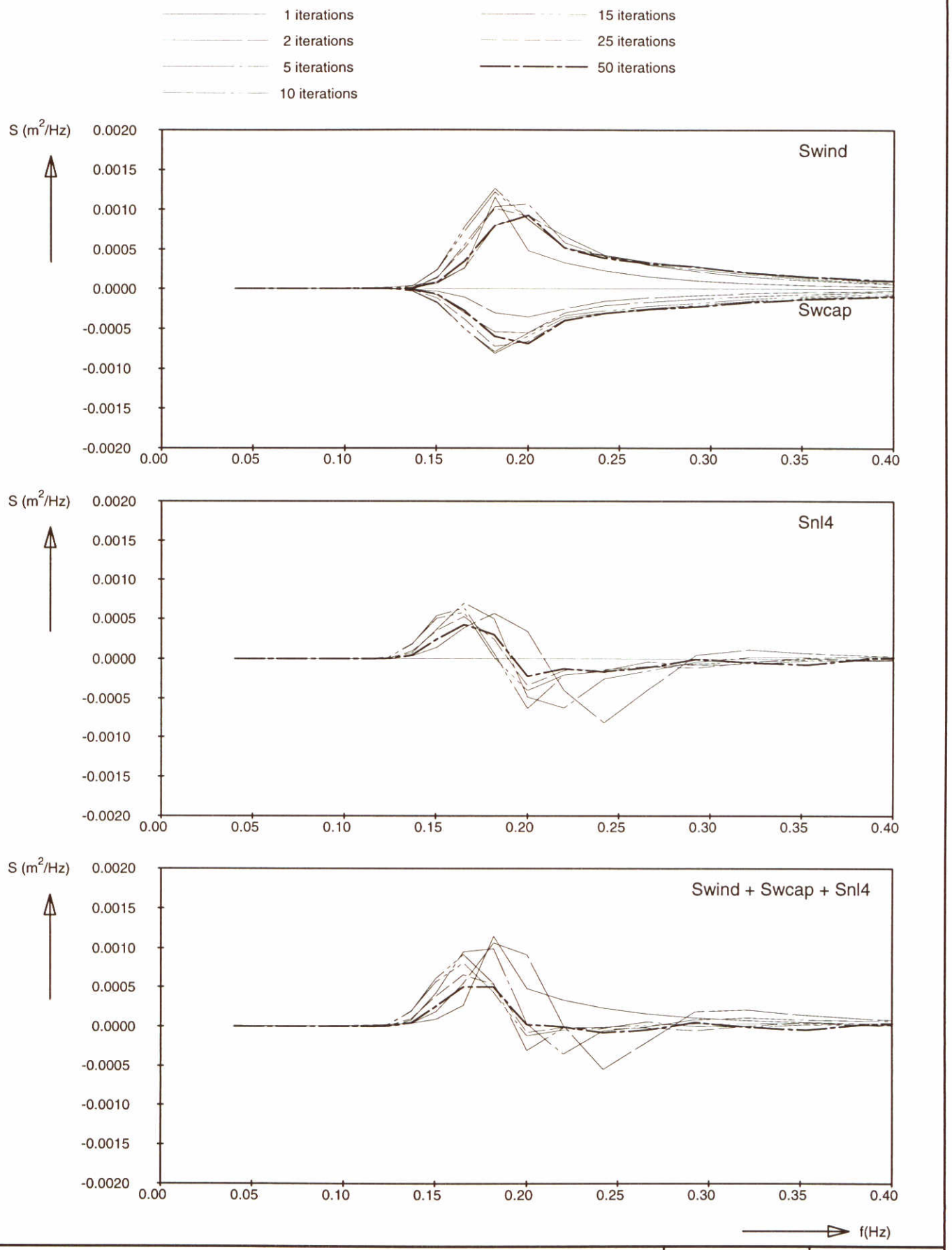

Source terms at x = 12.5 km Adapted coefficient for quadruplets Lambda = 0.2	SWAN-1D	U_{10}=30 m/s
WL | delft hydraulics	H3496	Fig. 30c

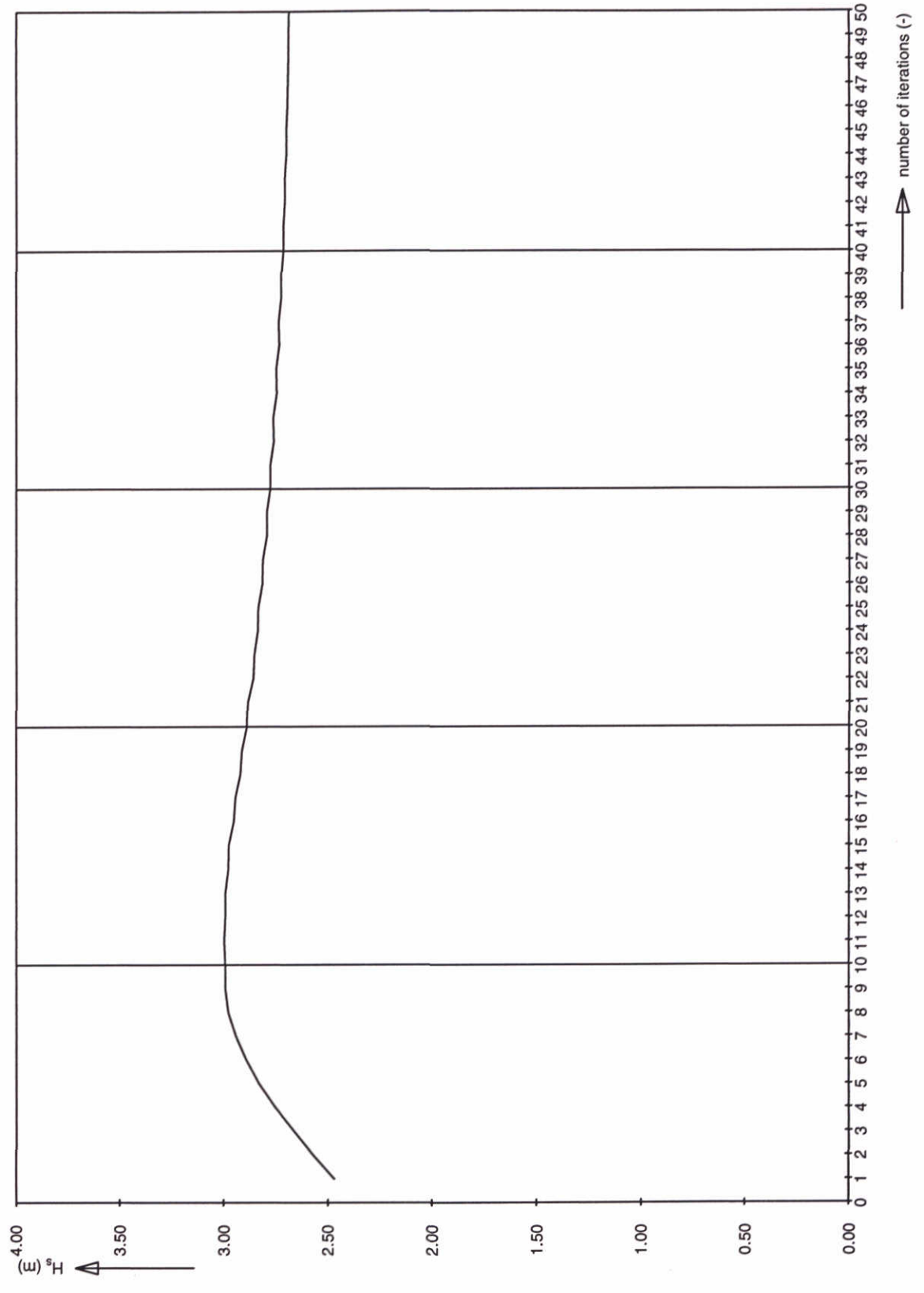

Significant wave height at 12.5 km Adapted coefficient for quadruplets Lambda = 0.2	SWAN-1D	U_{10}=30 m/s
WL | delft hydraulics	H3496	Fig. 30d

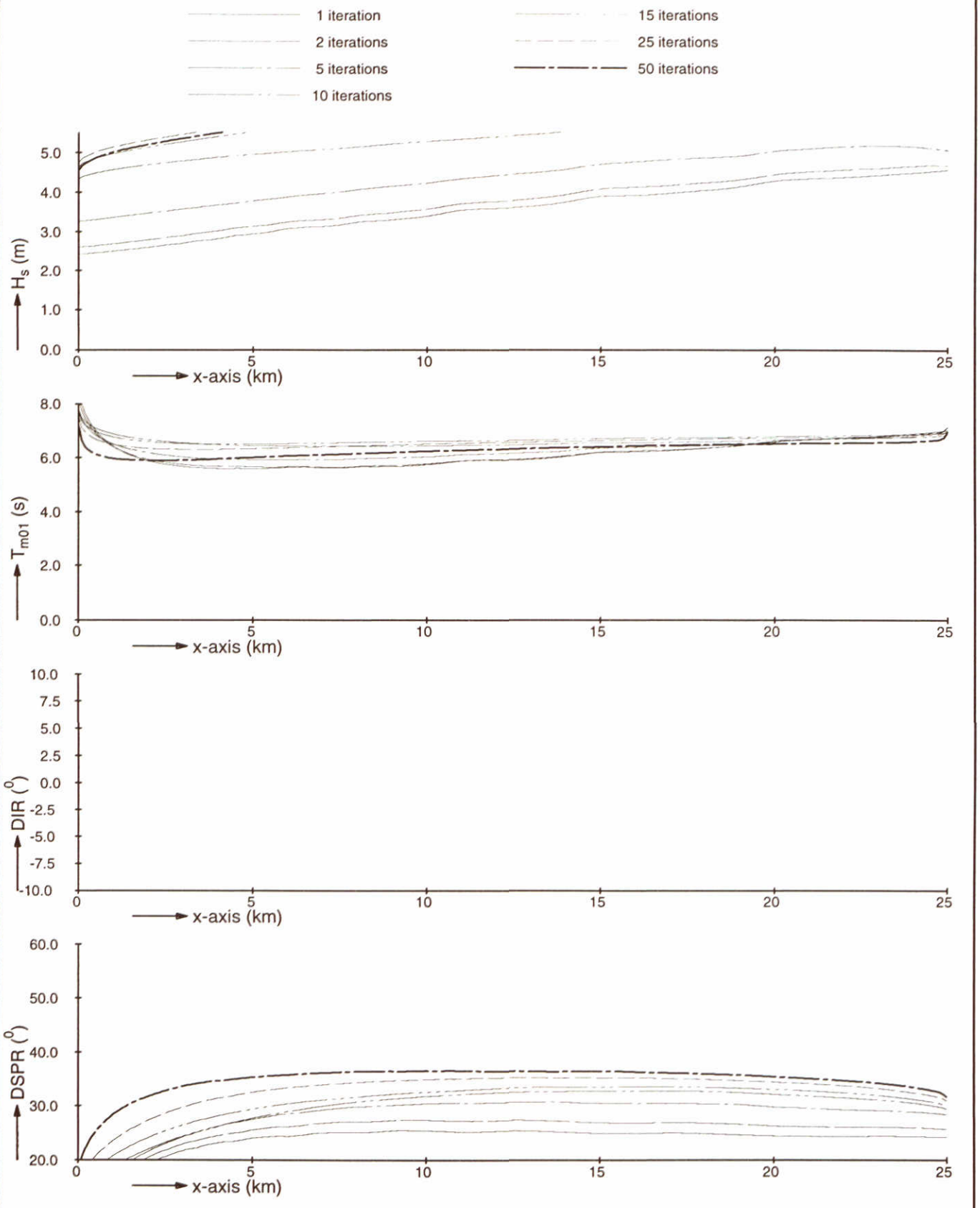

Model convergence behaviour using third-generation formulations
Adapted wind speed and direction
U_{10}=30 m/s, $U_{10,dir}$=45°

SWAN-1D | U_{10}=30 m/s

WL | delft hydraulics | H3496 | Fig. 31a

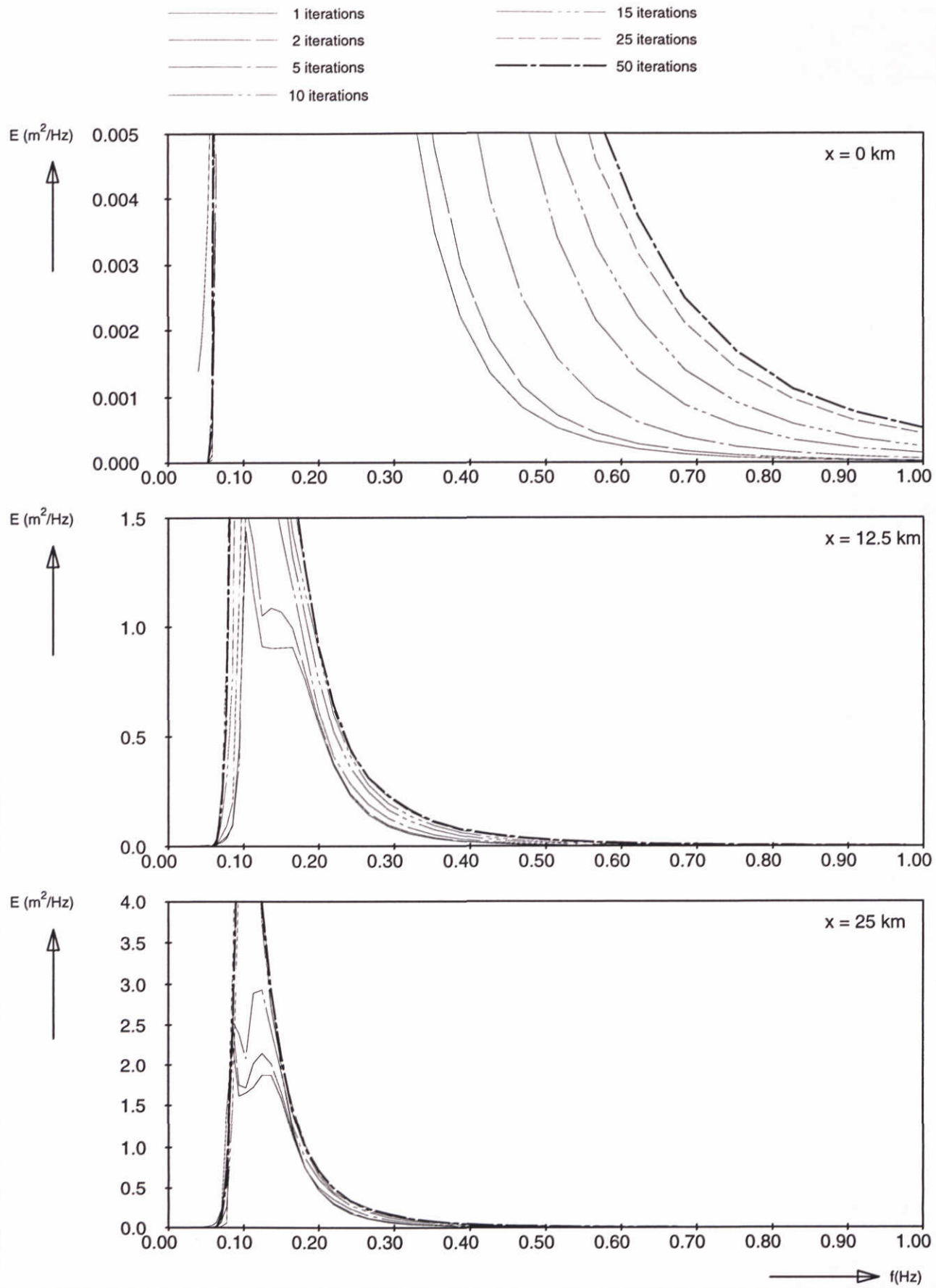

Frequency spectra at 3 locations Adapted wind speed and direction U_{10}=30 m/s, $U_{10,dir}$=45°	SWAN-1D	U_{10}=30 m/s
WL | delft hydraulics	H3496	Fig. 31b

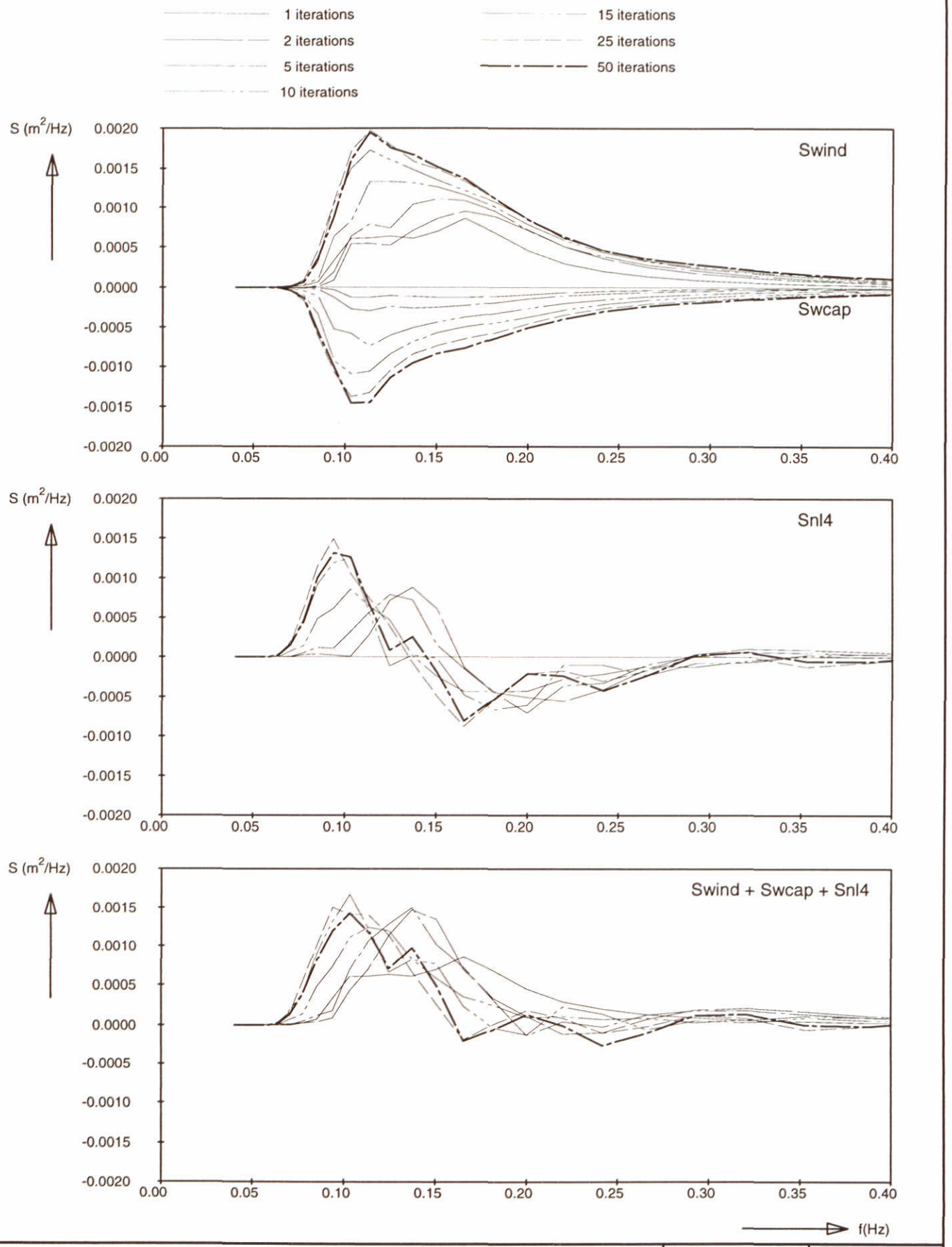

Source terms at x = 12.5 km Adapted wind speed and direction U_{10}=30 m/s, $U_{10,dir}$=45°	SWAN-1D	U_{10}=30 m/s
WL | delft hydraulics	H3496	Fig. 31c

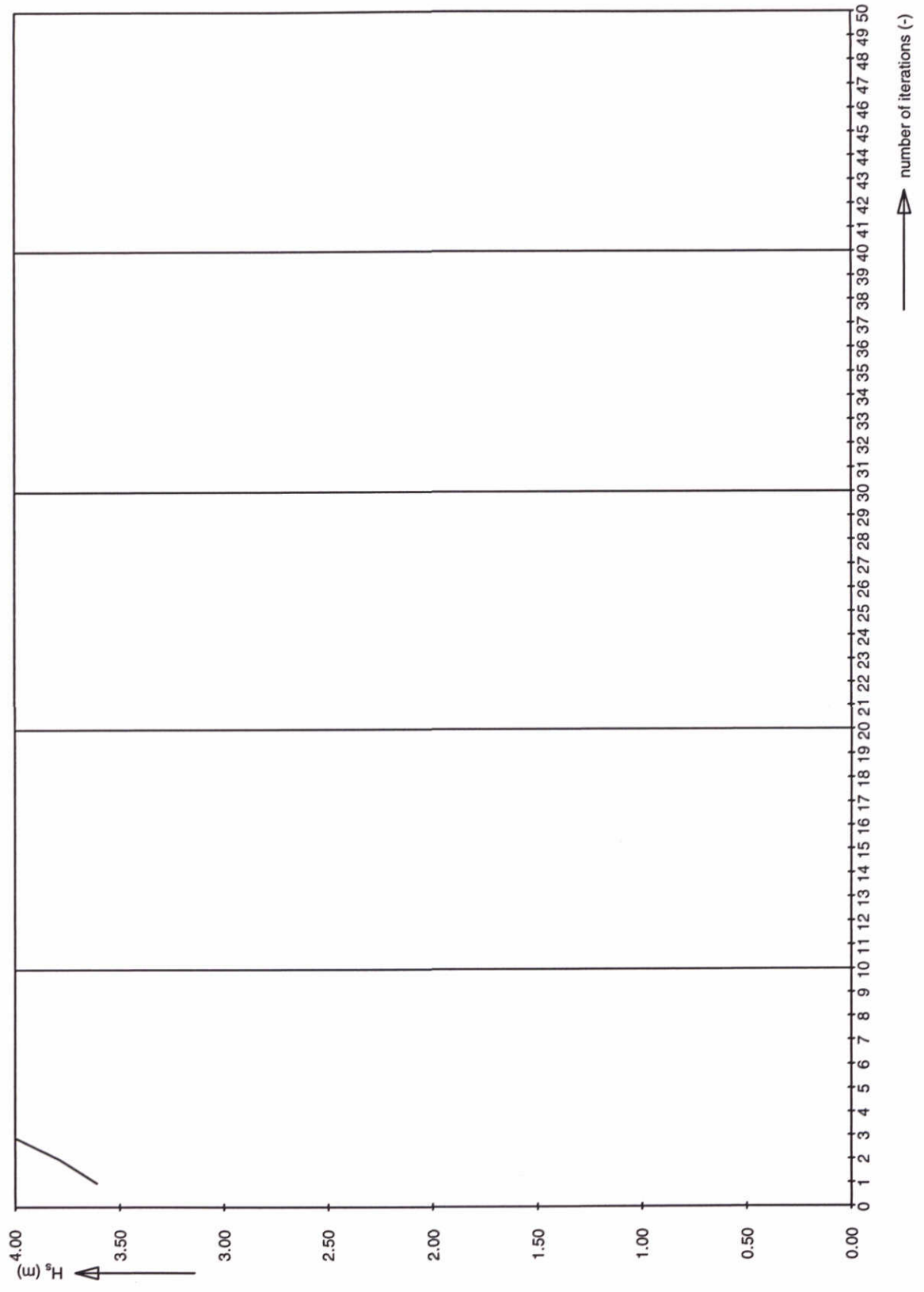

Significant wave height at 12.5 km Adapted wind speed and direction U_{10}=30 m/s, $U_{10,dir}$=45°	SWAN-1D	U_{10}=30 m/s
WL | delft hydraulics	H3496	Fig. 31d

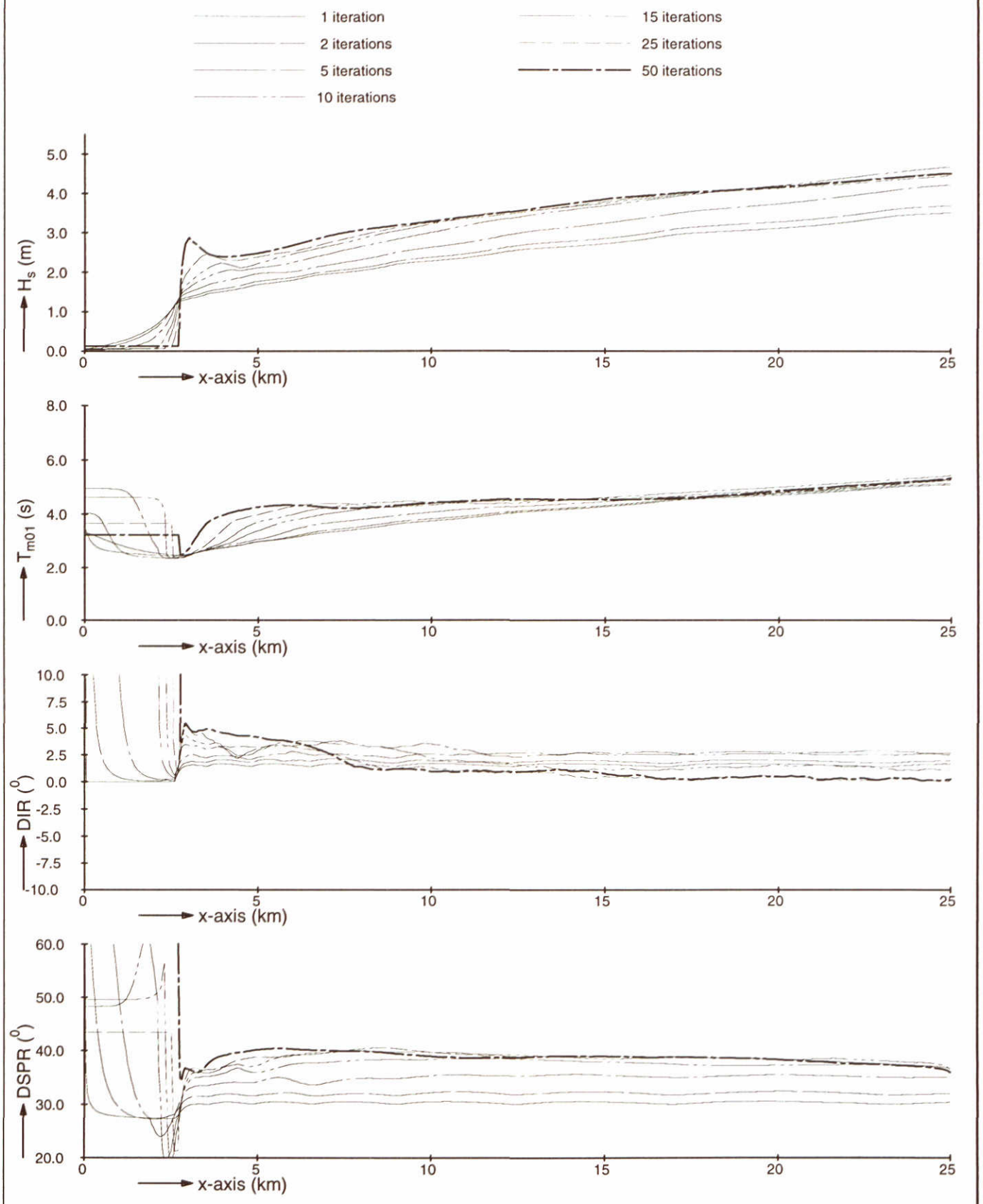

Model convergence behaviour using third-generation formulations
Adapted frequency range
f_{low} = 0.04 Hz, f_{high} = 0.3 Hz, MSC = 21

SWAN-1D | U_{10}=30 m/s

WL | delft hydraulics | H3496 | Fig. 32a

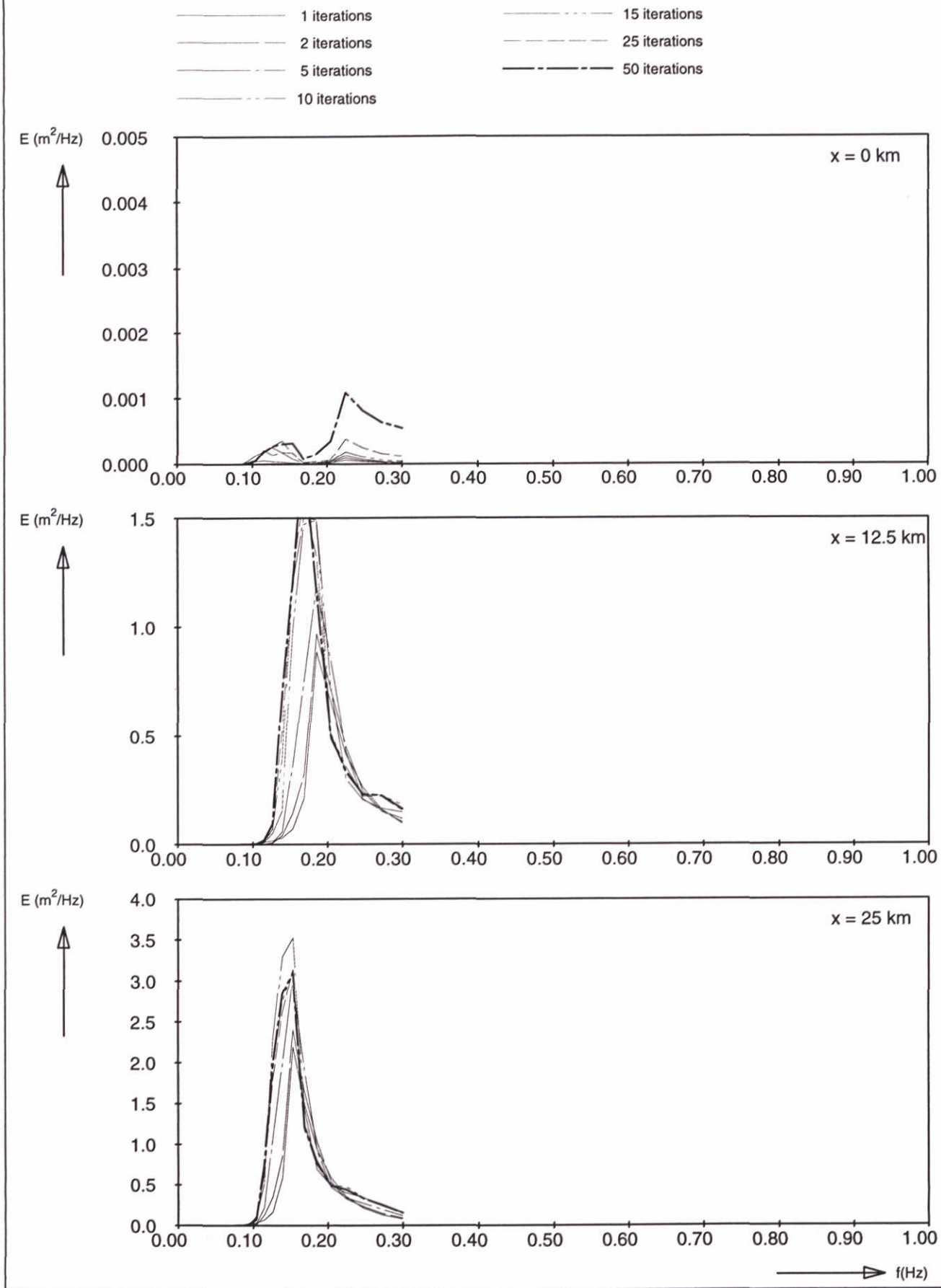

Frequency spectra at 3 locations Adapted frequency range f_{low} = 0.04 Hz, f_{high} = 0.3 Hz, MSC = 21	SWAN-1D	U_{10}=30 m/s
WL | delft hydraulics	H3496	Fig. 32b

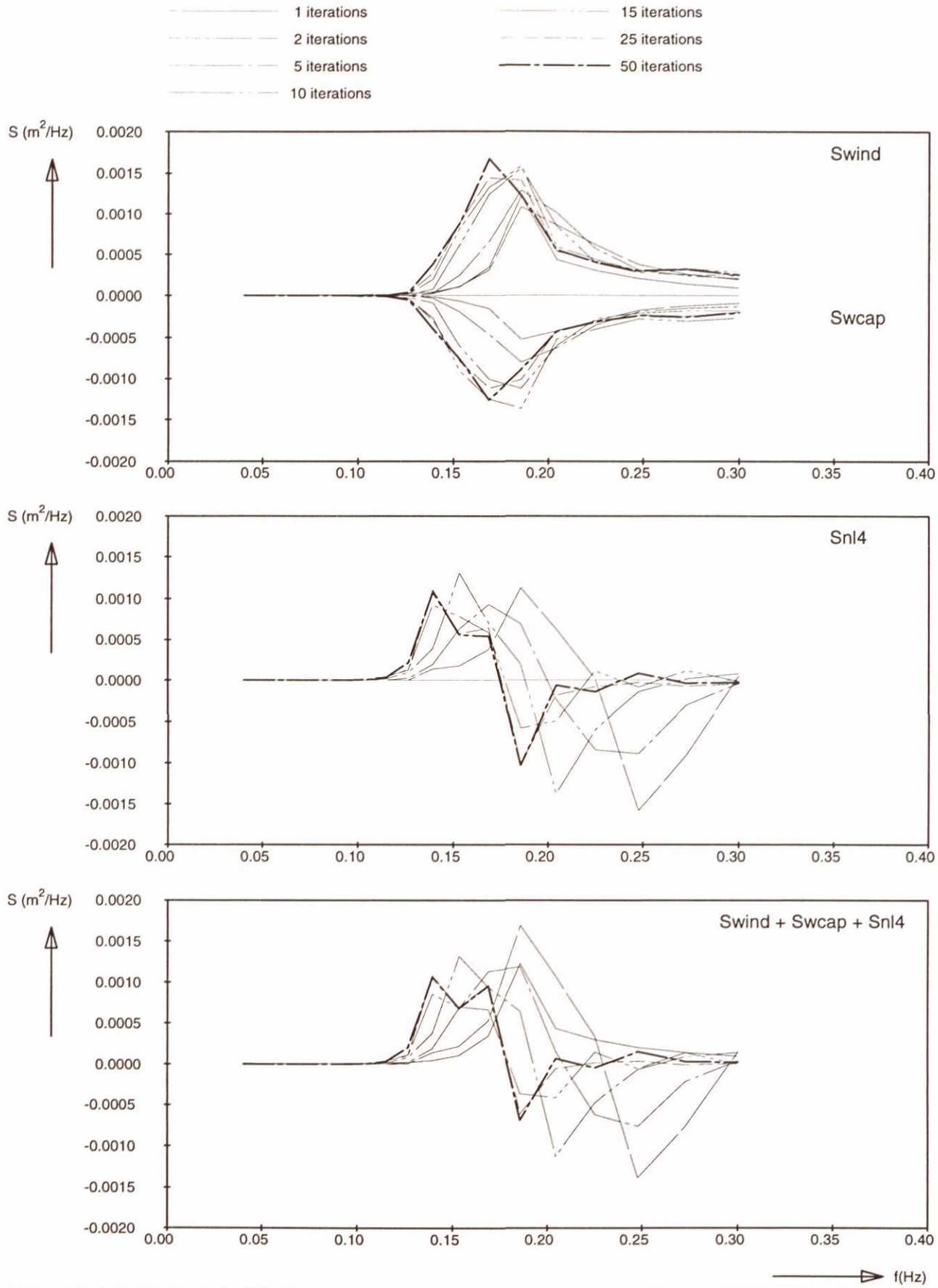

Source terms at x = 12.5 km
Adapted frequency range
f_{low} = 0.04 Hz, f_{high} = 0.3 Hz, MSC = 21

SWAN-1D

U_{10}=30 m/s

WL | delft hydraulics

H3496

Fig. 32c

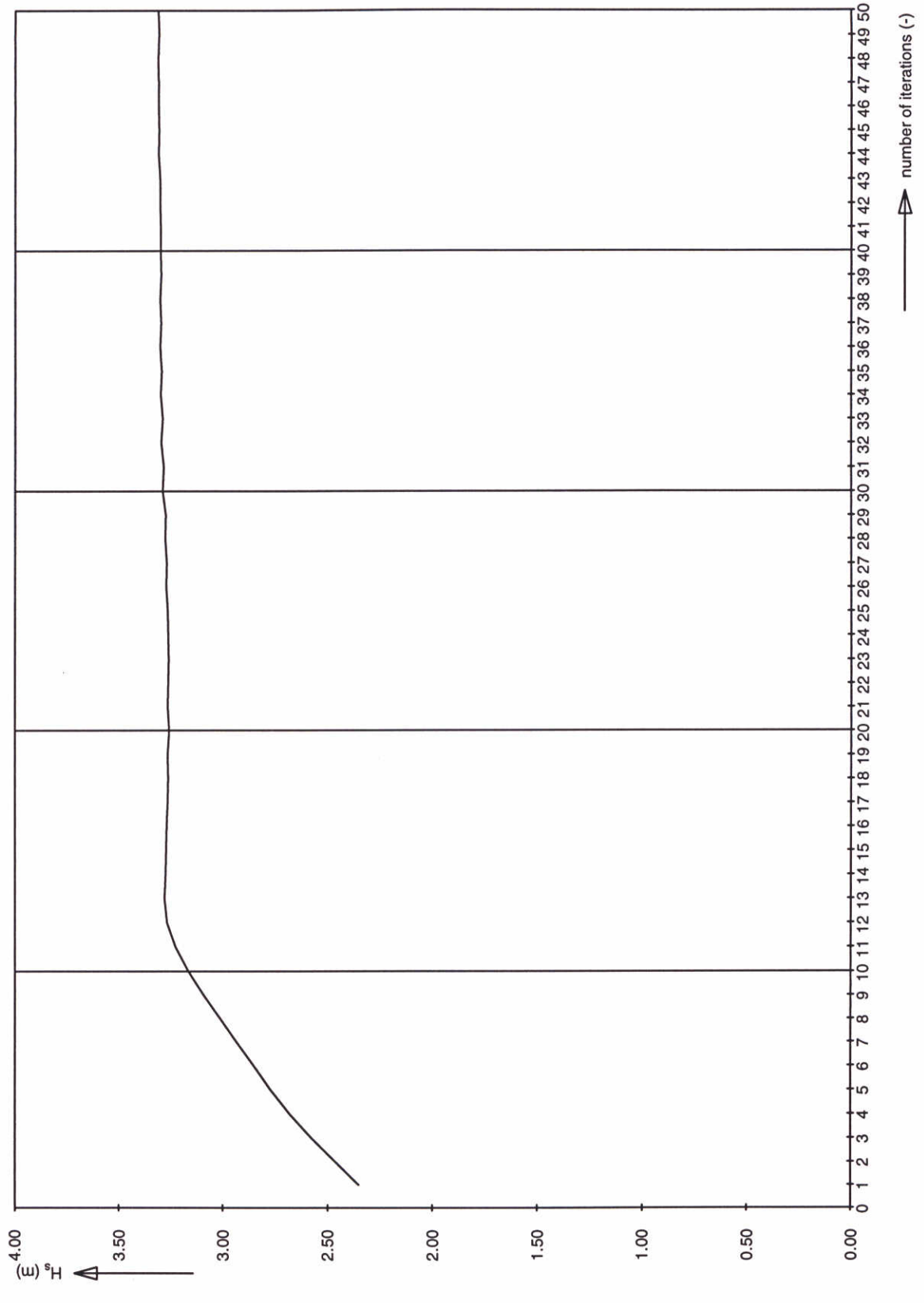

Significant wave height at 12.5 km Adapted frequency range f_{low} = 0.04 Hz, f_{high} = 0.3 Hz, MSC = 21	SWAN-1D	U_{10}=30 m/s
WL | delft hydraulics	H3496	Fig. 32d

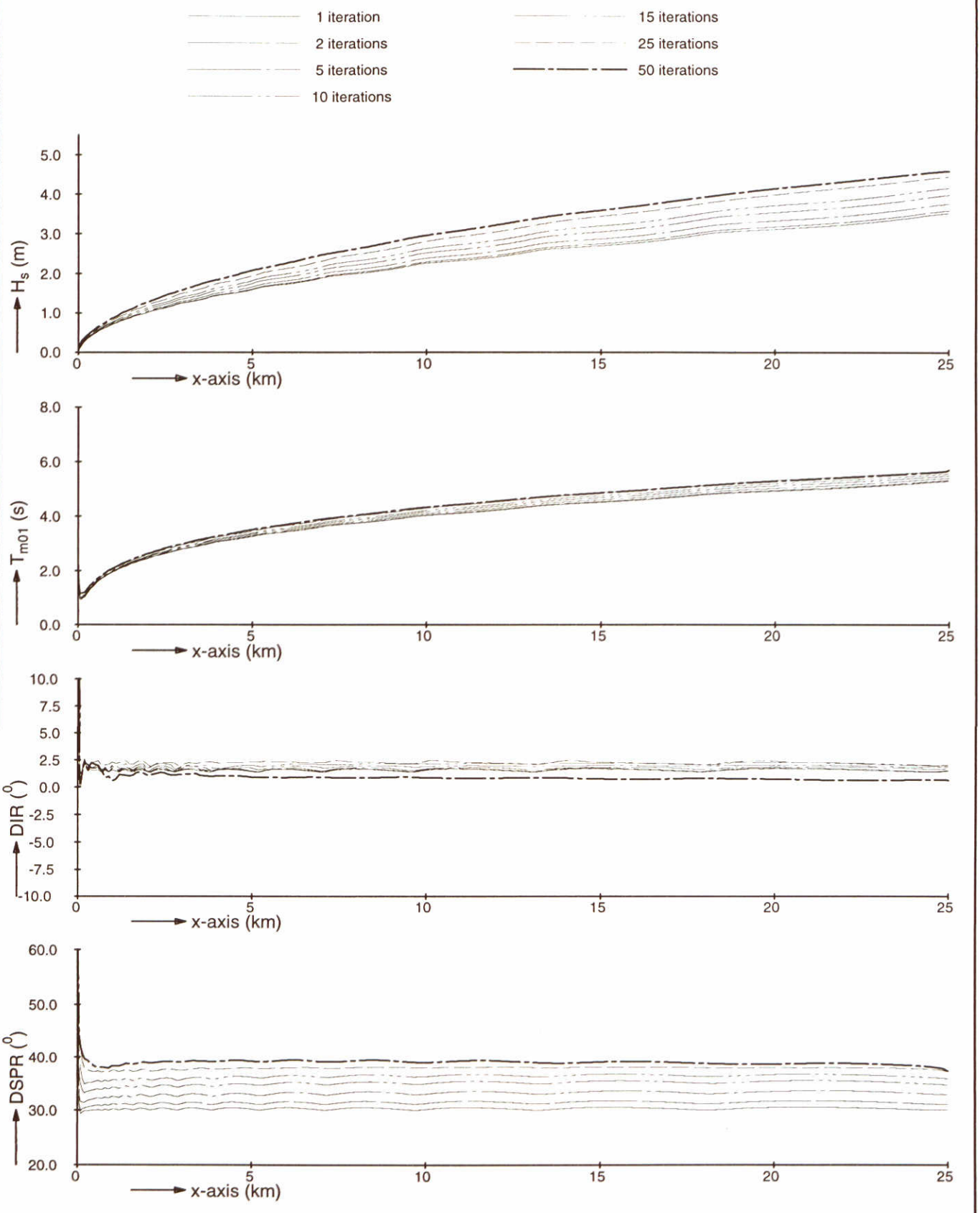

Model convergence behaviour using third-generation formulations
Adapted limter
Limiter = 2%

SWAN-1D

U_{10}=30 m/s

WL | delft hydraulics

H3496

Fig. 33a

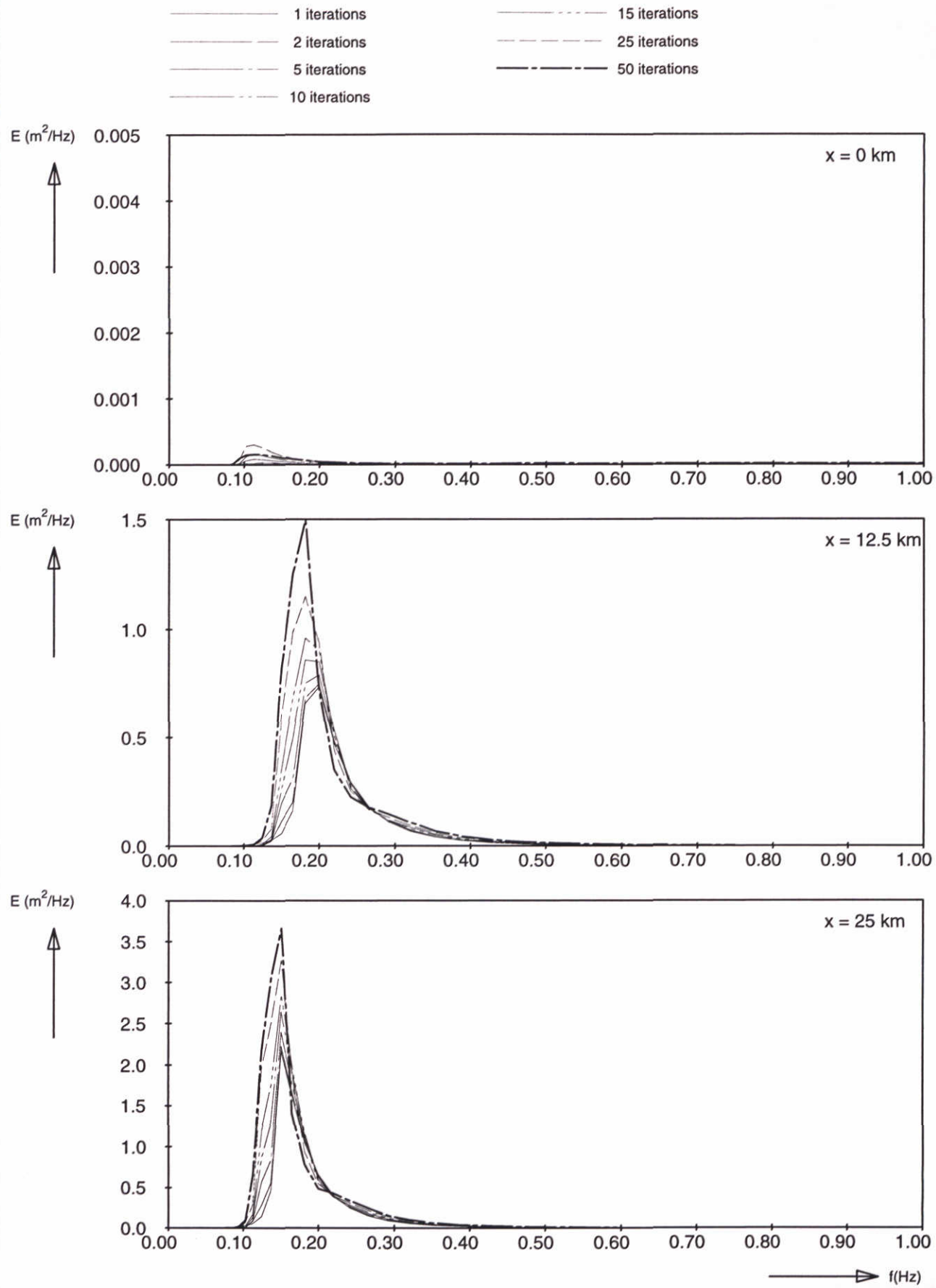

Frequency spectra at 3 locations Adapted limter Limiter = 2%	SWAN-1D	U_{10}=30 m/s
WL | delft hydraulics	H3496	Fig. 33b

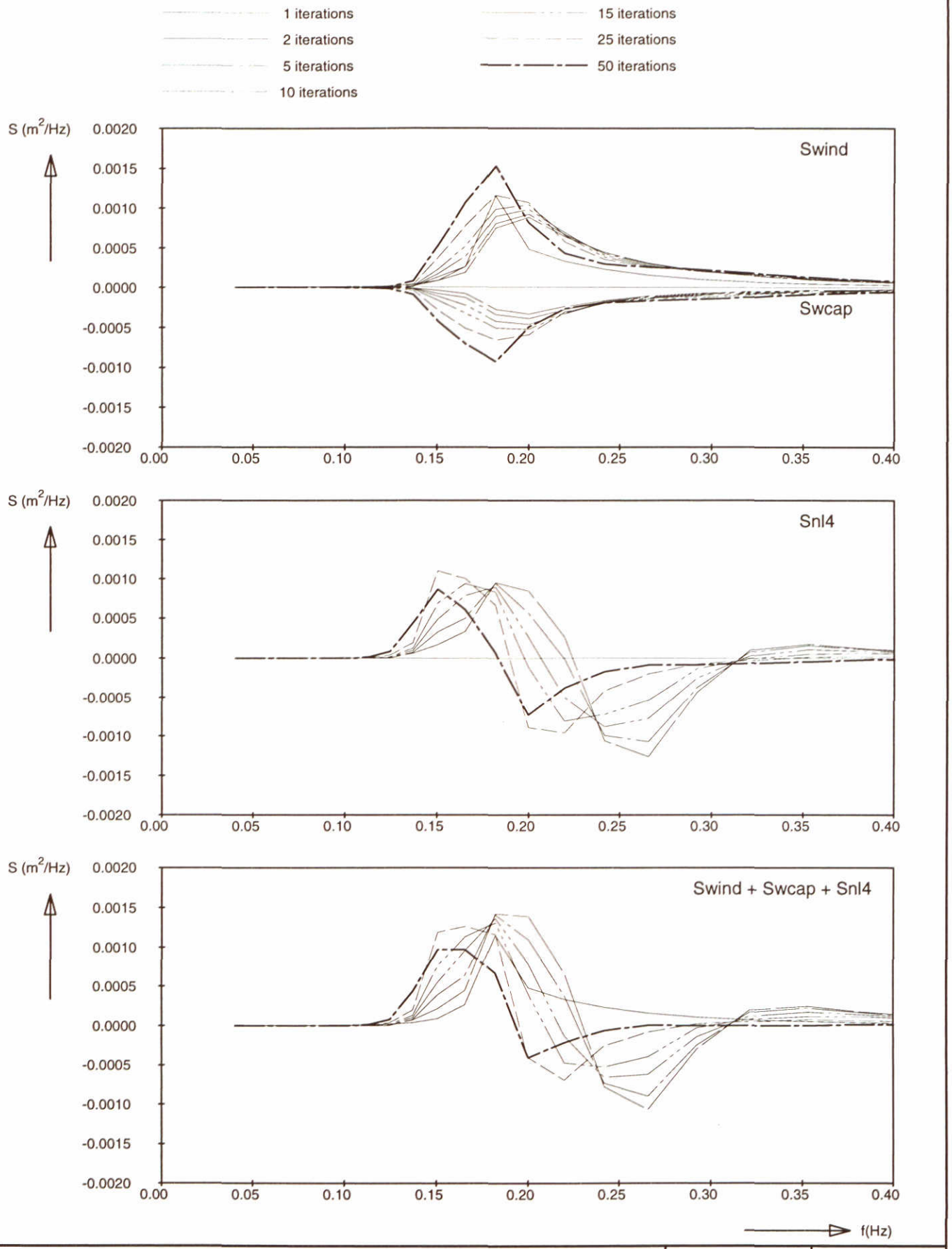

Source terms at x = 12.5 km Adapted limter Limiter = 2%	SWAN-1D	U_{10}=30 m/s
WL | delft hydraulics	H3496	Fig. 33c

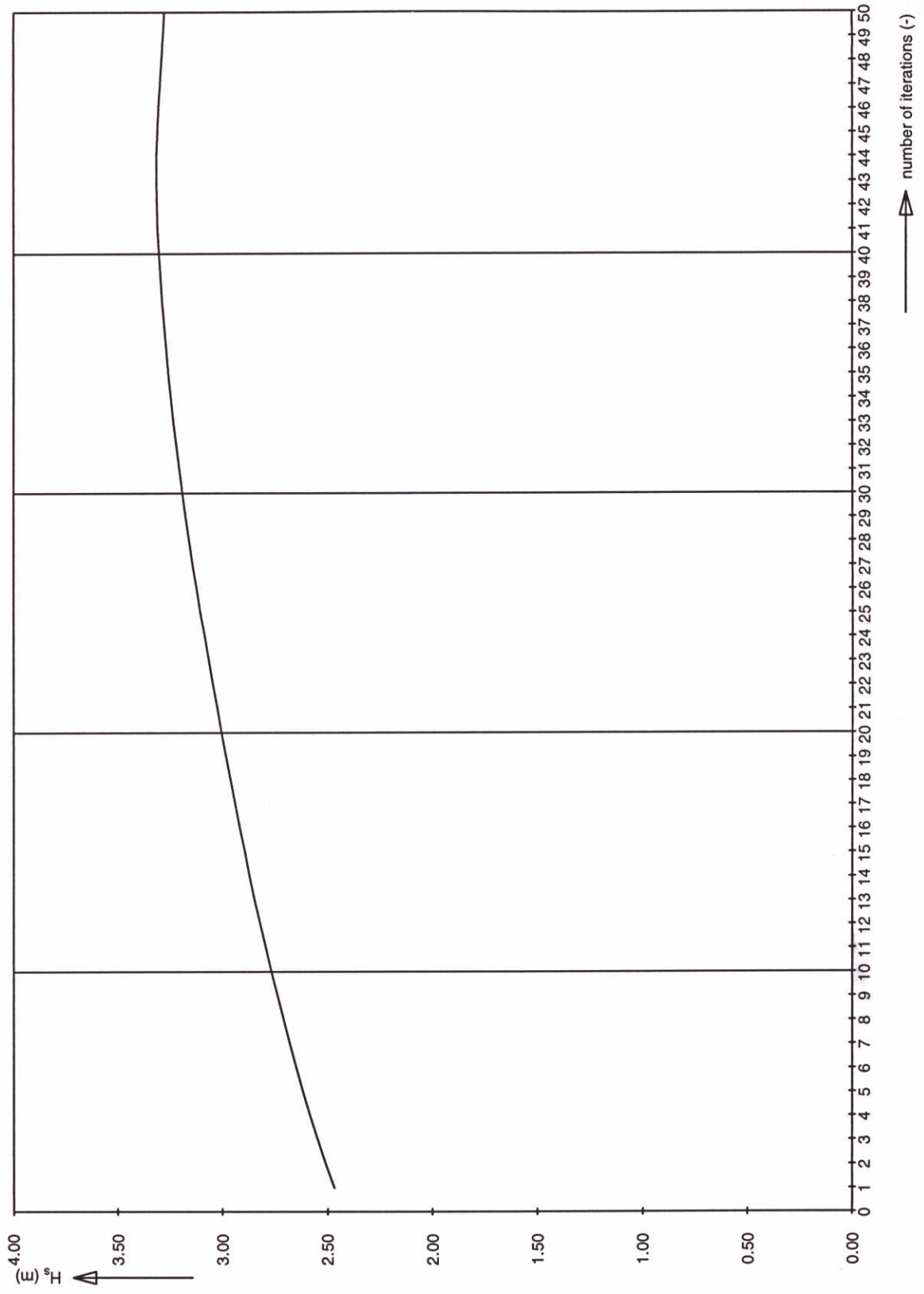

Significant wave height at 12.5 km Adapted limter Limiter = 2%	SWAN-1D	U_{10}=30 m/s
WL | delft hydraulics	H3496	Fig. 33d

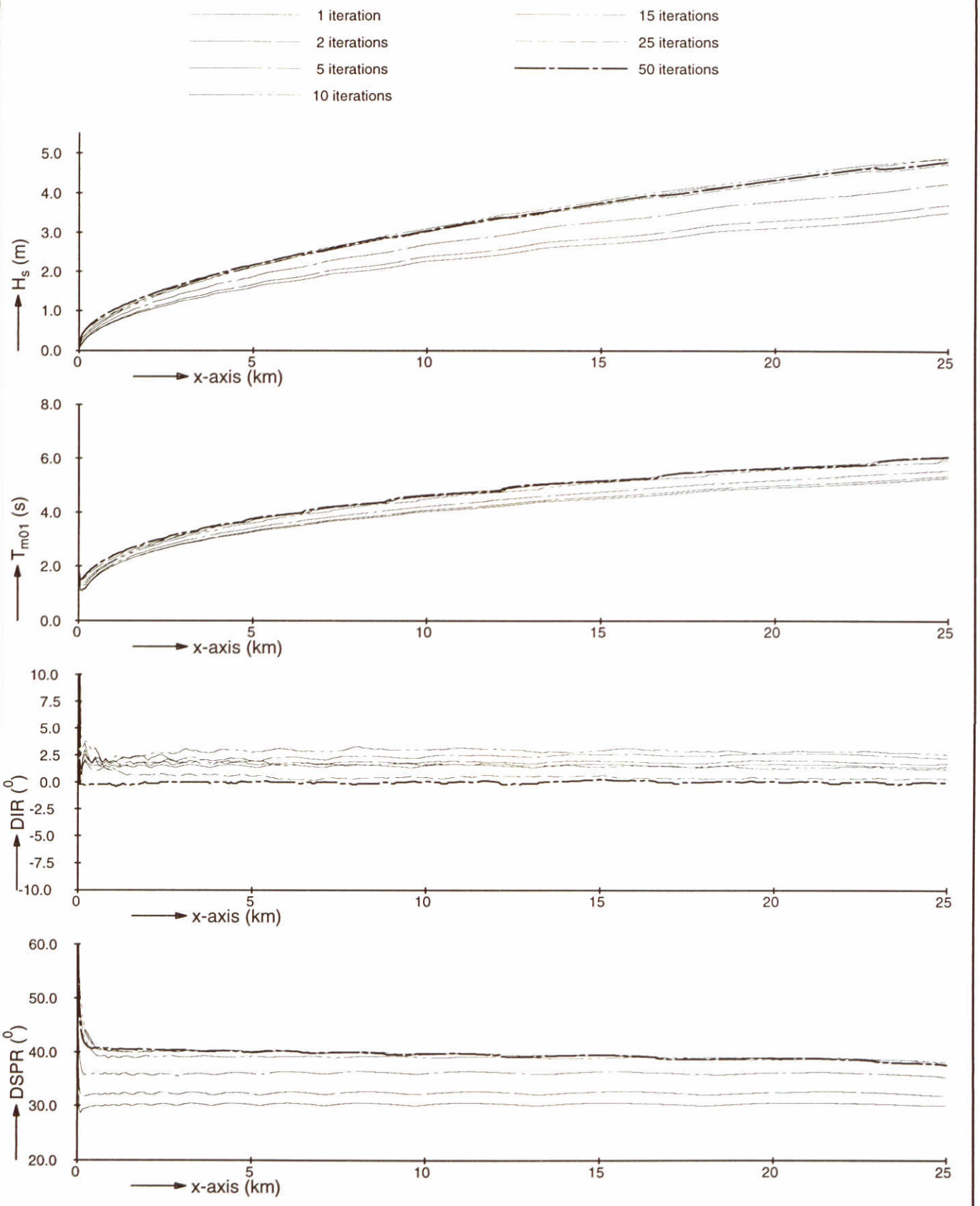

Model convergence behaviour using third-generation formulations Application of a self scaling cut-off frequency Coefficient δ = 1.5	SWAN-1D	U_{10}=30 m/s
WL | delft hydraulics	H3496	Fig. 34a

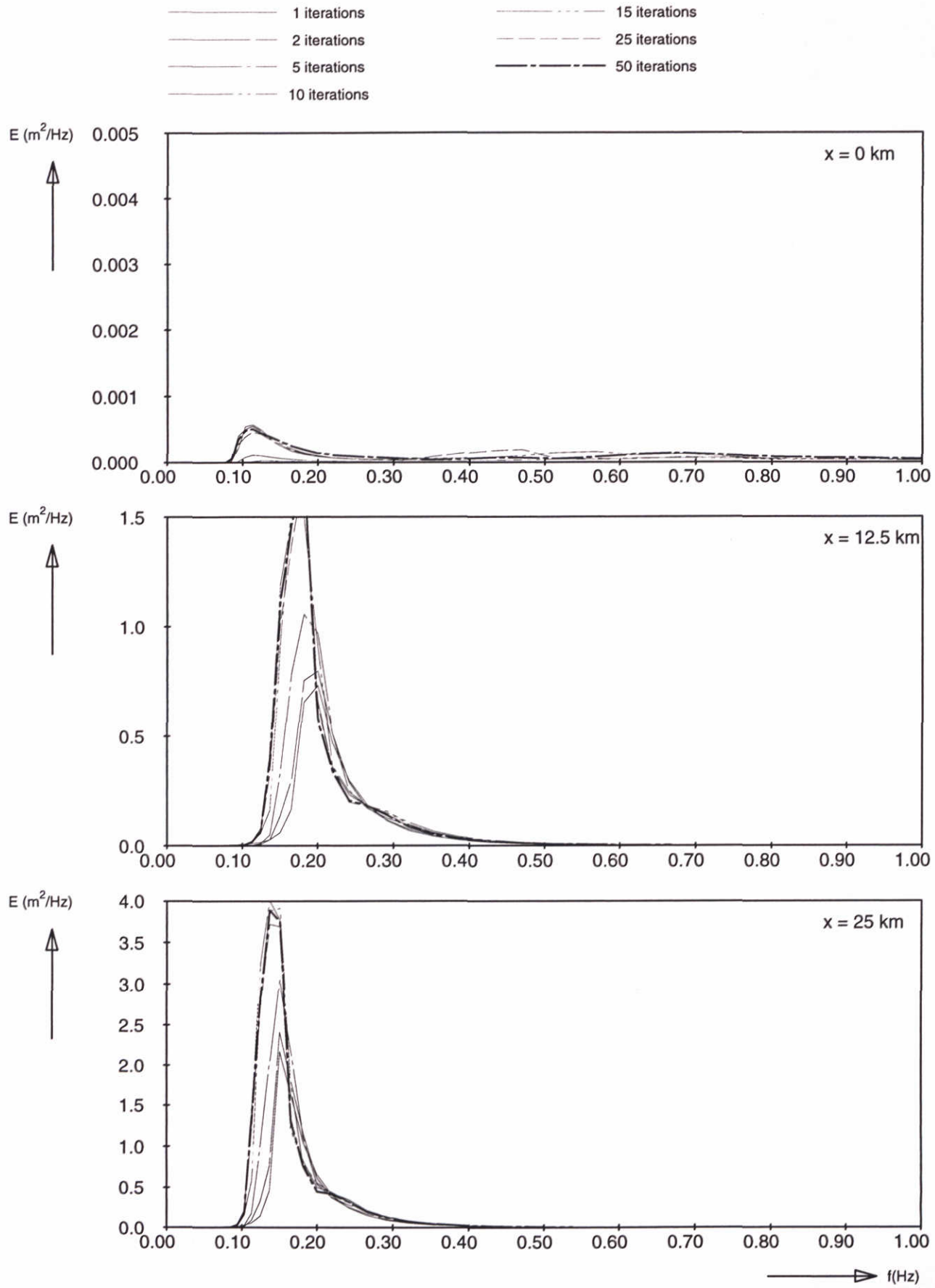

Frequency spectra at 3 locations Application of a self scaling cut-off frequency Coefficient δ = 1.5	SWAN-1D	U_{10}=30 m/s
WL | delft hydraulics	H3496	Fig. 34b

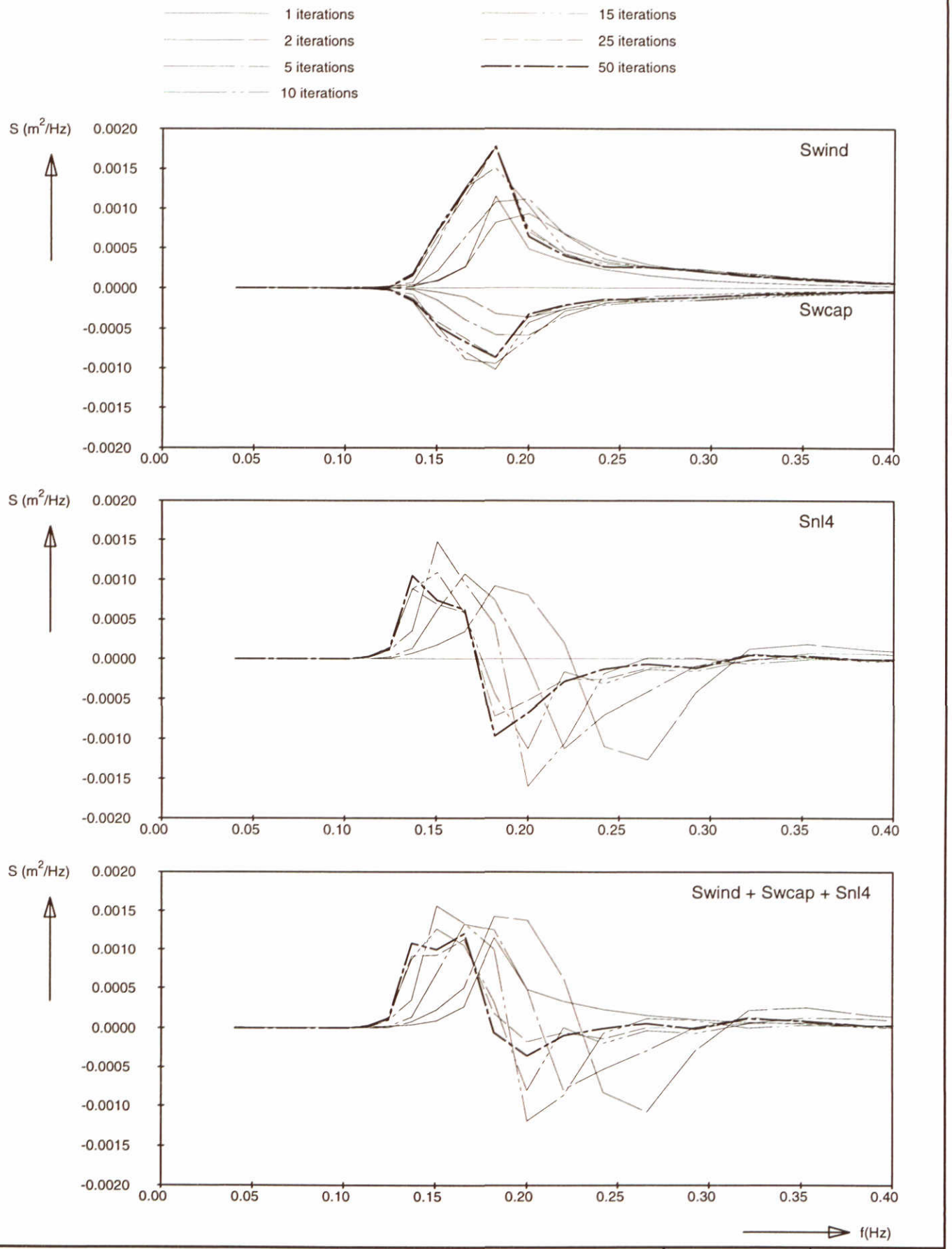

Source terms at x = 12.5 km
Application of a self scaling cut-off frequency
Coefficient δ = 1.5

SWAN-1D

U_{10}=30 m/s

WL | delft hydraulics

H3496

Fig. 34c

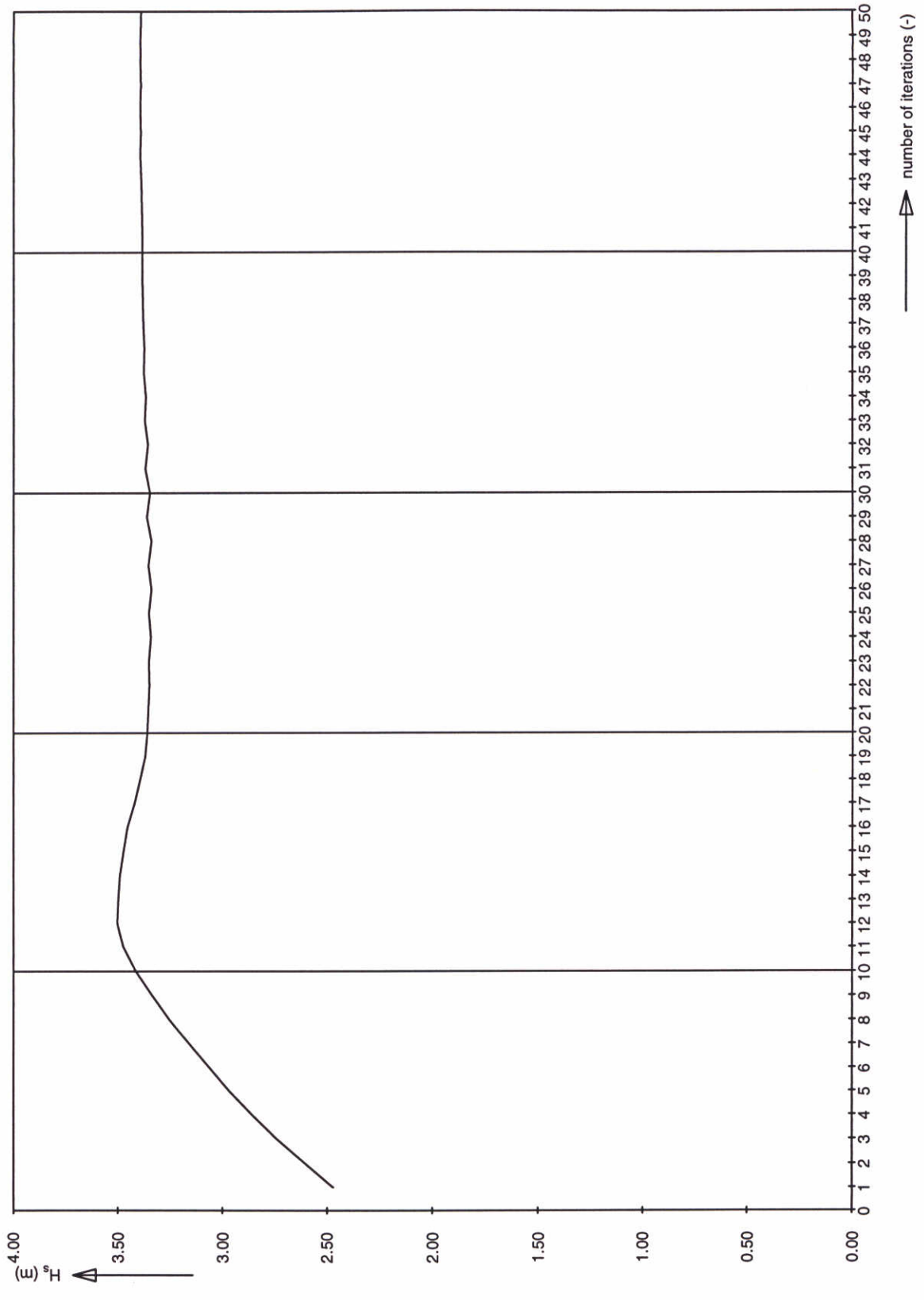

Significant wave height at 12.5 km Application of a self scaling cut-off frequency Coefficient δ = 1.5	SWAN-1D	U_{10}=30 m/s
WL | delft hydraulics	H3496	Fig. 34d

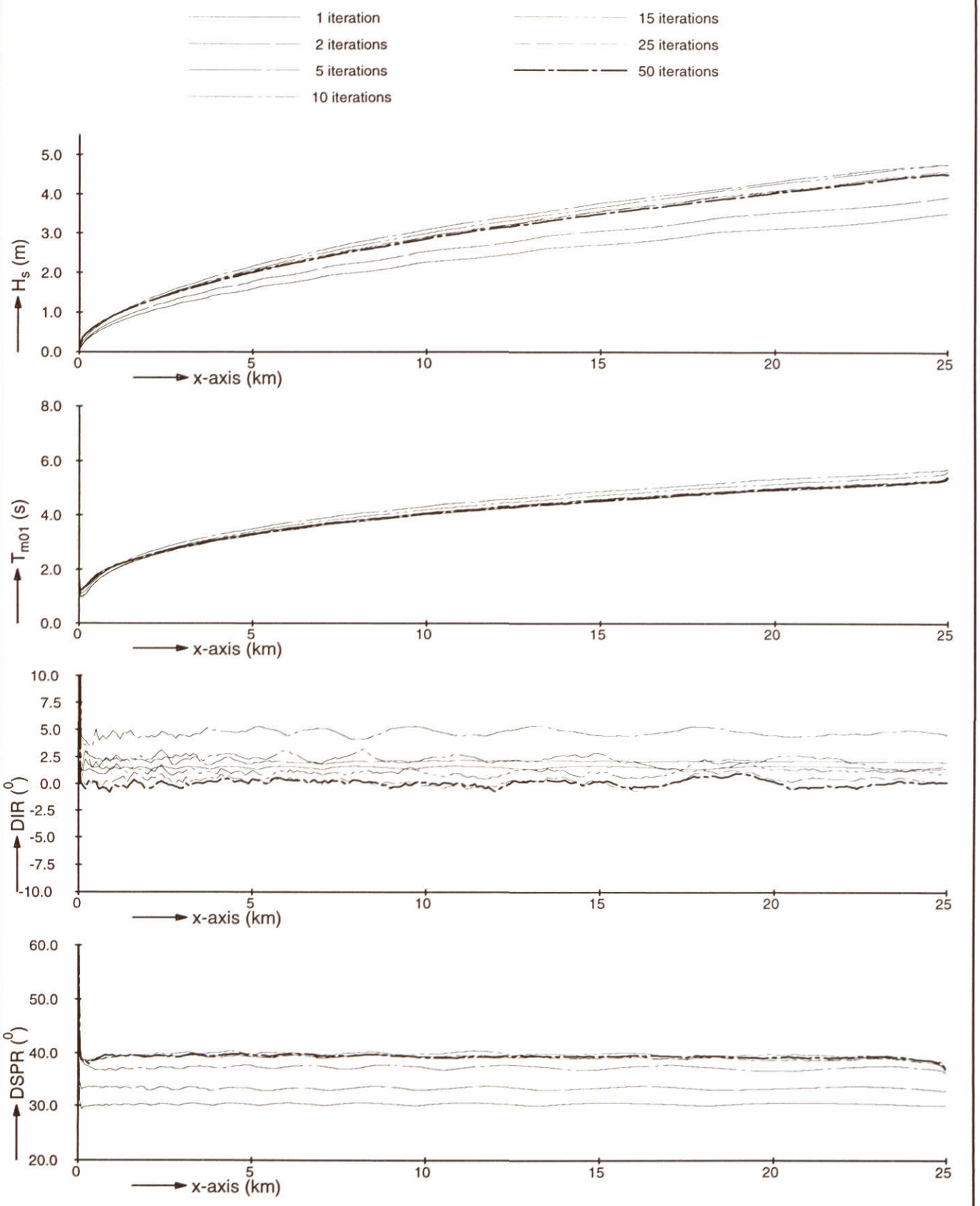

Model convergence behaviour using third-generation formulations
Adapted limiter
Limiter = 40%

SWAN-1D

U_{10}=30 m/s

WL | delft hydraulics

H3496

Fig. 35a

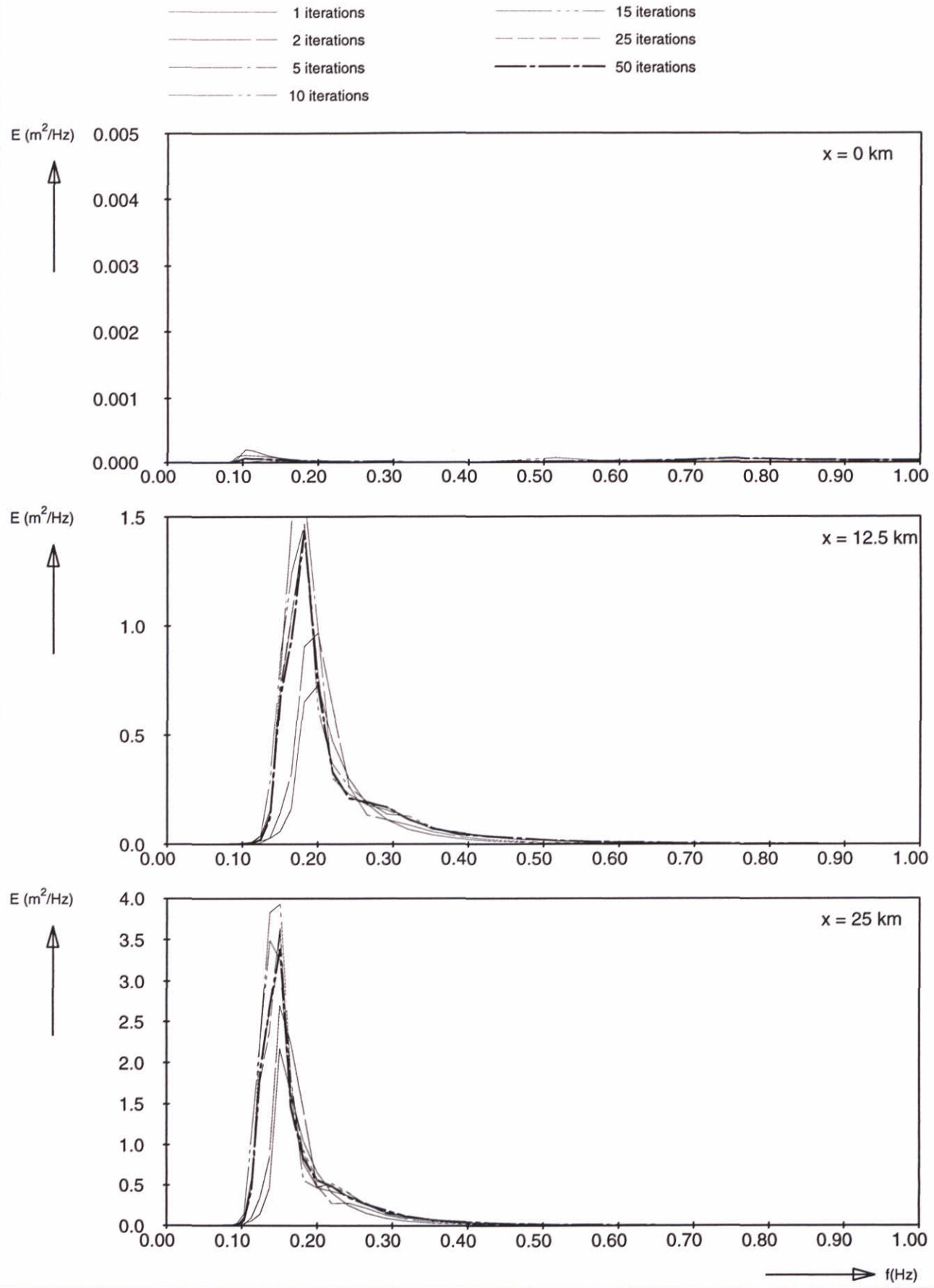

Frequency spectra at 3 locations Adapted limiter Limiter = 40%	SWAN-1D	U_{10}=30 m/s
WL | delft hydraulics	H3496	Fig. 35b

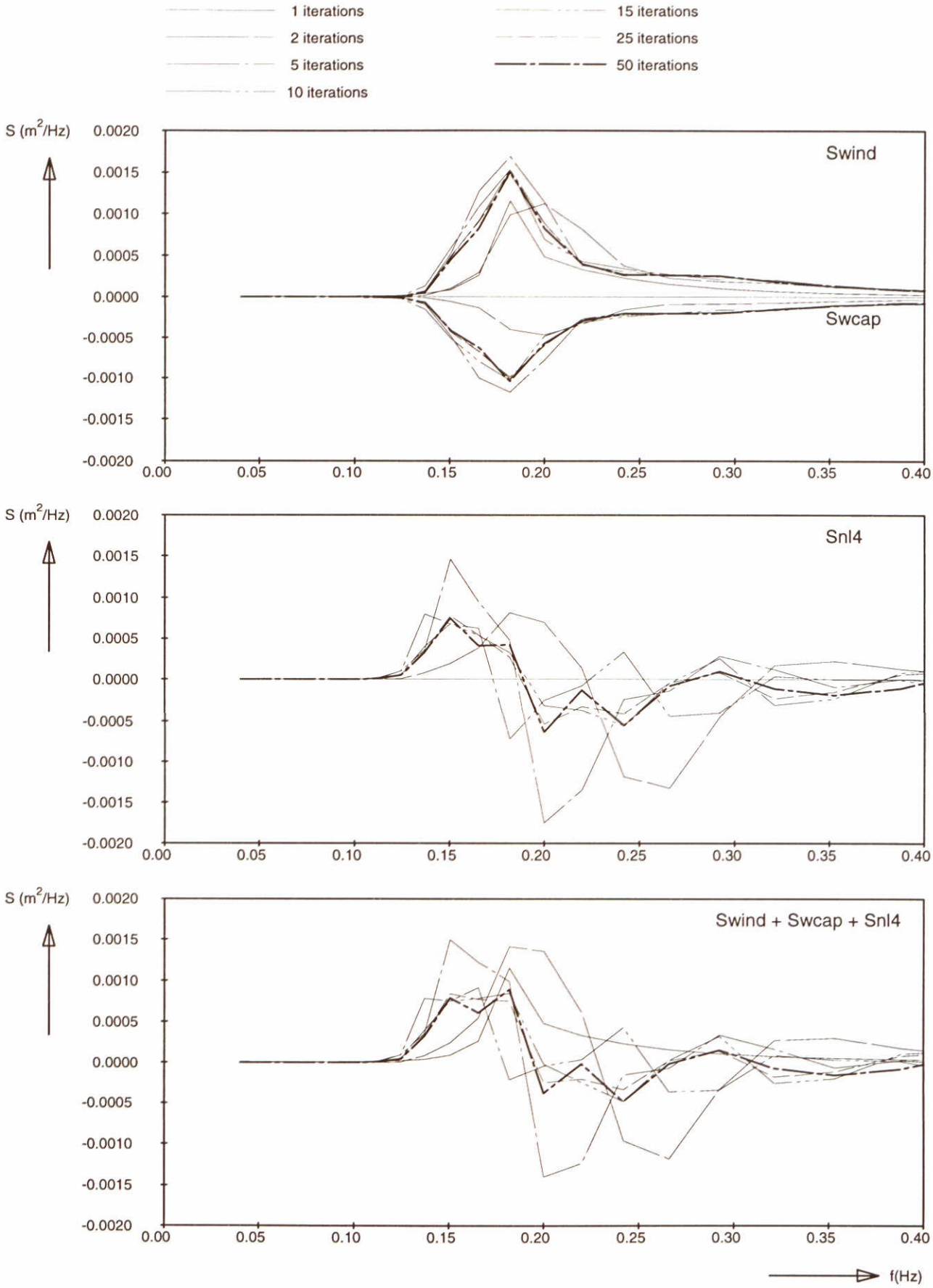

Source terms at x = 12.5 km Adapted limiter Limiter = 40%	SWAN-1D	U_{10}=30 m/s
WL | delft hydraulics	H3496	Fig. 35c

Significant wave height at 12.5 km Adapted limiter Limiter = 40%	SWAN-1D	U_{10}=30 m/s
WL | delft hydraulics	H3496	Fig. 35d

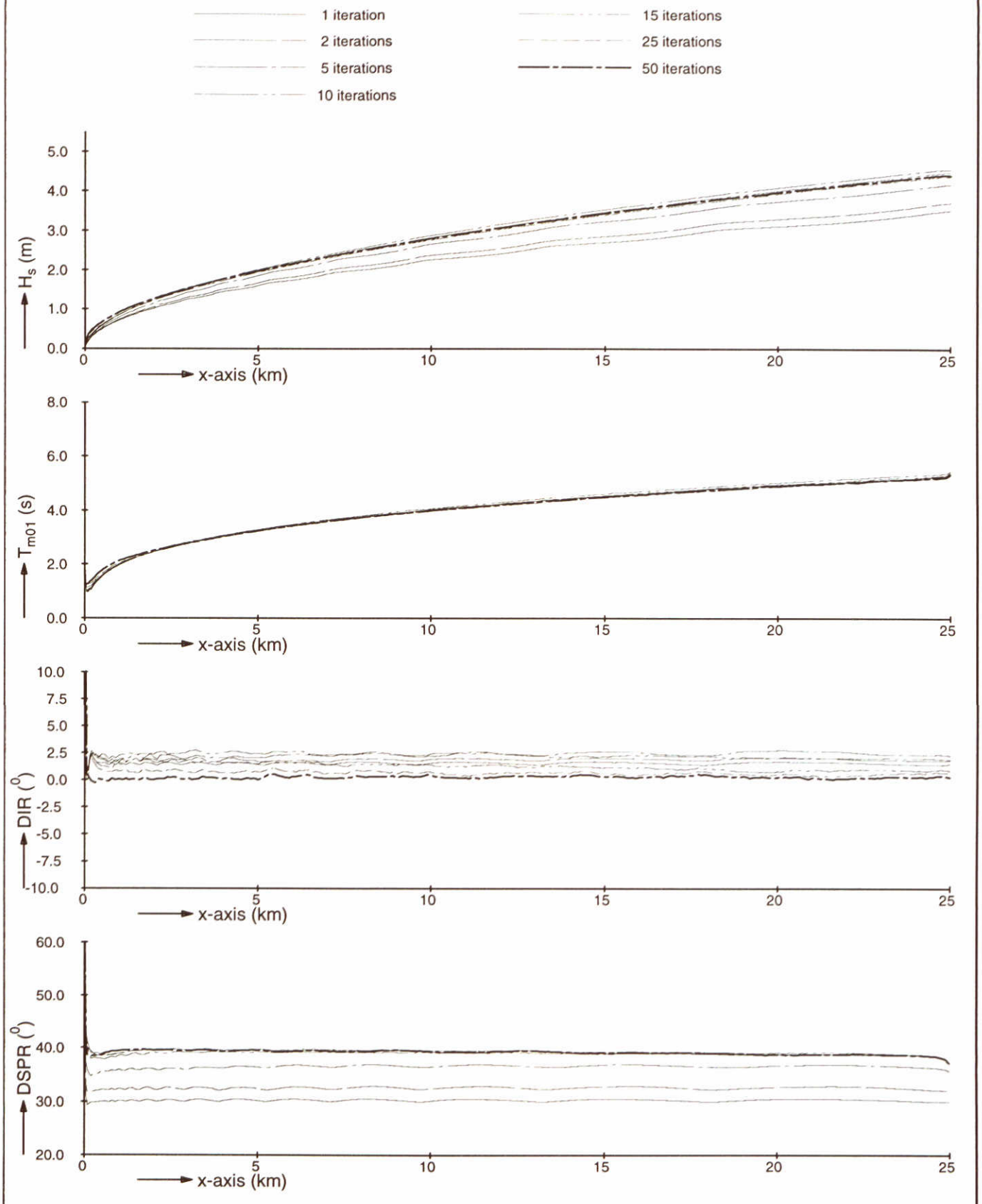

Model convergence behaviour using third-generation formulations Adapted limiter Distribution equal (f/f_m)	SWAN-1D	U_{10}=30 m/s
WL | delft hydraulics	H3496	Fig. 36a

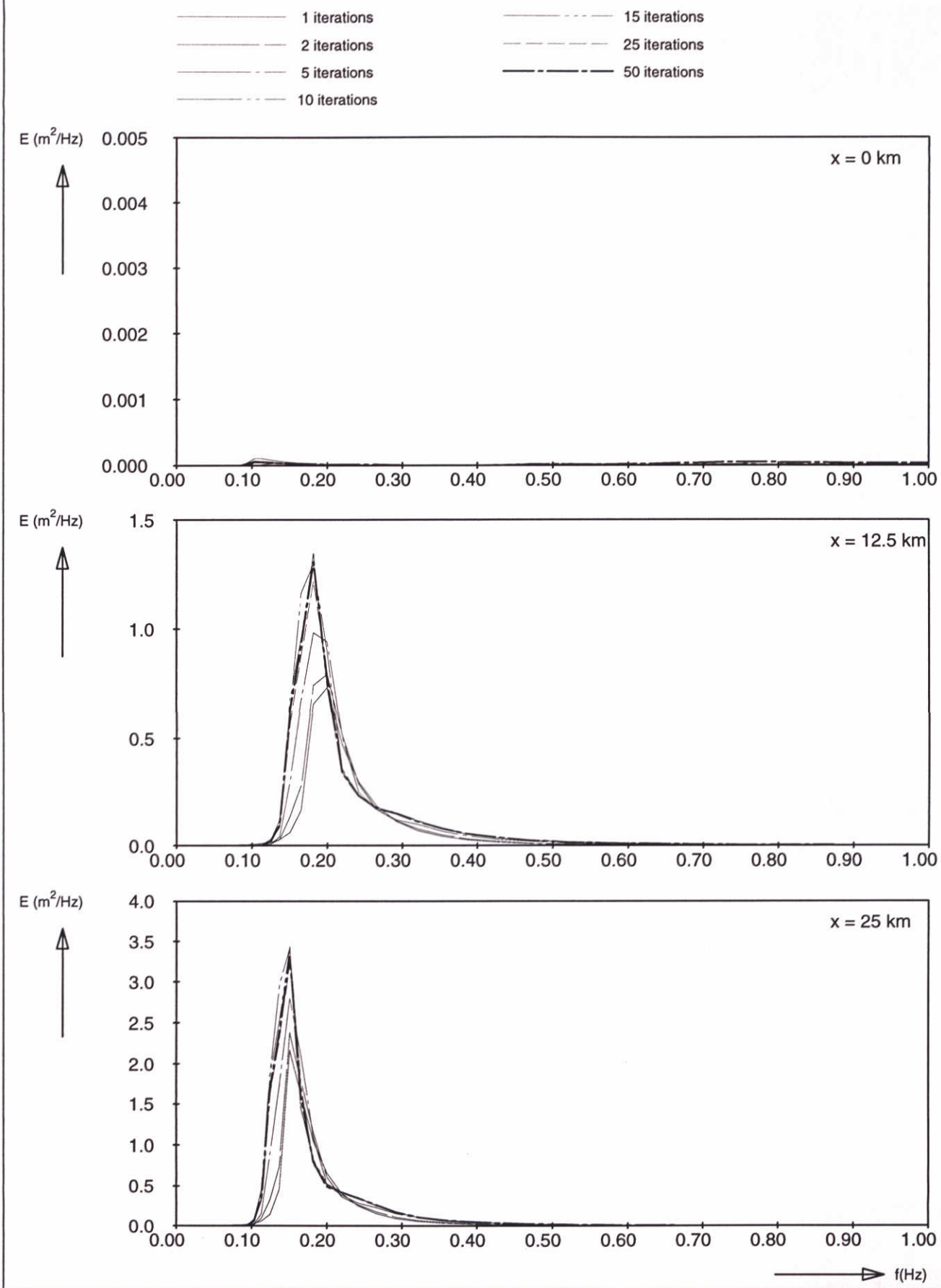

Frequency spectra at 3 locations Adapted limiter Distribution equal (f/f_m)	SWAN-1D	U_{10}=30 m/s
WL | delft hydraulics	H3496	Fig. 36b

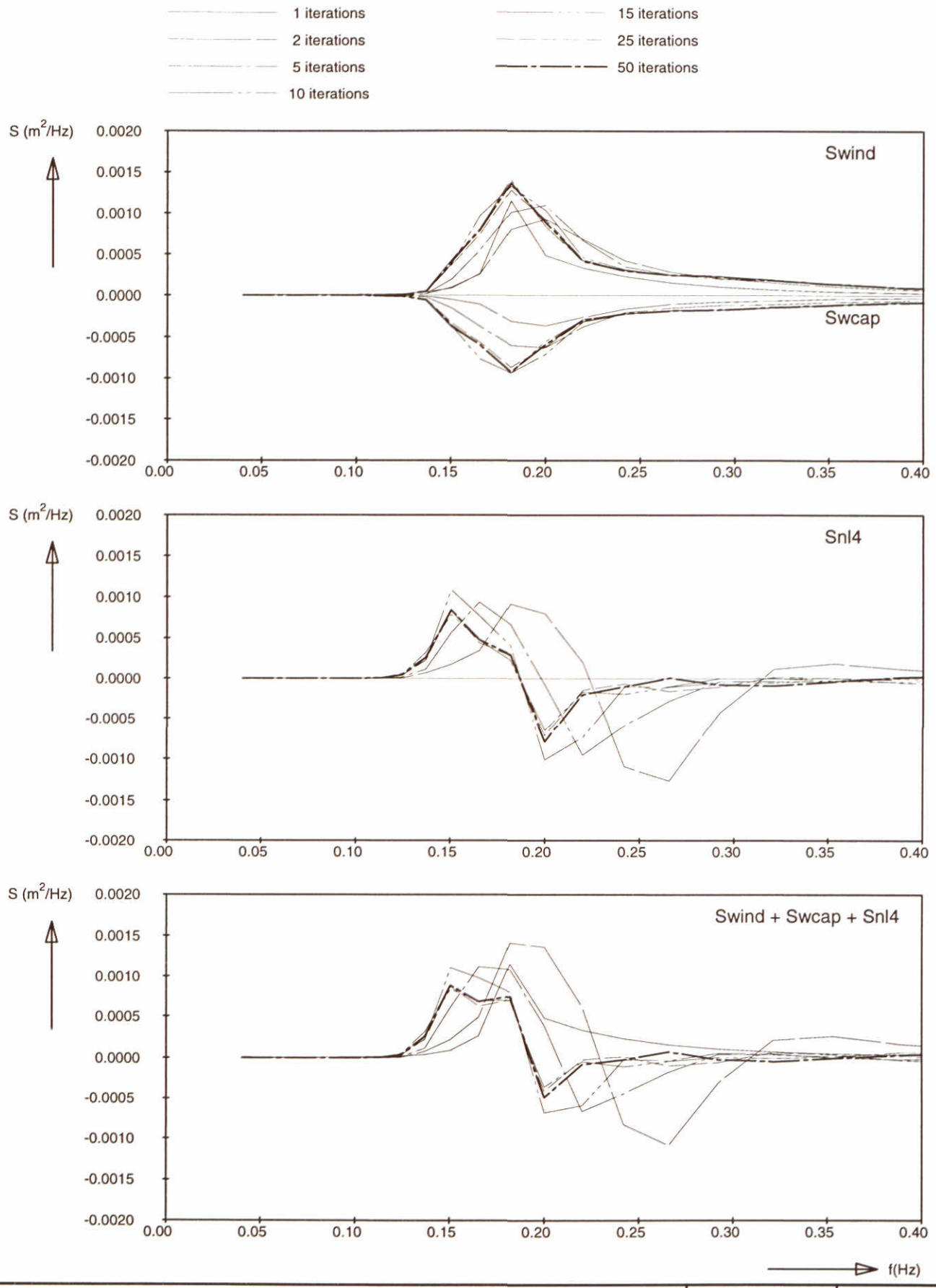

Source terms at x = 12.5 km Adapted limiter Distribution equal (f/f_m)	SWAN-1D	U_{10}=30 m/s
WL | delft hydraulics	H3496	Fig. 36c

Significant wave height at 12.5 km Adapted limiter Distribution equal (f/f_m)	SWAN-1D	U_{10}=30 m/s
WL | delft hydraulics	H3496	Fig. 36d

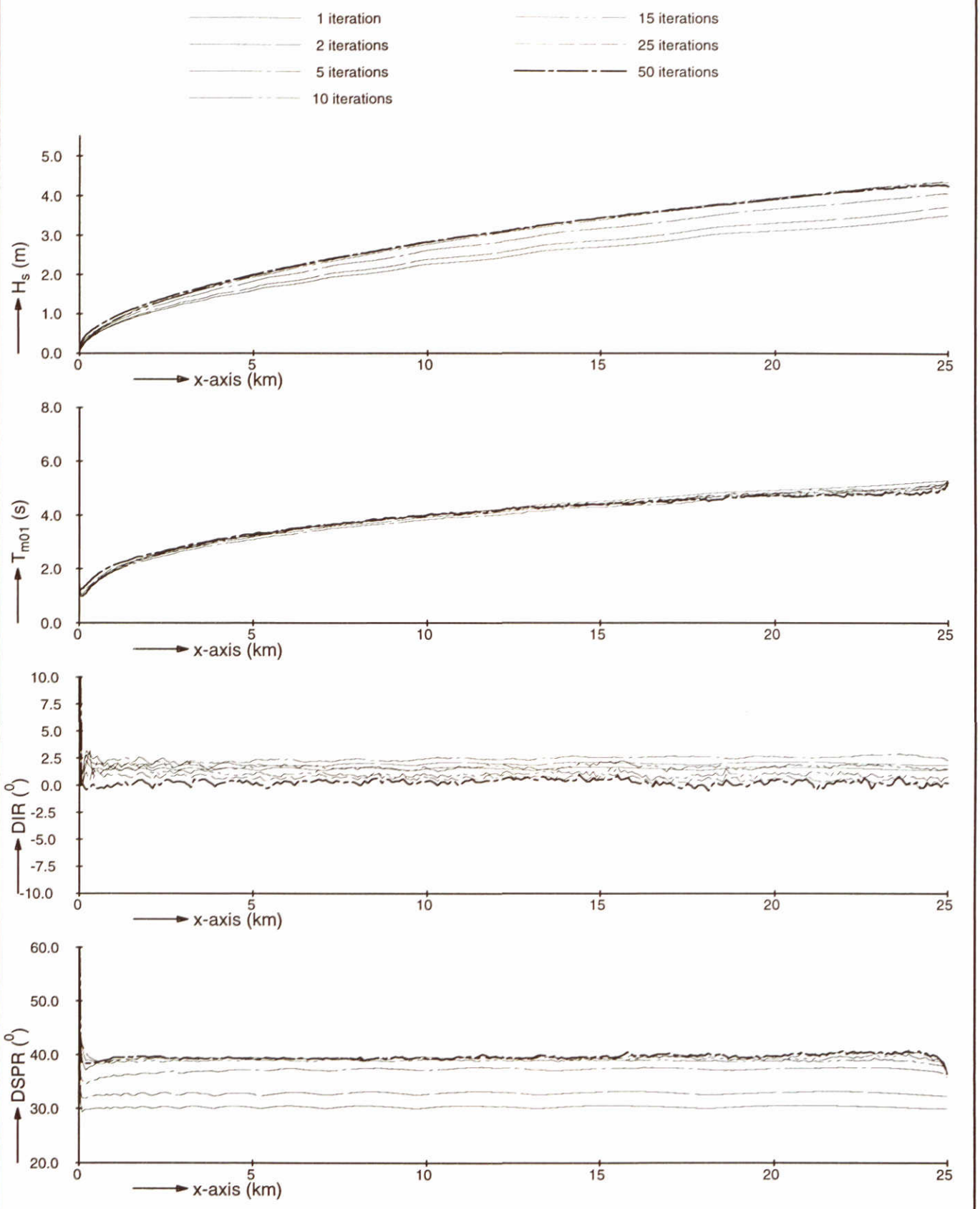

Model convergence behaviour using third-generation formulations Adapted limiter Distribution equal $(f/f_m)^2$	SWAN-1D	U_{10}=30 m/s
WL | delft hydraulics	H3496	Fig. 37a

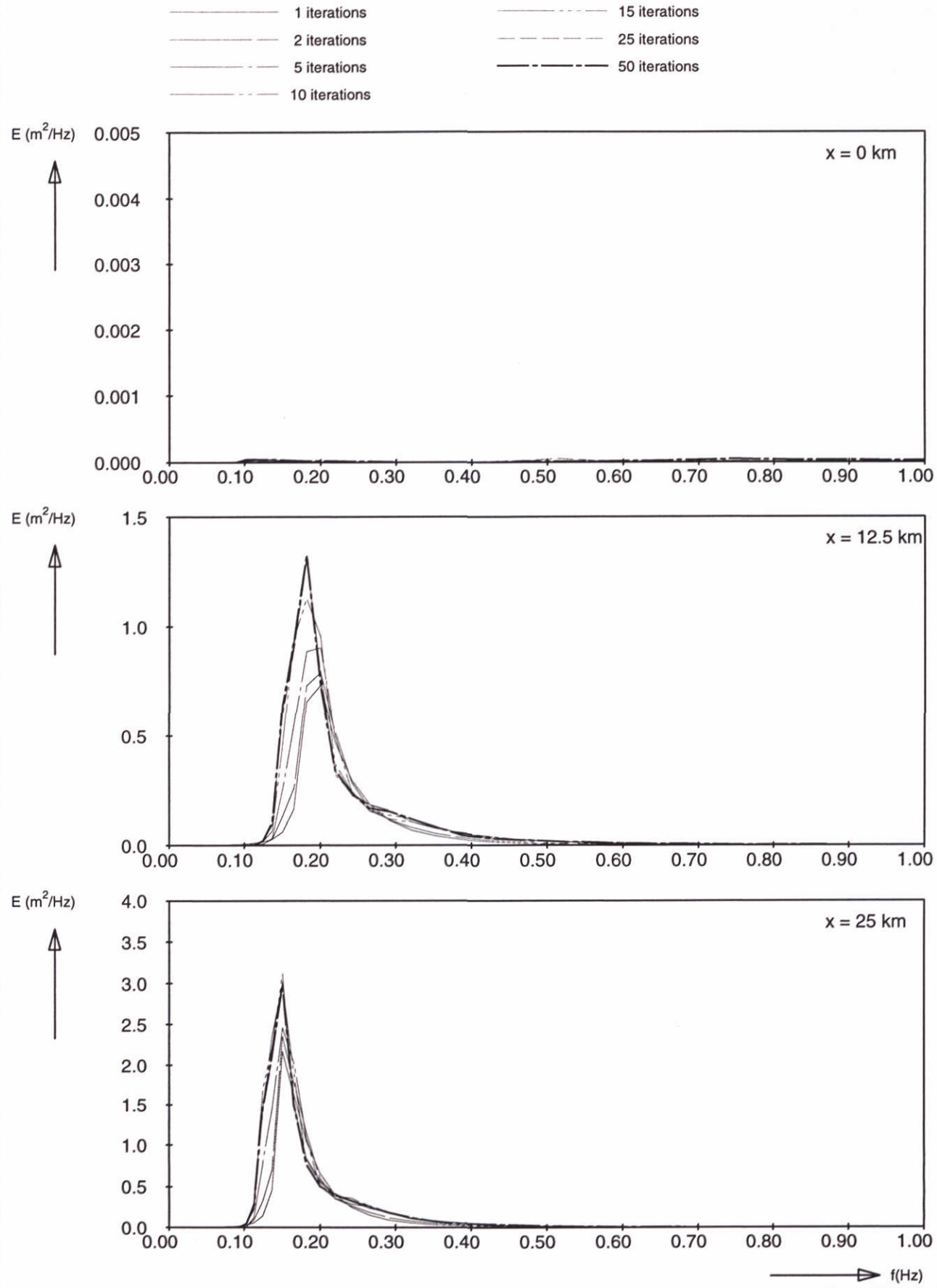

Frequency spectra at 3 locations Adapted limiter Distribution equal $(f/f_m)^2$	SWAN-1D	U_{10}=30 m/s
WL | delft hydraulics	H3496	Fig. 37b

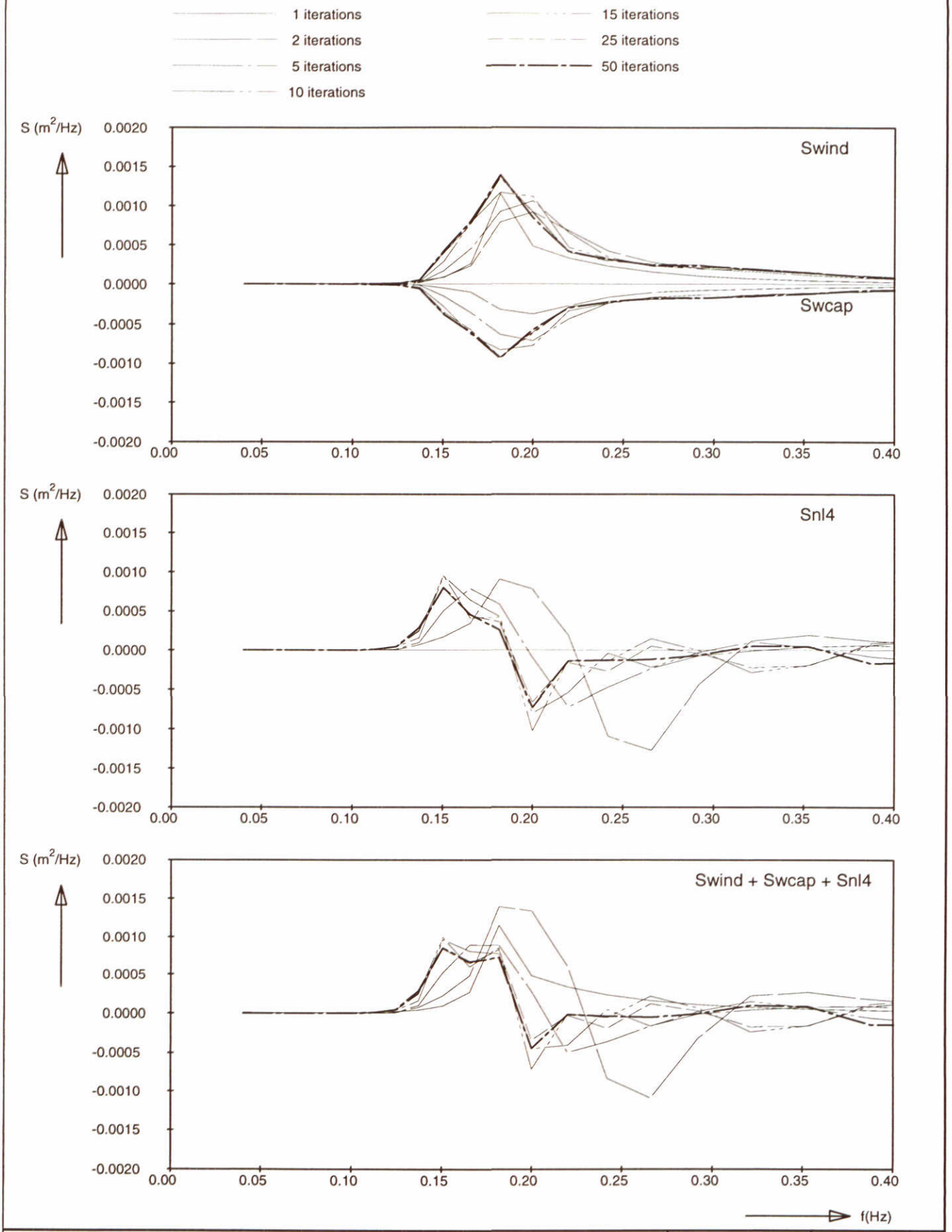

Source terms at x = 12.5 km Adapted limiter Distribution equal $(f/f_m)^2$	SWAN-1D	U_{10}=30 m/s
WL | delft hydraulics	H3496	Fig. 37c

Significant wave height at 12.5 km Adapted limiter Distribution equal $(f/f_m)^2$	SWAN-1D	U_{10}=30 m/s
WL | delft hydraulics	H3496	Fig. 37d

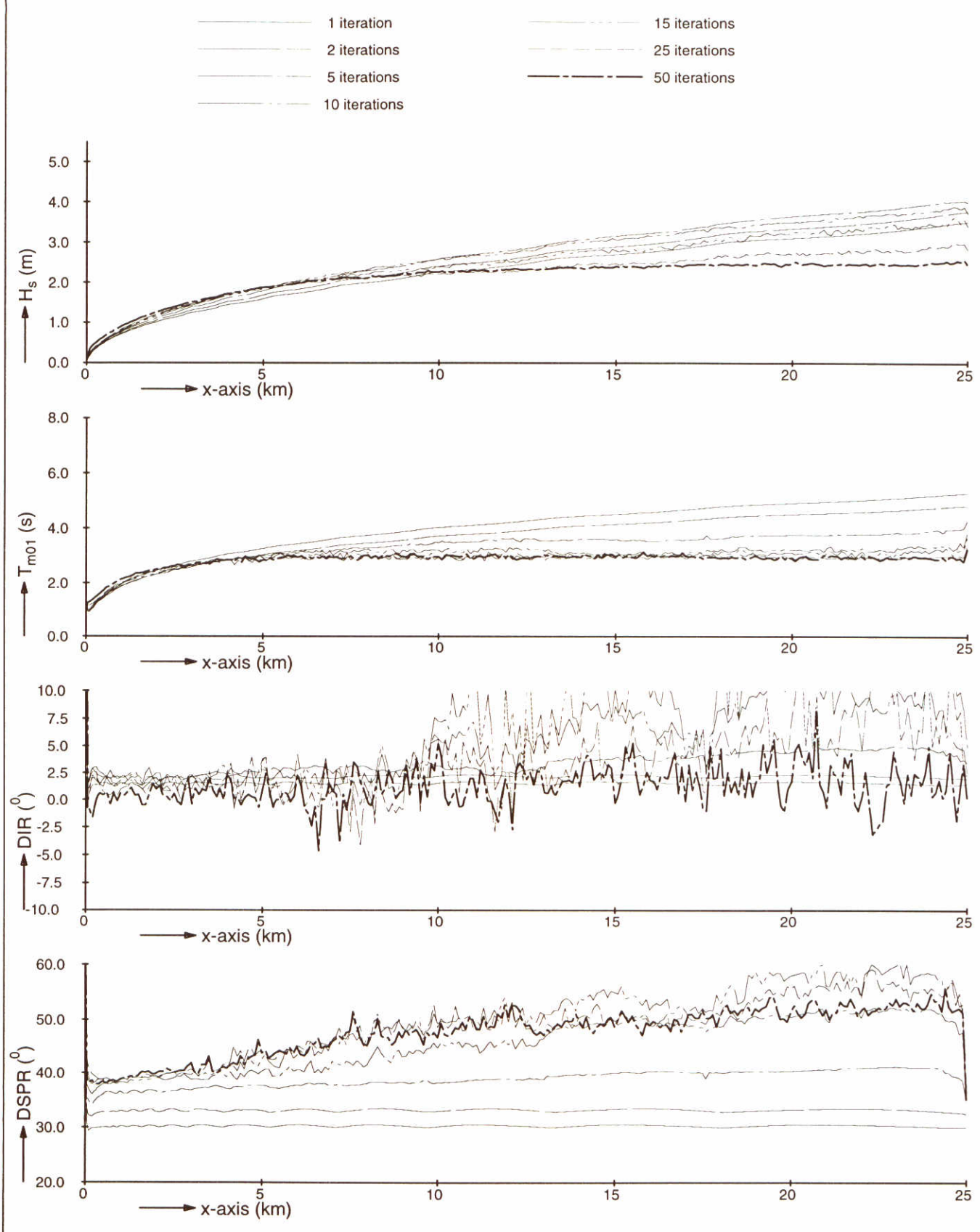

Model convergence behaviour using third-generation formulations
Adapted limiter
Distribution equal $(f/f_m)^3$

SWAN-1D

U_{10}=30 m/s

WL | delft hydraulics

H3496

Fig. 38a

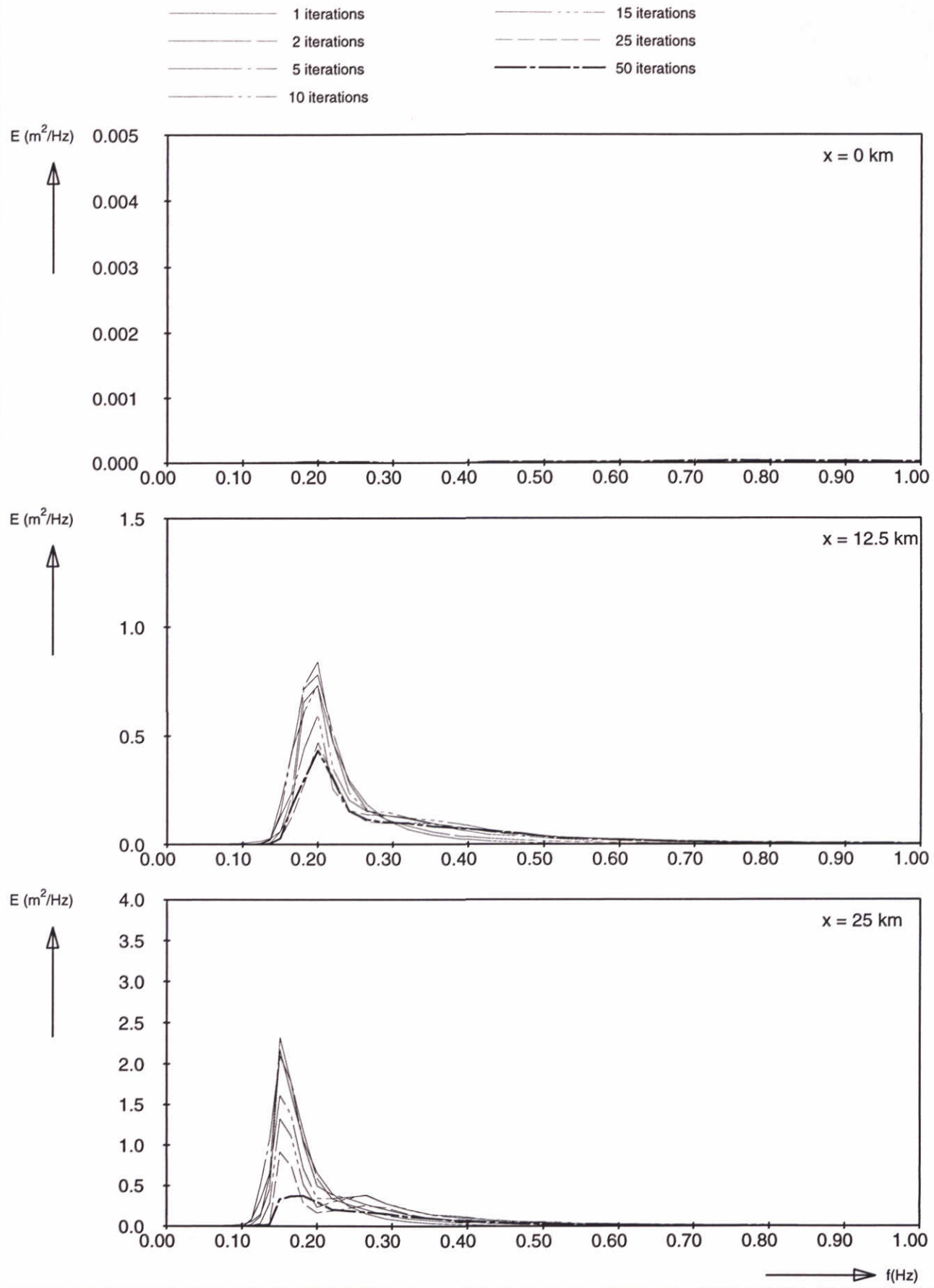

Frequency spectra at 3 locations Adapted limiter Distribution equal $(f/f_m)^3$	SWAN-1D	U_{10}=30 m/s
WL | delft hydraulics	H3496	Fig. 38b

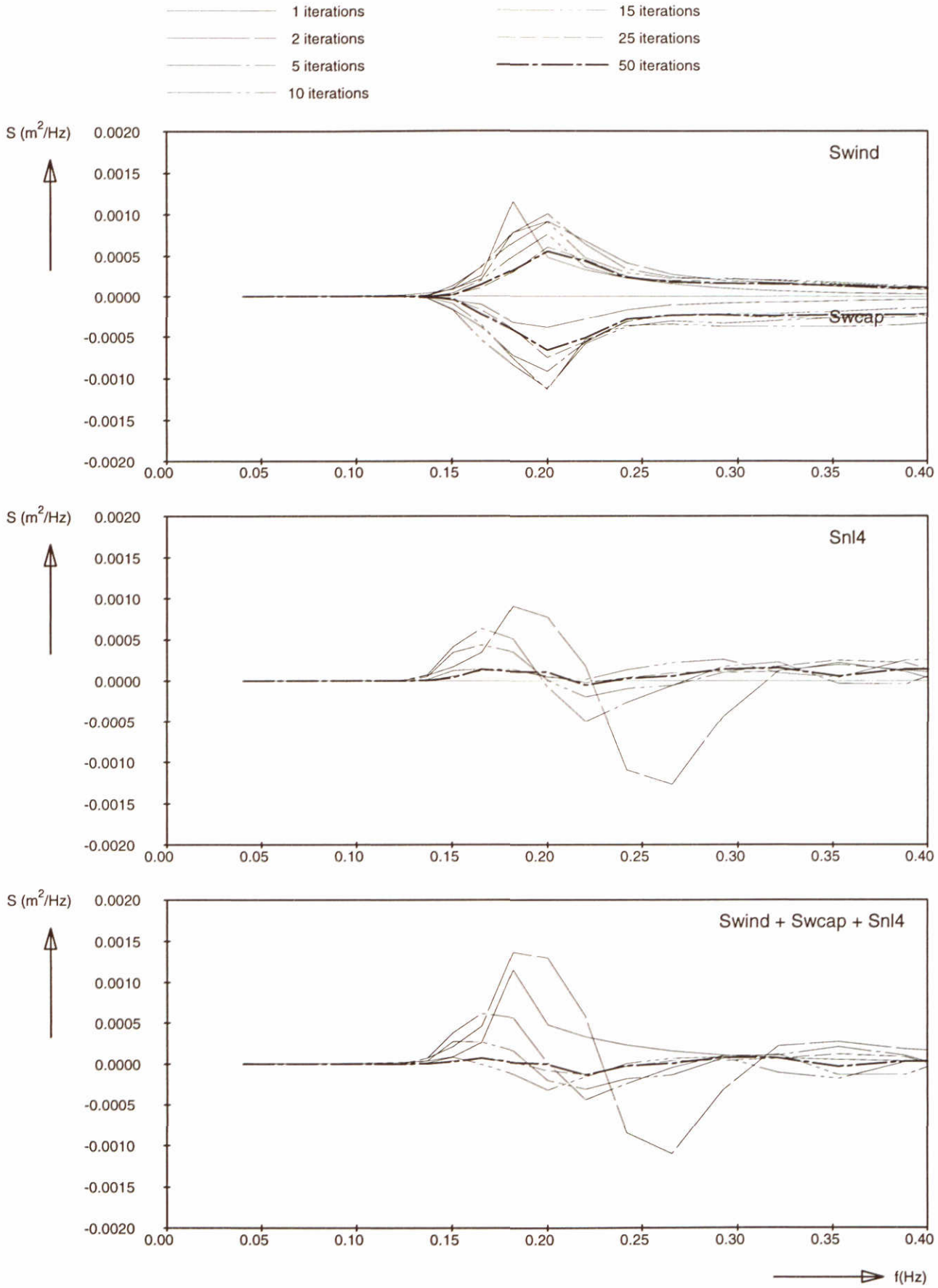

Source terms at x = 12.5 km Adapted limiter Distribution equal $(f/f_m)^3$	SWAN-1D	U_{10}=30 m/s
WL | delft hydraulics	H3496	Fig. 38c

Significant wave height at 12.5 km Adapted limiter Distribution equal $(f/f_m)^3$	SWAN-1D	U_{10}=30 m/s
WL | delft hydraulics	H3496	Fig. 38d

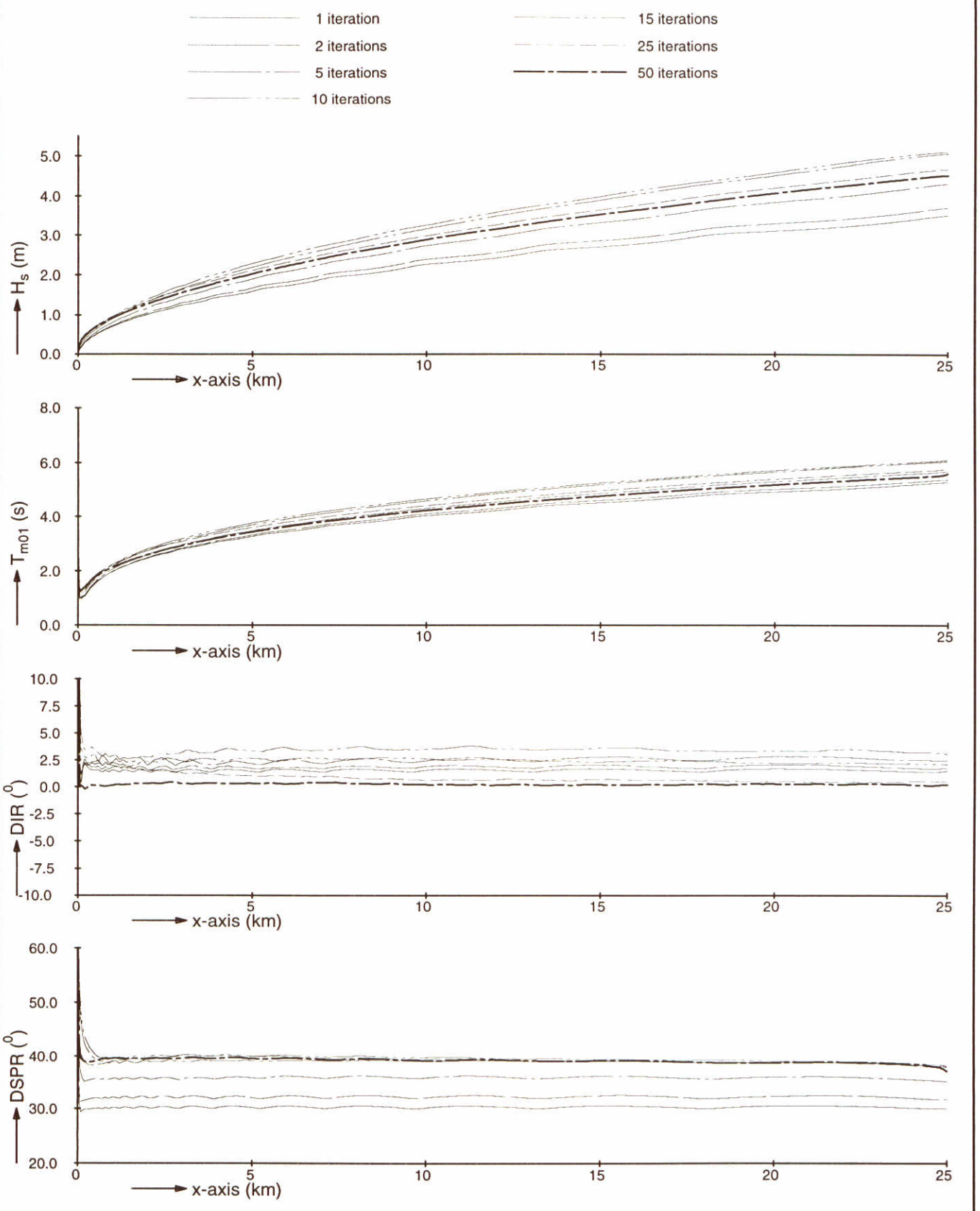

Model convergence behaviour using third-generation formulations
Adapted limiter
Distribution equal f_m/f

SWAN-1D

U_{10}=30 m/s

WL | delft hydraulics

H3496

Fig. 39a

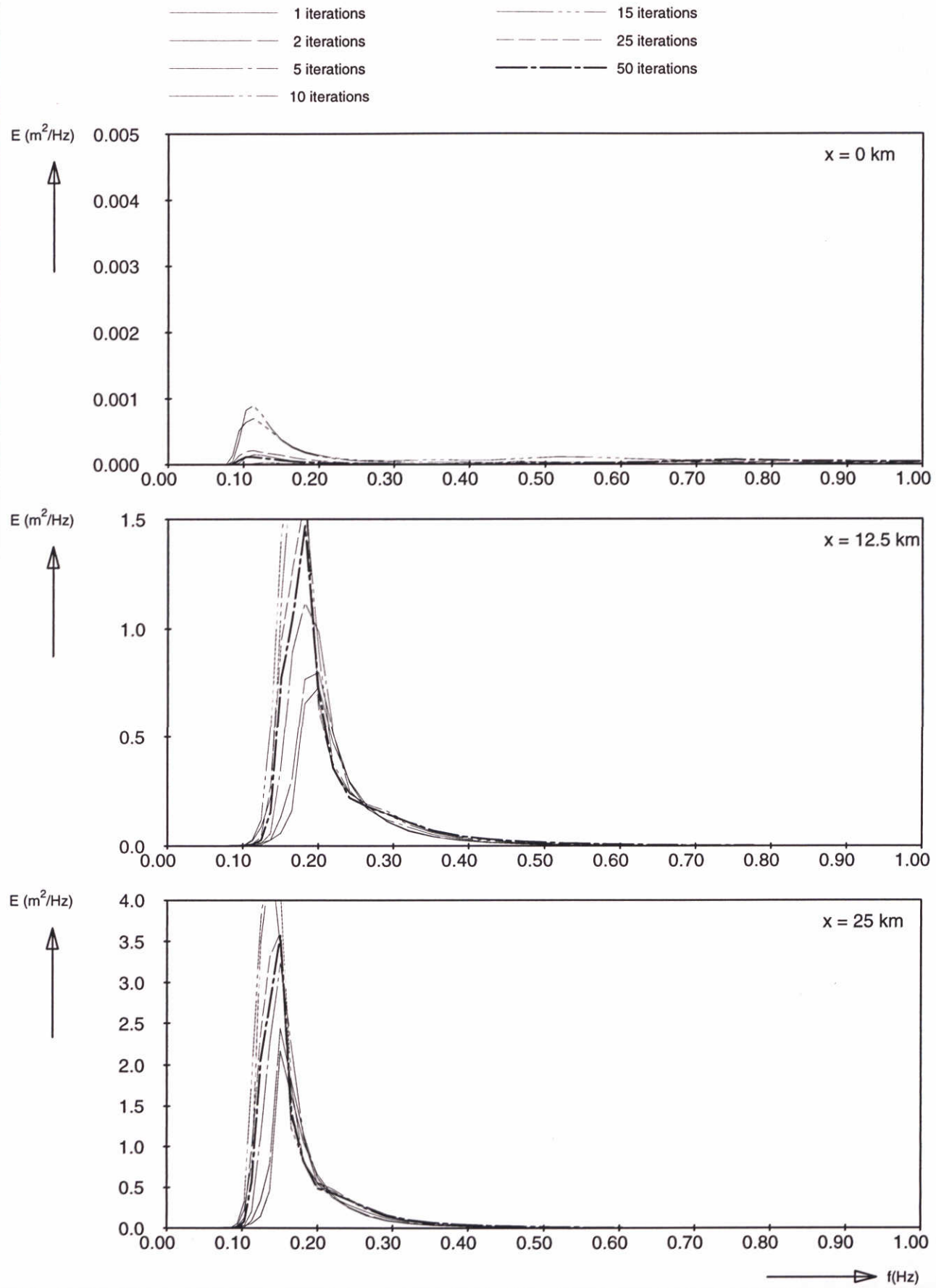

Frequency spectra at 3 locations Adapted limiter Distribution equal f_m/f	SWAN-1D	U_{10}=30 m/s
WL | delft hydraulics	H3496	Fig. 39b

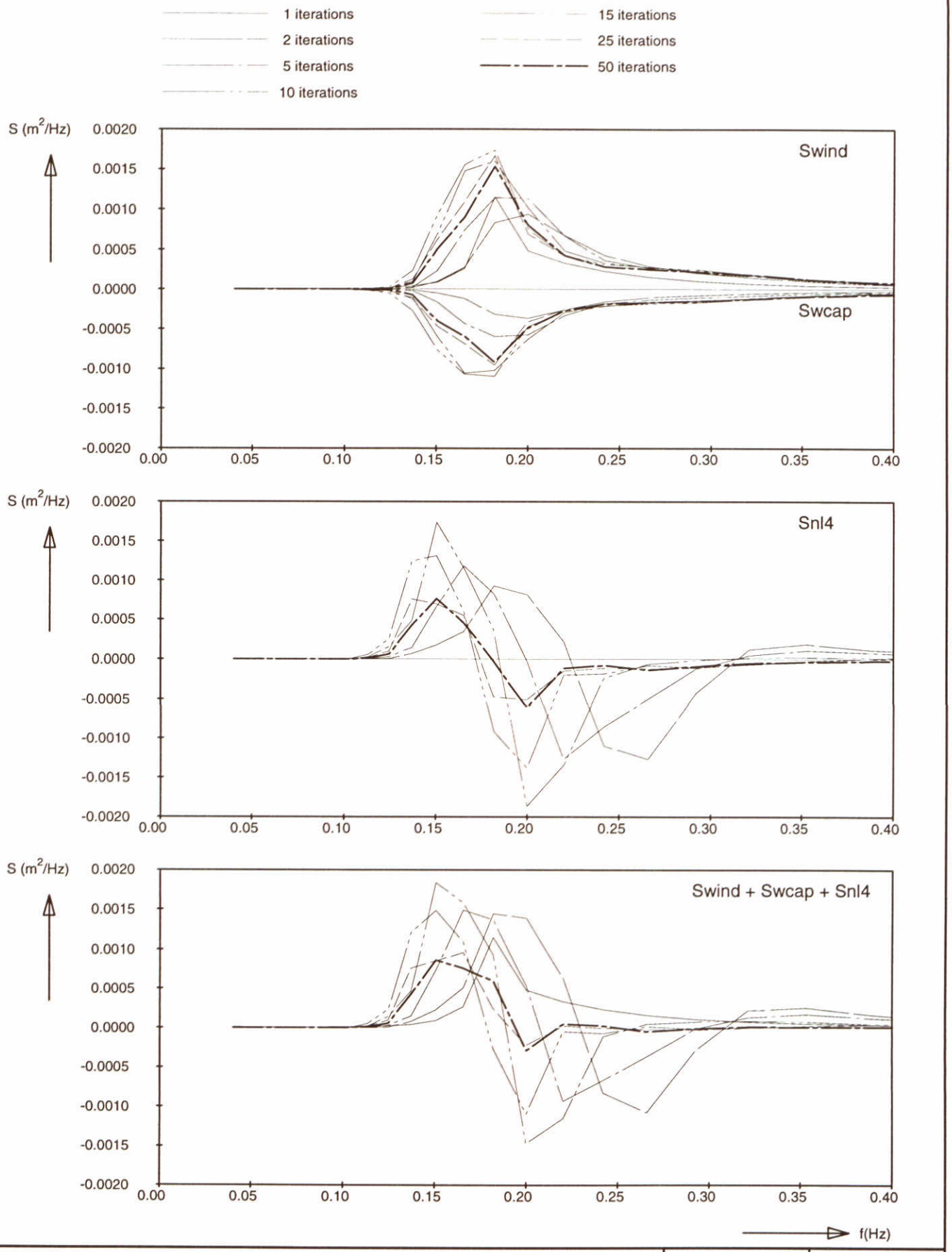

Source terms at x = 12.5 km Adapted limiter Distribution equal f_m/f	SWAN-1D	U_{10}=30 m/s
WL | delft hydraulics	H3496	Fig. 39c

Significant wave height at 12.5 km Adapted limiter Distribution equal f_m/f	SWAN-1D	U_{10}=30 m/s
WL | delft hydraulics	H3496	Fig. 39d

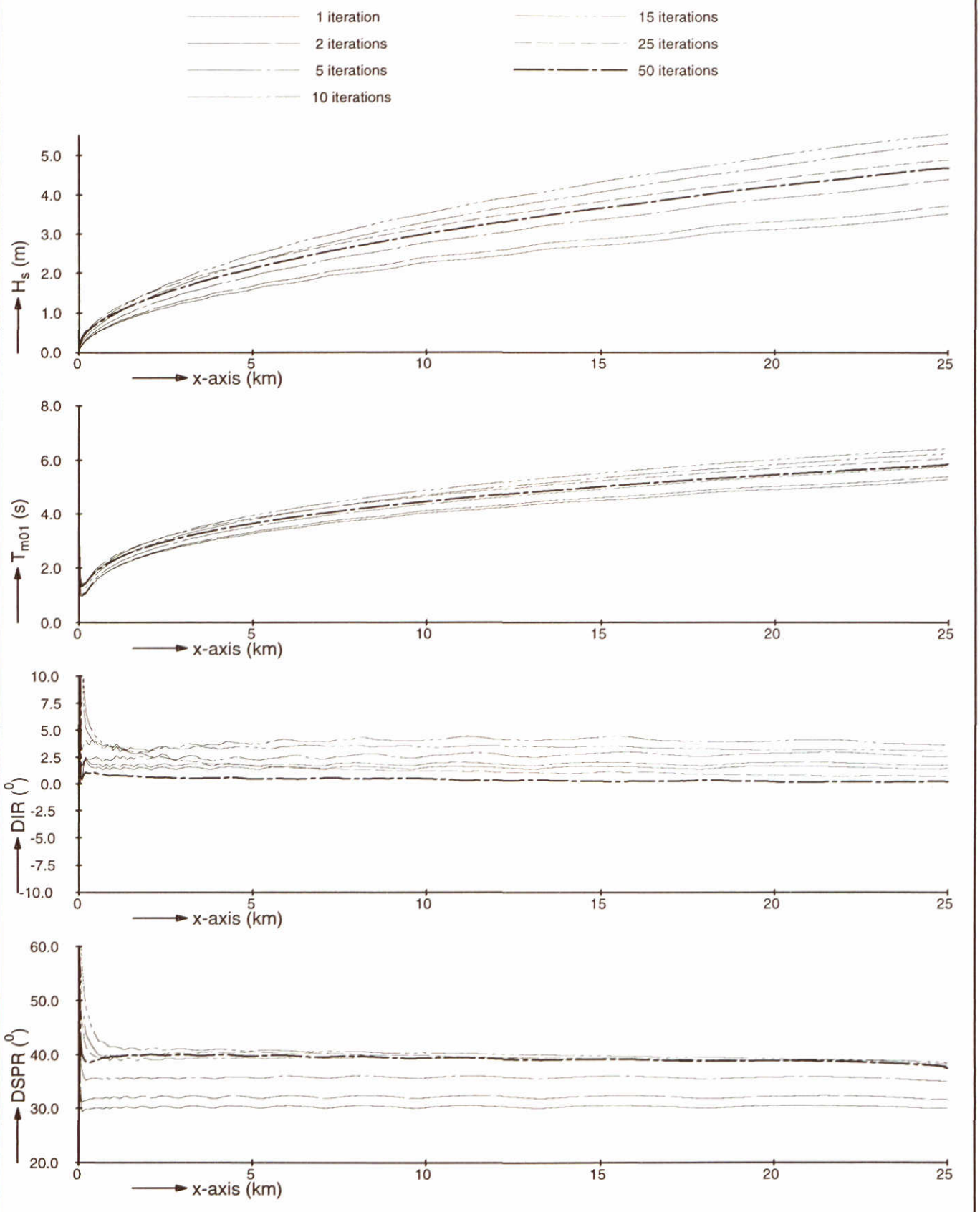

Model convergence behaviour using third-generation formulations Adapted limiter Distribution equal $(f_m/f)^2$	SWAN-1D	U_{10}=30 m/s
WL | delft hydraulics	H3496	Fig. 40a

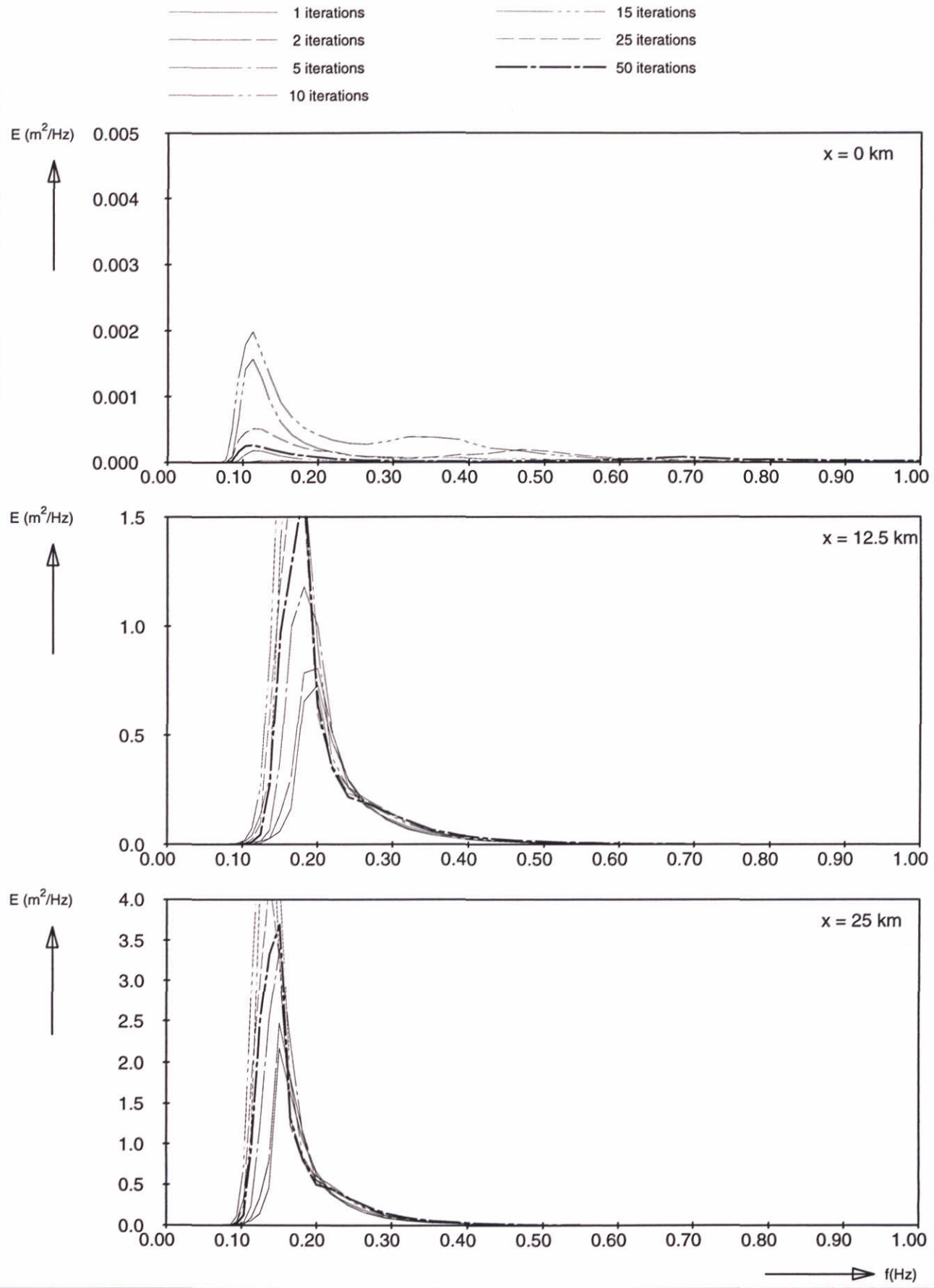

Frequency spectra at 3 locations Adapted limiter Distribution equal $(f_m/f)^2$	SWAN-1D	U_{10}=30 m/s
WL | delft hydraulics	H3496	Fig. 40b

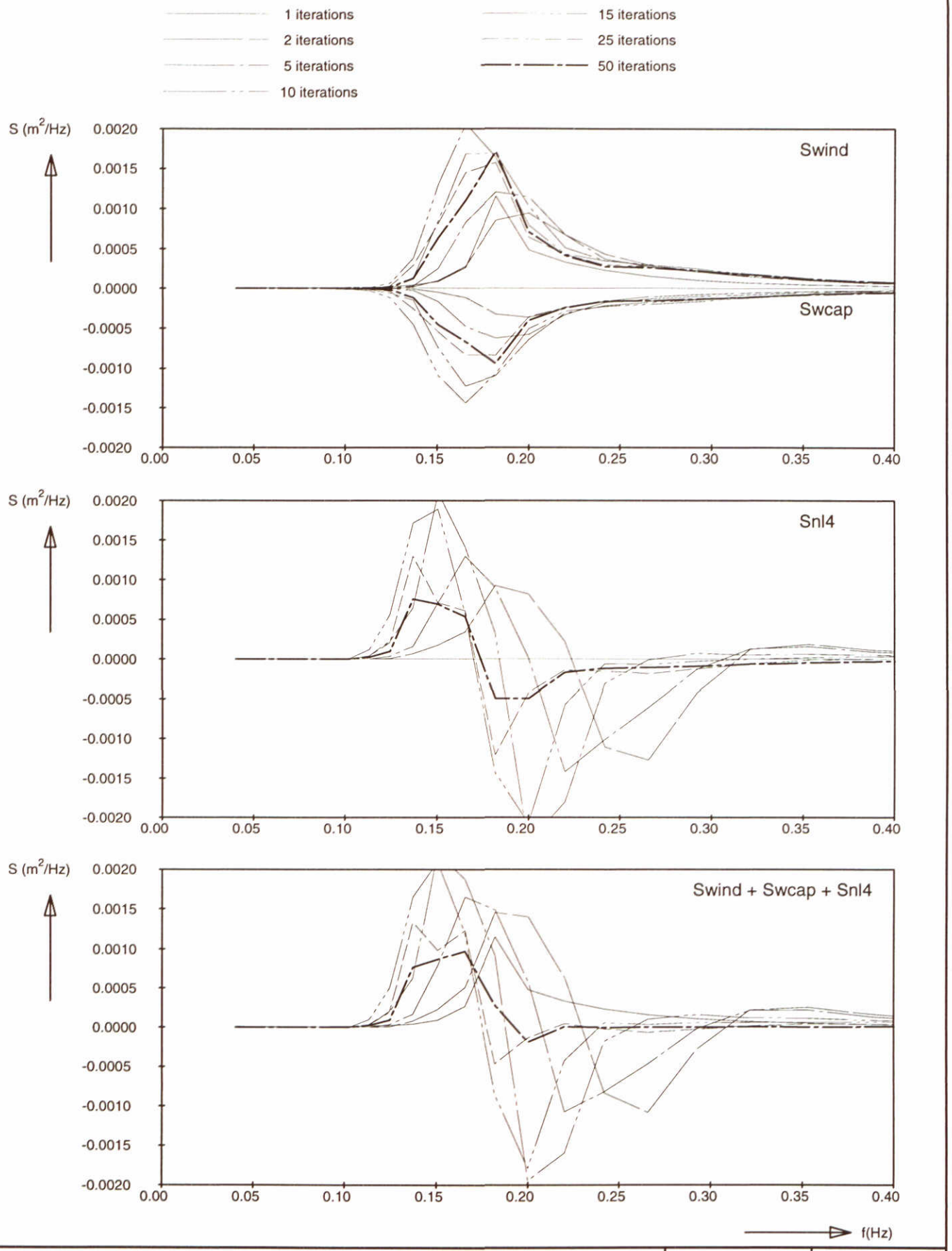

Source terms at x = 12.5 km Adapted limiter Distribution equal $(f_m/f)^2$	SWAN-1D	U_{10}=30 m/s
WL | delft hydraulics	H3496	Fig. 40c

Significant wave height at 12.5 km Adapted limiter Distribution equal $(f_m/f)^2$	SWAN-1D	U_{10}=30 m/s
WL | delft hydraulics	H3496	Fig. 40d

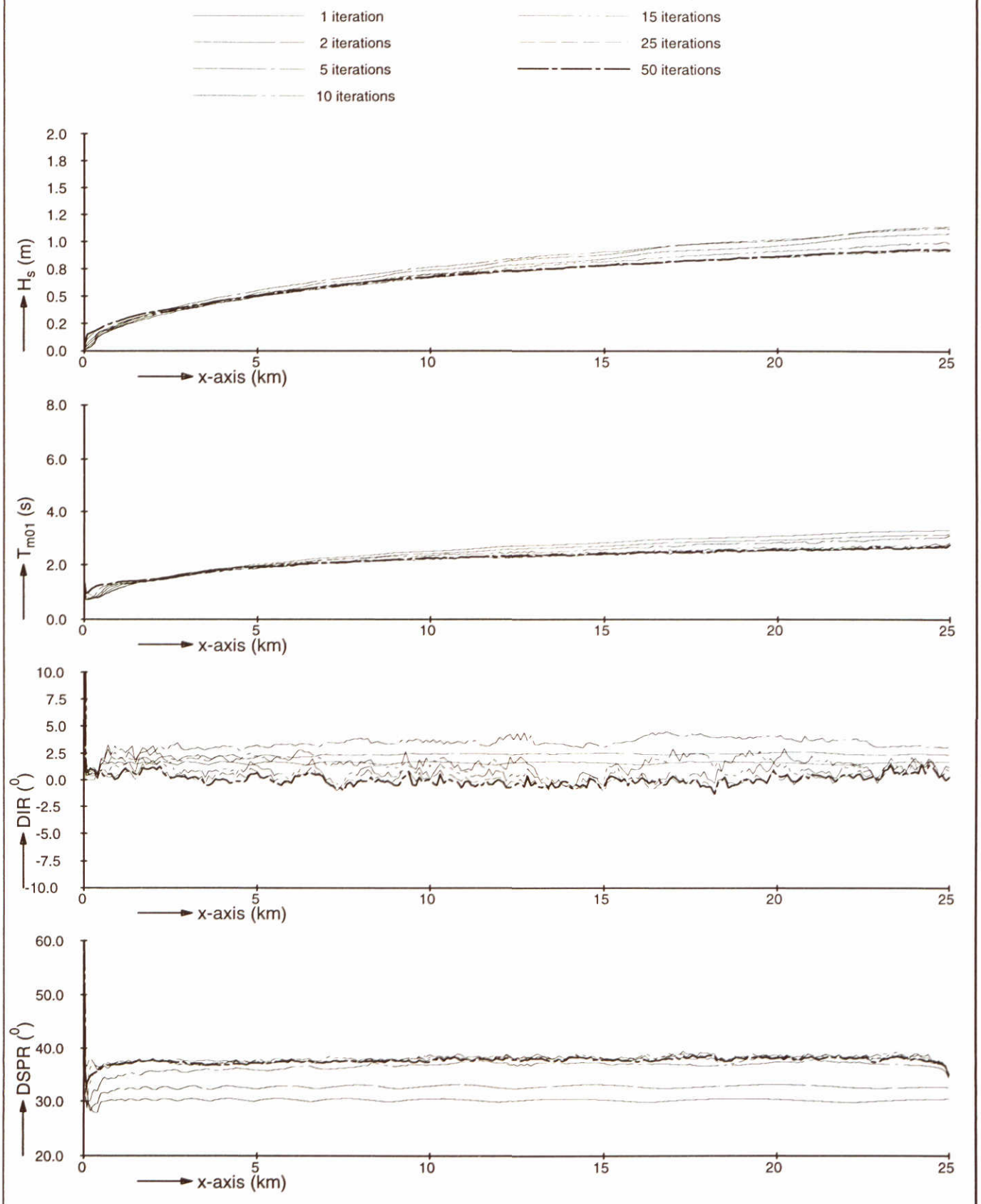

Model convergence behaviour using third-generation formulations
Adapted limiter
Distribution equal $(f/f_m)^2$

SWAN-1D

U_{10}=10 m/s

WL | delft hydraulics

H3496

Fig. 41a

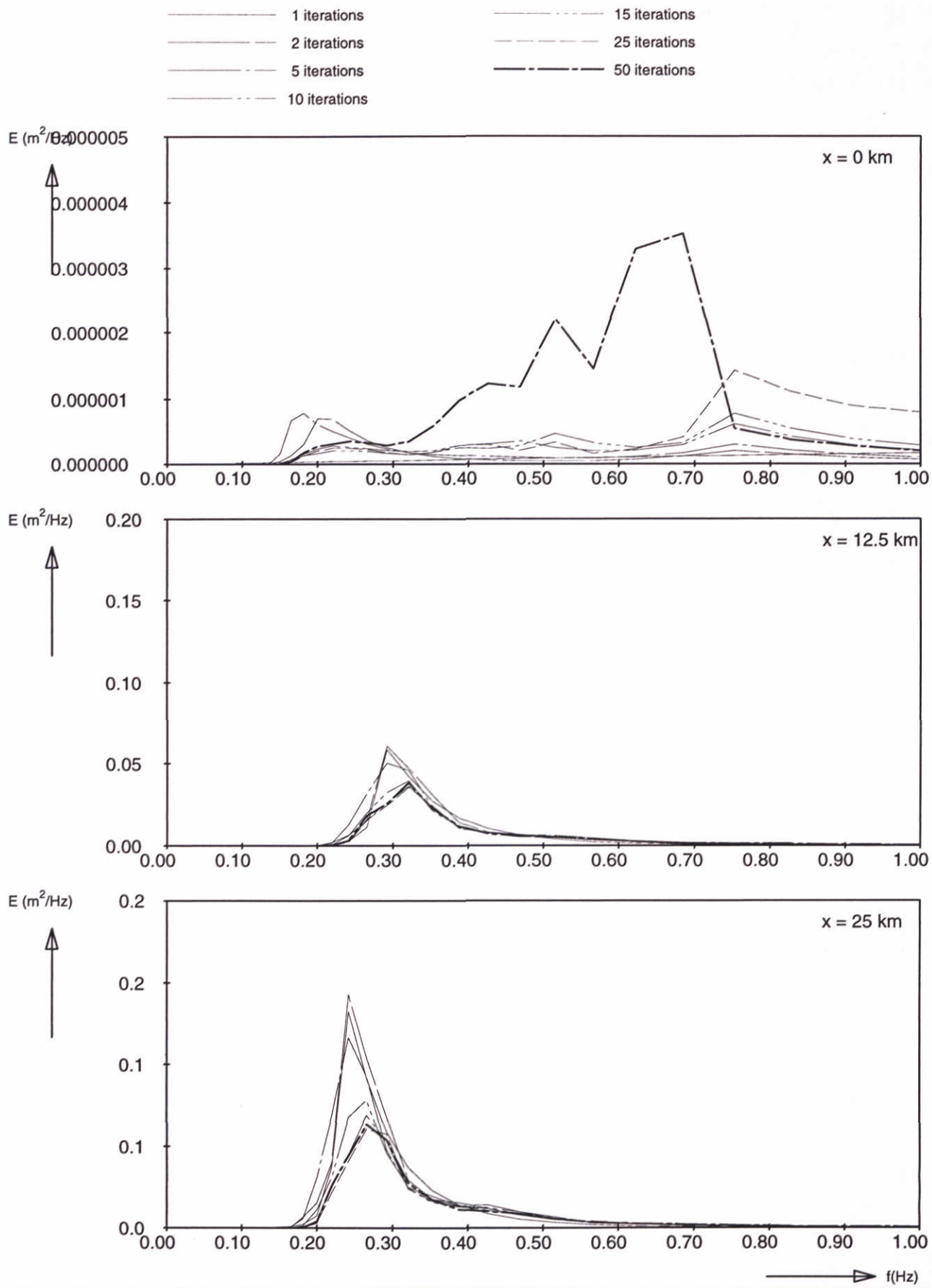

Frequency spectra at 3 locations Adapted limiter Distribution equal $(f/f_m)^2$	SWAN-1D	U_{10}=10 m/s
WL | delft hydraulics	H3496	Fig. 41b

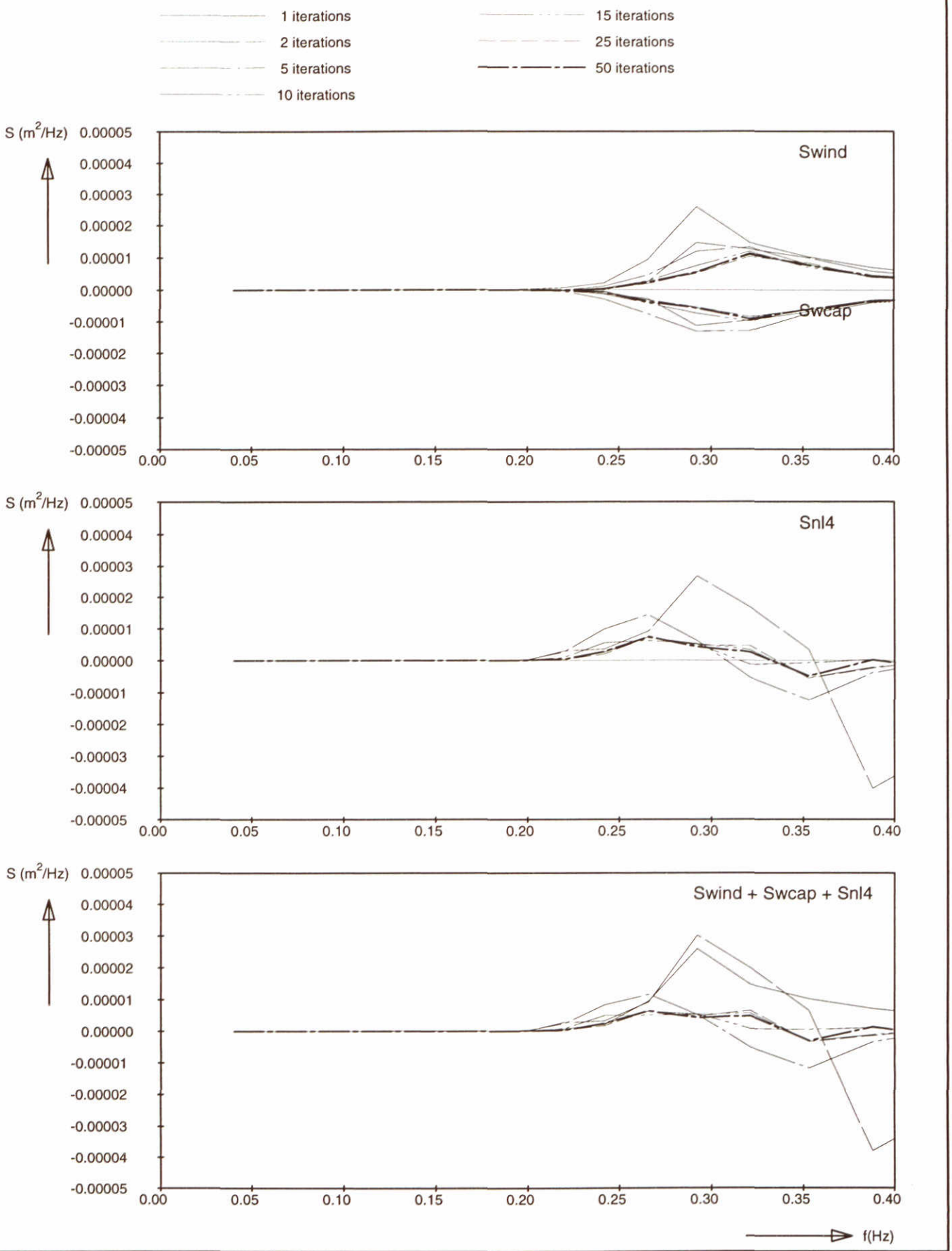

Source terms at x = 12.5 km Adapted limiter Distribution equal $(f/f_m)^2$	SWAN-1D	U_{10}=10 m/s
WL | delft hydraulics	H3496	Fig. 41c

Significant wave height at 12.5 km Adapted limiter Distribution equal $(f/f_m)^2$	SWAN-1D	U_{10}=10 m/s
WL | delft hydraulics	H3496	Fig. 41d

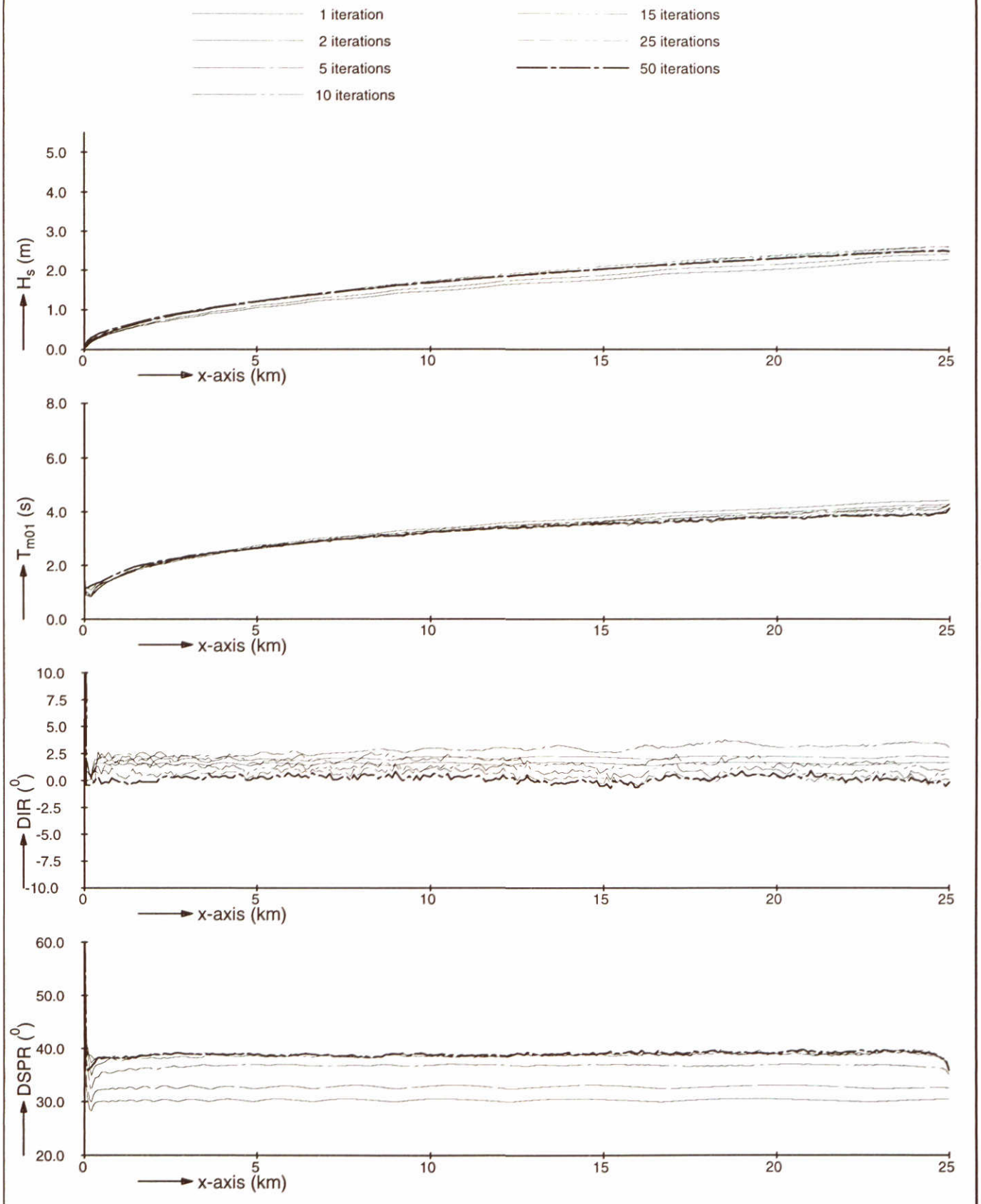

Model convergence behaviour using third-generation formulations Adapted limiter Distribution equal $(f/f_m)^2$	SWAN-1D	U_{10}=20 m/s
WL | delft hydraulics	H3496	Fig. 42a

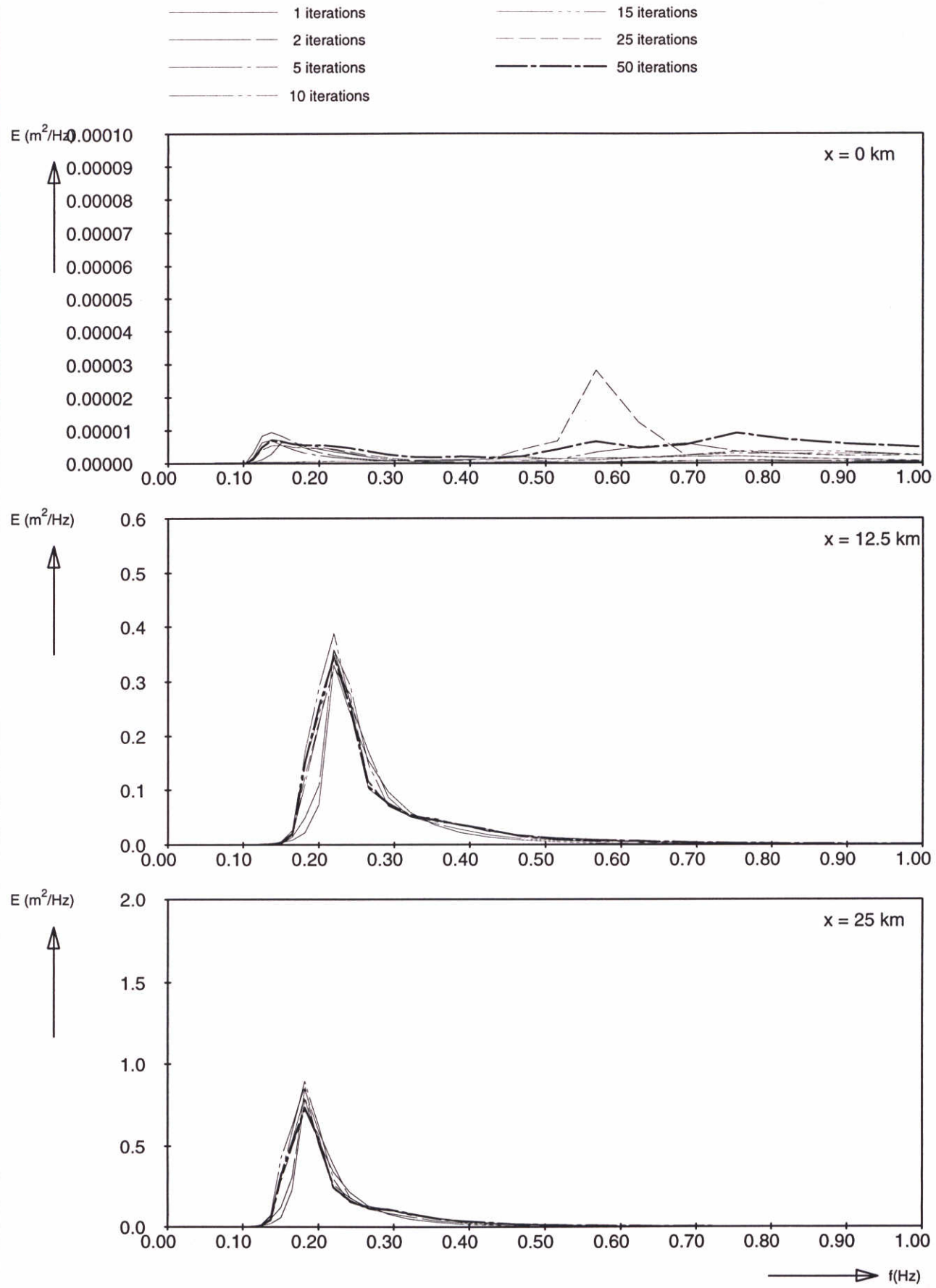

Frequency spectra at 3 locations Adapted limiter Distribution equal $(f/f_m)^2$	SWAN-1D	U_{10}=20 m/s
WL | delft hydraulics	H3496	Fig. 42b

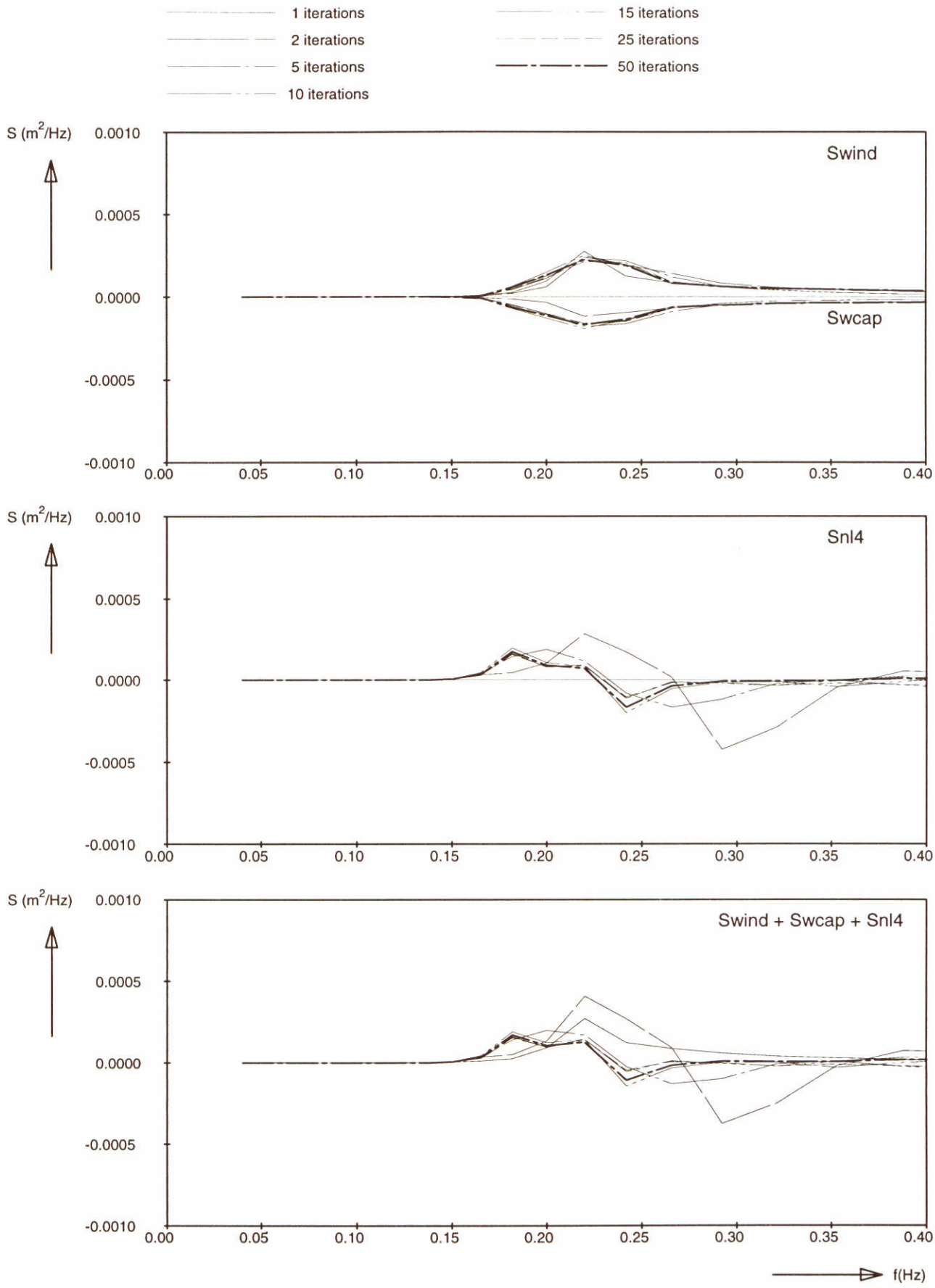

Source terms at x = 12.5 km Adapted limiter Distribution equal $(f/f_m)^2$	SWAN-1D	U_{10}=20 m/s
WL | delft hydraulics	H3496	Fig. 42c

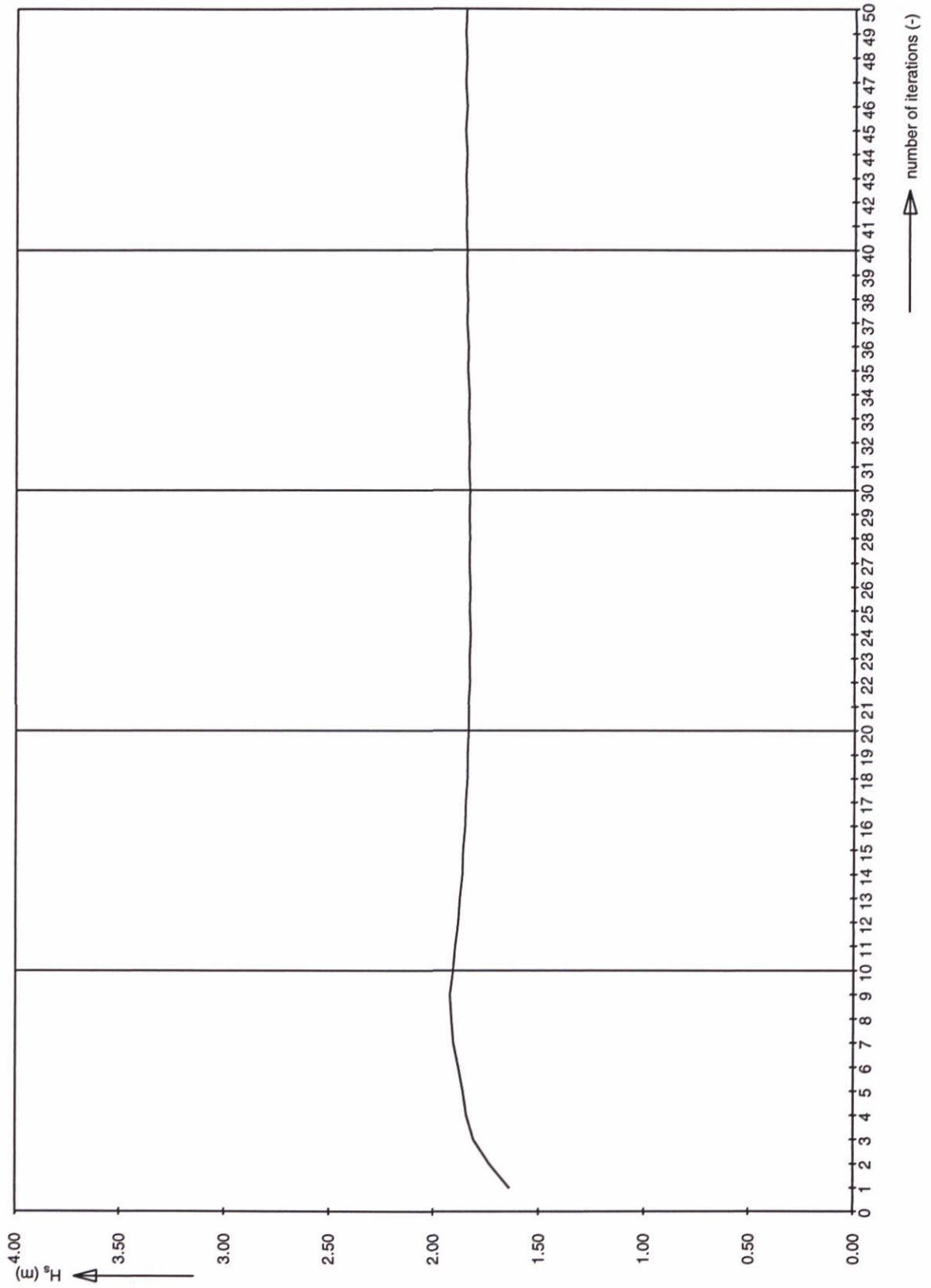

Significant wave height at 12.5 km Adapted limiter Distribution equal $(f/f_m)^2$	SWAN-1D	U_{10}=20 m/s
WL | delft hydraulics	H3496	Fig. 42d

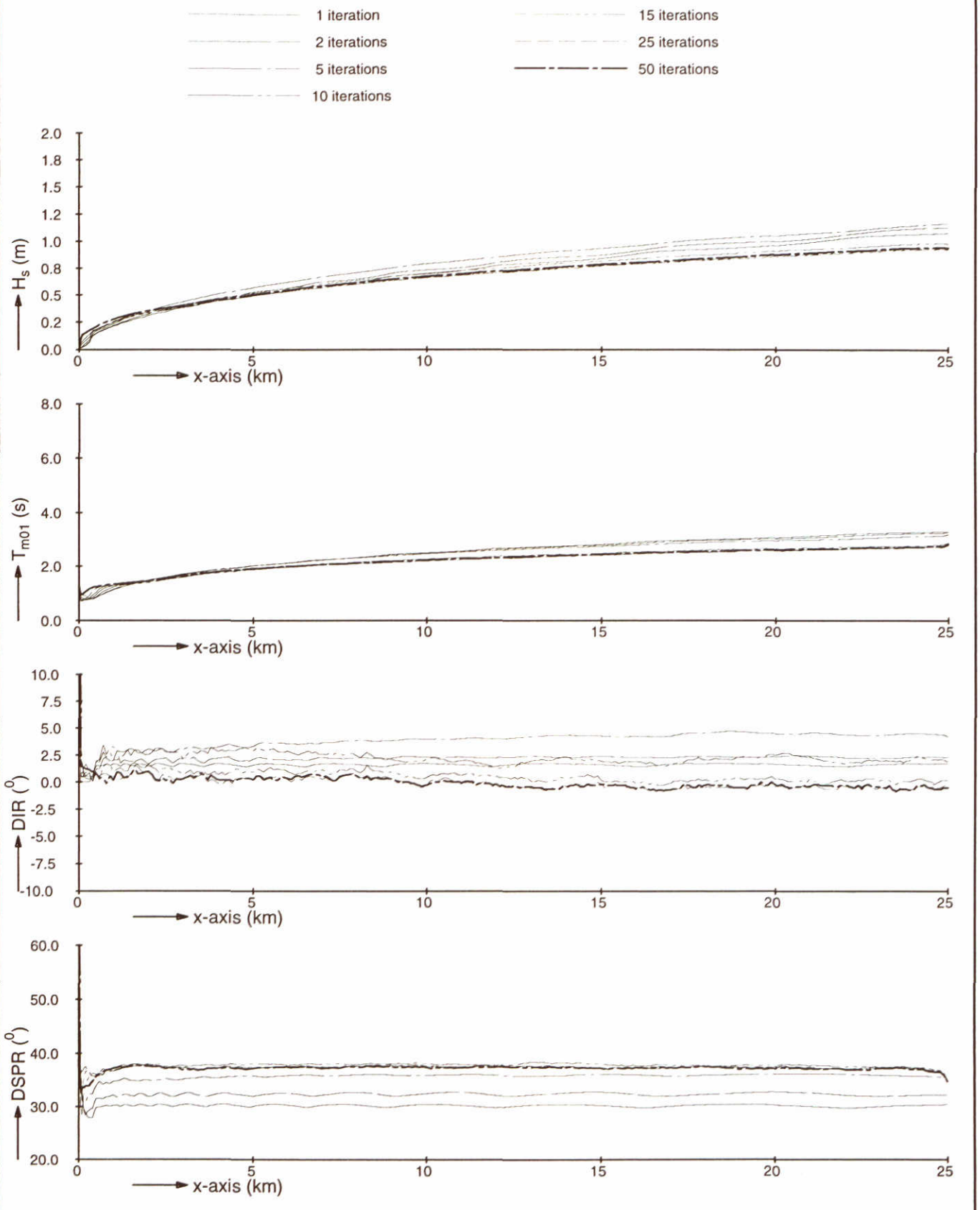

Model convergence behaviour using third-generation formulations
Adapted limiter
Distribution equal f/f_m

SWAN-1D | U_{10}=10 m/s

WL | delft hydraulics | H3496 | Fig. 43a

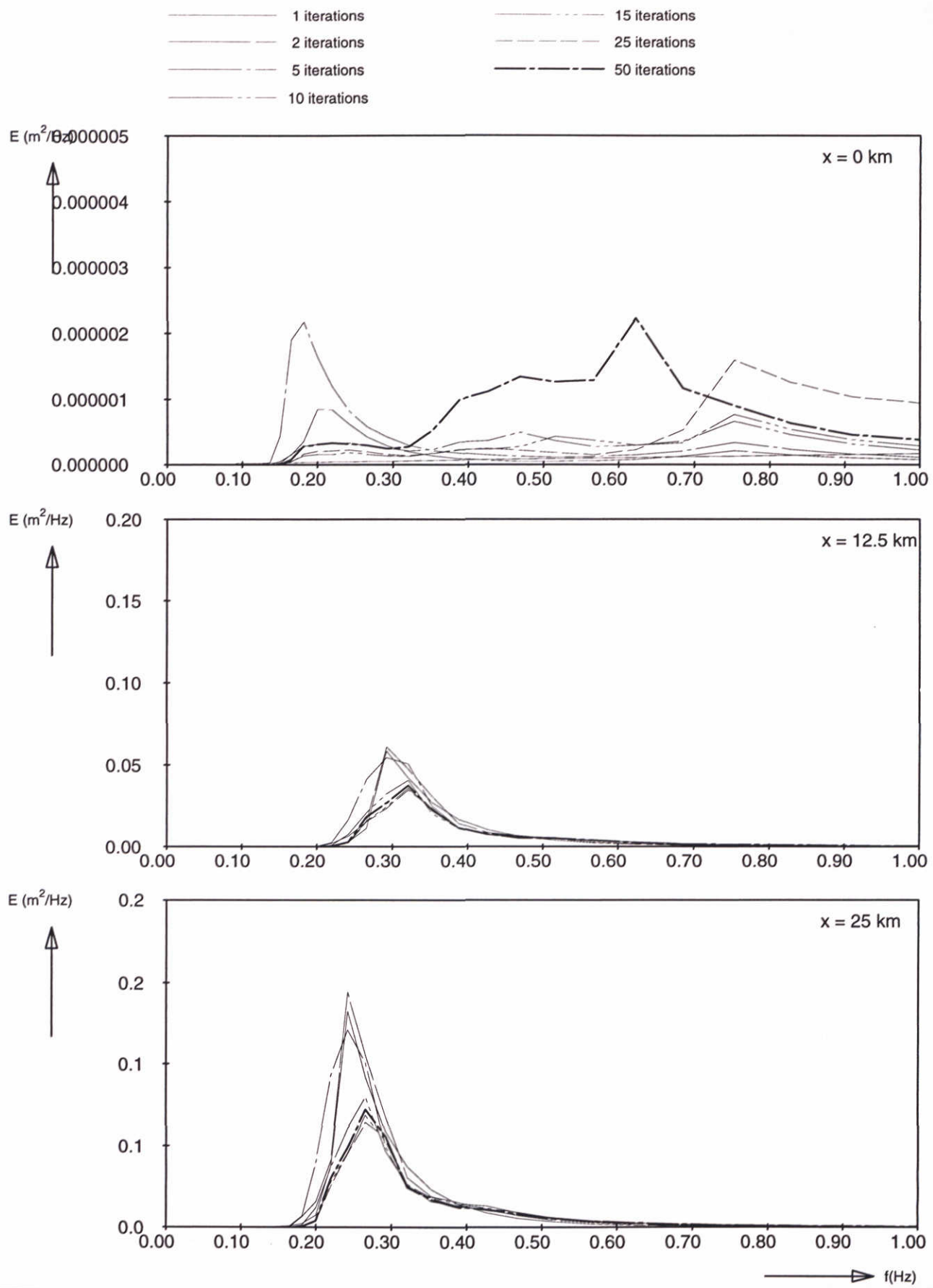

Frequency spectra at 3 locations Adapted limiter Distribution equal f/f_m	SWAN-1D	U_{10}=10 m/s
WL | delft hydraulics	H3496	Fig. 43b

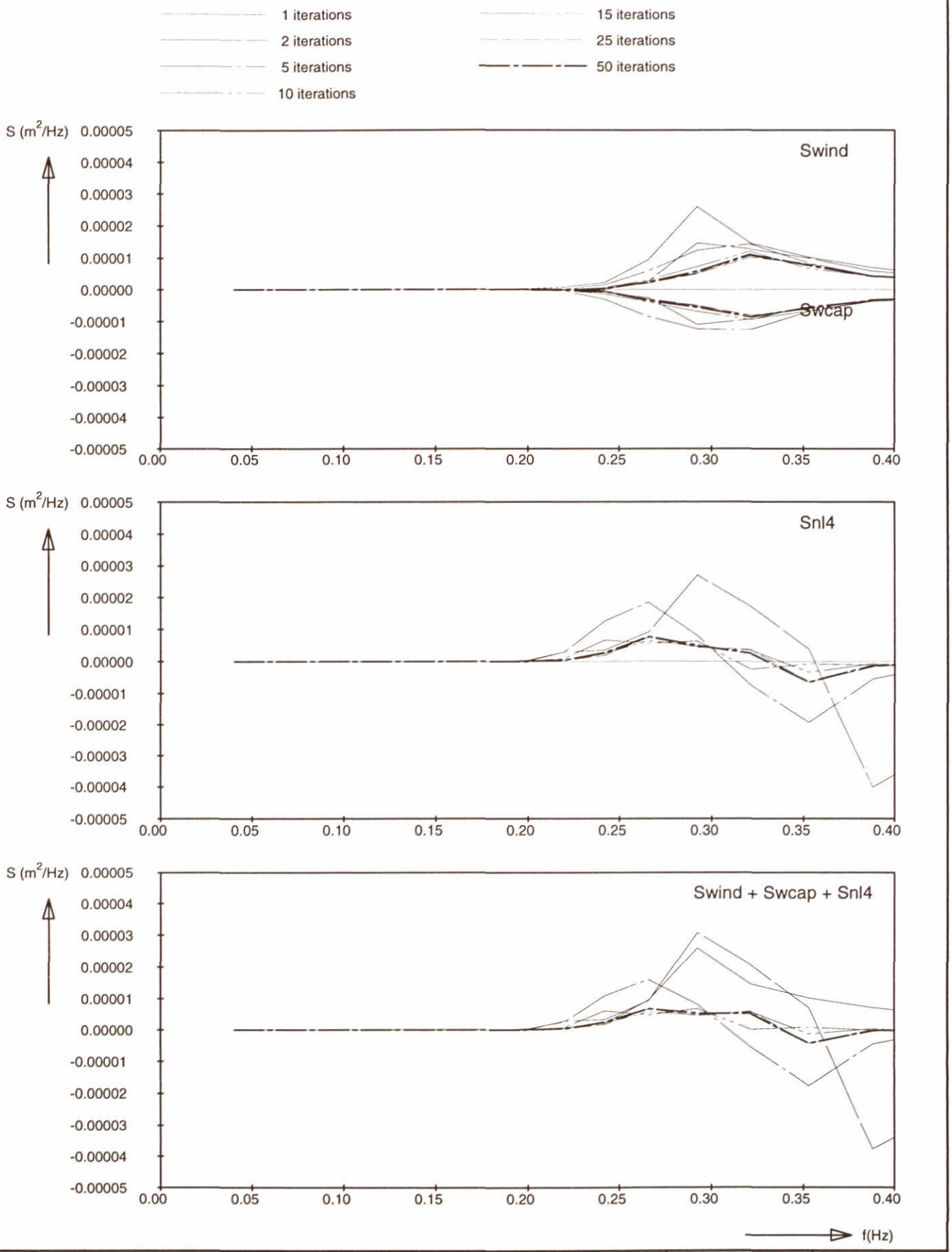

Source terms at x = 12.5 km Adapted limiter Distribution equal f/f_m	SWAN-1D	U_{10}=10 m/s
WL | delft hydraulics	H3496	Fig. 43c

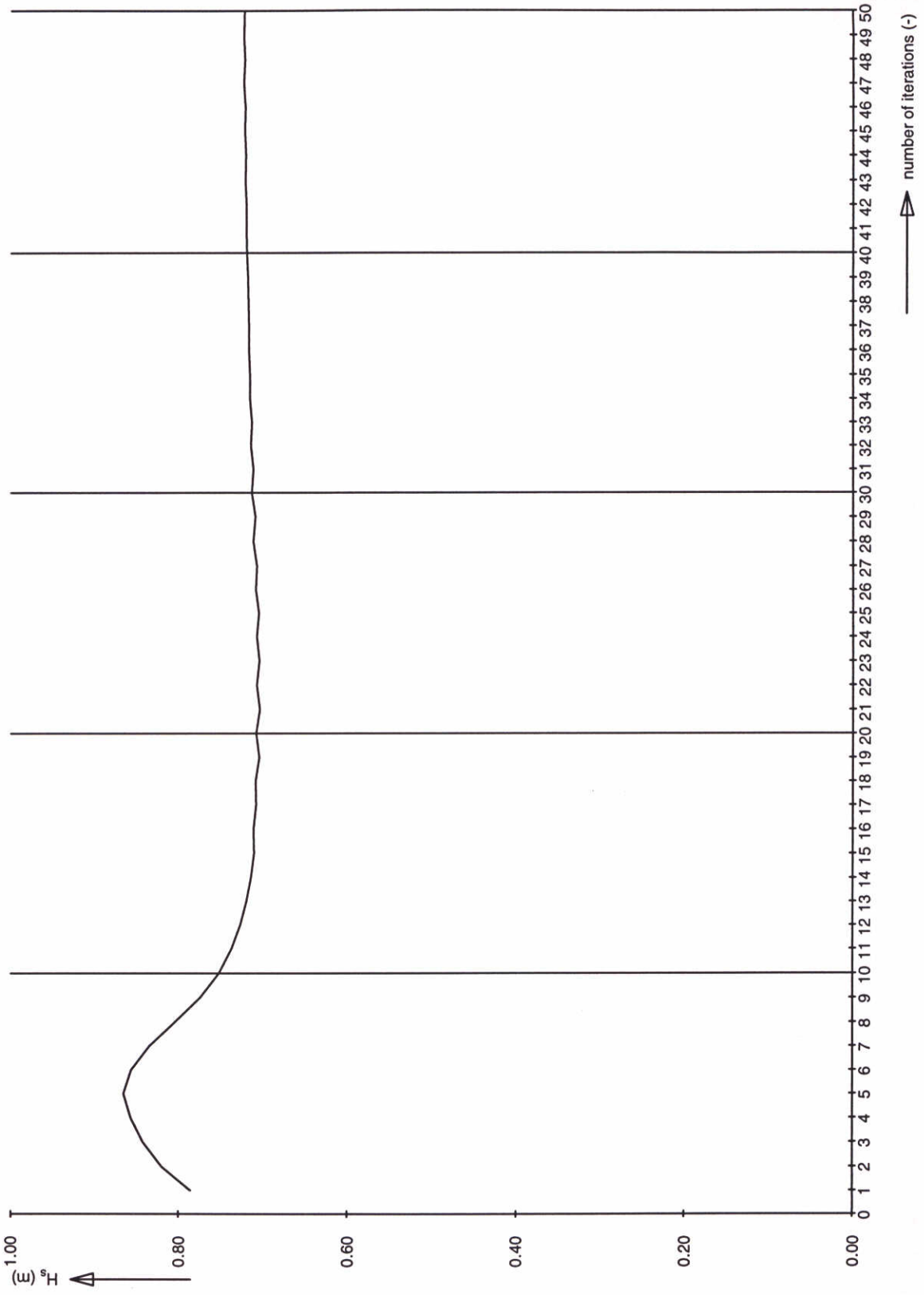

Significant wave height at 12.5 km Adapted limiter Distribution equal f/f_m	SWAN-1D	U_{10}=10 m/s
WL | delft hydraulics	H3496	Fig. 43d

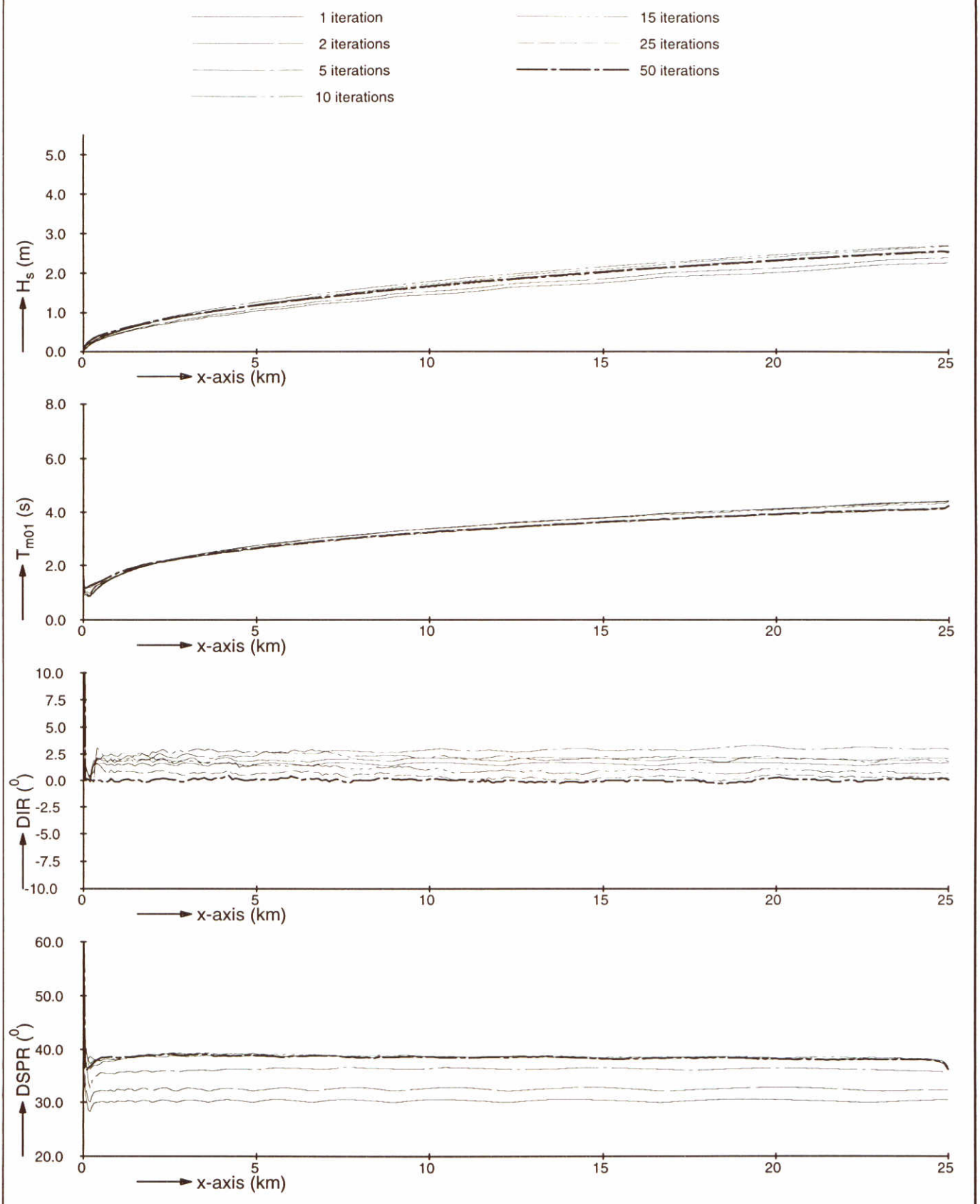

Model convergence behaviour using third-generation formulations Adapted limiter Distribution equal f/f_m	SWAN-1D	U_{10}=20 m/s
WL | delft hydraulics	H3496	Fig. 44a

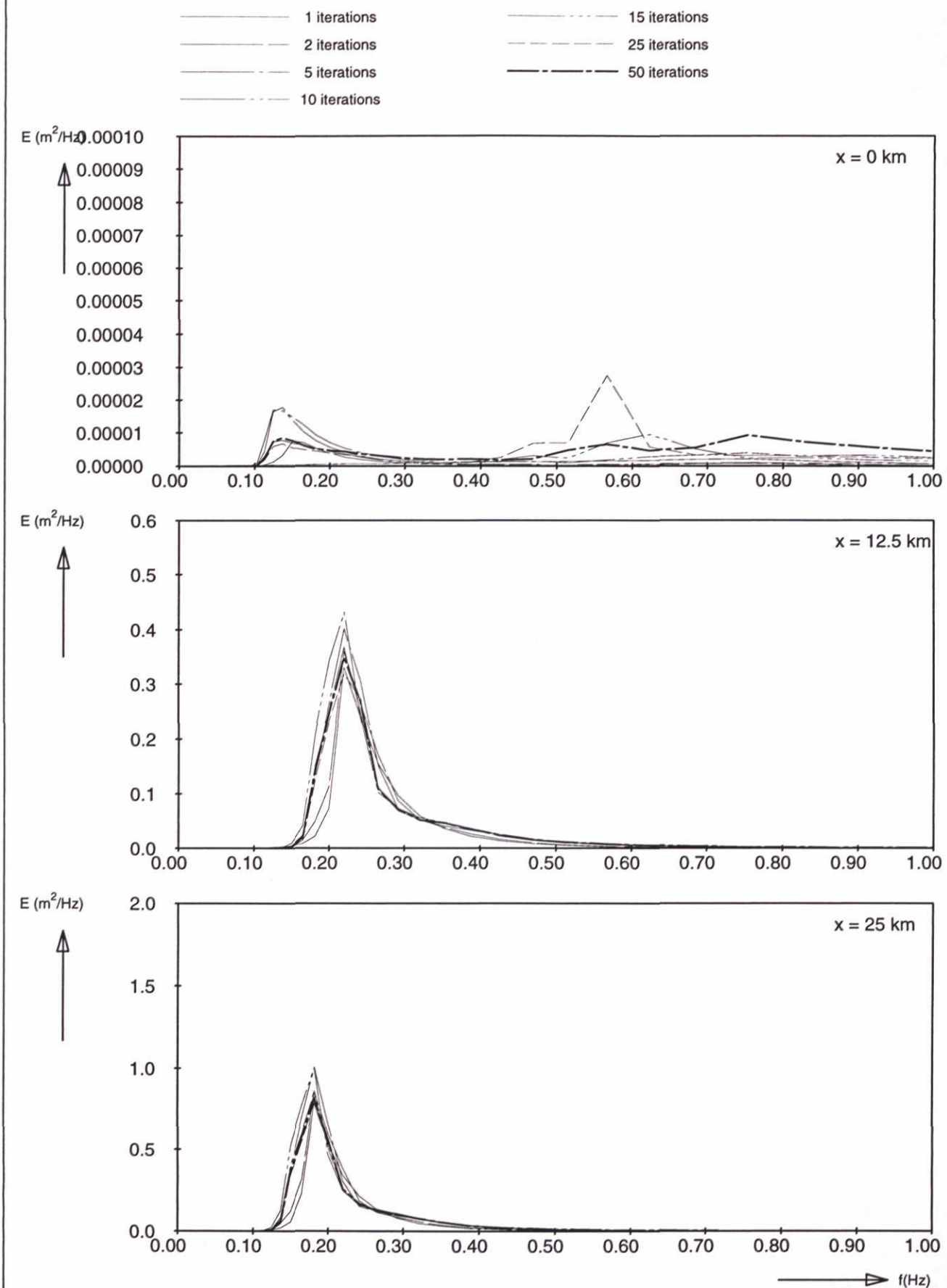

Frequency spectra at 3 locations Adapted limiter Distribution equal f/f_m	SWAN-1D	U_{10}=20 m/s
WL | delft hydraulics	H3496	Fig. 44b

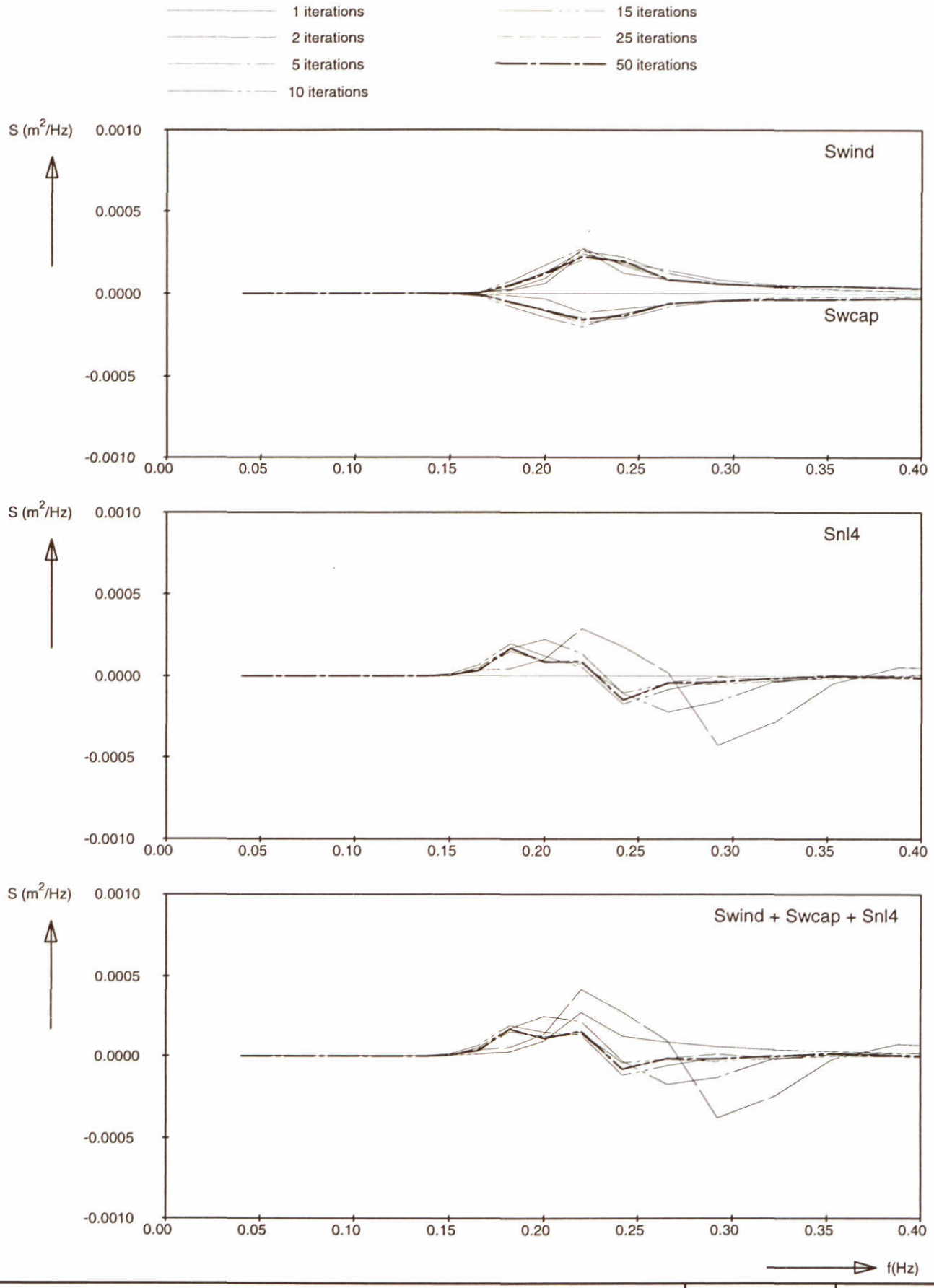

Source terms at x = 12.5 km Adapted limiter Distribution equal f/f_m	SWAN-1D	U_{10}=20 m/s
WL | delft hydraulics	H3496	Fig. 44c

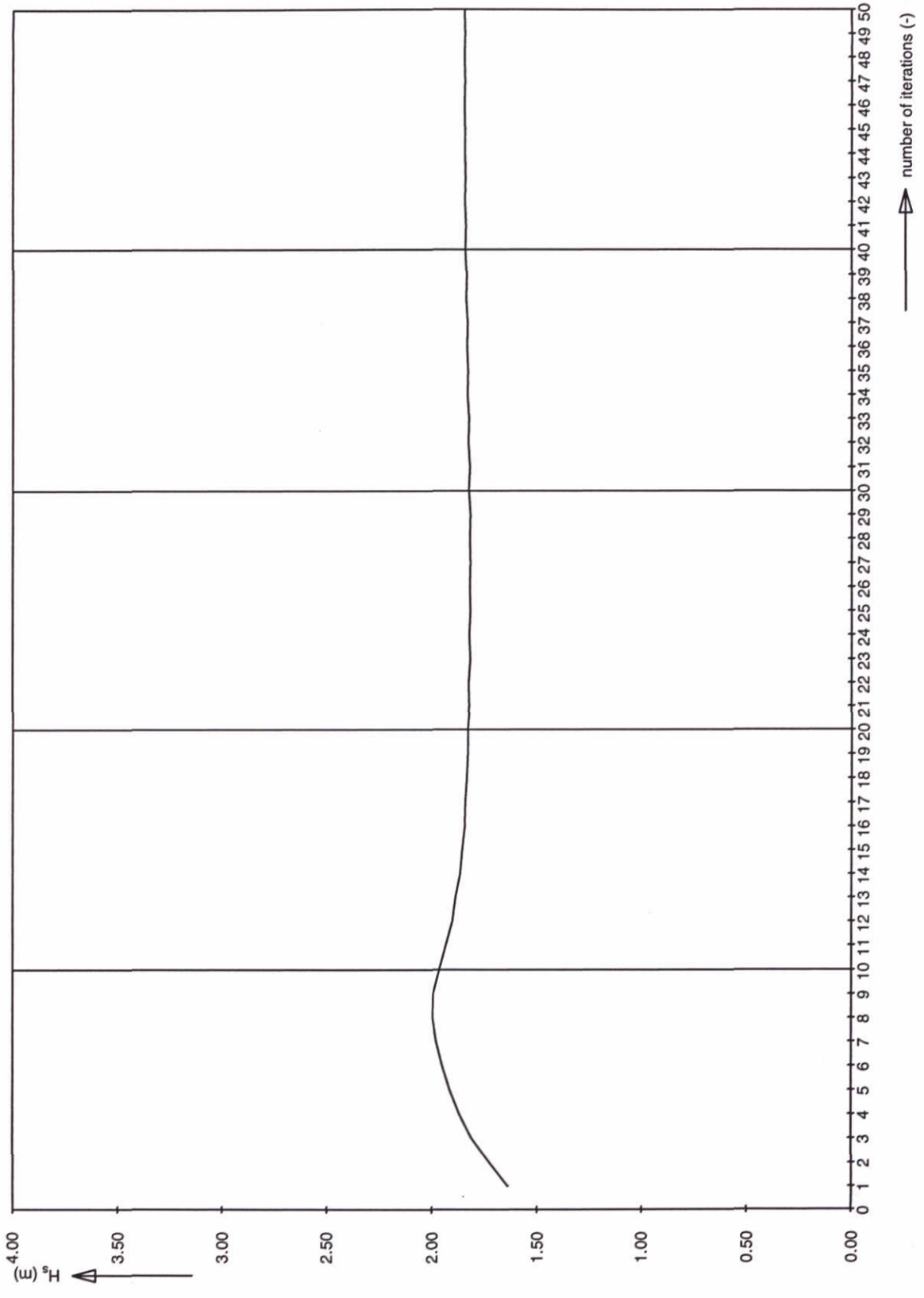

Significant wave height at 12.5 km Adapted limiter Distribution equal f/f_m	SWAN-1D	U_{10}=20 m/s
WL | delft hydraulics	H3496	Fig. 44d

Appendices

A Listing of SWAN input file

A listing of the standard SWAN input file (case 4) is given in this appendix.

```
$*****************************************
$
PROJ 'SWAN '    '4'
$
$ iteration:  1
$
$************* MODEL INPUT *****************
$
MODE STAT ONED
$
SET LEVEL=6. DEPMIN=.05 MAXERR = 150
$
CGRID 0. 0. 0. 25000. 0. 250 0 CIRCLE 36 0.04 1. 34
$
INP  BOTTOM 0. 0. 0. 1 0 25000. 1.
READ BOTTOM 1. '../bottom/deep.bot' 4 FREE
$
WIND 30. 0.
$
GEN3
OFF BREAK
$ FRIC
$ TRIAD
$
NUM ACCUR 1.e-5 1.e-5 1.e-5 100. 1
$
$******** output requests *********
$
CURVE 'curve' 0. 0. 500 25000. 0.
TABLE 'curve' HEAD   'h4_i01.tbl' DIST DEP HS TM01 DIR DSPR QB DISS
TABLE 'curve' NOHEAD 'h4_i01.out' DIST DEP HS TM01 DIR DSPR QB DISS
$
POINT 'point' 0. 0. 12500. 0. 25000. 0.
SPEC  'point' SPEC1D ABS 'h4_i01.sp1'
$
TEST POINTS 125 0 S1D 'h4_i01.src'
POOL
COMPUTE
STOP
```

WL | delft hydraulics

Rotterdamseweg 185
postbus 177
2600 MH Delft
telefoon 015 285 85 85
telefax 015 285 85 82
e-mail info@wldelft.nl
internet www.wldelft.nl

Rotterdamseweg 185
p.o. box 177
2600 MH Delft
The Netherlands
telephone +31 15 285 85 85
telefax +31 15 285 85 82
e-mail info@wldelft.nl
internet www.wldelft.nl